Open Research Online

The Open University's repository of research publications
and other research outputs

The mechanism of nucleophilic substitution at silicon

Thesis

How to cite:

Lau, Juliana C.Y. (1986). The mechanism of nucleophilic substitution at silicon. PhD thesis. The Open University.

For guidance on citations see FAQs.

© 1986 The Author

Version: Version of Record

Copyright and Moral Rights for the articles on this site are retained by the individual authors and/or other copyright owners. For more information on Open Research Online's data policy on reuse of materials please consult the policies page.

oro.open.ac.uk

DX 72762/87
UNRESTRICTED

THE MECHANISM OF NUCLEOPHILIC SUBSTITUTION AT SILICON

A thesis presented for the degree of Doctor of Philosophy by Juliana C.-Y. Lau at the Chemistry Department of the Open University in September 1986.

Date of submission: September 1986

Date of award: 21 November 1986

ProQuest Number: 27775897

All rights reserved

INFORMATION TO ALL USERS
The quality of this reproduction is dependent on the quality of the copy submitted.

In the unlikely event that the author did not send a complete manuscript
and there are missing pages, these will be noted. Also, if material had to be removed,
a note will indicate the deletion.

ProQuest 27775897

Published by ProQuest LLC (2020). Copyright of the Dissertation is held by the Author.

All Rights Reserved.
This work is protected against unauthorized copying under Title 17, United States Code
Microform Edition © ProQuest LLC.

ProQuest LLC
789 East Eisenhower Parkway
P.O. Box 1346
Ann Arbor, MI 48106 - 1346

Statement

The work embodied in this thesis was carried out by the author during the period September 1983 to September 1986 in the Chemistry Department of the Open University. This work has not been published in any form.

Acknowledgements

I like to thank Dr. A.R. Bassindale for being my supervisor, Dr. P.G. Taylor for commenting on my thesis and the Open University for the student grant.

I especially like to thank my parents for their support and Dr. T. Stout for modifying and writing part of the DNMR4 program as well as all the graphic programs.

Abstract

Using multinuclear n.m.r. spectroscopy (^{1}H, ^{13}C, ^{29}Si and ^{17}O), the interactions of diastereotopic ($PhCHMeSiMe_2X$; X=Cl, Br, OSO_2CF_3) and chiral ($PhMeHSiX$; X=Cl, OSO_2CF_3) silanes with a diverse range of nucleophile (Nu = amides, ureas, pyridines, phosphine oxide and amines) are examined in detail.

The dominant species in the diastereotopic silylating solutions are four coordinate 1:1 ionic $[PhCHMeSiMe_2\text{-}Nu]^+X^-$ adducts. These complexes undergo exchange with nucleophiles and their parent silanes at a rate limited by the initial attack of nucleophile or counterion at the silicon atom of the adduct. The halide counterions of stable silane-nucleophile adducts can also induce isomerization of uncomplexed silanes.

The kinetic and thermodynamic results are consistent with the operation of two different mechanisms for the racemizations of $PhCHMeSiMe_2X$ (X=Cl, Br). Racemization involving less stable silane-nucleophile complexes may proceed via rate determining attack by a second molecule of nucleophile at the adduct, formed in the initial, rapid, pre-equilibrium step. Two molecules of nucleophile are utilized resulting in an order of 2 or 1.5 in nucleophile, depending upon the degree of ion-pair dissociation. An alternative pathway is preferred with increasing stability of the silane-nucleophile salt. Adduct formation is followed by halide exchange leading to racemization of silane. One molecule of nucleophile is required in this case corresponding to a first or a half order in nucleophile.

The kinetic results are correlated with the rate of alcoholysis reported by Frye, the relative equilibrium constant for the formation of $[Me_3Si\text{-}Nu]^+X^-$ complexes and the donor strength of nucleophile as measured by Taft's Beta values. The good correlation with the Beta values provides evidence that the rate of racemization is dependent upon the nucleophilicity of the donor species. The excellent linear correlation

with Frye's ln k_1 values further verifies the mechanism first postulated by Chojnowski. Rapid pre-equilibrium formation of $[R_3Si\text{-}Nu]^+X^-$ adducts is followed by slow attack of a second molecule of nucleophile.

With strong nucleophiles, four coordinate ionic $[PhMeHSi\text{-}Nu]^+Cl^-$ salts undergo second nucleophilic attacks yielding stable pentacoordinate $[PhMeHSi\text{-}(Nu)_2]^+Cl^-$ ionic adducts. The collapse of the N-methyl resonances of DMF observed in the interactions of PhMeRSiCl (R=H, Me) with DMF may serve as an indication of N-silylation of DMF.

Contents

List of figures

Chapter 3 Kinetic studies on the racemization of diastereotopic silanes

List of tables

Chapter 4 Thermodynamic studies on the racemization of diastereotopic silanes

Chapter 6 Experimental

List of abbreviations

asym asymmetric stretch

br broad

Beta (a scale of nucleophilicity assigned by Taft)

2,6DBP 2,6-Di-tert-butylpyridine

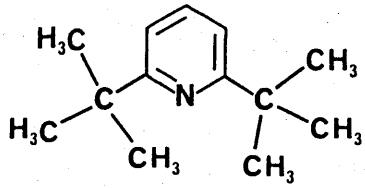

DMEU 1,3-Dimethyl-2-imidazolidinone (N,N'-Dimethylethyleneurea)

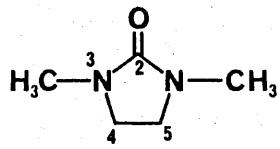

DMF N,N-Dimethylformamide

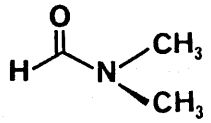

2,4DMP 2,4-Dimethylpyridine

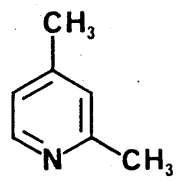

2,6DMP 2,6-Dimethylpyridine

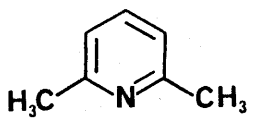

3,5DMP 3,5-Dimethylpyridine

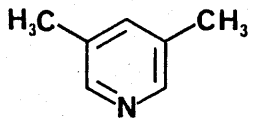

DMPU 1,3-Dimethyl-3,4,5,6-tetrahydro-2(1H)-pyrimidinone
(N,N'-Dimethylpropyleneurea)

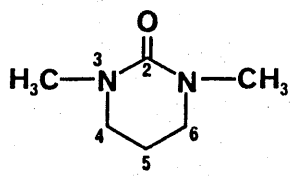

Et_3N Triethylamine

HMPA Hexamethylphosphoramide (hexamethylphosphoric triamide)

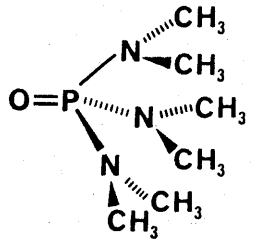

J coupling constant (measured in Hertz)

k_{obs} observed pseudo-first order rate constant

m multiplet

mmol millimole(s)

n order of reaction in nucleophile

NMI N-Methylimidazole (1-methylimidazole)

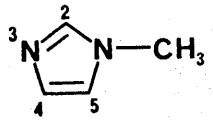

NMP 1-Methyl-2-pyrrolidone

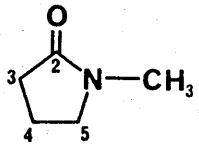

NMPO 1-Methyl-2-pyridone

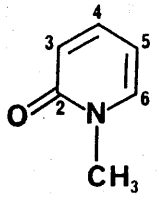

no not observed

nr not recorded

Nu nucleophile

OTf^-	trifluoromethanesulphonate (triflate), $OSO_2CF_3^-$
py	pyridine

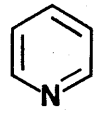

q	quartet
qn	quintet
R	alkyl group
sbr	slightly broadened
s.d.	standard deviation
sym	symmetric stretch
t	triplet
TMS	tetramethylsilane, Me_4Si
TMU	1,1,3,3-tetramethylurea

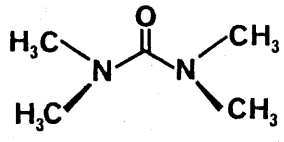

vbr	very broad
vsh	very sharp
v	chemical shift or infrared frequency

Chapter 1 Literature survey

1.1 The importance of organosilicon chemistry

Organosilicon compounds are increasingly important in many areas of chemistry, especially in organic synthesis. There are three main areas where organosilicon reagents are particularly useful. The reaction pathway and hence the stereochemical outcome can be controlled in certain cases, for example the Peterson reaction. Undesirable side reactions can be eliminated by providing temporary protection to functional groups, such as hydroxy, amino or thiol moieties,[1,2,3,4] as silyl derivatives. Silicon compounds can also serve as catalysts to enhance the reactivity of some reagents. This can be clearly illustrated by the group transfer polymerization process, where the silyl ether group initiates the chain polymerization reaction.[5] In each of these areas, it is essential to have a detailed understanding of the precise role of silicon compounds in order to design more efficient reagents.

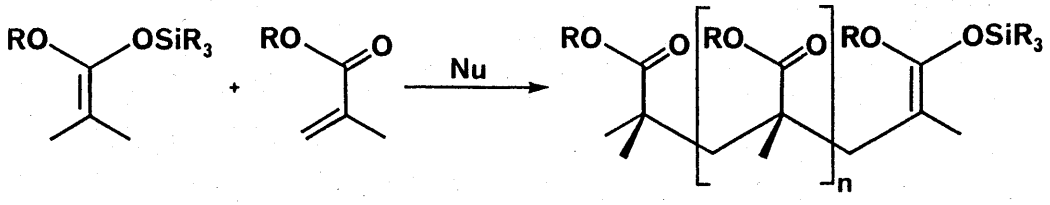

Scheme 1.1.1 Group transfer polymerization

1.1.1 Background of the project

Nucleophiles such as amines are generally believed to promote silylation reactions hence they are frequently used in combination with silylating agents.[1,2,6] Three different silylation mechanisms are currently postulated to account for the precise mode of action of nucleophiles.

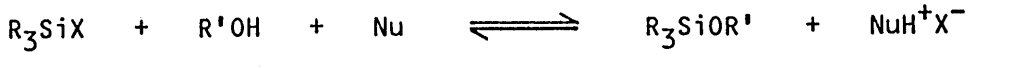

Scheme 1.1.2 Nucleophile activated silylation of alcohol

It was initially thought that the nucleophile was acting only as a base, scavenging protons and driving the equilibrium towards products. In this mechanism the nucleophile is not involved in the activated complex. However this has been disputed by Chaudhary and Hernandez,[7] who provided evidence that enhancement by nucleophiles is not related to their basicities, although a base may be required to regenerate the catalyst in specific cases.

Corriu[8] proposed that expansion of coordination at silicon is involved in the initial step, leading to penta- and hexacoordinate molecular intermediates as illustrated in Scheme 1.1.3. In the third mechanism, Chojnowski[9] suggested that a four coordinate ionic silane-nucleophile complex is formed in a rapid pre-equilibrium step. The silylated species then becomes the active intermediate in the subsequent rate determining bimolecular displacement. However this concept of ionic adduct formation was questioned by Corriu.

$$R_3SiX + Nu \rightleftharpoons \underset{\text{5 coordinate}}{R_3SiXNu} \rightleftharpoons \underset{\text{6 coordinate}}{R_3SiXNuHOR'} \longrightarrow R_3SiOR' + HX + Nu$$

Scheme 1.1.3 Proposal by Corriu

$$R_3SiX + Nu \rightleftharpoons \underset{\text{4 coordinate}}{[R_3SiNu]^+X^-} \longrightarrow R_3SiOR' + HX + Nu$$

Scheme 1.1.4 Proposal by Chojnowski

With the latter two mechanisms being kinetically identical, it is vital to have a better understanding of the exact nature of the intermediate species formed during silylation reactions. It is this aspect, together with the kinetic and the thermodynamic behaviour, of nucleophile induced silylations which is investigated in this study. A knowledge of the stereochemistry at silicon and the kinetic behaviour are particularly valuable in the elucidation of the mechanism of silylation reactions.

1.1.2 Outline of the project

This work has bearing on the mechanism of substitutions at silicon which is the fundamental reaction in the synthesis of siloxane polymers. Functionalized silanes having diastereotopic methyl groups attached to the silicon atom, $RCHMeSiMe_2X$ (R=Et, ^tBu, Ph; X=Cl, Br, OSO_2CF_3), were synthesised. The majority of the work concentrates upon the nature of the interactions of these compounds with a diverse range of nucleophiles. Structural changes in both silanes and nucleophiles, as well as their kinetic and thermodynamic behaviour are assessed in detail. In several cases, solid-nucleophile adducts were isolated and characterized. The structural and electronic factors governing the interactions between silanes and nucleophiles are briefly surveyed by studying silanes with various aryl or alkyl groups.

Multinuclear n.m.r. spectroscopy has proved to be an extremely powerful, easy and convenient tool for obtaining structural and dynamic information, thus it is predominantly employed in this work. For instance silicon-29 n.m.r. spectra provide useful information on the coordination number at silicon. The dynamic n.m.r. technique (DNMR) is particularly valuable in studying chemical exchange processes and obtaining kinetic data as well as thermodynamic parameters, by examining the exchange-broadened spectra using total bandshape analysis. This method has numerous advantages over other classical kinetic approaches. A more detailed analysis on this technique is given in a later section.

1.2 Physical properties of organosilicon compounds

A comparison of the chemistry of silicon and carbon is useful to fully comprehend and hence predict the behaviour of organosilicon compounds. The successful and extensive use of organosilicon reagents in organic synthesis can be interpreted in terms of the fundamental physical properties of silicon. These include the electronegativity of silicon, the bond strengths of silicon to other elements, hyperconjugation and the

participation or lack of involvement of its valence p- and empty d-orbitals.

The major difference between the chemistries of carbon and silicon is often interpreted with reference to the possible expansion of coordination at silicon. Hypercoordinate carbon compounds are not common in organic chemistry but they play an important part in organometallic chemistry; a pentacoordinate carbon species with trigonal bipyramidal geometry has been isolated.[10,11] In contrast, a large number of penta- and hexacoordinate silicon complexes have been identified, many of which have been characterized by X-ray crystallography.[12] The relative ease of silicon in extending its coordination shell to accommodate more than four ligands can be related to its size, the bond lengths, hyperconjugation and the utilization of low lying vacant d-orbitals for bonding.

The addition of an extra valence shell of electrons, descending down each group of the periodic table, is reflected in the increase in the covalent radii of the elements. Silicon is considerably larger than carbon (77 pm for C and 117 pm for Si);[13] nucleophilic attack is therefore facilitated. In nucleophilic substitution at carbon the bond to the leaving group must be broken, at least partially, prior to nucleophilic attack. In the case of silicon, the bond can be broken more readily owing to its increased length compared with the carbon analogues (189 pm for Si—C and 154 pm for C—C bond).[6] Furthermore, the pentacoordinate transition state is less sterically hindered and more stable therefore its formation is facilitated. The combination of these factors helps to minimise steric strain and stabilize extra covalency at silicon, thus the reactivity is promoted by lowering activation energies.

Several scales of electronegativity have been established, however the values remain relatively consistent whichever scale is chosen. Silicon is significantly less electronegative than carbon (H, 2.79; C, 2.35; Si, 1.64),[6] thus polarization of the $Si^{\delta+}—C^{\delta-}$ bond results. This also helps to explain the greater susceptibility of silicon towards

nucleophilic attack, although it is also important to take into account of electronic factors, for example the presence of electron donating (+I) substituents on silicon, which may offset this trend.

Compared with their carbon analogues, silicon forms markedly stronger single bonds with electronegative elements (oxygen, fluorine and chlorine) but weaker ones with carbon, nitrogen and hydrogen. The relative inertness of the Si—F bond to hydrolysis reflects upon the fact that it is one of the strongest single bonds known. It is rather surprising that the Si—X bonds can be cleaved more readily than the corresponding bonds to carbon, considering their significant strengths. This may be attributed to the greater polarizability of the bonds relative to their carbon counterparts. Partial double bond character, as a consequence of $p\pi$-$d\pi$ bonding is believed to be responsible for the considerable strength of the Si—O bond; the dative oxygen 2p lone pairs overlap with the empty 3d orbitals of the adjacent silicon. A more quantitative illustration is shown in the following table.

Table 1.2.1
Approximate bond dissociation energies of Si—X and C—X bonds[14]

Bond	Bond dissociation energy ($kJmol^{-1}$)	Bond	Bond dissociation energy ($kJmol^{-1}$)
Si-C	318	C-C	334
Si-N	320	C-N	335
Si-H	339, 378, 382	C-H	340
Si-Cl	471	C-Cl	335
Si-O	531	C-O	340
Si-F	807	C-F	452

There are three main areas of organosilicon chemistry where d-orbital participation is considered to be important. They are useful in the formation of additional δ bonds, the stabilization of reaction intermediates and transition states, as well as in the formation of

internal π bonds by accepting electrons from atoms such as nitrogen, halogens, oxygen or carbon in moieties capable of conjugation.

The utilization of d-orbitals to form δ bonds is well established as demonstrated by the octahedral hexafluorosilicate ion, SiF_6^{2-}, where silicon forms six $3sp^3d^2$ hybrid bonds with the fluorine atoms. The fast S_N2 reactions at silicon of chiral silicon compounds observed by Sommer[15] are consistent with the hypothesis that the involvement of d-orbitals lowers the transition state energies. The contribution of d-orbitals in the π-bonding of silicon is, nevertheless, highly controversial; a comprehensive account of the arguments has been covered by several authors[13,16,17,18] and will not be discussed in detail here.

The extent of d-orbital contribution by silicon has been investigated by Kanyha et al.[19] using multinuclear n.m.r. spectroscopy and evidence for $p\pi$-$d\pi$ bonding is provided. Ebsworth[13] proposed that d-orbital participation is not essential for the expansion of coordination. Pitt[20] preferred to employ the hyperconjugation or δ-δ^* conjugation hypothesis in explaining the electronic properties of organosilicon compounds. However Nagy et al.[17] stressed that both the hyperconjugation effect and d-orbital contribution have to be considered in interpreting any experimental outcome.

A recent detailed review on the theoretical aspects of bonding in carbon-functionalized silanes has been provided by Ponec.[18] He concluded that both concepts should only be treated as simplistic models, however no alternative hypothesis was proposed. A more sophisticated quantum mechanical treatment is necessary to fully understand the bonding in organosilicon compounds, nevertheless the d-orbital participation and hyperconjugation approaches serve as useful and qualitative guides.

1.3 Stereochemistry and coordination at silicon

Hypercoordinate silicon complexes are formed as a result of the interactions between neutral tetracoordinate silanes and nucleophiles, which normally contain one or more electronegative atoms such as fluorine, chlorine, oxygen or nitrogen. Aliphatic or heterocyclic amines and nitriles are typical nitrogen donor ligands; however no open chain complexes containing oxygen donor species have been observed to date.

It is important to assign the geometry of a silane-nucleophile adduct correctly, otherwise confusion in the coordination number at silicon may result. A compound of known molecular composition may adopt a number of geometrical structures.[21] For example a R_3SiNuX species may exist in two different geometries, four coordinate tetrahedral ionic or pentavalent trigonal bipyramidal covalent with sp^3d hybridization at silicon. Similarly, for an adduct with a formula of R_3SiXNu_2, there are two possibilities, it can be either a pentacoordinate trigonal bipyramidal ionic species or alternatively a six coordinate covalent octahedral compound having sp^3d^2 hybridization at the silicon atom.

Multinuclear n.m.r. spectroscopy, conductivity measurements and X-ray crystallography have proved to be extremely helpful for determining the coordination number at silicon. The structures of the pyridine-Me_3SiX (X=I, Br) solids were resolved by Hensen et al.[22] with the application of X-ray crystallography. Chojnowski[9] used phosphorus-31 n.m.r. and conductivity studies to characterize 1:1 HMPA-Me_3SiX (X=I, Br, Cl) adducts. The phosphorus-31 n.m.r. chemical shifts of the adducts were very similar, irrespective of the counterion, thus indicating that the complexes adopt a four coordinate tetrahedral geometry. The formation of ionic complexes was confirmed by the findings from conductivity measurements. However these observations have been strongly questioned by Corriu.[8]

Some examples of penta- and hexacoordinate silicon complexes, which have been isolated and identified, are presented in Figure 1.3.1. The

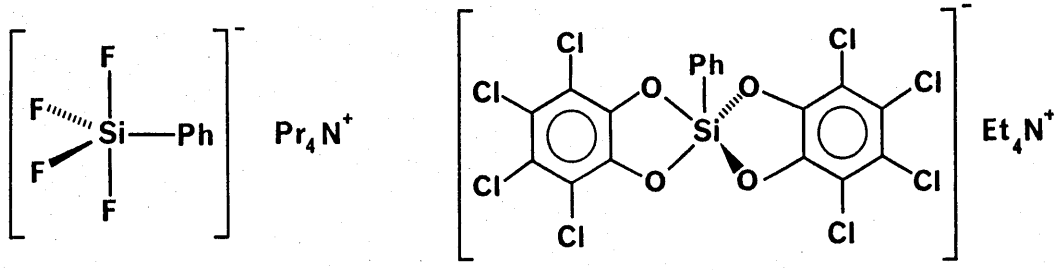

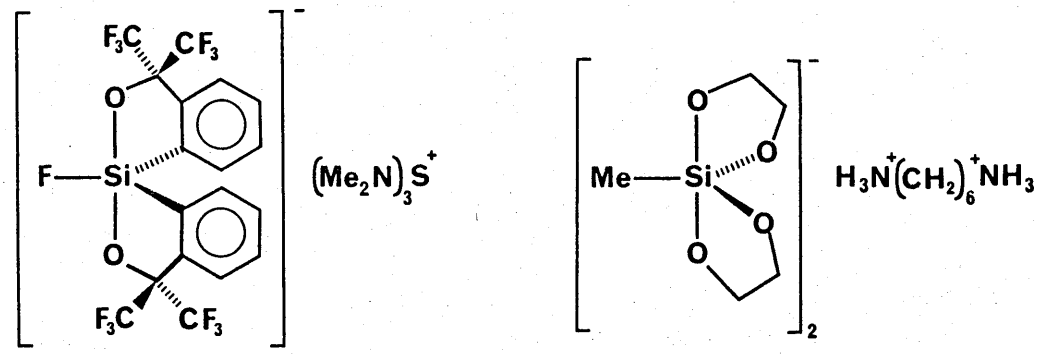

pentacoordinate complexes

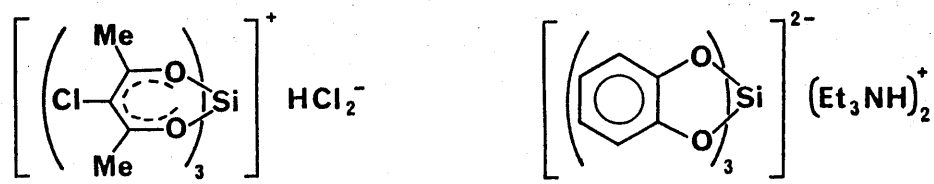

hexacoordinate complexes

Figure 1.3.1 Examples of penta- and hexacoordinate silicon complexes

stereochemistry of hexacoordinate silicon compounds is usually octahedral with several electronegative ligands. The majority of five coordinate silicon complexes have a trigonal bipyramidal structure, although a series of silicon compounds with geometries varying from trigonal bipyramidal to square pyramidal was reported by Holmes.[12] Pseudorotation has recently gained popularity as an alternative mechanism for nucleophilic substitution at silicon, although this proposal has been presented before.[15] Internal ligand exchange or pseudorotation is a distinct feature in the chemistry of trigonal bipyramidal molecules, thus the observation by Holmes is a particularly interesting one.

1.4 Silicon-29 n.m.r. spectroscopy

The changes in the chemical shifts of the carbon and the proton atoms attached to a silicon atom often provide considerable information about the changes in the environment and the stereochemistry at silicon. Moreover, silicon-29 n.m.r. spectroscopy has proved to be an even more powerful tool and has become a routine technique in the structural elucidation of organosilicon compounds.[23,24,25,26] The knowledge gained from the peripheral nuclei may not be related to the actual events taking place at the site of coordination i.e. the silicon atom. Its use as an analytical technique has expanded rapidly over the last decade, in parallel with the development of improved multinuclear n.m.r. spectrometers of increasing sensitivity. Nonetheless difficulties are still encountered in making silicon-29 n.m.r. measurements.

Silicon-29 has a low natural abundance of 4.67% and a negative gyromagnetic ratio γ of -0.555, which means that under proton decoupling conditions the nuclear Overhauser effect enhancement (NOE) is negative, causing a reduction or cancellation of the silicon-29 signal intensity. Its characteristic long spin-lattice relaxation (T_1) prolongs the data accumulation times, which hinders the observation of silicon-29 n.m.r. signals. Fortunately, the recent introduction of special pulse sequences,[27] particularly the polarization transfer techniques,

together with the application of paramagnetic relaxation reagents have overcome these problems by enhancement of sensitivity.

1.4.1 Sensitivity enhancement techniques

Transition metal complexes such as chromium acetylacetonates, $Cr(acac)_3$, can serve as paramagnetic relaxation agents. The presence of a small concentration (ca. 1%) of these compounds can increase the sensitivity of silicon-29 n.m.r. by shortening its spin-lattice relaxation time and allowing faster pulsing. However the drawback of this approach is that these reagents may contaminate the samples under investigation, and react with the organosilicon compounds producing undesirable side reactions.

The fundamental mechanism of polarization transfer involves the application of a weak irradiation on a sensitive nucleus with a large gyromagnetic ratio and considerable Boltzmann population difference. The nuclear spin polarization induced is then transferred from the sensitive nucleus e.g. proton to the insensitive one such as silicon-29, thus the intensity of a silicon-29 signal is increased significantly. The degree of enhancement of the silicon signal normally depends upon the number of coupled protons.[24] Another advantage of this technique is that the short relaxation time of the proton nuclei enables fast pulsing, which may reduce the recording time by 30 to 300 fold.[27]

In the INEPT method (Insensitive Nuclei Enhancement by Polarization Transfer), the enhancement is governed by the pulse parameters, which can be evaluated from the $^{1}H—^{29}Si$ coupling constants. Improper use of these parameters may lead to signal distortion or cancellation, therefore it is essential to have a knowledge of coupling constants.

1.4.2 Factors affecting silicon-29 chemical shifts

In spite of the numerous suggestions for reference compounds, tetramethylsilane (TMS) is now accepted as the reference standard for silicon-29 as well as for carbon-13 and proton n.m.r. spectra. At present, the span of silicon-29 n.m.r. chemical shifts reported is greater than 500 ppm, although most organosilanes can be found within a 250 ppm range.[23,24]

Silicon-29 n.m.r. chemical shifts are generally influenced by both electronic and steric effects, introduced by the substituents.[26] These inter-related factors may reinforce or oppose each other. The silicon chemical shifts are dependent upon the electric field and magnetic anisotropy of the neighbouring groups and the polarization of the Si—X bonds, which is controlled by the electronegativities of the substituents. These inductive effects can lead to a decrease in the nuclear shielding at silicon. Nevertheless, back donation as a consequence of the involvement of d-orbitals in $p\pi$-$d\pi$ bonding increases nuclear shielding. The coordination number at silicon as well as the deviation from the tetrahedral bond angle are also major factors affecting the silicon chemical shifts.

As yet, no satisfactory theory has been developed to encompass both electronic and steric effects in predicting the silicon-29 chemical shifts. An empirical attempt in correlating the substituent electronegativities with the silicon chemical shifts yields a U-shaped curve for a given series of silanes.[23,24] For example, with Me_nSiX_{4-n}, where X is an electronegative substituent; as the methyl groups are replaced by chlorine atoms an initial increase followed by a gradual decrease in chemical shift is observed. Prediction is made easier when the structural changes occur at a site remote from the silicon, since the silicon shielding becomes dependent mainly upon the electronic effects of the substituent.

The solvent dependence of silicon-29 n.m.r. chemical shifts are usually not significant (smaller than 1 ppm), however pronounced chemical shift changes of greater than 5 ppm have been observed for specific classes of organosilanes. An excellent linear correlation[28] is obtained when the silicon chemical shifts of a series of silanols and silylamines are plotted against the Gutmann solvent donor number,[29,30] which measures the electron pair donor ability of the solvent. Such changes in chemical shifts are normally accounted for by solvent-solute interactions. Strong hydrogen bonding of the type $R_3Si—O—H\leftarrow\!\!-\!\!-\!\!-$:donor together with repulsion of the O—H bonding electrons with the donor solvent electron pair contribute to an increase in the electron density at silicon. This indicates that solvent donicity plays an important role in the chemical shifts of silanols, with basic solvents inducing pronounced shifts to lower frequency.

1.4.3 Structural elucidation

As emphasized earlier, silicon-29 n.m.r. offers a unique approach for determining the coordination number at silicon, since the chemical shifts of extracoordinate silicon complexes deviate significantly from those observed for comparable tetravalent silicon compounds. For example in the formation of silatranes, a shift of about 20 ppm to lower frequency on going from four to five coordination is reported.[31] Although the chemical shift ranges for each coordination number at silicon overlap considerably, the assessment of the stereochemistry at silicon from a given silicon chemical shift is relatively straightforward provided that analogous silicon compounds with the same R groups are compared. The currently recognized chemical shifts for penta- and hexacoordinate silicon complexes range from -176 ppm to -53 ppm and -200 ppm to -120 ppm respectively.[23,24]

X-ray crystallography and the recently developed high resolution solid state n.m.r. have become invaluable for studying hypercoordinate silicon species, which dissociate readily into their individual components in solutions. These two techniques are also useful for investigating

whether the structures remain consistent in both solid and solution phases, by comparing with the data obtained from solution state n.m.r. studies. Good agreement between structures resulting from solution state n.m.r. and that from solid state n.m.r. together with x-ray studies has been reported.[24]

1.5 Dynamic nuclear magnetic resonance spectroscopy

1.5.1 General background

Dynamic n.m.r. (DNMR) is an application of n.m.r. spectroscopy employed to examine the changes in n.m.r. spectra arising from a chemical exchange process.[32,33] N.m.r. spectra provide considerable information concerning the changes in the environment of magnetic nuclei, induced by exchanges between sites with different chemical shifts and/or different coupling constants.

The line shape of a n.m.r. signal is related to the life time of the species under study, which can be expressed as the reciprocal of a rate constant as well as a function of Larmor frequency and spin-spin transverse relaxation time (T_2). A dynamic process usually causes a change in the Larmor frequencies and the magnetization of the species, therefore the line shape of n.m.r. signals is dependent upon chemical exchange processes. Hence evaluation of rate constants of such processes is feasible by examining the variation in the line shape of n.m.r. signals.[32,33]

The growing popularity of this technique may be due, in part, to the advent of sophisticated n.m.r. spectrometers since line shapes depend very crucially on field homogeneity, together with fast digital computers for storing and calculating spectral data using a quantum mechanical density matrix technique. Furthermore, it possesses several advantages compared with other classical kinetic methods.[33]

DNMR can be applied to fast, first or pseudo-first order and reversible processes. Activation parameters as well as a diverse range of rate constants (10^{-1} to 10^{-6} s^{-1}) with energy barriers of 20 to 100 $kJmol^{-1}$ can be evaluated. It provides direct information about the nuclei affected by exchange, which is often very difficult to achieve by other methods. Systems at thermodynamic equilibrium and/or degenerate systems, in which exchanges lead to molecules indistinguishable from the original ones, can be investigated using this technique. Dynamic processes can also be studied over a wide range of temperatures since n.m.r. spectra of many compounds are temperature dependent. Furthermore, this method is invaluable in that it helps in the elucidation of exchange pathways, mechanisms and conformational transformations using standard n.m.r. equipment.

Some typical examples of dynamic reactions studied by DNMR are inversions of lone electron pairs on nitrogen and phosphorus, inversions of cyclic and heterocyclic rings, degenerate valence isomerizations, intramolecular rearrangements and hindered rotations around sterically crowded systems with partial double bond character, for instance the hindered rotation of the C(O)—N bond in N,N-dimethylformamide. The theoretical background and the statistical treatment of this technique are extremely complicated. This topic has been reviewed elsewhere[33] and thus will not be discussed here.

1.5.2 Line broadening of n.m.r. signals

The bandshape of a n.m.r. signal is determined by parameters such as the chemical shifts of each exchanging magnetic environment or site (v), the coupling constants (J), the populations of each site (p), and the natural linewidth (w) which is related to the spin-spin transverse relaxation times (T_2).

Consider a two-spin system where nucleus A is undergoing chemical exchange with nucleus B, induced either by the addition of a catalyst or

an increase in temperature, the chemical shifts are ν_A and ν_B with linewidths w_A and w_B respectively. At slow rates of exchange, slight line broadening of each species is observed, the broadening becomes more pronounced as the rates increase until the two signals merge and coalesce. Further increases in the exchange rate cause gradual sharpening of the signal until eventually an averaged signal with natural linewidth is observed. The chemical shift of this signal is governed by two factors; the relative populations and the positions of the two exchanging species (A and B), as demonstrated by the following equations.

$$\nu_{observed} = \nu_A p_A + \nu_B p_B \qquad \text{Equation 1.5.1}$$

$$p_A + p_B = 1 \qquad \text{Equation 1.5.2}$$

An illustration of the changes in the line shape of the two n.m.r. signals as a result of the exchange between two equally populated, uncoupled sites is given in Figure 1.5.1. The signals of species with equal populations broaden rapidly in a symmetrical manner, accompanied by a change in the chemical shifts.

Comparatively little use has been made of silicon-29 n.m.r. in dynamic n.m.r. line shape analysis, this may be largely owing to the signal-to-noise problem. In many cases, a further obstruction arises from the greater separation of the peaks, which can result in the disappearance of the signal into the baseline at coalescence.

1.5.3 Evaluation of rate constants

One of the main objectives of studying the exchange-broadened n.m.r. spectra is the evaluation of rate constants. There are various methods of analysing the n.m.r. spectra of exchanging systems;[33] the complete line shape technique is the most accurate and reliable, however it is time-consuming and laborious. For very simple, uncoupled spin systems, approximate rate constants can be calculated using simplified methods.

Figure 1.5.1 Line broadening of n.m.r. signals

Calculated bandshapes for an uncoupled, two site exchange system with equal populations ($P_A = P_B$, $T_2 = 0.2$, $\delta\nu = 600Hz$), scaled to the height of the reference peak C.

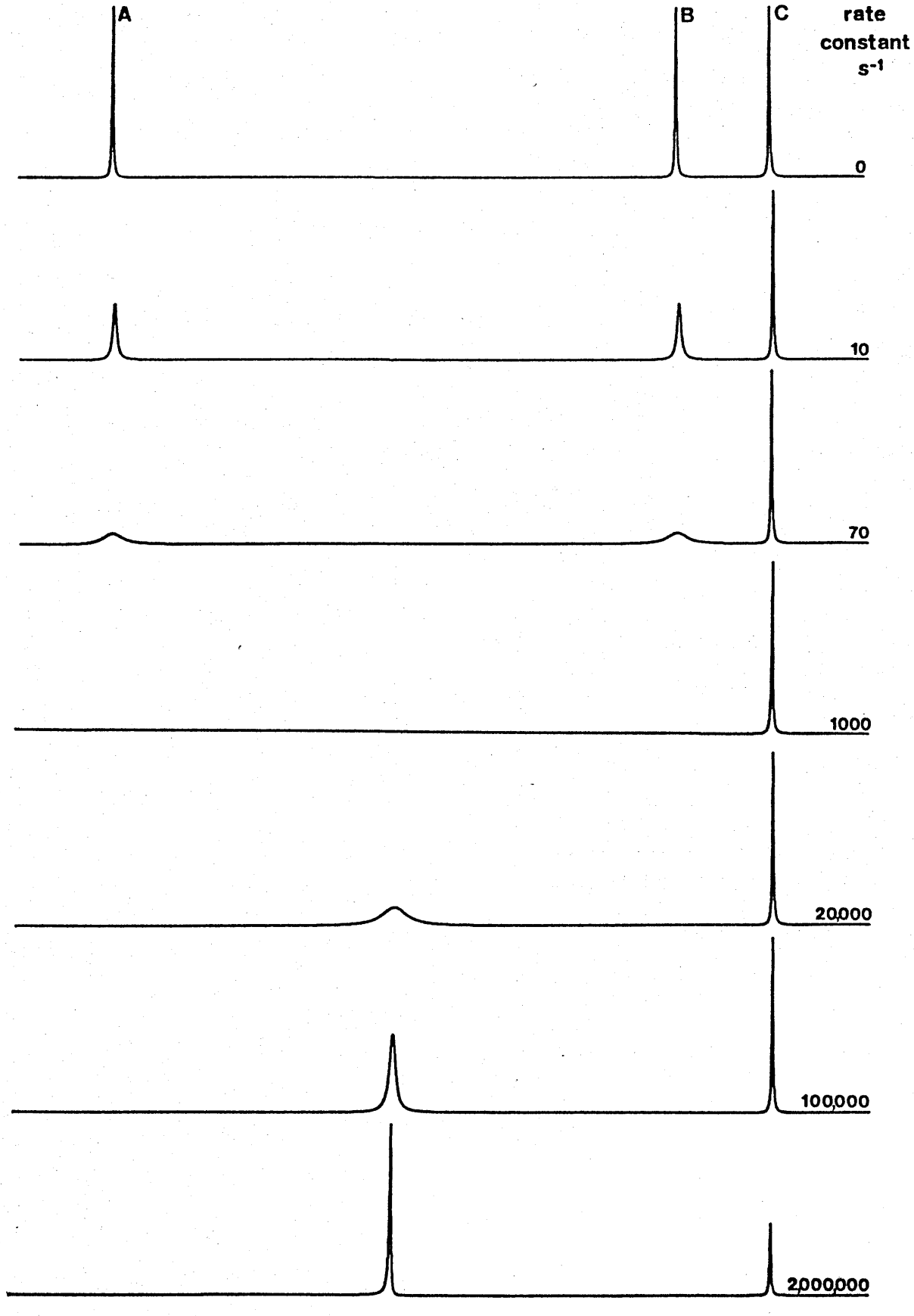

These rely upon the relations between rate constant and the readily measured parameters such as peak separations, bandwidths at half maximum intensity, ratio of maximum to minimum intensity.

The equation derived from the separation of exchanging sites (where $\delta\nu$ is measured in Hertz) at coalescence is one of the most commonly used expression for obtaining an approximate rate constant.

$$k = \frac{\pi\delta\nu}{\sqrt{2}} \qquad \text{Equation 1.5.3}$$

However this expression is only valid if the peak separation ($\delta\nu$) and the rate constant (k) are much greater than the linewidth in the absence of exchange. If this condition is fulfilled, the calculated rate constant is reasonably accurate. The main limitation of this approach is that it provides the rate constant at one temperature only.

Precautions must be exercised for a non-exchanging system to obtain symmetrical, narrow lines with Lorentzian linewidths, otherwise significant errors will be introduced into the total line shape analysis. The concept behind this technique is to compare the entire experimental spectrum, recorded at a specific temperature, with a series of theoretical spectra calculated for different rate constants. The computer evaluated spectra can be plotted on the same scale as the experimental spectrum. The best possible fit and hence the correct rate constant can be found by trial and error matching, either visually or by a computer, of the spectra. If computer matching is adopted it is advisable to make a visual comparison of the final calculated spectra with the experimental ones to eliminate obvious errors. A comparison of the experimental and theoretical data will be provided in the following chapter. More sophisticated computing programs are now available to suit individual needs. This line shape analytical approach is superior to the one-parameter approximation methods since all the information contained in the bandshape is analysed, therefore it is less susceptible to systematic errors and errors in the measurements.

1.5.4 Evaluation of activation parameters

According to Arrhenius, molecules must possess an excess quantum of energy known as the activation energy (E_a) prior to reaction, thus the Arrhenius activation theory is based on the equilibrium established between the activated and unactivated molecules. The treatment of this equilibrium with the van't Hoff isochore gives the Arrhenius equation.

$$k = A\, e^{-E_a/RT} \qquad \text{Equation 1.5.4}$$

Activation parameters can be indirectly measured by examining the variation in the line shapes of n.m.r. signals at different temperatures to determine the rate constants for the series of temperatures studied.[32,33] However this approach relies upon two important assumptions, namely, the temperature independence of the peak separation and the linewidth at half-height of the n.m.r. signals in the absence of exchange.

An Arrhenius plot of the natural logarithm of the observed rate constant against the reciprocal of temperature yields the Arrhenius activation energy (E_a) and the pre-exponential or frequency factor (A) for the reaction investigated, both E_a and A are also assumed to be independent of temperature. From transition state theory the activation parameters, the enthalpy ($\Delta H^{\ddagger}$) and the entropy ($\Delta S^{\ddagger}$) of activation, together with the free energy of activation ($\Delta G^{\ddagger}$), can be evaluated using the following equations. It is important to note that all three entities are temperature dependent.

$$\Delta H^{\ddagger} = E_a - RT \qquad \text{Equation 1.5.5}$$

$$\Delta S^{\ddagger} = R \ln\left(\frac{hA}{Kk_BT}\right) - R \qquad \text{Equation 1.5.6}$$

$$\Delta G^{\ddagger} = \Delta H^{\ddagger} - T\Delta S^{\ddagger} \qquad \text{Equation 1.5.7}$$

k_B is the Boltzmann constant with the value 1.3805×10^{-23} JK^{-1}, h is Planck's constant 6.626×10^{-34} Js, T is the absolute temperature in Kelvin and K is the transmission coefficient which is the fraction of activated molecules reaching the transition state and proceeding to form product molecules, it is usually set as 1.

The importance of this temperature dependence factor can be reduced by applying the Eyring equation which is based on statistical thermodynamics. The plot of ln(k/T) against 1/T gives a straight line with a slope of $-\Delta H^{\ddagger}/R$ and an intercept of $\ln(Kk_B/h) + \Delta S^{\ddagger}/R$.

$$k = K \left(\frac{k_B T}{h}\right) \exp\left(\frac{-\Delta H^{\ddagger}}{RT}\right) \exp\left(\frac{\Delta S^{\ddagger}}{R}\right) \qquad \textbf{Equation 1.5.8}$$

1.5.5 Analysis of errors

As mentioned earlier, additional line broadening due to magnetic field inhomogeneity and partial saturation of the resonance signal may introduce a large systematic error. Fortunately these errors can be eliminated by using an internal standard which is not affected by the exchange process under investigation.

It is crucial to have a reasonable chemical shift difference in order to achieve an accurate determination of the rate constants; this is particularly essential when the experiment is performed over a narrow temperature range. The assumption that the peak separation and the linewidth at half-height of the n.m.r. signals, in the absence of exchange, are temperature independent may not be always valid. It may be necessary to measure their temperature dependence during slow exchange and extrapolate to temperatures where fast exchange take place. The precision of the $\Delta H^{\ddagger}$ and $\Delta S^{\ddagger}$ values depends upon a large chemical shift separation and a wide temperature range.

The accuracy of the rate constants may be greatly improved if the simulation is based near the coalescence region rather than near the fast

and slow exchange limits. The poor signal-to-noise ratio around the coalescence point may also create considerable problems in the comparison of the experimental and theoretical data.

1.6 Stereochemistry of nucleophilic substitution at silicon

As in many reactions, nucleophilic displacements at silicon are affected by the nature of the substrate, the leaving group, the nucleophile and the solvent. Unlike carbon, substitution reactions at silicon generally proceed with high stereoselectivity, either retention or inversion of configuration at silicon and only rarely racemization.

1.6.1 Frontier-orbital hypothesis

Anh and Minot[34] provided a theoretical Frontier-orbital treatment to rationalize the geometry of attack by nucleophile at silicon. This Frontier-orbital approximation is based upon the Salem orbital treatment of the Walden inversion. It is assumed that the major interaction during a reaction is that between the HOMO (Highest Occupied Molecular Orbital) of the nucleophile and the LUMO (Lowest Unoccupied Molecular Orbital) of the silane δ^*_{Si-X}.

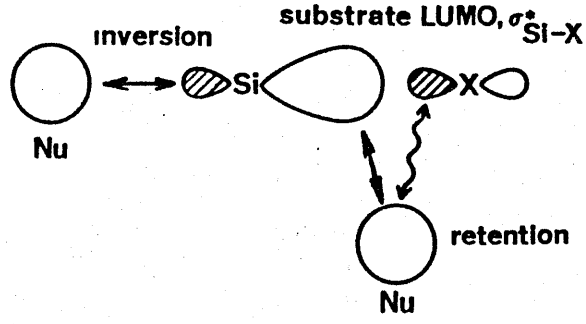

Figure 1.6.1 Geometry of attack by nucleophile

As described in Figure 1.6.1, the front side attack of nucleophile on the hybrid orbital of silicon leads to retention of configuration. When the

unfavourable out-of-phase overlap between the nucleophile and the orbital of the leaving group predominates, inversion of configuration takes place with the nucleophilic attack at the rear side of the molecule, opposite to the leaving group.

The site of attack depends upon the extent of in-phase or out-of-phase overlap between the HOMO and the LUMO orbitals.[35] The electronegativity of the leaving group and the nature of the nucleophile have dramatic effects on the size of the LUMO and the HOMO orbitals respectively. The s character at the silicon atom increases as the leaving group becomes more electronegative, a bigger lobe between silicon and the leaving group results and retention of configuration is therefore favoured. Rear side attack is enhanced with a soft nucleophile having diffuse valence orbitals since the unfavourable out-of-phase overlap with the leaving group dominates and cannot be ignored, thus inversion of configuration is observed. The energy level of the HOMO orbital of the nucleophile is also an important factor in determining the geometry of attack.

1.6.2 The structure of silanes

The reactivity of a silane is a delicate balance between steric and electronic effects of the substituent, the latter includes the inductive and conjugative effects together with anchimeric assistance. Retardation of the solvolytic rate of trialkylchlorosilane is observed when an electron releasing group, for example an isopropyl group, or a sterically bulky ligand such as the phenyl ring or naphthyl group is introduced to the silicon skeleton.[36,37]

The successful application of steric parameters, derived from the reactivities of carbonyl compounds, to the reactions at silicon allowed Cartledge[38] to establish a set of parameters to describe the steric effects at silicon specifically. Sommer[15] stressed that cyclic silanes behave very differently mechanistically and stereochemically from acyclic

ones. Nucleophilic substitution of cyclic silanes normally occurs with retention of configuration, if the leaving group is not a part of the ring. However a shift towards inversion is observed when both the silicon atom and the leaving group are in a strained ring.

1.6.3 The leaving group

The dependence of the reactivity of silanes, $R^1R^2R^3SiX$, towards nucleophiles upon the nature of the leaving group is reflected by the observations made by Corriu.[35] The tendency of halosilanes to undergo racemization and the preference for inversion over retention of stereochemistry upon nucleophilic attack at silicon both follow the same trend as that of the relative ability of the leaving group to be displaced. However the attempted correlation of the stereochemistry of nucleophilic displacement at silicon with the pK_a of the conjugate acid of the leaving group or its electron polarizability has not been satisfactory.

Corriu further proposed that the ability of silicon compounds to pentacoordinate is not related to the electronegativities of the substituents but depends upon the tendency of the Si—X bonds to be stretched under the influence of an incoming nucleophile. His extensive n.m.r. studies on the $o\text{-}(Me_2NCH_2)C_6H_4SiRX_2$ and $o\text{-}(Me_2NCH_2)C_6H_4SiXR^1R^2$ systems indicate the formation of an intramolecular Si—N bond, leading to the expansion of coordination at silicon. The relative ease of pentacoordination at silicon can be summarized by the following sequence.

$$X = Br, Cl, OAc > SR, F > OR, H$$

The variable temperature fluorine-19 n.m.r. studies on a very similar silane $o\text{-}(Me_2NCH_2)SiMeFX$[35] led Corriu to define a scale of relative apicophilicity of the various substituents on silicon. Apicophilicity is a measure of the ability of the ligands on silicon to adopt an apical position within the trigonal bipyramidal framework relative to the

nucleophile. The apical and equatorial fluorine atoms can be distinguished owing to their different ^{19}F n.m.r. resonances. As the temperature is lowered the n.m.r. signal either shifts to lower field indicating that it is apical, or to higher field showing that it is equatorial. The fluorine atom occupies the apical position when X=H, OR or NR_2 or equatorial when X=Cl. Moreover when X=p-$YC_6H_4CO_2$ (Y=H, OMe, NO_2), a mixture of the two configurations results, the ratio of F_{axial} to $F_{equatorial}$ depends upon the nature of the para substituent Y.

Analogous to the ease of pentacoordination, apicophilicity is not affected by electronegativity. Furthermore the ease of expansion of coordination at silicon, the increasing apicophilicity, the increasing rate of racemization as well as the increasing proportion of inversion of configuration all follow the same order.

1.6.4 The attacking nucleophile

The stereochemistry at silicon is usually affected by the nature of the nucleophile. Nucleophilic substitution at silicon normally proceeds with inversion of configuration for silanes with good leaving groups such as bromide and chloride, except with very hard nucleophiles. Apart from the case with Ph_2CHLi, retention of configuration is predominantly observed when poor leaving groups such as H are involved. However with moderately good leaving groups, such as SR, F or OMe, the stereochemical outcome is largely governed by the nature of the incoming nucleophile.

According to Corriu[35], for a given leaving group, hard nucleophiles lead to retention whereas soft nucleophiles give inversion of configuration at silicon. Hard nucleophiles, for instance Ar^-, $PhC{\equiv}C^-$ and RLi, have localized negative charge and prefer equatorial attack on silicon giving retention; however, the reverse is observed for good leaving groups for example bromide and chloride. Soft nucleophiles, such as benzyl or allyl anions as well as Grignard reagents with more covalent

C—Mg bonds, possess delocalized negative charge and tend to attack from an apical position yielding inversion, unless the leaving group is exceptionally poor. By altering the properties of the solvent, the nature of the nucleophile can be reversed, from a hard to a soft one, thus a corresponding change in the product stereochemistry results.

The general relationships between the various contributing factors affecting the stereochemical outcome of nucleophilic substitution at silicon can be outlined as follows.

	H < OMe << F, SR << Cl < Br, OCOR, OTs
Stereochemistry:	retention → inversion
Nature of nucleophile:	hard → soft
Racemization ability:	→
Pentacoordination ability:	→
Ease of displacement:	→

1.6.5 The solvent effects

Prediction of the stereochemical outcome of nucleophilic substitution at silicon is further complicated by the dual characteristic of a solvent, namely, its donicity and its dielectric constant. The donicity of a solvent measures its Lewis base strength or its ability to behave as a nucleophile. The dielectric constant describes the dipole-dipole interactions within the solvent molecule and reflects the ability to solvate charged species. However it should be noted that the polarity or the dipole moment is also responsible for the solvating potential of a solvent. The balance between the nucleophilicity and the dielectric constant of a medium is important in determining the outcome of a reaction.

Consider the simple process of the ionization of a covalent compound to give a pair of dissociated ions, as illustrated by the following scheme.

$$S: \quad + \quad A{:}B \quad \rightleftharpoons \quad (SA)^{+}\,(:B)^{-} \quad \rightleftharpoons \quad (SA)^{+} \quad + \quad (:B)^{-}$$

solvent — ion pair — separate solvated ions

Scheme 1.6.1 Formation of unassociated solvated ions

The initial formation of the ion pair, as a result of ionization, depends largely upon the nucleophilic property of the medium, contrary to the classical belief that the ionizing power of a solvent depends on its dielectric constant. The dielectric constant of a solvent is the major factor in determining the degree of dissociation of the ions in the subsequent step. Thus the concentration of the fully dissociated ions is governed by both properties.

It is therefore crucial to distinguish the role of a solvent in nucleophilic displacements at silicon. For example, the stereochemical outcome of the reaction between chlorosilanes and methanol is completely altered from one producing inversion to one yielding retention, merely by changing from a non-polar solvent to a polar one such as HMPA, DMF or DMSO. Using solvents with very low dielectric constant but moderate donicity to study the racemization of chlorosilanes, Corriu[35] discovered that, in these systems, the nucleophilicity of the solvent becomes much more important than its ability to stabilize and solvate a charged intermediate.

Several solvent parameters have been defined as measures of the solvent properties. Gutmann[29,30] believed that the strength of a coordinate donor-acceptor bond depends partly on the donor and acceptor properties of the donor and acceptor respectively, and hence proposed two parameters a donor number (DN) and an acceptor number (AN). The donor number (DN) is based on the measured reaction enthalpy in the 1:1 adduct formation between the solvent (donor) and antimony pentachloride ($SbCl_5$, reference acceptor) in 1,2-dichloroethane. It is therefore a reflection of the solvent—$SbCl_5$ bond strength, when the entropy components are assumed to be constant.

The reference for the acceptor number (AN) is taken as the phosphorus-31 chemical shift of the 1:1 adduct formed between antimony pentachloride and triethylphosphine oxide ($Et_3P{=}O$) in 1,2-dichloroethane, and is given an arbitrary value of 100. The acceptor number is defined by the phosphorus-31 chemical shifts of $Et_3P{=}O$ in the acidic solvents under investigation.

Drago[39] suggested that the reaction enthalpy of the acid-base interaction is governed by two empirical and independent factors, namely, the covalent and electrostatic contributions to bonding. They correlated and predicted the reaction enthalpies of adduct formation in gas phase and in poorly coordinating solvent using the following equation. E measures the abilities of the acid (acceptor) and base (donor) to participate in ionic bonding, whereas C describes their abilities in covalent bonding.

$$-\Delta H = E_{acid}\, E_{base} + C_{acid}\, C_{base} \qquad \text{Equation 1.6.1}$$

Using a linear solvation energy relationship, Taft et al.[40,41,42] proposed a much more complex equation encompassing all the possible factors contributing to solvent effects. The classical Lewis definition of acidity and basicity is based on the abilities to accept and donate an electron pair respectively. An alternative definition has been recently introduced by Taft and his coworkers, they relate the acidity and the basicity properties to the hydrogen bonding ability. Thus the different solvatochromic variables incorporated in Taft's unified scale are hydrogen bond basicity and acidity, the coordinate covalency parameter to allow for various functional groups, the solvent dipolarity and the Hildebrand solubility parameters.

The hydrogen bond basicity (β) is defined as the ability of a solvent molecule to act as a hydrogen bond acceptor in a solvent-solute interaction. Conversely, the hydrogen bond donor acidity (α) measures the ability of the solvent to donate a proton during the solvent-solute hydrogen bond formation. The solvent dipolarity (π^*) relates the ability

of the solvent or solute to participate in dipolar interactions, which can be either between dipoles and/or dipoles with induced dipoles. The Hildebrand solubility parameter or cohesive energy density (δ_H) is a measure of the interrupted solvent-solvent interactions in creating a suitably sized cavity for the solute in the solvent.

1.7 Mechanisms for nucleophilic substitution at silicon

Several mechanistic pathways have been postulated for the highly stereospecific nucleophilic substitution reactions at silicon. The stereochemical outcome of the displacement reactions is predominantly governed by the geometry or site of attack of the incoming nucleophile. Analogous to the nucleophilic substitution processes at carbon, a back side (180^{o}) attack of the nucleophile opposite to the leaving group produces an inversion of configuration. Conversely, retention at silicon requires a front side nucleophilic attack at 90^{o} to the leaving group.

Extensive coverage on this subject has been provided by various authors[3,14,15,35,43] therefore only a brief summary is outlined here. The major discrepancies between these recently proposed mechanisms do not relate to the direction of nucleophilic attack, but lie mainly with the interpretation of the reaction pathways which concerns the structures of transition states and intermediates.

1.7.1 Background knowledge

The pioneering survey by Sommer[44] on the stereochemistry and mechanistic pathways of organosilicon compounds triggered many further studies on this aspect of organosilicon chemistry. The S_N1 process is exceedingly rare, if it happens at all,[3] for organosilicon compounds. This is because the much more rapid S_N2 reaction takes precedence and is not due to the incapability of silicon to stabilize a positive charge. This is supported by the recent observation by Lambert on the Ph_3Si^+

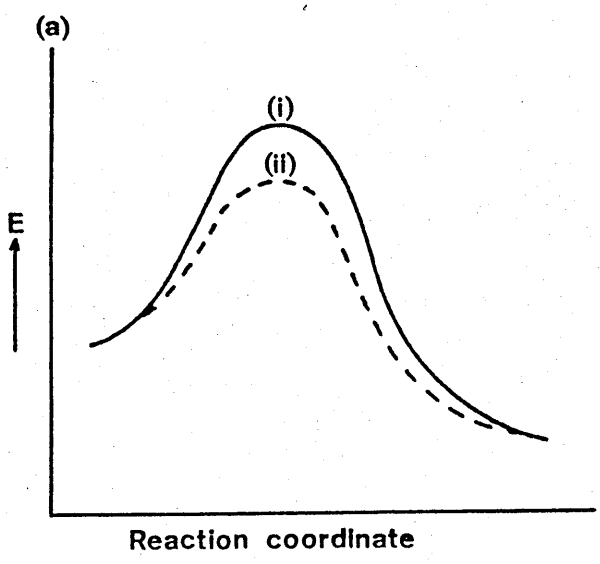

(a) i. S_N2-C transition state

ii. S_N2-Si transition state

Rate = k_2 [R_3SiX] [Nu]

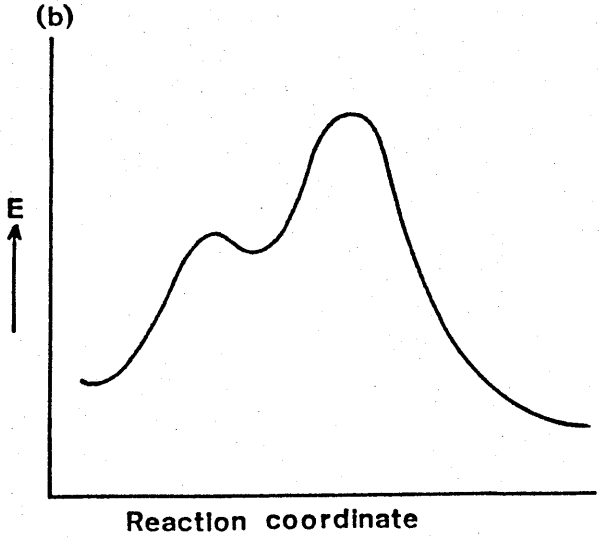

(b) S_N2^*-Si

Rapid pre-equilibrium formation of a five coordinate intermediate, followed by rate limiting conversion to product.

$$\text{Rate} = \frac{k_1}{k_{-1}} k_2 [R_3SiX] [Nu]$$

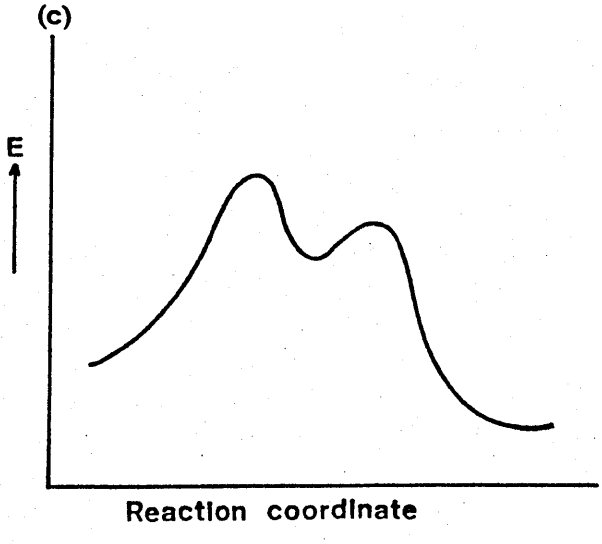

(c) S_N2^{**}-Si

Rate determining formation of intermediates, followed by rapid dissociation to products.

Rate = k_1 [R_3SiX] [Nu]

Figure 1.7.1 Reaction energy diagrams of the S_N2 processes at silicon

species.[45] Eaborn[46] has also observed S_N1 solvolysis but in some special, highly hindered systems.

The displacement reaction at silicon which proceeds with inversion of configuration undoubtedly undergoes an S_N2 mechanism, resembling that at carbon. However in the case of silicon, the process can either involve a pentacoordinate transition state or a pentacoordinate intermediate (S_N2^*-Si and S_N2^{**}-Si)[15] depending on the reaction pathway and the rate determining step.

The greater stability of the transition state for S_N2-Si reactions, as compared with carbon, can be attributed to the reduced steric strain of the pentacovalent species due to longer bonds as well as the possibility of 3d-orbital participation. The reaction energy diagrams and the corresponding rate laws are shown in Figure 1.7.1. The preference for S_N2^*-Si and S_N2^{**}-Si mechanisms increases as the alkyl groups in R_3SiX are progressively replaced by highly electronegative group X.

The S_Ni-Si mechanism involving a quasicyclic transition state is responsible for the retention of configuration at silicon,[15] by offering electrophilic assistance to the leaving group. The actual geometry of the transition state is speculated to be either a tetragonal pyramid or a trigonal bipyramid. Nevertheless this is in contrast to the work of Corriu,[35] who proposed that inversion of configuration can be promoted when the electrophilic part of the attacking species is a metal ion M^+. Solvation in polar media and other factors which stabilize the M^+ ion should decrease the proportion of retention at silicon.

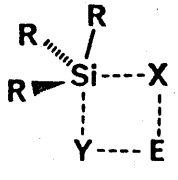

X - leaving group

E - electrophilic part of attacking species EY

Figure 1.7.2 S_Ni-Si mechanism

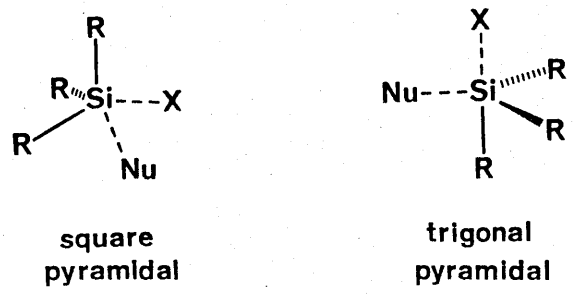

Figure 1.7.3 Geometry for transition states

The three currently postulated mechanisms are slightly different from the proposals of Sommer. Corriu[8] strongly supports the formation of penta- and hexacoordinate molecular intermediates whereas Chojnowski provides evidence for the involvement of ionic intermediates. Inspired by the stereochemistry and mechanisms of phosphorus chemistry, pseudorotation has recently been proposed as the alternative route for displacements at silicon.[47,48]

1.7.2 Pseudorotation

The Berry pseudorotation hypothesis has been widely accepted as a mechanistic pathway for intramolecular ligand exchange in a trigonal bipyramidal molecule, which is commonly observed in phosphorus compounds.

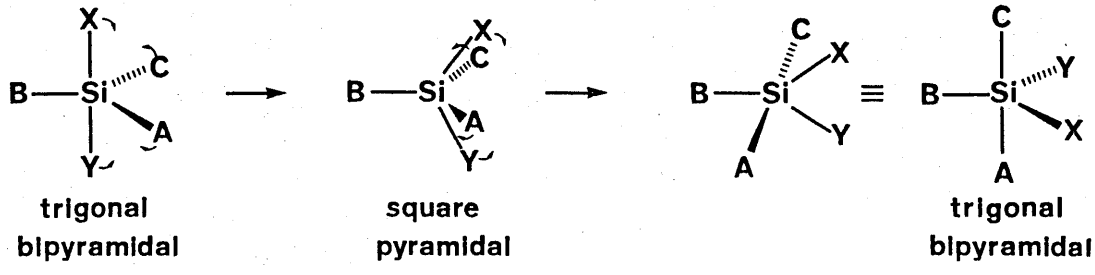

Scheme 1.7.1 Pseudorotation mechanism

The fundamental concept of this intramolecular rearrangement process is illustrated by Scheme 1.7.1. It involves the interconversions of the

axial ligands, X and Y, with two of the equatorial ligands, C and A, leaving the third equatorial group B, known as the pivot ligand, unaltered. During a pseudorotation, A and C which are originally equatorial become axial. Similarly, the ligands X and Y are converted from apical to equatorial positions.

The stereochemical outcome of the process can be predicted with the assistance of several empirical rules. The attack of the incoming nucleophile and the departure of the leaving group take place in the apical positions, which are normally preferred by electronegative substituents. Cyclic systems such as four and five membered rings are constrained to occupy one apical and one equatorial positions.

The recognition and the growing popularity of the application of the pseudorotation concept in organosilicon chemistry are reflected by the increasing number of publications on the stereomutation of penta-coordination silicon intermediate by intramolecular ligand exchange. From the fluorine-19 n.m.r. studies on the SiF_5^-, $RSiF_4^-$ and $R_2SiF_3^-$ (R=Me or Ph) systems, Muetterties[49] suggested that rapid isomerization processes via pseudorotations are taking place. A different rationalization of these spectral results is offered by Janzen[50] and Corriu,[35] who proposed that the ligand exchange is induced by the nucleophile assisted hydrolysis of these fluorosilanes.

Additional support comes from the variable temperature fluorine-19 n.m.r. studies by Farnham and Harlow[51] as well as Martin and Stevenson.[52,53] The spectra of pentacoordinate spirosiliconate anions are unaffected by concentration, solvent and the presence of nucleophiles such as HMPA; moreover rapid interconversion of the diastereotopic CF_3 groups is observed at 70°C. They therefore conclude that intramolecular Berry pseudorotation or a Si—O bond dissociation-reassociation process is responsible for such observations. The X-ray crystallographic characterization of pentacoordinate silicon complexes, with geometries ranging from trigonal bipyramidal to square pyramidal, by Holmes et

al.[12] provides further contribution to the evidence in support of this phenomenon.

Corriu originally suggested that the pseudorotation process at silicon may involve a higher activation energy, compared with the corresponding reaction at phosphorus. Furthermore the relative apicophilicity of the ligands in five coordinate silanes is different for the analogous pentacoordinate phosphorus compounds. However in more recent publications,[54,55] Corriu has been more prepared to adopt pseudorotation as a possible mechanism for nucleophilic substitution at silicon.

1.7.3 Mechanisms involving hypercoordinate silicon intermediates

On the basis of kinetic studies, Corriu[8,35] proposed a mechanism involving reversible nucleophilic back side attack on a silane to give a pentacoordinate molecular intermediate. The attack of a second molecule, such as water, alcohol or another nucleophile molecule, on this five coordinate silicon species is postulated to be the rate determining step. The product of this second rate limiting step of the racemization reaction may be either a pentacoordinate siliconium ion (C) or a hexacoordinate octahedral species (B).

The isolation and characterization of the ionic adducts between HMPA and Me_3SiX (X=I, Br) led Chojnowski[9] to propose a slightly different mechanism. The formation of an ionic adduct between a silane and a nucleophile occurs in a rapid pre-equilibrium initial step. This ionic adduct becomes the active intermediate in the subsequent rate determining step. Overall retention as a result of two consecutive inversions is observed in solvolysis induced by the attack of water or alcohol. However racemization can occur from the attack of a second nucleophile molecule on the ionic adduct. The low or negative enthalpy of activation for racemization and solvolysis can be accounted for by the exothermic formation of the ionic adduct in the pre-equilibrium step. Strong

support for this mechanism has been obtained by Bassindale and Stout[56] as well as Frye.[57]

Both mechanisms are shown in the scheme 1.7.2 and obey the same experimentally observed rate law.

$$\text{Racemization rate} \propto [\text{silane}][\text{nucleophile}]^2$$

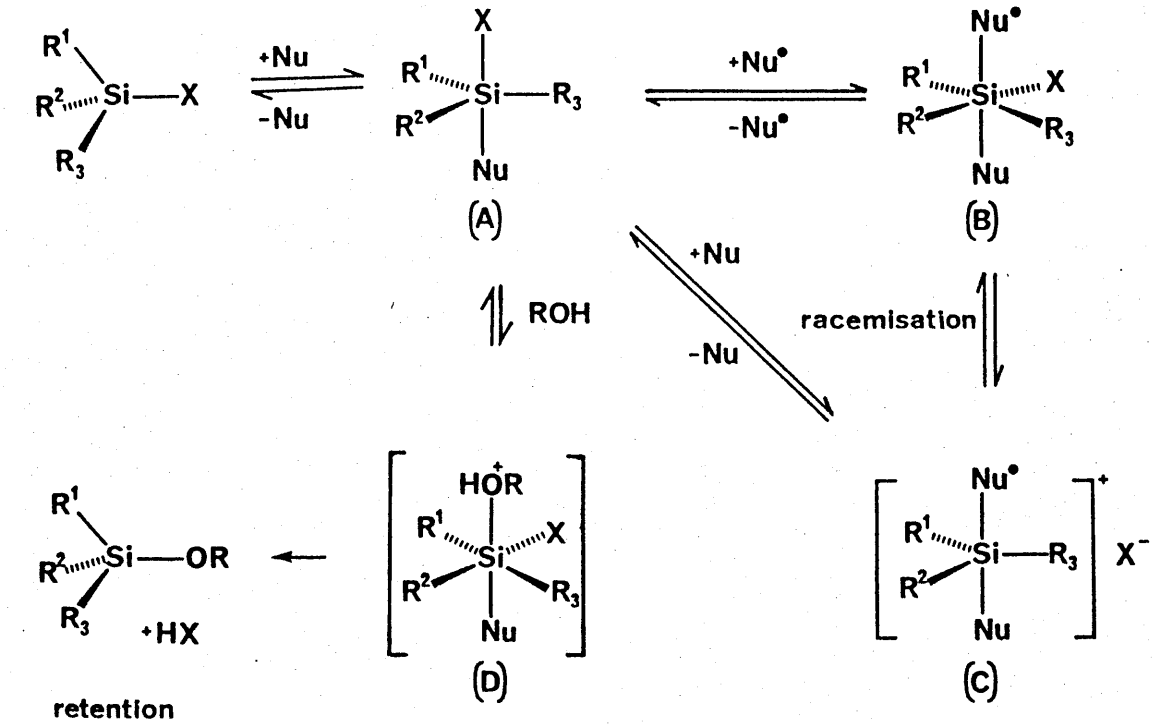

Mechanism proposed by Corriu

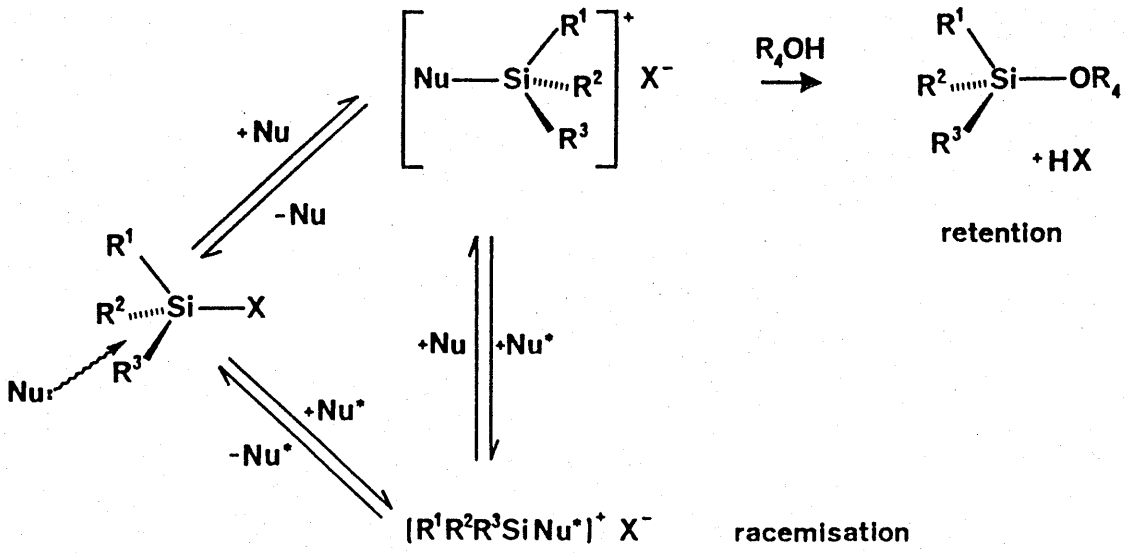

Mechanism proposed by Chojnowski

Scheme 1.7.2 Mechanisms proposed by Corriu and Chojnowski

Chapter 2 The nature of the silane-nucleophile adduct

2.1 Introduction

Several different structures of silane-nucleophile adducts have been proposed as described in Section 1.7. Therefore it is essential to understand the exact nature of the dominant species present during silylation, prior to investigating the kinetic and thermodynamic behaviour as well as establishing the mechanism.

Numerous spectroscopic methods are available for monitoring the course of a reaction and identifying the species present in the reaction mixture. In selecting an experimental technique, the time scale of observation is a crucial factor in determining whether the various species present during a dynamic process can be differentiated. The minimum lifetime necessary for the observation of distinguishable entities increases as the transition energy of the exchanging species decreases.[58] For the commonly employed techniques, the minimum half life decreases in the following order: physical separation such as chromatography, magnetic resonance spectroscopy (n.m.r., e.s.r.), vibrational and electronic spectroscopy (infrared, Raman, ultraviolet, optical rotatory dispersion) and diffraction measurements (X-ray, electron, neutron). The time scale of physical separation studies is fairly long, so they are not applicable for examining rapid silylation reactions. N.m.r. spectroscopy provides a suitable time scale, allowing detailed studies of silylation reactions which take place on a time scale ranging from 10^{-1} to 10^{-5} second. It also enables the individual exchanging species to be detected.

Another significant advantage of n.m.r. spectroscopy is its efficacy for studying the stereochemistry of nucleophilic displacement of optically active silanes, without having to resolve a racemic mixture into its constituent enantiomers by physical separation. Furthermore, unlike the other techniques such as optical rotatory dispersion and polarimetry, n.m.r. offers direct information on the chemical environments of the nuclei under study. Thus the structural changes induced in both silanes and nucleophiles during the interaction can be examined in detail by

n.m.r. spectroscopy in a non-intrusive manner. This technique is also frequently employed for determining the optical purity of mixtures of optically active species.[59,60] This is complementary to the polarimetric method which does not always give accurate values for optical purities because of the very low specific rotations exhibited by some mixtures of enantiomers.[60]

In achiral media, enantiomers are indistinguishable because they are isochronous and have superimposed chemical shifts. In contrast, diastereomers show different chemical and physical properties, for example melting point, solubility, infrared and n.m.r. spectra, and consequently are usually distinguishable even in achiral surroundings.[60] It is therefore not surprising that enantiomers are usually converted into diastereomers for optical resolution.[59] The resolution of racemates normally involves the interaction with an excess of a resolving agent, for instance an optically pure chiral compound, to produce a mixture of diastereomers. Based on a similar principle, the interactions between optically active halophenylmethylsilanes, PhMeHSiX (X=Cl, OSO_2CF_3), and nucleophiles were examined in an optically pure chiral solvent such as R-(+)-limonene.

The influence of chirality on n.m.r. spectra is not limited to the optically active centres. For instance, when a group of the general structure $R'RSiX_2$, where Si is a prochiral atom, is in the neighbourhood of a moiety that lacks symmetry (R') the environments of the X substituents become non-equivalent or diastereotopic. A pair of diastereomers are produced if these two diastereotopic groups are replaced separately by a ligand different from any of those attached to the prochiral centre. For example, two diastereomers are formed when the two diastereotopic hydrogen atoms of 2-methylbutanol, $EtCH(Me)CH_2OH$, are substituted individually. Diastereotopic groups are not interchangeable by any symmetry operations and possess different chemical as well as physical properties. Their anisochrony is reflected in their different chemical shifts in either achiral or chiral solvents.

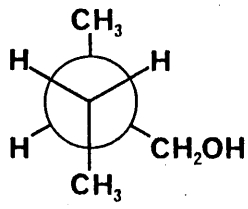

Figure 2.1.1 Diastereotopic 2-methylbutanol

The major factor affecting the magnitude of the difference in chemical shifts of two diastereotopic groups[61] is based on the specific differences in the environments of the two groups. These include the type and the anisotropy of the other parts of the molecule, the spatial distances between the two groups as well as conformational effects.

Changes in the magnitude of chemical shift non-equivalence can also be induced by altering the temperature, the solvent or the concentration, together with the population of each conformer. The effects resulting from changes in concentration are related to those induced by changes in solvent, simply because a change in concentration can alter the properties of the medium.

The magnitude of the chemical shift non-equivalence diminishes with increasing distance between the prochiral centre and the asymmetric moiety in the molecule. This is due to the conformational interactions between the centres and the anisotropic effects of substituents become less important at long distance, however this concept is not applicable to the diastereotopic system, $RCHMeSiMe_2X$, studied in this project. A more detailed analysis of these factors will be provided in the following discussion section.

Interconversion between the environments of stereochemically non-equivalent groups is observed as a consequence of conformational changes or tautomerisation.[58] However, the chemical shift non-equivalence is cancelled and an average signal results if the exchange is fast. As

explained earlier, the time scale of observation relative to the rate of interchange is vital in determining whether the stereochemical non-equivalence is maintained. If the exchange is rapid compared with the time scale of observation the two groups will be indistinguishable, whereas the reverse is observed if the exchange is slow. An energy barrier to interconversion of about 50 $kJmol^{-1}$ is sufficient for detection by n.m.r. spectroscopy at ambient temperature.[58]

It is desirable to choose a simple system which enables easy observation of the detailed structural changes in both donor and acceptor. Extensive studies have been performed on halotrimethylsilanes, Me_3SiX (X=Cl, Br, I, OSO_2CF_3),[8,9,62,63,64,65] since they are widely used in organic synthesis. However the kinetic behaviour of these silanes is difficult to monitor, therefore an alternative system was designed.

A series of carbon functionalized halosilanes with diastereotopic methyl groups attached to the silicon atom, $RCHMeSiMe_2X$ (R=Et, ^tBu, Ph; X=Cl, Br, OSO_2CF_3), were synthesised. The similarities between this system and the halotrimethylsilanes will be outlined in a later section. The n.m.r. chemical shift titration studies, at both ambient and variable temperatures, concentrate upon the interactions of the diastereotopic silanes as well as the chiral chloromethylphenylsilane with two strong nucleophiles; hexamethylphosphoramide (an oxygen donor) and N-methyl-imidazole (a nitrogen donor). The nuclei adjacent to the silicon atom are most affected as a consequence of silylation. Therefore the analysis of the chemical shift titration results mainly focuses on the variation in the chemical shifts and the observed line shapes of the SiMe peaks in the proton, carbon-13 and silicon-29 spectra for both diastereotopic and optically active silanes. In several cases, solid silane-nucleophile adducts were isolated and characterized by n.m.r. and infrared spectroscopies together with elemental microanalysis.

2.2 Studies on halomethylphenylsilanes PhMeHSiX (X=Cl, OSO_2CF_3)

As a result of interaction with an optically pure chiral medium, each optical isomer of a chiral silane should, in principle, be anisochronous leading to two resonances with appreciably different chemical shifts in the silicon-29 n.m.r. spectrum. The introduction of a nucleophile will lead to variation in the chemical shifts, owing to changes in the configuration at silicon, thus valuable information concerning the stereochemistry of nucleophilic displacement may be obtained.

Nevertheless the results were rather disappointing; when methylphenylsilyl trifluoromethanesulphonate (triflate) was added to an optically pure chiral solvent, R-(+)-limonene, the colour of the mixture became red and an exothermic reaction with vigorous effervescence occurred. Hydrosilylation[35] of the chiral solvent by the silane could account for this observation. This reaction may be catalysed by trifluoromethanesulphonic (triflic) acid which may be present as a trace impurity in the silyl triflate. Addition of a strong base, triethylamine, solved this problem by removing the triflic acid.

Nonetheless neither the optical isomers of the chlorosilane, PhMeHSiCl, nor the silyl triflate, $PhMeHSiOSO_2CF_3$, could be resolved in the n.m.r. spectrum with the optically pure chiral solvent employed. The inability of the chiral solvent to separate the enantiomers of each silane may be due to weak solute-solvent interactions; further attempts at resolving these silanes were abandoned since it was difficult to select a suitable resolving agent without creating unwanted side reactions. For example, the commercially available chiral lanthanide shift reagent, Europium (III)-tris(1,1,1,2,2,3,3)-heptafluoro-7,7-dimethyl-4,6-octadionate $Eu(FOD)_3$, is liable to be silylated.

2.3 Diastereotopic silanes $RCHMeSiMe_2X$ (X=Cl, Br, OSO_2CF_3)

2.3.1 Structural effects

Chlorination of 2-hydroxy-3,3-dimethylbutane, $^tBuCH(OH)Me$, into its chloride derivative, $^tBuCH(Cl)Me$, the precursor for $^tBuCHMeSiMe_2H$, was complicated by the accompanying rearrangement reaction yielding 2-chloro-2,3-methylbutane, $Me_2CHCClMe_2$, as shown in Scheme 2.3.1. These two isomers have very similar properties, for example boiling point and retention time on a gas chromatogram,[66] their separation was therefore extremely difficult and hence the preparative work on this butyl derivative was not continued.

$$^tBuCH(OH)Me + SOCl_2 \longrightarrow {}^tBuCH(Cl)Me + Me_2CHCClMe_2$$

Scheme 2.3.1

Difficulties were not encountered in the syntheses of sec-butyldimethylhalosilanes, $EtCHMeSiMe_2X$ (X=Cl, OSO_2CF_3), and methylbenzyldimethylhalosilanes, $PhCHMeSiMe_2X$ (X=Cl, Br, OSO_2CF_3). However, in both the proton and the carbon-13 n.m.r. spectra, chemical shift non-equivalence of the two diastereotopic SiMe signals of the sec-butyldimethylhalosilanes was not observed; this phenomenon is often known as accidental isochrony.[67]

In contrast, two individual resonances were observed for the SiMe groups of the $PhCHMeSiMe_2X$ (X=Cl, Br, OSO_2CF_3) systems. Nevertheless, the chemical shift separations of these two diastereotopic peaks in the chloro- and bromosilanes were very small in the proton spectra, and only a broad singlet was recorded for the triflate. The chemical shift separations are different in the proton and carbon-13 n.m.r. spectra, which may be due to the greater chemical shift range for the carbon-13 nucleus. The intermolecular nucleophilic attack of the sulphonyl oxygen atom at the silicon atom of a neighbouring silyl triflate molecule is too fast to be monitored on the proton time scale, hence an average, broad singlet results for the silyl triflate. A summary of the n.m.r. data of

the two diastereotopic SiMe groups in both systems is given below. The n.m.r. data were recorded in chloroform-d_1 and referenced to an external standard.

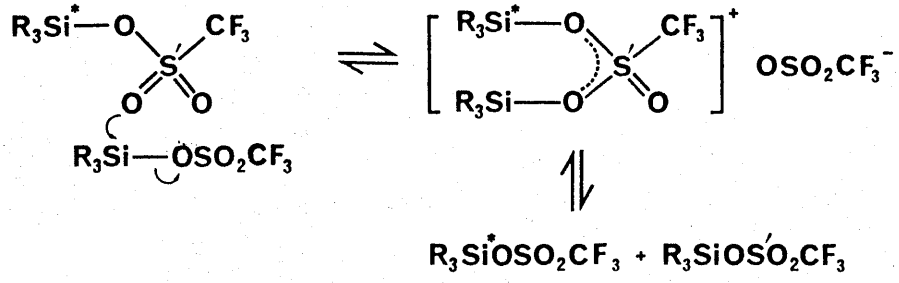

Scheme 2.3.2 Intermolecular exchange between silyl triflates

Silane	SiMe n.m.r. signals δ(ppm) (peak separation Hz)	
	Proton	Carbon-13
$EtCHMeSiMe_2H$	0.10d, 3.7Hz 0.09d, 3.7Hz	-5.9, -6.3 (9.1Hz)
$EtCHMeSiMe_2Cl$	0.37	0.06
$EtCHMeSiMeOSO_2CF_3$	0.39 sbr	-3.33
$PhCHMeSiMe_2H$	0.11d, 3.7Hz 0.07d, 3.7Hz	-5.2, -5.4 (3.9Hz)
$PhCHMeSiMe_2Cl$	0.40, 0.42 (1.8Hz)	0.8, -0.3 (23.3Hz)
$PhCHMeSiMe_2OSO_2CF_3$	0.47 sbr	-2.8, -3.8 (24.6Hz)
$PhCHMeSiMe_2Br$	0.54, 0.56 (1.8Hz)	0.5, 1.8 (29.8Hz)
$(PhCHMeSiMe_2)_2O$	-0.16	-1.0, -1.1 (2.6Hz)

Table 2.3.1 N.M.R. data of the diastereotopic silanes

The interpretation of the results demonstrates that the magnitude of chemical shift non-equivalence depends upon the anisotropy of the R group,[59,61] since the only difference between the two systems lies in the nature of the R group. In the sec-butyl substituent, EtCHMe, both the ethyl and the methyl groups are very similar in size and are essentially isochronous. Therefore it is not surprising that the magnitude of the observed non-equivalence is very small, in fact the chemical shift separation was not detectable in either the carbon-13 or the proton n.m.r. spectrum. Conversely, the phenyl group is very

different both in size and in magnetic anisotropy compared with the methyl group in the methylbenzyl substituent, PhCHMe. Thus the chemical shift non-equivalence is expected to be fairly large which is indeed observed.

Apart from the anisotropic effects of the substituents attached to the asymmetric moiety adjacent to the prochiral centre, another method of inducing a larger separation of the diastereotopic peaks is to use a n.m.r. spectrometer with a higher magnetic field strength. Thus two separate signals may be observed for the sec-butyldimethylhalosilanes with more powerful n.m.r. spectrometers.

Because a reasonable chemical shift difference between the diastereotopic resonance is essential for kinetic and thermodynamic studies, all the titration studies concentrated upon the methylbenzyldimethylhalosilanes, $PhCHMeSiMe_2X$ (X=Cl, Br, OSO_2CF_3), so as to compare with the kinetic and thermodynamic results.

As mentioned before, the diastereotopic systems, $RCHMeSiMe_2X$, bear a close resemblance to and can be regarded as a trimethylhalosilane, Me_3SiX (X=Cl, Br, OSO_2CF_3), with one of the methyl groups being replaced by the chiral RCHMe moiety. The major difference between the RCHMe substituent and the methyl entity is the steric bulk on the chiral group. Their resemblance is illustrated by their similar silicon-29 n.m.r. chemical shifts in chloroform-d_1, when $PhCHMeSiMe_2X$ (X=Cl, Br, OSO_2CF_3) are compared with the corresponding Me_3SiX.

Table 2.3.2 Comparison of $PhCHMeSiMe_2X$ with Me_3SiX

$PhCHMeSiMe_2X$	Silicon-29 n.m.r. (ppm)	Me_3SiX	Silicon-29 n.m.r. (ppm)
X=Cl	32.4	X=Cl	31.0
X=Br	30.8	X=Br	27.6*
$X=OSO_2CF_3$	40.4	X=OTf	43.4

* recorded in dichloromethane-d_2

2.3.2 The effects of conformation and temperature

For the methylbenzyldimethylhalosilanes, $PhCHMeSiMe_2X$, there are three possible staggered conformations around the Si—C(Me) bond, as depicted by the Newman projections in Figure 2.3.1. Owing to the free rotation of the Si—C(Me) bond, each rotamer has a similar population. Nevertheless, the residual chemical shift non-equivalence of the diastereotopic SiMe groups is preserved as required by the symmetry rules, this is known as the "intrinsic non-equivalence" or the "intrinsic anisochronism".[58,61]

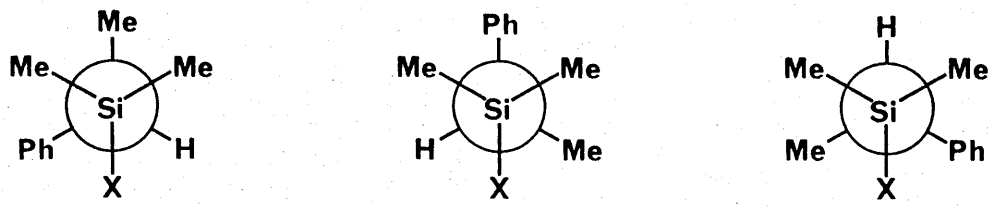

Figure 2.3.1 Three conformers of $PhCHMeSiMe_2X$

Generally, temperature affects the magnitude of the chemical shift difference by altering either the relative conformer populations or the individual chemical shifts. With the degeneracy of rotation about the Si—C(Me) bond, varying the temperature will not significantly alter the populations of the three rotamers. The variable temperature studies on the samples of $PhCHMeSiMe_2X$ (X=Cl, Br or a mixture of Cl and Br) in benzene-d_6 prove that the chemical shift difference between the two diastereotopic SiMe groups is independent of temperature. No changes in the chemical shift separations were recorded, when the samples were subjected to a variation in temperature spanning between 330K and 280K.

2.3.3 Effects of solvent and concentration

The magnitude of the chemical shift non-equivalence is often significantly solvent dependent, owing to the medium effects on the relative population of the conformers and the individual chemical shifts.

Aromatic solvents normally have a more marked effect on the magnitude of the chemical shift separation, for instance non-equivalence can be observed under conditions where diastereotopic signals are accidentally degenerate in aliphatic solvents.[61]

The solvent and the related concentration effects on the chemical shift difference of the methylbenzylchlorodimethylsilane, $PhCH(Me)SiMe_2Cl$, were examined. From the interpretation of the data, as given in the following tables, it seems that solvent effects are not pronounced in this diastereotopic system. Only a change of 5Hz in the chemical shift difference is observed on diluting the silane with polar dichloromethane-d_2, whereas the separation remains unaltered on dilution with benzene-d_6.

Table 2.3.3 Solvent effect on chemical shift difference of the diastereotopic signals of $PhCHMeSiMe_2Cl$

Solvent	Dielectric constant (ϵ)	Polarity (E_T)	Chemical shift difference of diastereotopic signals (Hz)
C_6D_6	2.3	34.5	25.9
$C_6D_5.CD_3$	2.4	33.9	25.9
$CDCl_3$	4.8	39.1	23.3
CD_2Cl_2	8.9	41.1	24.6
CD_3NO_2	35.9	46.3	23.3

Table 2.3.4 Concentration effect on chemical shift difference of diastereotopic peaks of $PhCHMeSiMe_2Cl$

C_6D_6 (v/v %)	Separation (Hz)	CD_2Cl_2 (v/v %)	Separation (Hz)
91%	25.9	91%	24.6
45%	25.9	45%	20.7
18%	25.9	18%	19.4
9%	25.9	9%	19.4

2.4 Interactions of $PhCHMeSiMe_2X$ (X=Cl, Br, OSO_2CF_3) with N-methylimidazole (NMI)

The interactions between the donor (NMI) and acceptors were examined by adding successive aliquots of NMI to a solution of silane $PhCHMeSiMe_2X$ (X=Cl, Br, OSO_2CF_3). The spectral data recorded during the chemical shift titrations are provided in the tables in the experimental chapter; some of the data are presented in the accompanying graphs. N-Methylimidazole is a powerful nitrogen donor and is capable of forming stable four coordinate ionic adducts with silanes.[63] The proton signals attached to the C_4 and C_5 atoms of 1-methylimidazole were obscured by the phenyl resonances of the silane, therefore information concerning the structural changes in NMI is based on the C_2—H and N—Me signals.

In each case, the spectral results were accompanied by two distinct features, namely, line broadening and upfield shifts of the n.m.r. peaks. The degree of line broadening depends upon the nature of the counterion or the leaving group, and provides useful information on the relative rate of exchange as well as the extent of the dynamic equilibrium, established between the silane and its imidazolium adduct.

In comparison with the uncomplexed NMI, the C_2—H signal shifted downfield due to complexation of the nucleophile with silane. Addition of excess NMI induced upfield shifts of the NMI resonances which may be attributable to medium effects and chemical exchange. The general upfield shifts of the silane signals can be rationalized in terms of the changes in the electron distribution in the silane molecule on complexation with NMI. The utilization of the lone pair on the nitrogen atom of NMI in forming the dative Si—N bond destroys the magnetic anisotropy of nitrogen, and causes an increased shielding of the adjacent silicon atom as well as its neighbouring moieties. The imidazolium cation becomes less deshielded owing to an increase in the electron density, which is most pronounced at the C_2 position as demonstrated by the following resonance structures.

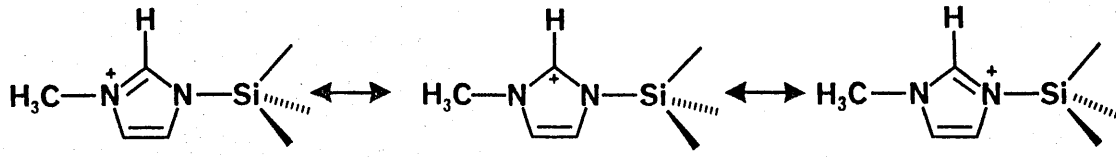

Figure 2.4.1 Resonance structures of NMI on complexation

In all three cases (X=Cl, Br, OSO_2CF_3), the changes in the chemical shifts of NMI in both proton and carbon-13 n.m.r. spectra follow the analogous trends observed by Pugmire and Grant[68] as well as Barlin and Batterham[69] for the protonation of imidazole by hydrogen chloride. However, the possibility of protonation in these cases can be entirely ruled out based upon the evidence from silicon-29 n.m.r. spectra and the absence of any peaks due to hydrolysed products in the spectra of the three nuclei.

2.4.1 Interaction of $PhCHMeSiMe_2Cl$ with NMI

The isolation and identification of the four coordinate adduct, readily formed between $PhCHMeSiMe_2Cl$ and NMI with a 1:1 stoicheiometry, strongly suggest that a penta- or a hexacoordinate silicon intermediate is not the dominant species in solution. The n.m.r. spectral data of the solid adduct in solution were similar to those of the mixture of the individual components in solution. For example, the chlorosilane gave a silicon-29 chemical shift of 32.4 ppm whereas a slightly broadened signal at 30.1 ppm was recorded for the adduct. Furthermore, line broadening of the NMI peaks was observed in both proton and carbon-13 spectra. These observations are consistent with a rapid dissociation of the complex in solution, as a consequence of nucleophilic attack of the chloride counterion at the silicon atom of the adduct, regenerating the chlorosilane and free NMI. Thus the dynamic exchange between the free and the complexed NMI molecules is responsible for the slight line broadening of the NMI resonances.

Except for some of the NMI signals, the observed line shapes in the chemical shift titration study did not display significant broadening, indicative of either a very fast or a very slow exchange. Moreover, the peaks arising from the two exchanging species, the chlorosilane and its imidazolium complex, were indistinguishable in the proton, carbon-13 and silicon-29 spectra. This is compatible with a fast dynamic process.

Besides affecting the nature of the medium, increasing the proportion of NMI also drives the equilibrium further towards the adduct and causes upfield shifts of the resonances. This is manifested by the low frequency shift of 6 ppm in the silicon-29 spectra, from 32.4 to 26.1 ppm with a five molar excess of NMI.

2.4.2 Interaction of $PhCHMeSiMe_2Br$ with NMI

$PhCHMeSiMe_2Br$ also forms a solid adduct with 1-methylimidazole, though unlike its chloride analogue, examination of the spectral data reveals that no substantial dissociation of the solid in solution takes place, reflecting the greater stability of the adduct. Apart from the elemental microanalytical results, further evidence for the existence of the four coordinate ionic complex was based on the proton, carbon-13 and silicon-29 n.m.r. spectra. The upfield shift of the silicon-29 peak to 23.5 ppm for the adduct, together with the increased deshielding of the NMI resonances, particularly at the C_2 position, confirm the formation of the dative Si—N bond, leading to increasing shielding in the silane and increasing deshielding in the NMI molecules on complexation.

In contrast to the chlorosilane, the results from the titration of $PhCHMeSiMe_2Br$ exhibited slightly different behaviour, both the variation in the chemical shifts and the broadening of the observed line shapes were more pronounced. These trends are fully consistent with a slower exchange accompanied by a larger equilibrium constant for adduct formation, corresponding to the observed stability of the bromosilane-NMI complex. This is clearly demonstrated by the extremely broad nature of

the singlet for the diastereotopic SiMe groups, the two exchanging CH quartets and the NMI peaks in the proton spectrum of a 2:1 mixture of silane to NMI.

The faster time scale of the carbon-13 and silicon-29 spectra enables the two exchanging silicon entities to be distinguished. The silicon-29 spectrum of a mixture of the two species in similar proportion produced two broad resonances, which are attributable to the uncomplexed bromosilane at 30.8 ppm and its adduct at 25.2 ppm. The successive increase in the concentration of NMI drives the equilibrium in favour of the complex, the dynamic process accelerates and eventually the normal line shapes are reproduced.

2.4.3 Interaction of $PhCHMeSiMe_2OSO_2CF_3$ with NMI

The general chemical shift trends, especially in the carbon-13 and silicon-29 spectra, resulting from the titration of the silyl triflate are in accord with those observed in the titration of the corresponding bromosilane described in the previous section. Nevertheless, intense broadening was not observed as a consequence of the much slower exchange between the two silyl species. Furthermore, when the silane to NMI ratio was at 2:1 the two silicon compounds existed in relatively equal ratios, separate signals in the spectra of all three nuclei were recorded for moieties adjacent to silicon, such as the SiMe, CH and CMe groups. The deshielded NMI resonances in the proton spectra provide important evidence for the formation of a four coordinate ionic silane-NMI complex, resembling that observed for the trimethylsilyl systems.

More interestingly, the two exchanging silicon species produced three resonances for the diastereotopic SiMe moieties in both proton and carbon-13 n.m.r. spectra. Owing to the slow dynamic process and the comparatively long lifetime of the triflate-NMI complex, the two diastereotopic SiMe entities in the adduct were detected.

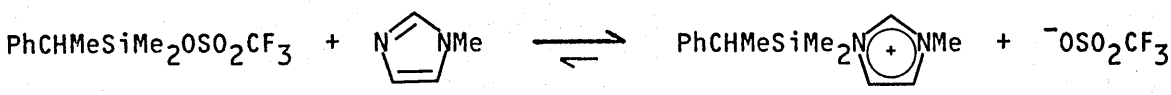

Scheme 2.4.1

The third SiMe resonance is undoubtedly due to the uncomplexed silyl triflate. The averaging of the two diastereotopic signals cannot be accounted for by the intermolecular exchange of the free silyl triflate molecules, since coalescence is observed in the carbon-13 as well as proton n.m.r. spectra. Nucleophilic attack by the triflate anion of the adduct at the silicon atom of the unreacted triflate is probably the major contributing factor. By undergoing fast exchange, the two diastereotopic SiMe entities of the triflate are indistinguishable from those of the inverted isomer, therefore an average singlet results.

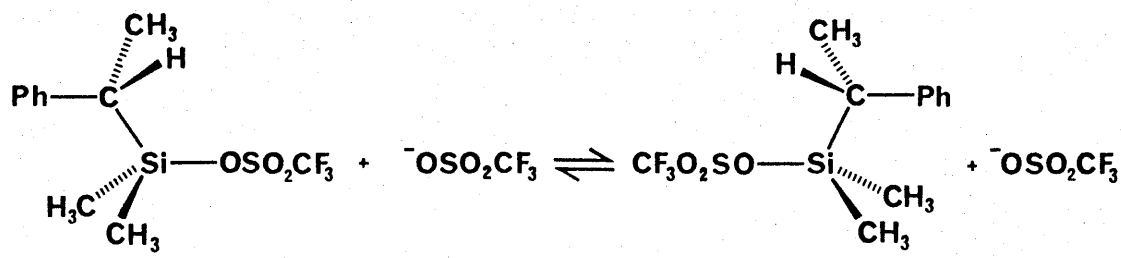

Scheme 2.4.2

As more NMI is introduced to convert the silyl triflate into its imidazolium salt, the stable ionic adduct becomes the dominant species in solution, thus the intensities of the silane signals diminish whilst those of the ionic complex increase. Nucleophilic attack of excess uncomplexed NMI at the silicon atom of the ionic adduct causes an inversion of configuration at silicon, hence coalescence of the two diastereotopic SiMe peaks results giving an average signal.

Figure 2.4.2
Proton n.m.r. titration studies of PhCHMeSiMe2X (X=Cl, Br, OTf) against NMI.

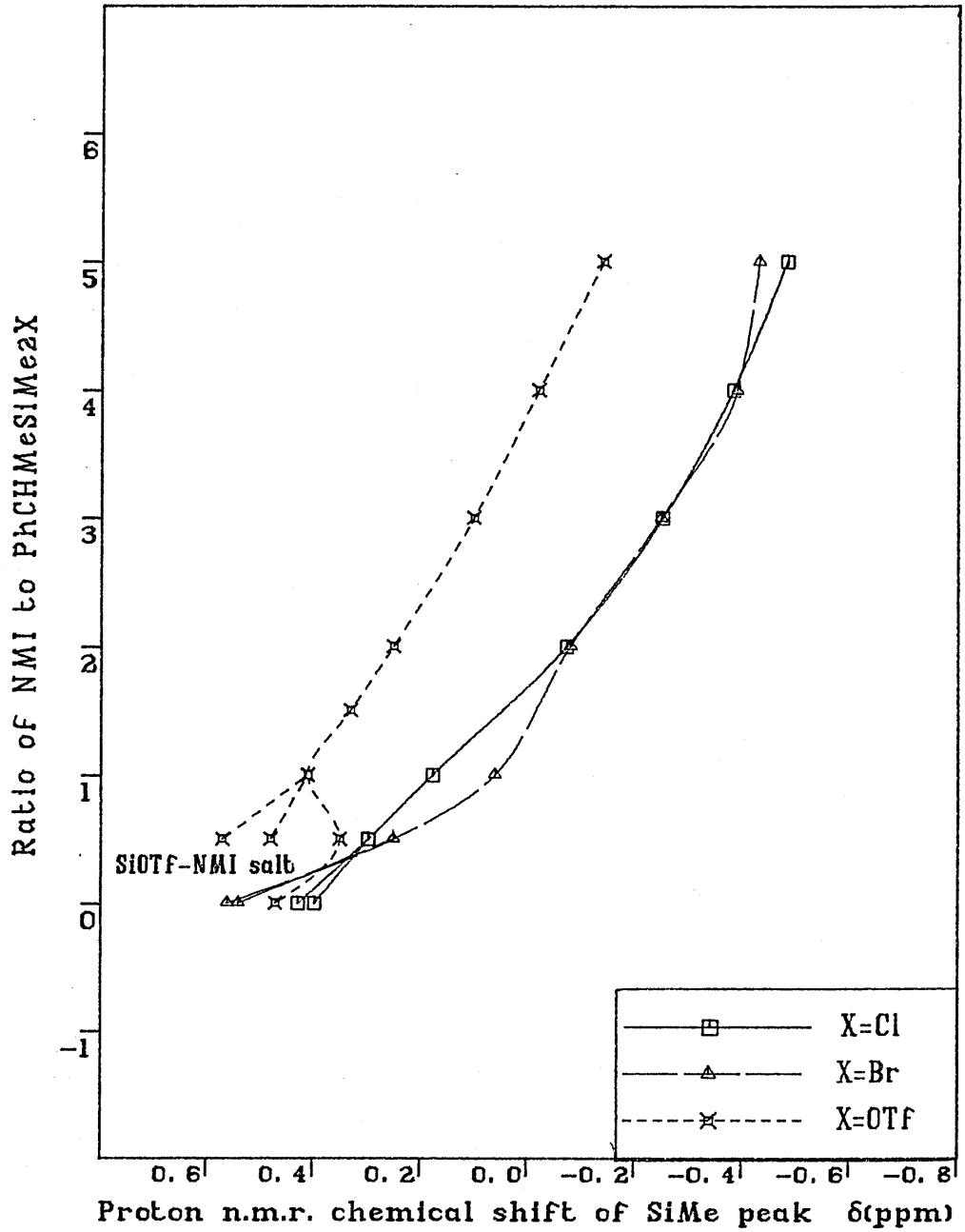

Figure 2.4.3
Carbon-13 n.m.r. titration studies of PhCHMeSiMe2X (X=Cl, Br, OTf) against NMI.

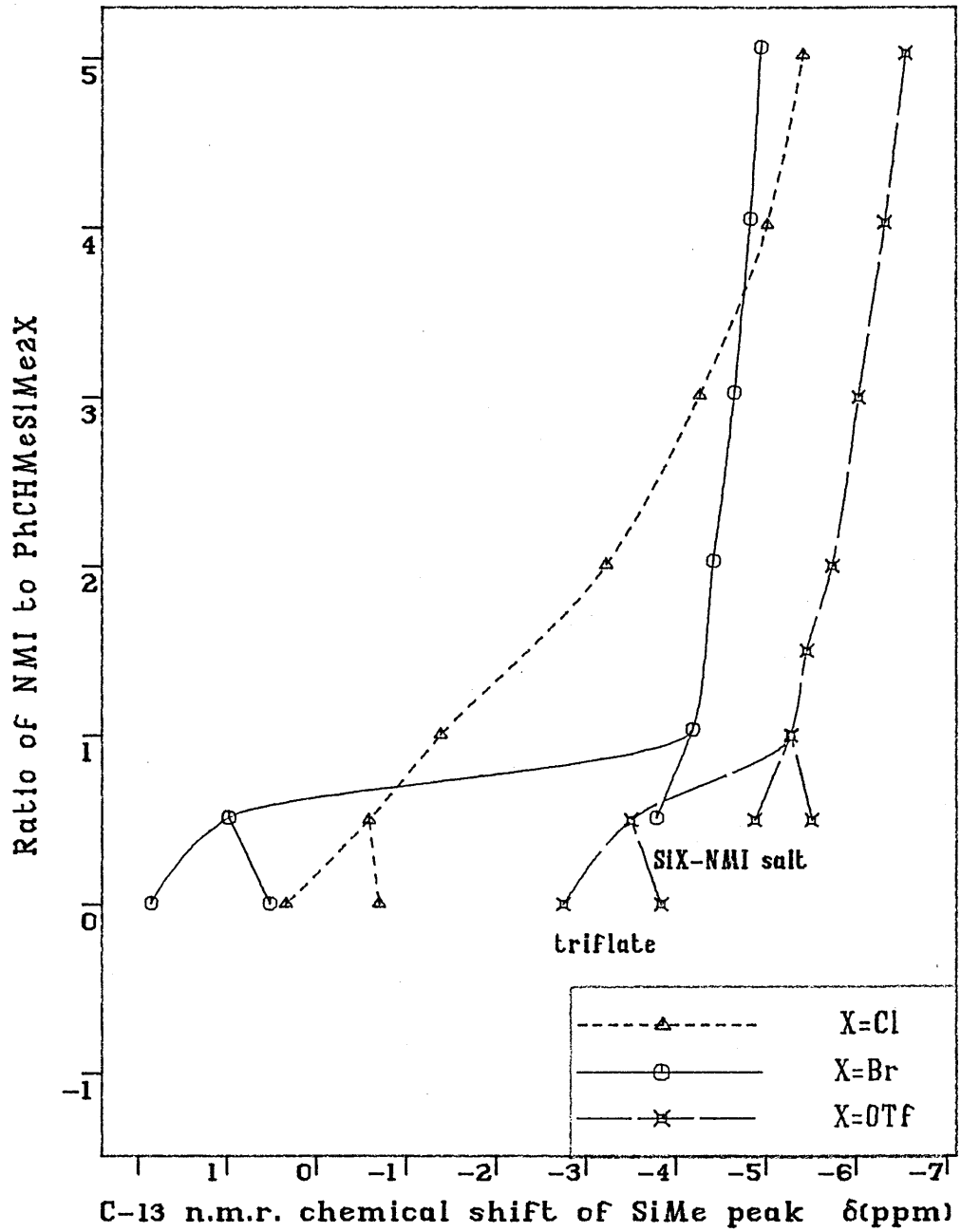

Figure 2.4.4
Silicon-29 n.m.r. titration studies of PhCHMeSiMe2X (X=Cl, Br, OTf) against NMI.

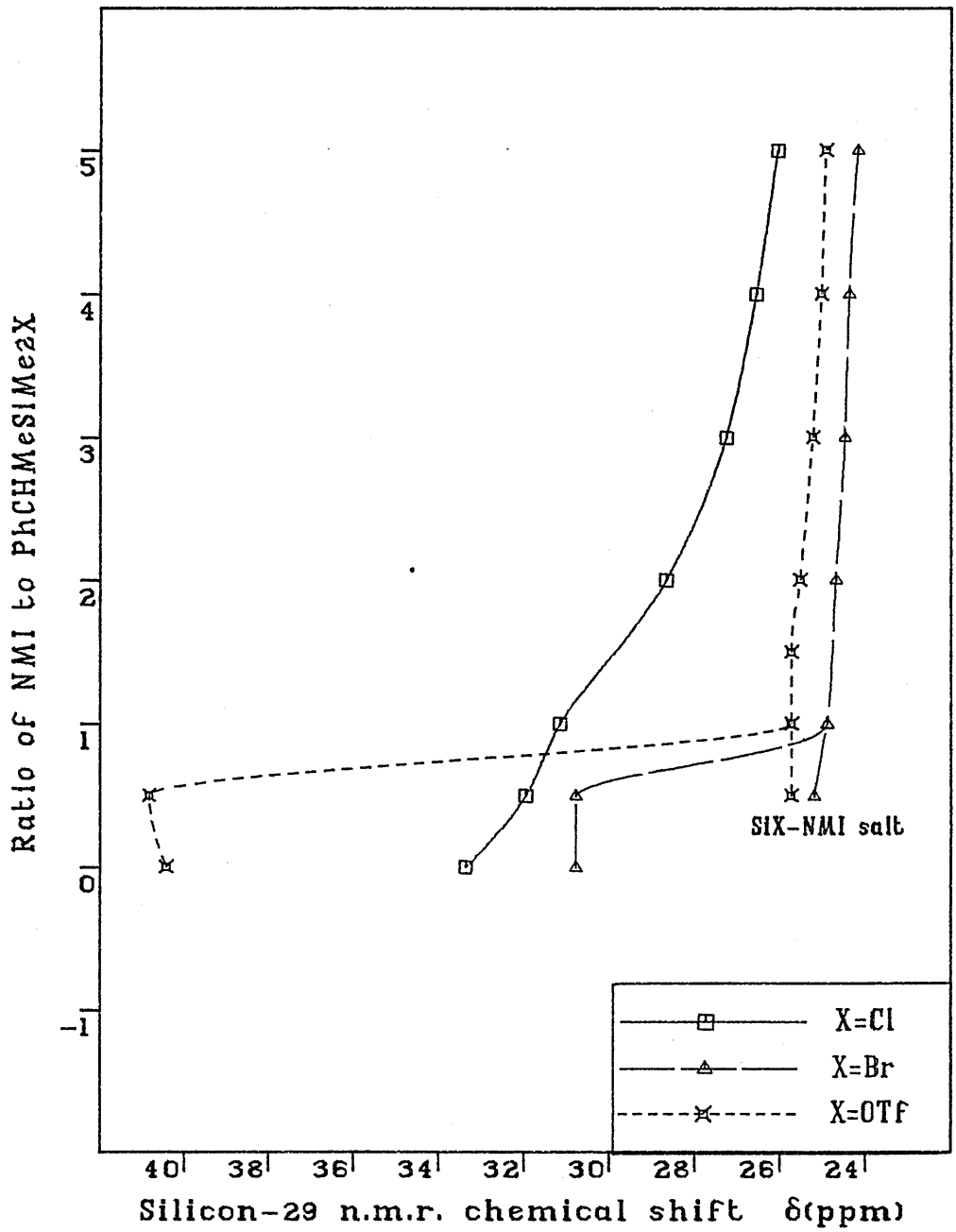

2.4.4 Comparison of the three systems

The dominant species in solution are believed to be the 1:1 four coordinate ionic silane-nucleophile adducts. This conclusion is based upon the results from the chemical shift titration, together with the isolation and characterization of the solid adducts. Furthermore, no evidence for expansion of coordination at silicon was noted. The similarity between the silicon-29 chemical shifts of the four coordinate adducts for different counterions (X=Cl, Br, OSO_2CF_3) indicates that the same type of complex, $PhCHMeSiMe_2N$⟨+⟩NMe X^- (X=Cl, Br, OSO_2CF_3), is present in each case.

The equilibrium constants for the exothermic adduct formation with NMI were found to increase in the following order with different counterions $Cl \ll Br < OSO_2CF_3$. The relative rates of exchange between the silane and its imidazolium complex deduced from the observed line shapes of n.m.r. resonances produced an entirely different trend. The exchange accelerates with counterions in the sequence $X=OSO_2CF_3 < Br < Cl$. These two opposing trends are consistent with the order of nucleophilicity and the solvation of each counterion involved.

The concentration of a silane-nucleophile adduct in a silylation mixture depends partly upon the relative difference between the bond energies of the Si—X and Si—Nu bonds. Thus more energy is required for the cleavage of the strong Si—Cl bond. As a result, the equilibrium lies towards the uncomplexed silane and free nucleophile in the case of chlorosilane with poor donor species.

The intramolecular nucleophilic attack of the counterion at the silicon atom of the ionic complex relies upon the nucleophilicity of the counterion. Thus, being a better nucleophile, the chloride ion attacks the silicon atom readily resulting in the dissociation of the complex into its individual components. In contrast, the stability of the complex is enhanced when the counterion is a large, diffuse and

polarizable species. The triflate anion can be solvated easily and is a poor nucleophile, which leads to a larger equilibrium constant.

Another interesting feature is the increase in the magnitude of the deshielding effect in the imidazolium cation with different counterions, which increases in the following order: X=Cl << OSO_2CF_3 < Br. Deshielding is not observed for the chlorosilane due to the low equilibrium constant for the imidazolium complex. In the remaining two systems, solvation of the counterion in the adduct is a decisive factor. In the absence of stabilization by solvent, the anion produced by the cleavage of the Si—X bond has to be solvated by the cationic charge. On the contrary to the large and polarizable triflate anion, the bromide ion is a relatively small, hard species and is less well solvated, therefore tight ion pairing is observed for the bromide ion with the imidazolium species acting as the solvent.

The interpretation of the spectral results of the interaction of $PhCHMeSiMe_2OSO_2CF_3$ with NMI also yields a very important finding. Being a potential nucleophile, the counterion of a stable complex can induce nucleophilic attack on the uncomplexed silane in the absence of added, more powerful nucleophile. This will be discussed in more detail later.

2.5 Interactions of $PhCHMeSiMe_2X$ (X=Cl, Br) with hexamethylphosphoramide (HMPA)

The chemical shift data for the interaction of $PhCHMeSiMe_2X$ (X=Cl, Br) with HMPA are tabulated in the experimental section; the proton, carbon-13 and silicon-29 spectral data of the diastereotopic SiMe moieties are illustrated graphically in accompanying figures. The chemical shift changes of these silanes with HMPA was similar to that found with NMI. In both cases, the CH peak of the silane molecule was obscured by the NMe doublet of HMPA in the proton spectra.

2.5.1 Interaction of $PhCHMeSiMe_2Cl$ with HMPA

Although broadening of the observed line shapes was insignificant, a gradual but small upfield shift of the n.m.r. resonances was recorded as the concentration of HMPA increased, indicating that the equilibrium was pushed towards the side of complex formation. The absence of any coupling between the phosphorus atom of HMPA and silane, together with the small lower frequency shift from 32.4 to 30.8 ppm in the silicon-29 spectra, are entirely consistent with the instability of the silane-HMPA complex. As a consequence of the rapid dissociation of the adduct initiated by the nucleophilic attack of the chloride counterion, as well as the fast forward reassociation reaction, a fast exchange was established between the two silicon species, which is in accord with the sharpness of the linewidths. Furthermore, the silicon-29 chemical shifts were characteristic of four coordinate silicon, implying that the presence of any penta- or hexacoordinate complex was not measurable.

At ambient temperature, the equilibrium constant for the formation of the four coordinate chlorosilane-HMPA adduct was very low, since a three molar excess of HMPA only induced a 2 ppm low frequency shift in the silicon-29 n.m.r. spectra. Therefore a variable temperature silicon-29 n.m.r. study was undertaken for a 1:1.5 mixture of chlorosilane and HMPA. Prior to the addition of HMPA, the chlorosilane solution was cooled from 300K to 180K to check for any changes in its chemical shift on lowering of temperatures. As expected, the chemical shift remained constant on cooling, the increase in the viscosity of the solution at low temperatures may account for the negligible 1 ppm downfield shift.

Cooling the mixture of chlorosilane and HMPA down to 200K, the silicon-29 signal moves 7 ppm upfield from an initial value of 30.1, which can be attributed to a trend towards the four coordinate ionic chloride salt formation at low temperatures. The intense broadening and the reduction in intensity of the silicon-29 peak around 200K provided strong evidence that the silane was undergoing an intermediate chemical exchange with the salt. On warming back to ambient temperature, a very similar spectrum

was recorded to that found initially, proving that the process of complex formation was reversible.

2.5.2 Interaction of $PhCHMeSiMe_2Br$ with HMPA

Complexes of HMPA with halotrimethylsilanes, Me_3SiX (X=Br, I), have been isolated and characterized by Chojnowski using microanalysis, phosphorus-31 n.m.r. spectroscopy and conductiometry.[9,70] Therefore it is likely that the silylation of HMPA by $PhCHMeSiMe_2Br$ may proceed via an analogous route forming a similar intermediate. This is confirmed by the n.m.r. data of the four coordinate $[PhCHMeSiMe_2\text{-}HMPA]^+Br^-$ solid complex isolated, which is also in accord with the observations from the ambient and variable temperature titrations with the chlorosilane.

Complex formation is reflected by the small higher field shift of the silane resonances, as well as the deshielding of the proton atoms of HMPA on silylation. Such shielding decrease is not experienced by the methyl carbon nuclei of HMPA. Analysis of the spectral data of the adduct in solution shows that the complex is largely undissociated in solution. For instance, the solid adduct produced a silicon-29 peak at 24.3 ppm, an upfield change of 6 ppm compared with the uncomplexed silane.

The titration of bromosilane with HMPA followed the same chemical shift trends as that for the chlorosilane. However the progressive low frequency shift and the broadening of the signals were more pronounced, indicative of a larger equilibrium constant for complex formation in the case of the bromosilane. The slow exchange of an equimolar mixture of silane and its HMPA complex, on the carbon-13 and silicon-29 n.m.r. time scale, allows the two entities to be detected separately in these two nuclei. Further addition of HMPA to this mixture disturbs and drives the equilibrium towards the formation of the stable bromosilane-HMPA complex. Thus in the presence of excess HMPA, the spectral data were characteristic of the dominant four coordinate adduct. The slight increase in the proton-phosphorus and carbon-phosphorus coupling

Figure 2.5.1
Proton n.m.r. titration studies of PhCHMeSiMe2X (X=Cl, Br) against HMPA.

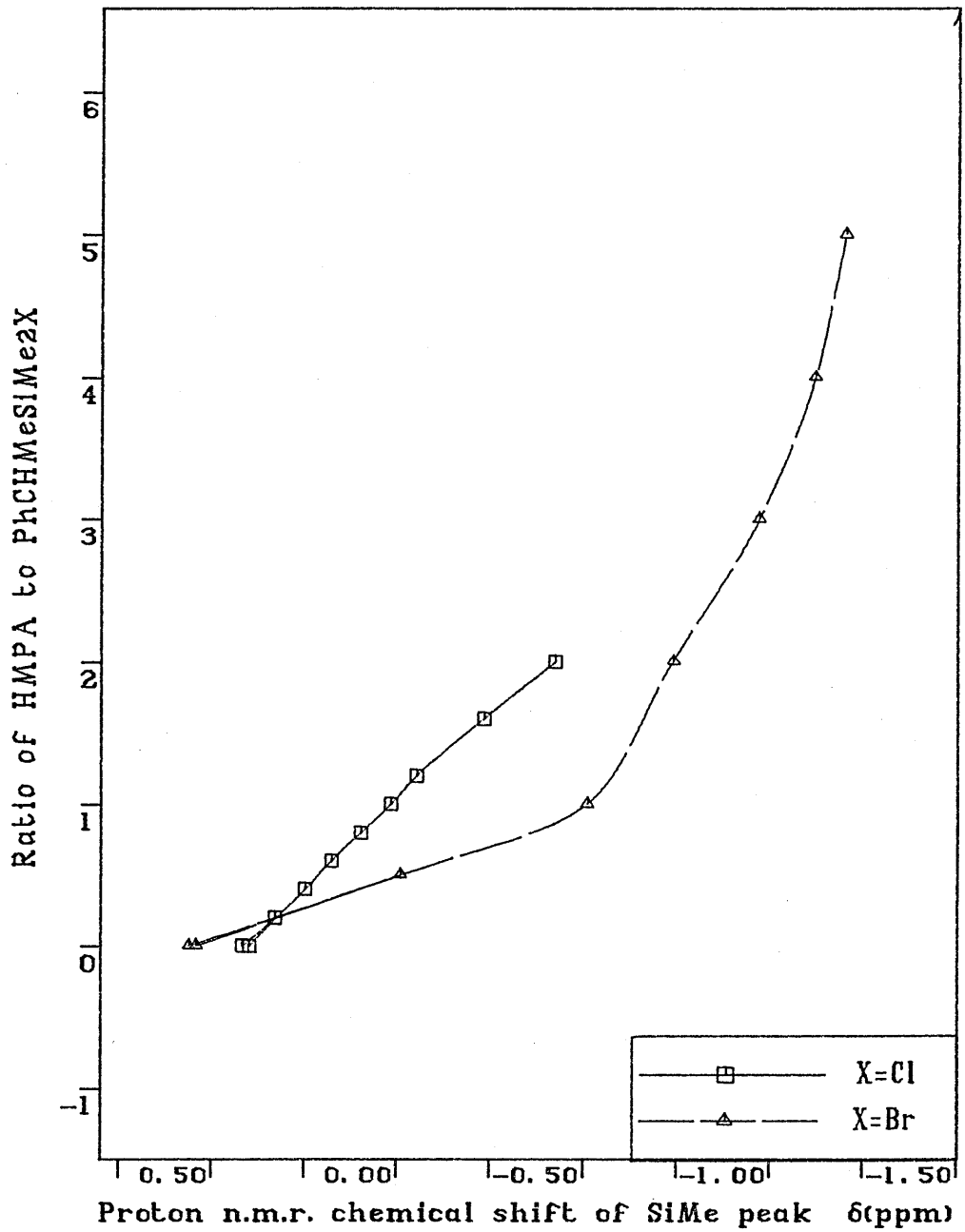

Figure 2.5.2
Carbon-13 n.m.r. titration studies of PhCHMeSiMe2X (X=Cl, Br) against HMPA.

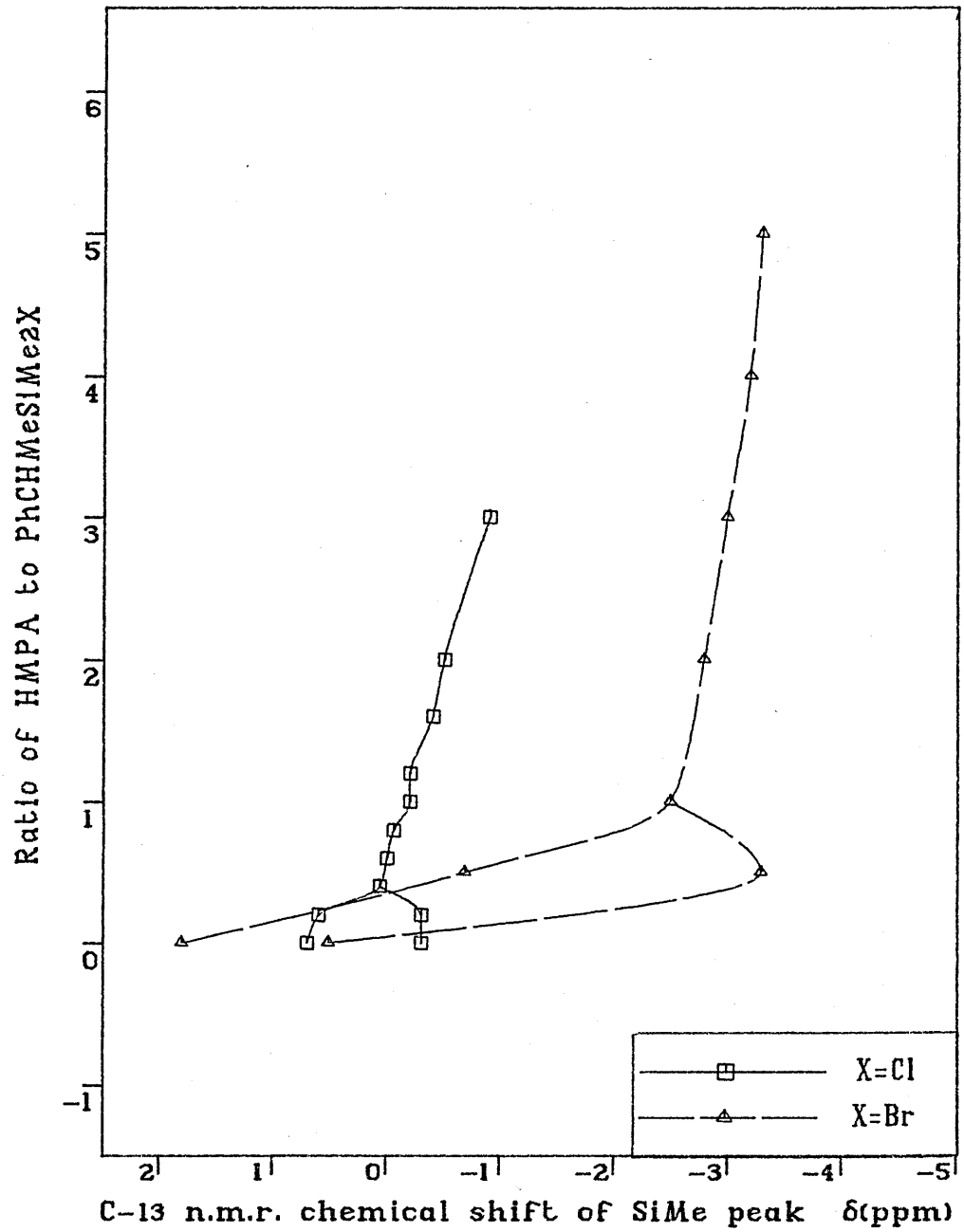

Figure 2.5.3
Silicon-29 n.m.r. titration studies of PhCHMeSiMe2X (X=Cl, Br) against HMPA.

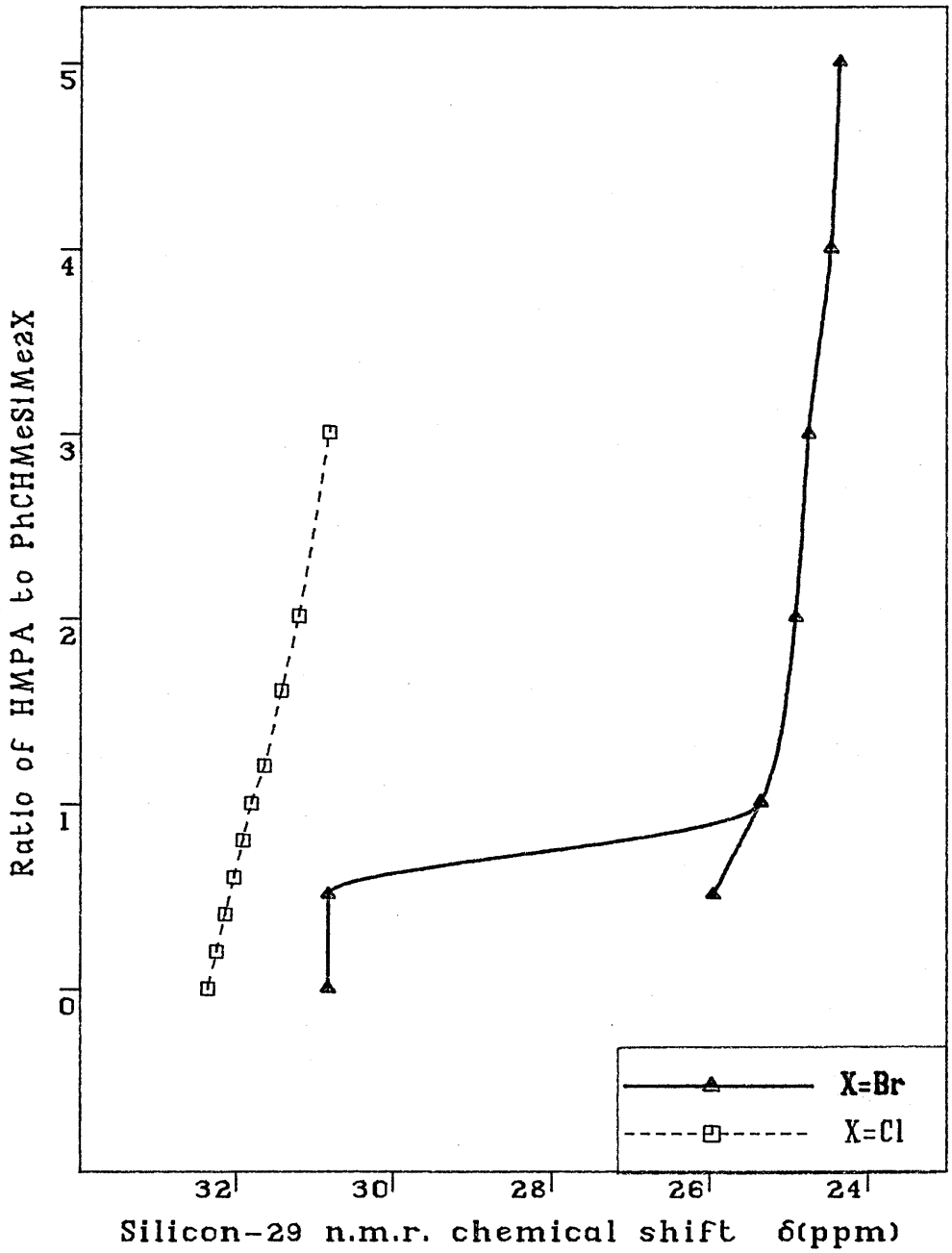

Figure 2.5.4
Variable temperature n.m.r. studies of PhCHMeSiMe2Cl and a 1 : 1.5 mixture of PhCHMeSiMe2Cl and HMPA.

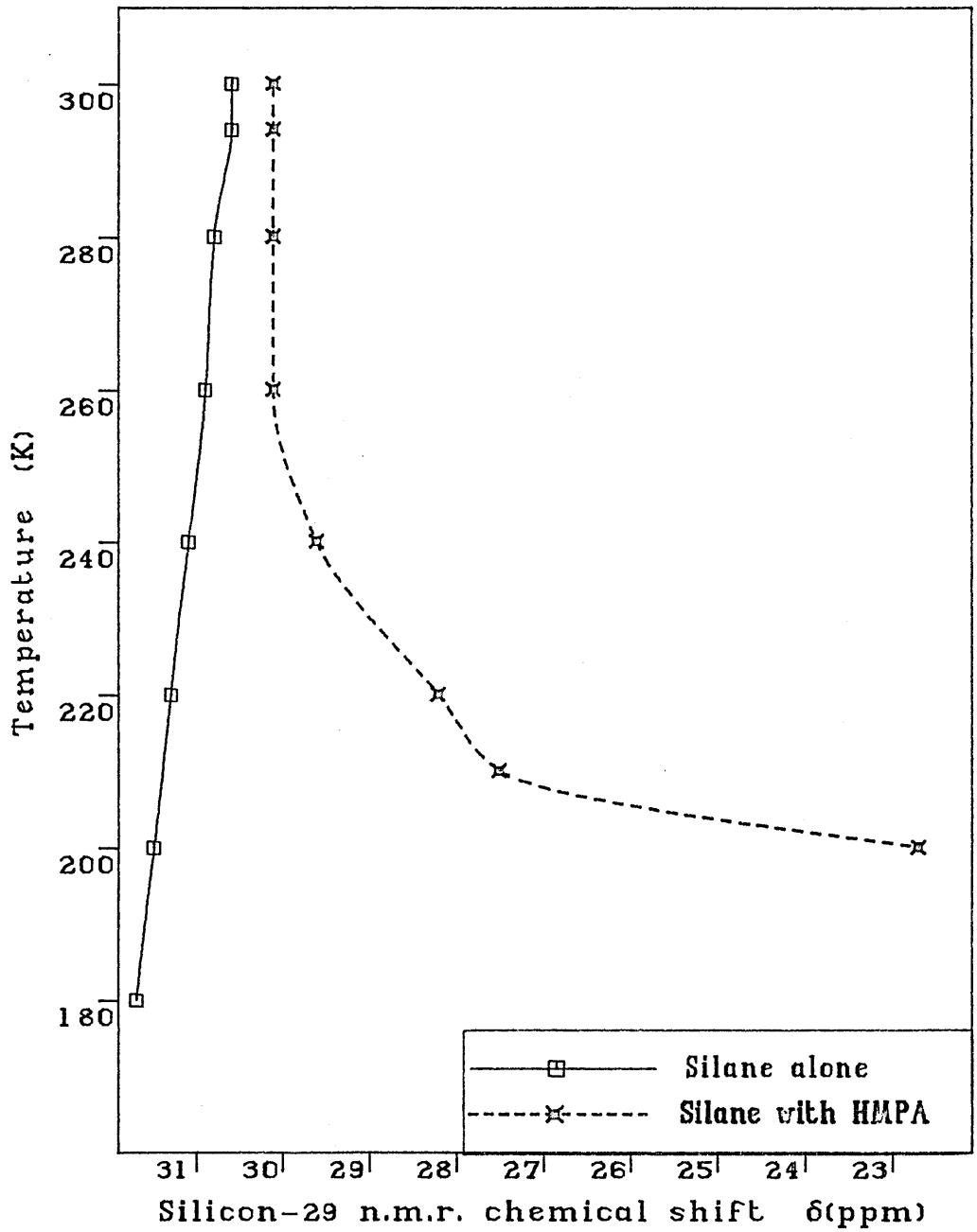

constants also serve as an indicator for the deshielding effect in the HMPA moiety on silylation.

2.5.3 Analysis of results

The interpretation of the chemical shift results, the variable temperature silicon-29 titration of the chlorosilane and HMPA mixture, together with the identification of the bromosilane-HMPA adduct, are fully consistent with a four coordinate ionic complex $[PhCHMeSiMe_2\text{-}HMPA]^+X^-$ (X=Cl, Br) being the dominant species in solution.

The ease of isolation of the solid $[PhCHMeSiMe_2\text{-}HMPA]^+Br^-$ adduct may reflect the greater facility of bromosilane for complex formation, in contrast to that of the chlorosilane, although the lattice energies of each adduct may also be important. Therefore it is predictable that the equilibrium constant for adduct formation increases with the counterions in the order X=Cl < Br. Moreover, the chlorosilane undergoes faster exchange with its HMPA complex compared with the corresponding bromosilane, due to the increased nucleophilicity of the chloride ion over the bromide anion.

These findings are comparable to those observed in the analogous silylation of NMI, which are mainly attributed to two determining factors, namely, the nucleophilicity and the solvating ability of the counterion. The chloride ion is small, hard and a good nucleophile, hence dissociation of the complex via attack of the chloride ion at silicon facilitates the exchange process. In contrast, the larger, diffuse bromide anion is comparatively well solvated and less nucleophilic which stabilize the adduct.

The relative rate of exchange between the silane and its adduct, deduced from the n.m.r. line shapes, increases with nucleophile in the order Nu=NMI < HMPA. This implies that either NMI is not as efficient as HMPA in nucleophilic attack at the silicon atom of a given silane, or the

counterion in the silane-nucleophile adduct is more tightly bound in the case of NMI. Therefore NMI is a poorer catalyst than HMPA for promoting chemical exchange between the silane and its adduct. Furthermore, the unsuccessful preparation of the $[PhCHMeSiMe_2\text{-}HMPA]^+Cl^-$ adduct provides some evidence that $PhCHMeSiMe_2Cl$ forms a more stable complex with the nitrogen donor. However, no such preference is detected in the case of the corresponding bromosilane, since stable $[PhCHMeSiMe_2\text{-}Nu]^+Br^-$ (Nu=NMI, HMPA) adducts have been isolated and identified.

2.6 The $[PhCHMeSiMe_2\text{-}NMPO]^+Br^-$ adduct

The potential of $PhCHMeSiMe_2Br$ for complex formation is further manifested by the synthesis of the solid $PhCHMeSiMe_2Br$-NMPO adduct. The n.m.r. spectral data of the adduct in solution are presented in the experimental chapter. N-Methylpyridone (NMPO) can exist in two tautomeric forms as described in the following scheme, however the oxo tautomer is the predominant species.

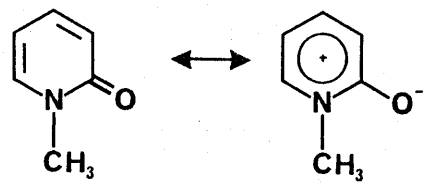

oxo

Scheme 2.6.1 Tautomers of NMPO

The analysis of the spectral data of the solid adduct in solution agrees well with the hypothesis that silylation takes place on the oxygen atom of NMPO. Only a small variation is detected in the chemical shifts of the silane in all three spectra, however the proton and carbon-13 n.m.r. chemical shift changes occur in NMPO on complexation are rather complicated.

Apart from the carbonyl carbon and C_5, deshielding is apparent in the proton and carbon-13 resonances of NMPO. The substantial higher field shift of the carbonyl carbon in the adduct indicates a reduction of

double bond character of the carbonyl group, which is consistent with silylation on oxygen. The enhanced deshielding of the N—Me and C_3—H moieties, adjacent to the carbonyl group, is also a consequence of O-silylation. The mesomeric and inductive delocalization of the positive charge into the ring system is the rationale behind the chemical shift variations in the other carbon atoms. The C_4—H and C_6—H groups are closer to the amide moiety, therefore experience more pronounced inductive effect and hence shift further downfield.

Based upon the spectral data of the NMPO signals as well as the silane resonances in the carbon-13 spectrum, evidence for O-silylation is very strong and dissociation of the complex in solution seems to be insignificant. Therefore, the unexpected similarity between the silicon-29 chemical shifts of the uncomplexed silane and the adduct may be merely coincidental.

2.7 Variable temperature titration studies of $PhCHMeSiMe_2Br$ with nucleophiles (NMI, HMPA)

In order to gain a more comprehensive knowledge of the exchange between the silane and its adduct, and also to ascertain that the chemical shift changes were reversible, variable temperature silicon-29 and carbon-13 n.m.r. studies were undertaken for 2:1 mixtures of $PhCHMeSiMe_2Br$ and nucleophiles (NMI, HMPA) in dichloromethane-d_2. All the recorded spectral data are shown in the appropriate tables in the experimental section. The plots of the silicon-29 and carbon-13 diastereotopic SiMe chemical shifts with temperatures are also provided in the figures.

$PhCHMeSiMe_2Br$ undergoes complexation readily with these two strong nucleophiles, producing stable four coordinate ionic adducts, therefore it is assumed that the 2:1 mixtures of $PhCHMeSiMe_2Br$ and nucleophiles essentially consist of equimolar quantities of the bromosilane and its complex.

Figure 2.7.1

Variable temperature carbon-13 n.m.r. titration studies of 2 : 1 mixtures of PhCHMeSiMe2Br and nucleophile (NMI, HMPA).

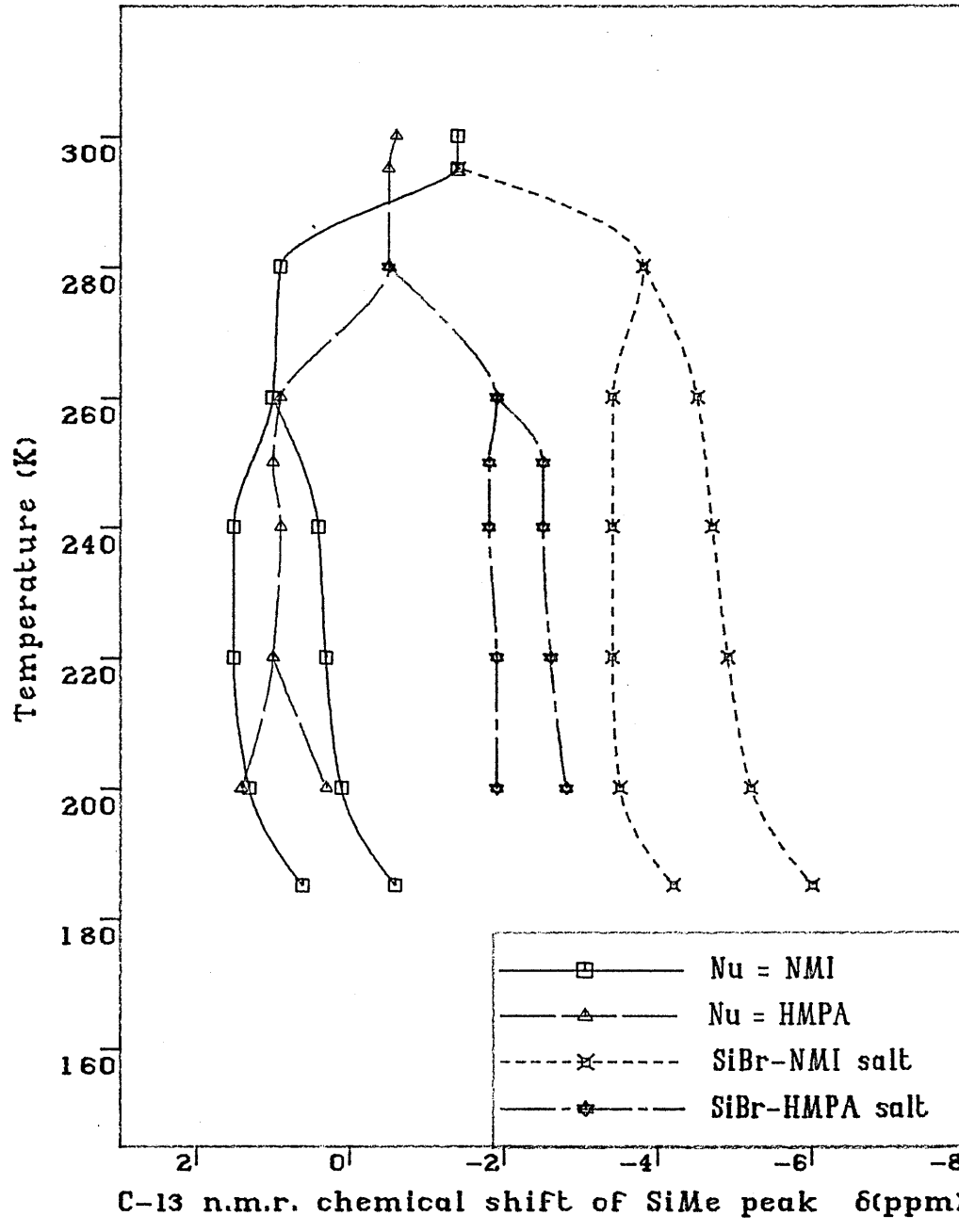

Figure 2.7.2
Variable temperature silicon-29 n.m.r. titration studies of 2 : 1 mixtures of PhCHMeSiMe2Br and nucleophile (NMI, HMPA).

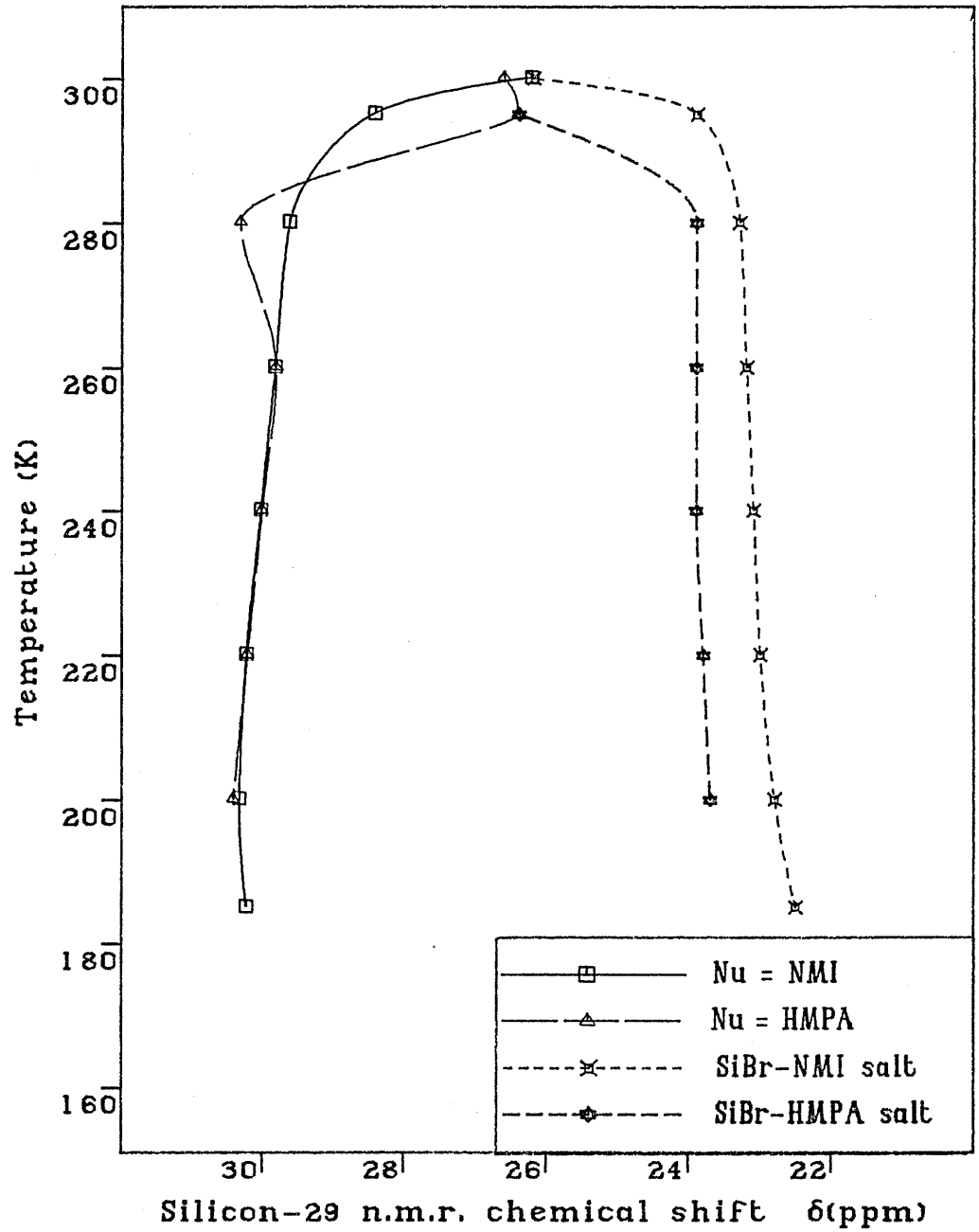

2.7.1 Variable temperature study of $PhCHMeSiMe_2Br$ with NMI

Prior to lowering the temperature of the probe, the mixture displayed silicon-29 and carbon-13 chemical shifts characteristic of signals resulting from the averaging of the silane and its complex. The extremely broad line shapes observed for groups directly attached to the silicon atom are in accord with a slow exchange established between the two silicon species.

As the temperature descended progressively from 300K to 185K, broadening became more significant. On reaching 260K, the two silicon entities were detected separately in the carbon-13 spectrum. The detailed examination of the diastereotopic SiMe resonances reveals a striking and somewhat unexpected finding.

On cooling to 280K, the very broad, average singlet split to produce two peaks with considerable linewidths, corresponding to the exchange between the uncomplexed silane and its imidazolium adduct. Interestingly, as the temperature continues to decrease, the adduct peak collapses to a doublet but the uncomplexed silane remains as an extremely broad singlet. The rate of exchange between these two silicon entities decelerates on cooling, and allows the anisochrony of the two diastereotopic SiMe groups in the complex to be detected, thus two SiMe peaks result.

However, the intense broadening of the singlet of the uncomplexed silane implies that the silane is undergoing chemical exchange. Since NMI is essentially associated with the silane in forming the imidazolium adduct, it is unlikely that this exchange reaction is induced by NMI, this is in accord with the sharpness of the resonances for the silane-NMI complex. This also proves that the adduct is not involved in the racemization of the silane under these conditions.

The nucleophilic attack of the bromide anion of the imidazolium adduct at the silicon atom of the uncomplexed silane is a possible alternative rationalization for such behaviour.[71] On continuous cooling to 240K,

the rate of this exchange reaction decreases further allowing both diastereotopic SiMe signals of the silane to be recorded. The increase in the viscosity of the medium at low temperatures may cause line broadening, leading to averaging of the phenyl resonances.

The silicon-29 n.m.r. spectra of the mixture were taken as the sample was gradually warmed back to ambient temperature; this also confirmed that the chemical shift changes were fully reversible. At low temperatures, the silicon-29 spectra consisted of two peaks due to the bromosilane and its imidazolium adduct respectively. On approaching ambient temperatures, the rate of exchange between these two silicon compounds increases, as indicated by the extreme broadening of the two signals. Eventually at 300K, coalescence occurs giving an average, broad singlet at 26.2 ppm.

2.7.2 Variable temperature study of $PhCHMeSiMe_2Br$ with HMPA

The general chemical shift trends produced by titrating $PhCHMeSiMe_2Br$ with HMPA are consistent with those observed with NMI. Nevertheless, compared with the NMI system, broadening and the subsequent separation into two distinct sets of silane and adduct peaks occurred at lower temperatures.

Deshielding of the methyl carbon nuclei of HMPA in the silylated species is insignificant, although there is a slight increase in the carbon-phosphorus coupling constant. The magnitude of the coupling constant decreases with increasing distance of carbon atom from the phosphorus atom. Therefore it is not surprising that carbon-phosphorus coupling is not detected in the diastereotopic methyl carbon peaks of the silane-HMPA complex even at low temperatures. Nonetheless, a small coupling is registered in the benzylic carbon signal of the adduct, this is possibly due to the presence of the electron releasing substituents on the benzylic carbon centre enhancing the spin-spin coupling. Similarly, silicon-phosphorus coupling can account for the doublet assigned to the

HMPA adduct in the silicon-29 spectra, this further supports the existence of the silane-HMPA complex in the mixture.

The difference between these two variable temperature studies is manifested by the diastereotopic SiMe resonances. On cooling to 250K, the two anisochronous, diastereotopic SiMe moieties of the HMPA adduct become visible whereas those of the uncomplexed silane remain as a singlet until 200K. However with the NMI system, the two SiMe signals of the NMI adduct as well as those of the free silane are already observable at 260K and 240K respectively. These results can be rationalized by assuming a more rapid nucleophilic attack of the bromide anion at the silicon atom of the free silane in the HMPA system. Nevertheless, the previous comparison of the interactions of $PhCHMeSiMe_2Br$ with nucleophiles (NMI, HMPA) at ambient temperature has demonstrated that both nucleophiles are capable of forming stable complexes with the bromosilane. The difference in the rate of this exchange reaction may therefore be governed by the stabilization of the bromide anion by each nucleophile, which is in accord with the observations from the conductivity studies of nucleophilic substitution of halotrimethyl-silanes.[9,70]

The conductivity of an equimolar solution of bromotrimethylsilane, Me_3SiBr, and HMPA is greater than an analogous solution of Me_3SiBr with N-trimethylsilylimidazole. This can be attributed to tighter ion pairing of the bromide ion in the bromosilane-imidazole complex, compared with the bromosilane-HMPA adduct. Thus the higher concentration of the free bromide anion in the HMPA complex enhances the attack at the electrophilic silicon atom.

The attack of bromide ion at the silicon atom of the silane-nucleophile complex leads to dissociation of the complex, yielding free nucleophile and silane with no net change of stereochemistry. Coalescence of the diastereotopic SiMe peaks in the silane-nucleophile complex can only be induced by the attack of a second molecule of nucleophile on the adduct, thus the diastereotopic SiMe signals for the $PhCHMeSiMe_2Br$-HMPA are

anisochronous at low temperatures. However, the bromide ion attack at the silicon atom of an uncomplexed bromosilane molecule results in bromide exchange, accompanied by inversion of configuration at silicon. This helps to explain the collapse of the diastereotopic SiMe peaks of the bromosilane.

2.8 Interactions of $PhCHMeSiMe_2Br$ with tetra-n-butylammonium bromide ($^nBu_4NBr$)

In order to demonstrate that the exchange is induced by the nucleophilic bromide anion of the silane-nucleophile adduct, tetrabutylammonium bromide was used as an alternative source of bromide ion complementary to the nucleophile. The chemical shift titrations of tetrabutylammonium bromide with $PhCHMeSiMe_2Br$ were carried out at various concentrations and under different conditions. The investigations were initially performed by introducing successive aliquots of $PhCHMeSiMe_2Br$ as well as a mixture of $PhCHMeSiMe_2Br$ and HMPA into solutions of tetrabutylammonium bromide. The effect of tetrabutylammonium bromide was further examined by dissolving it in a coalesced mixture of $PhCHMeSiMe_2Br$ and DMPU, and also by syringing DMPU to a solution of $PhCHMeSiMe_2Br$ containing a small quantity of tetrabutylammonium bromide. All the spectral data are tabulated in the experimental section. Apart from the diastereotopic SiMe signals, there were no apparent variations in the chemical shifts in the silicon-29, proton and carbon-13 spectra for all the systems investigated. However, the silicon-29 resonances gradually moved upfield when HMPA was present in the system due to complexation.

2.8.1 Interaction of $^nBu_4NBr$ with $PhCHMeSiMe_2Br$

Immediate coalescence of the two diastereotopic SiMe peaks of $PhCHMeSiMe_2Br$ occurred as the silane was added to a ten molar excess of $^nBu_4NBr$ solution. Further additions of $PhCHMeSiMe_2Br$ led to an equimolar mixture of $PhCHMeSiMe_2Br$ and $^nBu_4NBr$, however the SiMe signal remained as

a sharp singlet. These observations are consistent with the involvement of the bromide ion of tetrabutylammonium bromide, causing the collapse of the two SiMe resonances into a sharp singlet by attacking the electrophilic silicon.

2.8.2 Interaction of $^{n}Bu_4NBr$ with the $[PhCHMeSiMe_2\text{-}HMPA]^{+}Br^{-}$ adduct

As a consequence of the common ion effect, the dissociation of the stable four coordinate $[PhCHMeSiMe_2\text{-}HMPA]^{+}Br^{-}$ ionic complex should be favoured in the presence of tetrabutylammonium bromide. With a ten fold excess of tetrabutylammonium bromide, the extensive broadening of the silicon-29 n.m.r. signal at 28.4 ppm corresponds to the chemical exchange between the uncomplexed bromosilane and the silane-HMPA adduct. In comparison with the chemical shifts of the uncomplexed silane at 29.2 ppm and its HMPA salt at 24.3 ppm, the peak at 28.4 ppm indicates that the equilibrium lies towards the uncomplexed $PhCHMeSiMe_2Br$. This is consistent with the operation of a common ion effect enhancing the dissociation of the silane-HMPA adduct. Apart from exchanging with its HMPA complex, the uncomplexed silane also undergoes exchange with the bromide ion of tetrabutylammonium bromide, however this is a degenerate exchange and will not cause line broadening.

Nevertheless as the proportion of the silane-HMPA adduct increased, only a slightly broadened singlet at 24.2 ppm was recorded. Tetrabutyl-ammonium bromide can act as a common ion as well as a polar solvent. As the dominant species in solution, $^{n}Bu_4NBr$ pushes the equilibrium towards the side of the uncomplexed silane and free HMPA by facilitating the dissociation of the complex. Nonetheless, when the silane-HMPA adduct is present in a similar ratio, the relative proportion of bromide ion from tetrabutylammonium bromide decreases. Furthermore $^{n}Bu_4NBr$ may behave as a polar solvent stabilizing the ionic complex; these two factors drive the equilibrium towards the adduct formation.

2.8.3 Interaction of $PhCHMeSiMe_2Br$ with an equimolar quantities of tetrabutylammonium bromide and DMPU

Since the bromide ion is responsible for the coalescence of the two diastereotopic SiMe peaks of $PhCHMeSiMe_2Br$, further studies were undertaken to compare the nucleophilic strength of the bromide ion with that of a good nucleophile such as dimethylpropyleneurea (DMPU). The addition of $^nBu_4NBr$ to a bromosilane solution causes immediate collapse of the SiMe peaks yielding a very sharp singlet. However an extremely broad, coalesced resonance results when the same concentration of DMPU was added to an analogous bromosilane solution.

Furthermore, the introduction of an equimolar ratio of $^nBu_4NBr$ to a coalesced mixture of bromosilane and DMPU leads to instantaneous sharpening of the broadened SiMe peak. These findings are also in accord with the results obtained from the interaction of a mixture of $PhCHMeSiMe_2Br$ and $^nBu_4NBr$ with DMPU. The two diastereotopic SiMe resonances of the silane collapsed to a sharp singlet when only a small amount of $^nBu_4NBr$ was used. The observed line shapes and the chemical shifts are unaffected by the addition of a small quantity of DMPU. These results imply that the bromide ion is a more effective nucleophile than DMPU since it induces faster coalescence of the SiMe peaks.

2.8.4 Summary

The halide counterion of a four coordinate silane-nucleophile ionic complex is proved to be intimately involved in the racemization of halosilane. The concentration of the halide ion depends upon the stability of the four coordinate ionic adduct. $PhCHMeSiMe_2Br$ forms stable 1:1 ionic complexes with NMI and HMPA, however the $[PhCHMeSiMe_2\text{-}NMI]^+Br^-$ adduct is found to be more tightly ion paired in contrast to the HMPA counterpart. Thus in the NMI system, a smaller proportion of labile bromide ion is available for nucleophilic attack at the silicon atom of $PhCHMeSiMe_2Br$, resulting in a slower rate of exchange. The observations

from the titration studies of tetrabutylammonium bromide not only demonstrate the catalytic promotion of the bromide exchange of bromosilane by bromide ion, they also show that the common ion effect only becomes important when a large excess of free bromide ion is present in the system.

2.9 Interactions of a mixture of $PhCHMeSiMe_2Cl$ and $PhCHMeSiMe_2Br$ with nucleophiles (NMI, HMPA)

From the preceding discussion, it can be concluded that the stability of a four coordinate ionic silane-nucleophile complex is dependent upon the nature of the counterion. Furthermore, the magnitude of the equilibrium constant for complex formation for a given counterion is controlled by the attacking nucleophile. Comparisons of the $PhCHMeSiMe_2Br$ and $PhCHMeSiMe_2Cl$ titrations with nucleophiles (NMI, HMPA) indicate that the chlorosilane forms less stable ionic complexes and undergoes much faster chemical exchange with its adduct. In addition, the bromide ion of the adduct is well solvated and induces a rapid racemization of the bromosilane.

These findings are further verified by titrating an equimolar mixture of $PhCHMeSiMe_2Cl$ and $PhCHMeSiMe_2Br$ with nucleophiles (NMI, HMPA) at ambient and variable temperatures. The spectral data are provided in the appropriate tables in Chapter 6. Again, the proton, carbon-13 and silicon-29 chemical shifts of the diastereotopic SiMe groups are presented in the accompanying figures.

2.9.1 Interaction of the mixture of $PhCHMeSiMe_2Cl$ and $PhCHMeSiMe_2Br$ with HMPA

Coalescence of diastereotopic SiMe peaks was not observed in the variable temperature study on a 1:1 mixture of $PhCHMeSiMe_2Cl$ and $PhCHMeSiMe_2Br$, this is indicative of the absence of exchange between these two silicon

species. As a consequence of titrating the mixture with HMPA, both the proton and silicon-29 signals shifted slightly upfield, however such changes are not apparent in the carbon-13 spectra apart from the SiMe peaks. Only the silicon-29 signals as well as those resonances for moieties attached to the silicon atom in the proton and carbon-13 n.m.r. spectra show intense line broadening. With increasing concentration of HMPA, the CH resonance in the proton spectra became obscured by the HMPA doublet, therefore it is not possible to assign this signal. Although the proton atoms and the methyl carbon nuclei of HMPA are not deshielded significantly as would be expected on silylation, there is a slight increase in the proton-phosphorus and carbon-phosphorus coupling constant.

The changes in the proton chemical shifts follow a similar pattern to that observed in the carbon-13 spectra. Deductions from the proton, carbon-13 and silicon-29 spectral data are consistent with the operation of several dynamic processes. The addition of a 0.1 molar equivalent of HMPA to the mixture of silanes leads to an immediate coalescence of the two diastereotopic SiMe signals of $PhCHMeSiMe_2Br$ yielding a singlet, whereas those of the chlorosilane remain unchanged until more HMPA is introduced. This is in accord with the expected behaviour, since the bromosilane has a greater tendency in forming a stable complex with HMPA than its chloride counterpart. Thus nucleophilic attack by HMPA is mainly at the silicon atom of the bromosilane with the generation of bromide ion, which in turn promotes rapid halide exchanges of the chloro- and bromosilanes. Similarly, the small chloride ion produced by the attack of bromide ion at the chlorosilane can also induce halide exchanges of the two silanes.

The transient, unstable $[PhCHMeSiMe_2\text{-}HMPA]^+Cl^-$ adduct dissociates readily releasing uncomplexed HMPA, which then complexes with $PhCHMeSiMe_2Br$ or undergoes exchange with $[PhCHMeSiMe_2\text{-}HMPA]^+Br^-$. The attack of HMPA at the silicon atom of the $[PhCHMeSiMe_2\text{-}HMPA]^+Br^-$ complex is facilitated with respect to the isolated bromosilane, since HMPA is an excellent, neutral leaving group compared with the bromide ion. Thus the exchange

Figure 2.9.1

Proton n.m.r. titration study of a 1 : 1 mixture of PhCHMeSiMe2X (X=Cl, Br) against HMPA.

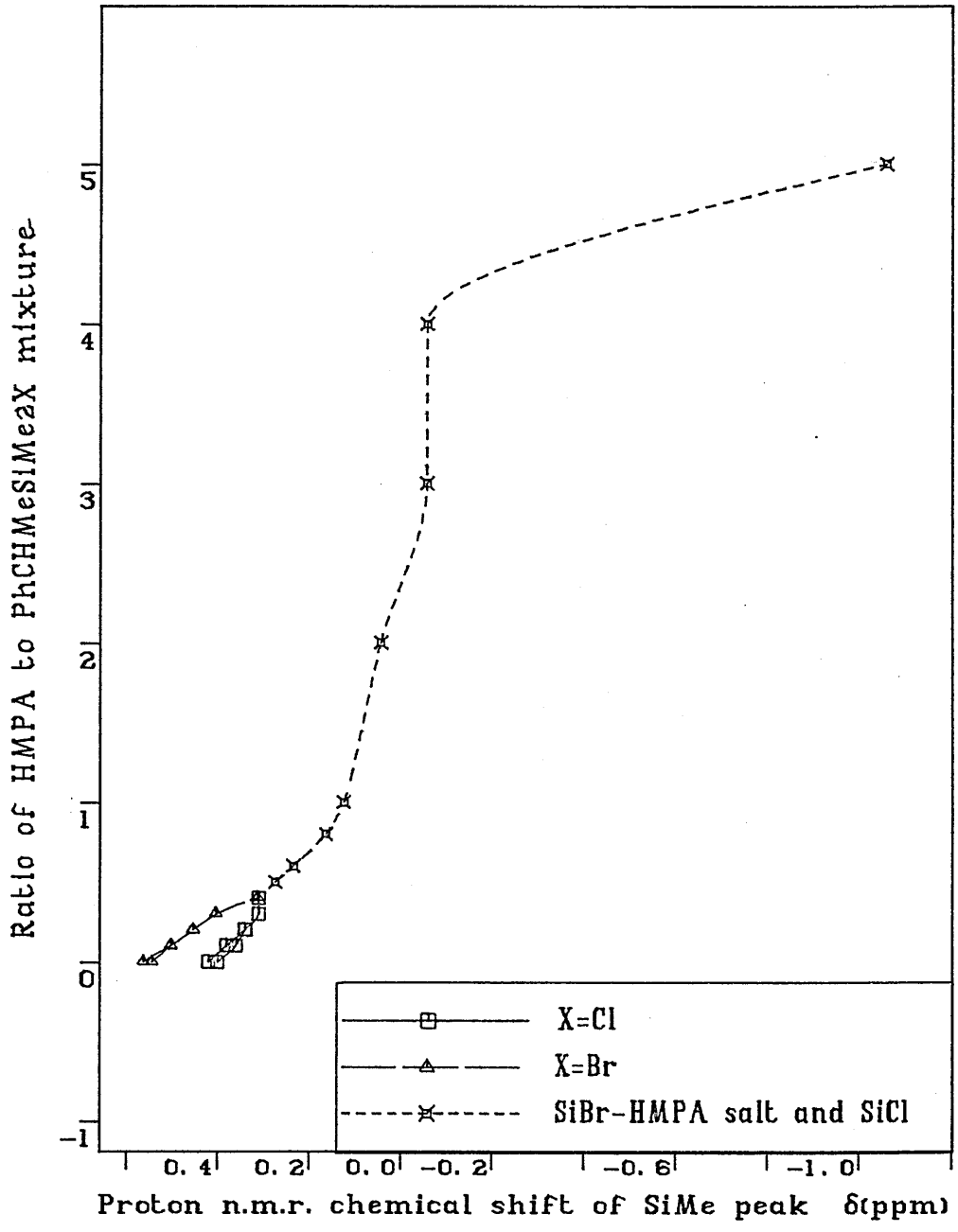

Figure 2.9.2

Carbon-13 n.m.r. titration study of a 1 : 1 mixture of PhCHMeSiMe2X (X=Cl, Br) against HMPA.

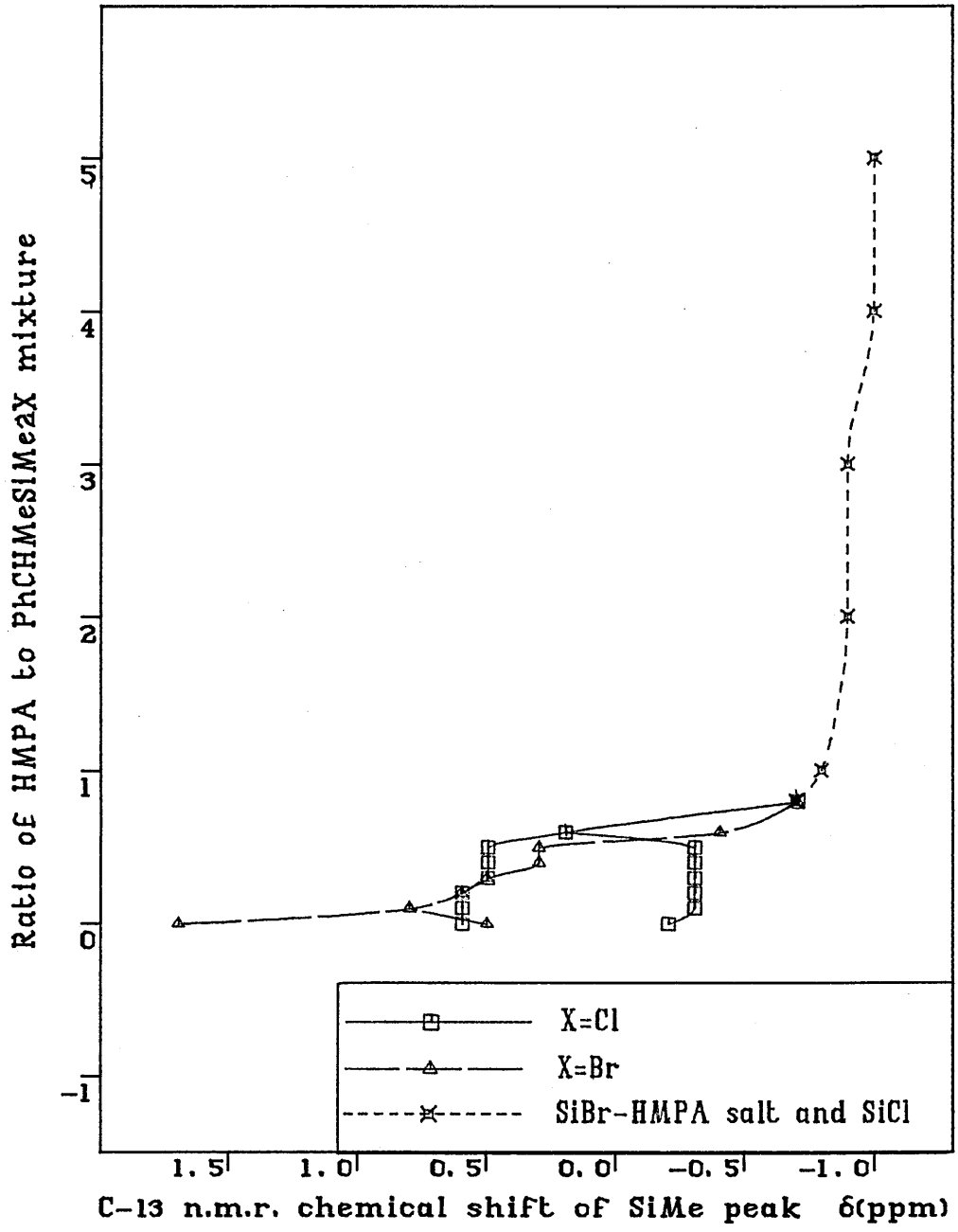

Figure 2.9.3

Silicon-29 n.m.r. titration study of a 1 : 1 mixture of PhCHMeSiMe2X (X=Cl, Br) against HMPA.

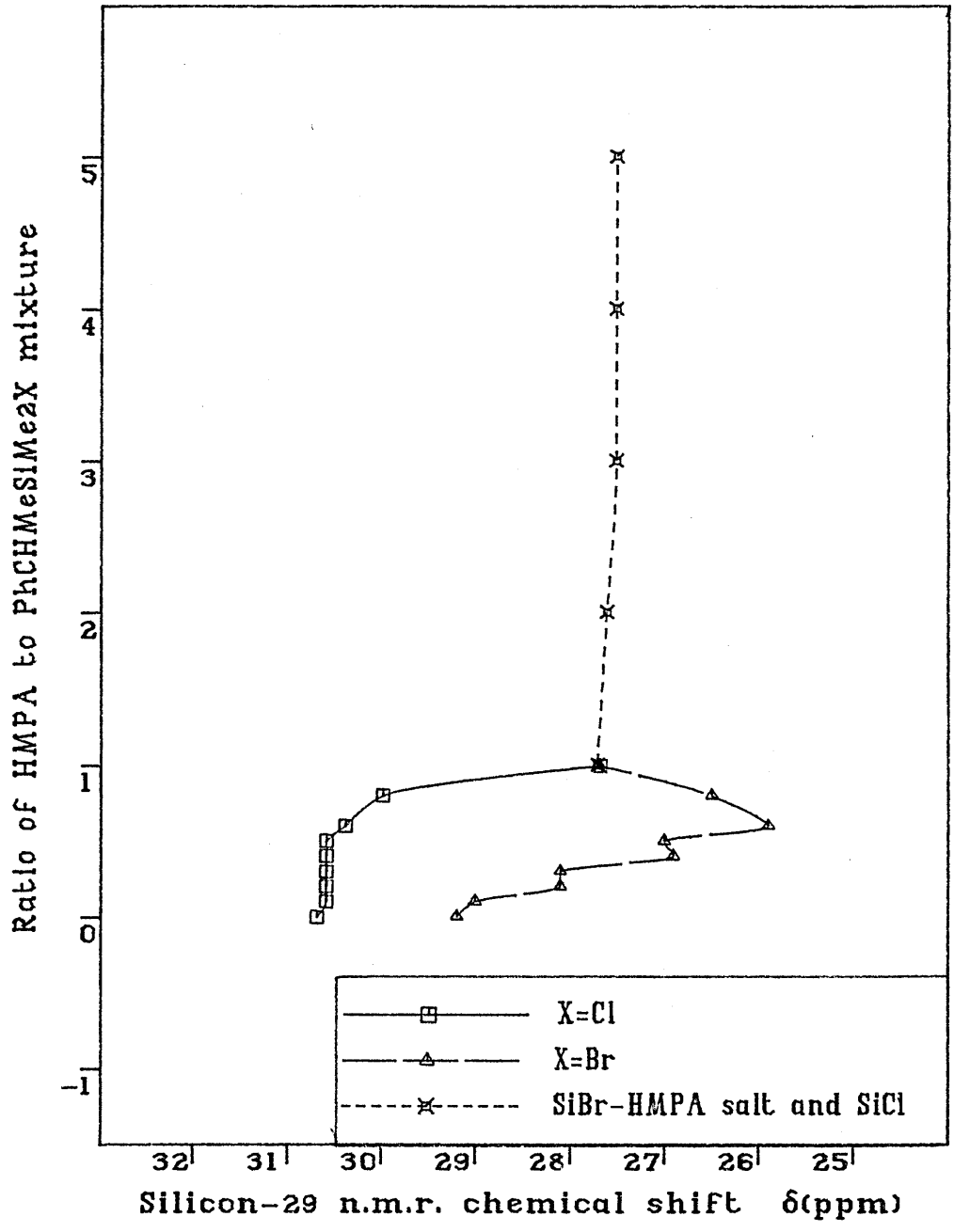

between $PhCHMeSiMe_2Br$ and its HMPA salt is greatly enhanced in the presence of the chlorosilane.

The formation of the bromosilane-HMPA ionic complex is favoured with increasing concentration of nucleophile. Hence $PhCHMeSiMe_2Cl$ and $[PhCHMeSiMe_2\text{-}HMPA]^+Br^-$ adduct become the major species present at high proportion of HMPA. Consequently, a dynamic equilibrium is also established between these two silicon species and averaging of the SiMe signals of $PhCHMeSiMe_2Cl$ results. This finding agrees well with the observation by Cartledge[72,73] on HMPA catalysed halide exchange between bromo- and chlorosilanes, which also take place via ionic intermediates.

2.9.2 Interaction of the mixture of $PhCHMeSiMe_2Cl$ and $PhCHMeSiMe_2Br$ with NMI

By analogy with the HMPA system, the chemical shift titration with NMI exhibits similar behaviour except for the proton spectra, where anomalous downfield shifts of the SiMe and CH signals are recorded. Furthermore, contrary to the HMPA titration, line broadening is more pronounced in the resonances of the groups adjacent to silicon, indicative of a slower exchange. Deshielding and broadening of the NMI peaks are significant particularly at the C_2 position, which strongly support the formation of an ionic imidazolium complex on silylation.

2.9.3 Variable temperature study on the mixture with HMPA

A variable temperature proton n.m.r. chemical shift study was performed on a mixture consisting of an equimolar ratio of $PhCHMeSiMe_2Cl$ and $PhCHMeSiMe_2Br$, together with a 0.45 molar equivalent of HMPA. Prior to varying the temperature of the probe, the proton n.m.r. spectrum of the sample and the very broad, average SiMe resonance were consistent with chemical exchanges taking place in the system. Apart from the SiMe and,

Figure 2.9.4

Proton n.m.r. titration study of a 1 : 1 mixture of PhCHMeSiMe2X (X=Cl, Br) against NMI.

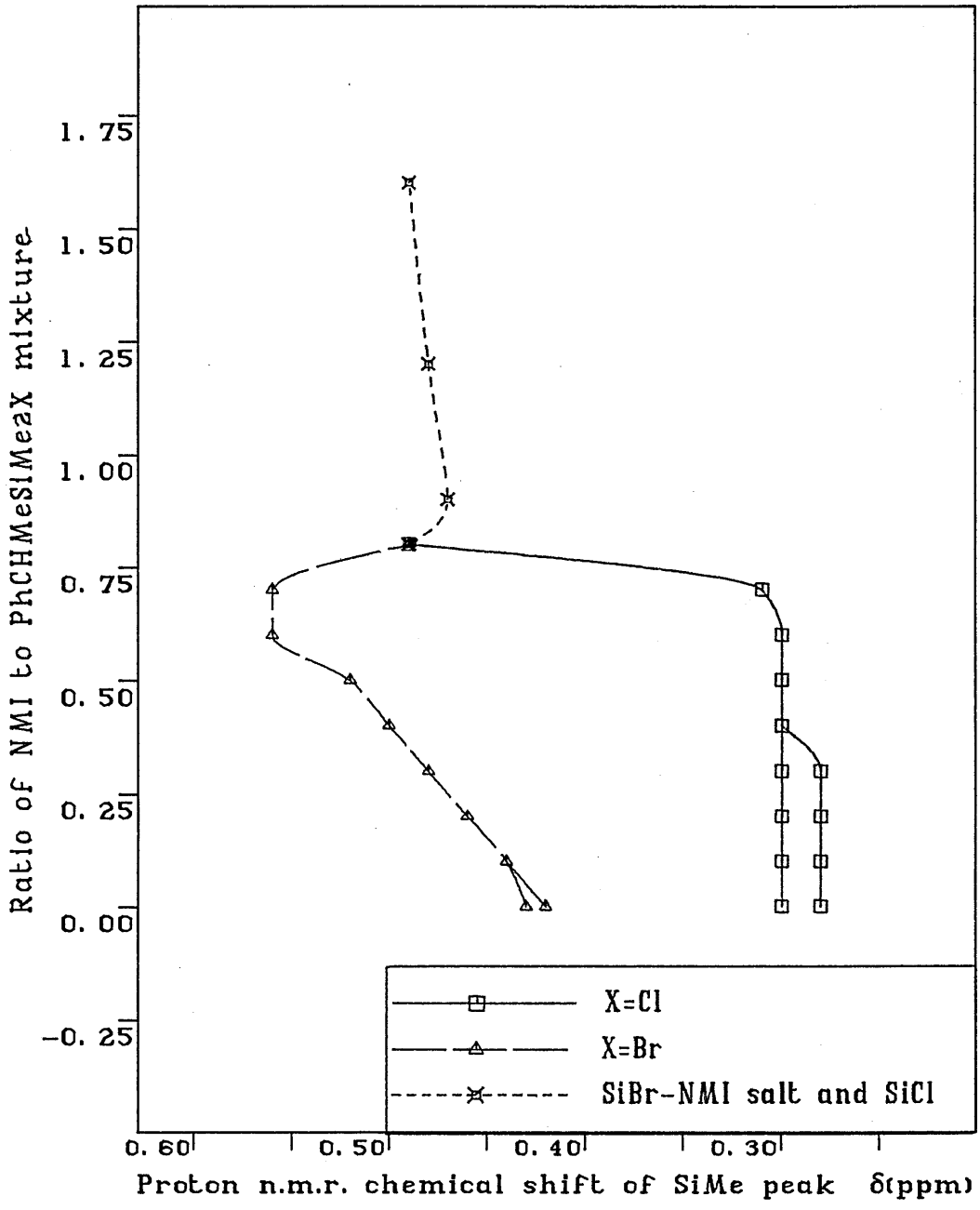

Figure 2.9.5

Carbon-13 n.m.r. titration study of a 1 : 1 mixture of PhCHMeSiMe2X (X=Cl, Br) against NMI.

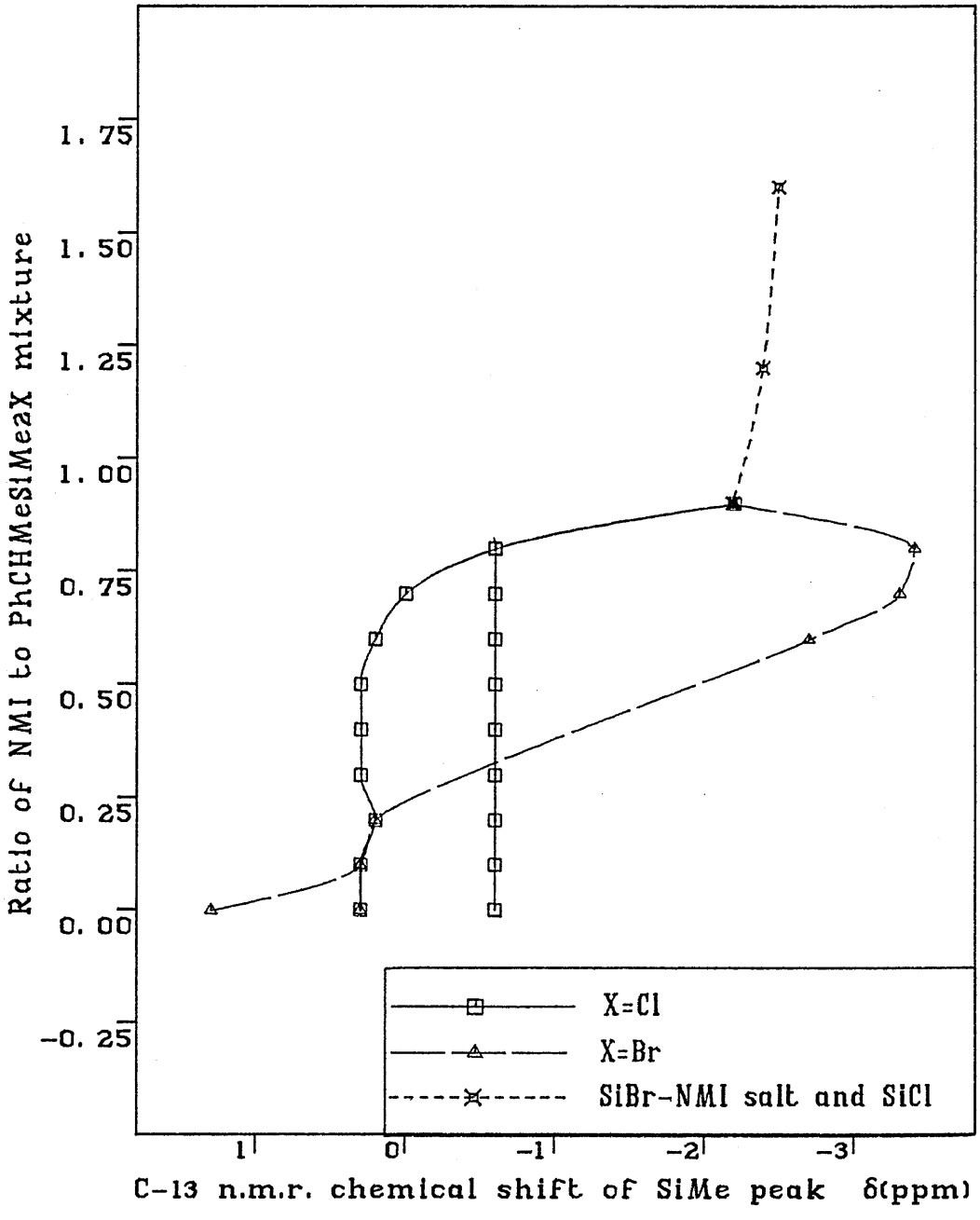

Figure 2.9.6

Silicon-29 n.m.r. titration study of a 1 : 1 mixture of PhCHMeSiMe2X (X=Cl, Br) against NMI.

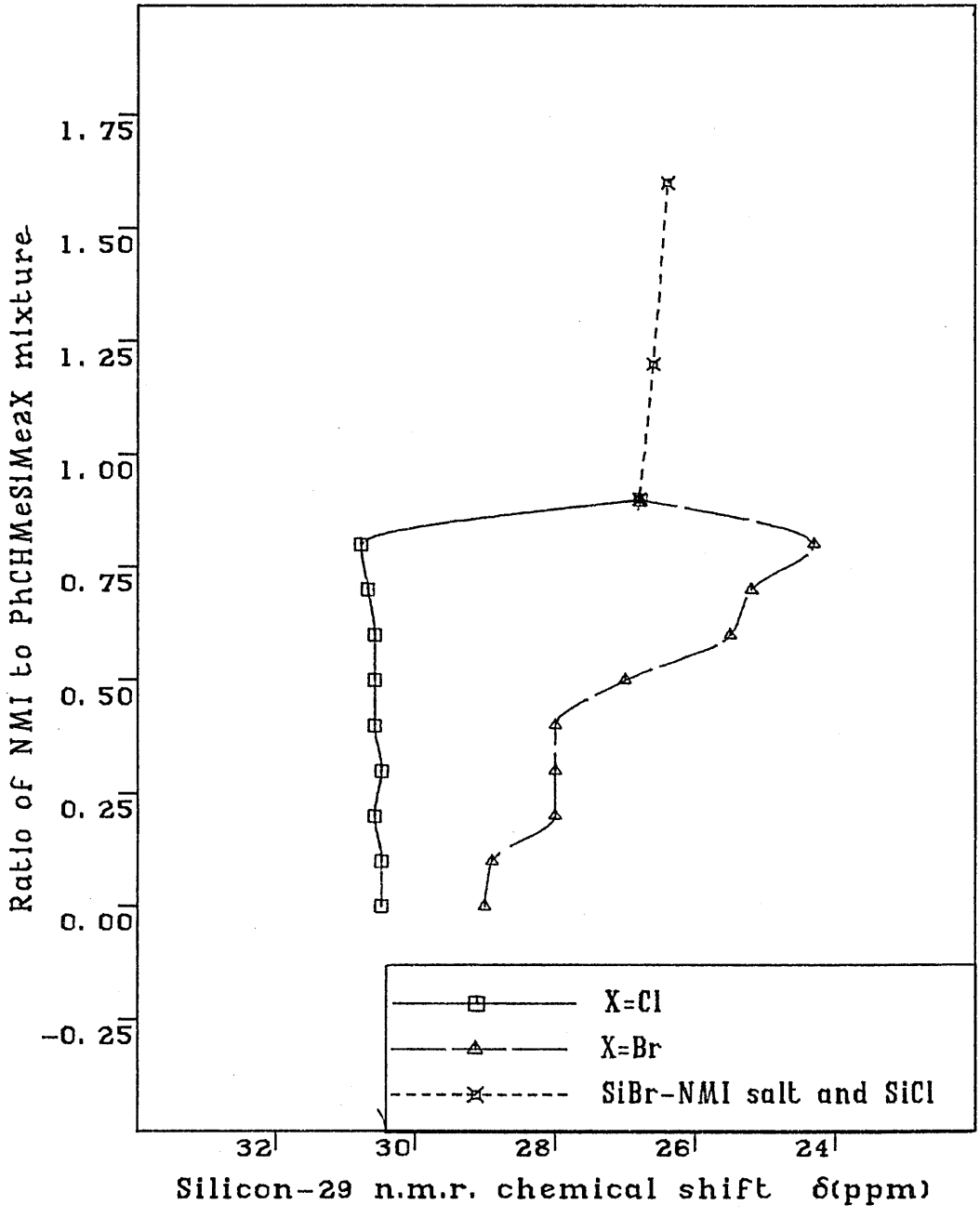

to a lesser degree, the Me signals, there is no apparent change in the remaining chemical shifts on progressive lowering of temperature.

On cooling to 290K, the SiMe singlet split to give two peaks at 0.33 and 0.37 ppm attributable to $PhCHMeSiMe_2Cl$ and the two exchanging silyl bromide species respectively. As the temperature continues to decrease, a shoulder gradually develops on the SiMe singlet of the chlorosilane. Eventually two symmetrical peaks at 0.31 and 0.28 ppm are observed, corresponding to the two diastereotopic groups in $PhCHMeSiMe_2Cl$. Such behaviour is in accord with the deceleration of the rate of exchange between the chlorosilane and the silane-HMPA adduct with decreasing temperatures.

In addition, rate retardation of the exchange between the bromosilane and its HMPA adduct results upon further cooling, accompanied by progressive line broadening of the coalesced singlet for these two exchanging silicon species. Finally at 250K, the proton spectrum gives two separate resonances for the diastereotopic SiMe groups of the HMPA adduct and a slightly broadened singlet for those of the bromosilane. Again, the collapse of the two SiMe signals in the bromosilane can be rationalized by rapid nucleophilic attack of the bromide ion, causing inversion at silicon of the bromosilane.

Thus the interpretation of the spectral data produces an order for the relative rate of the three dynamic processes, compared with the proton n.m.r. time scale. The exchange between $PhCHMeSiMe_2Cl$ and the $[PhCHMeSiMe_2\text{-}HMPA]^+Br^-$ complex is slower than the exchange of $PhCHMeSiMe_2Br$ with its HMPA adduct, which is in turn slower than the racemization of the bromosilane.

Figure 2.9.7
Variable temperature proton n.m.r. titration study of a 1 : 1 : 0.45 mixture of PhCHMeSiMe2X (X=Cl, Br) and HMPA.

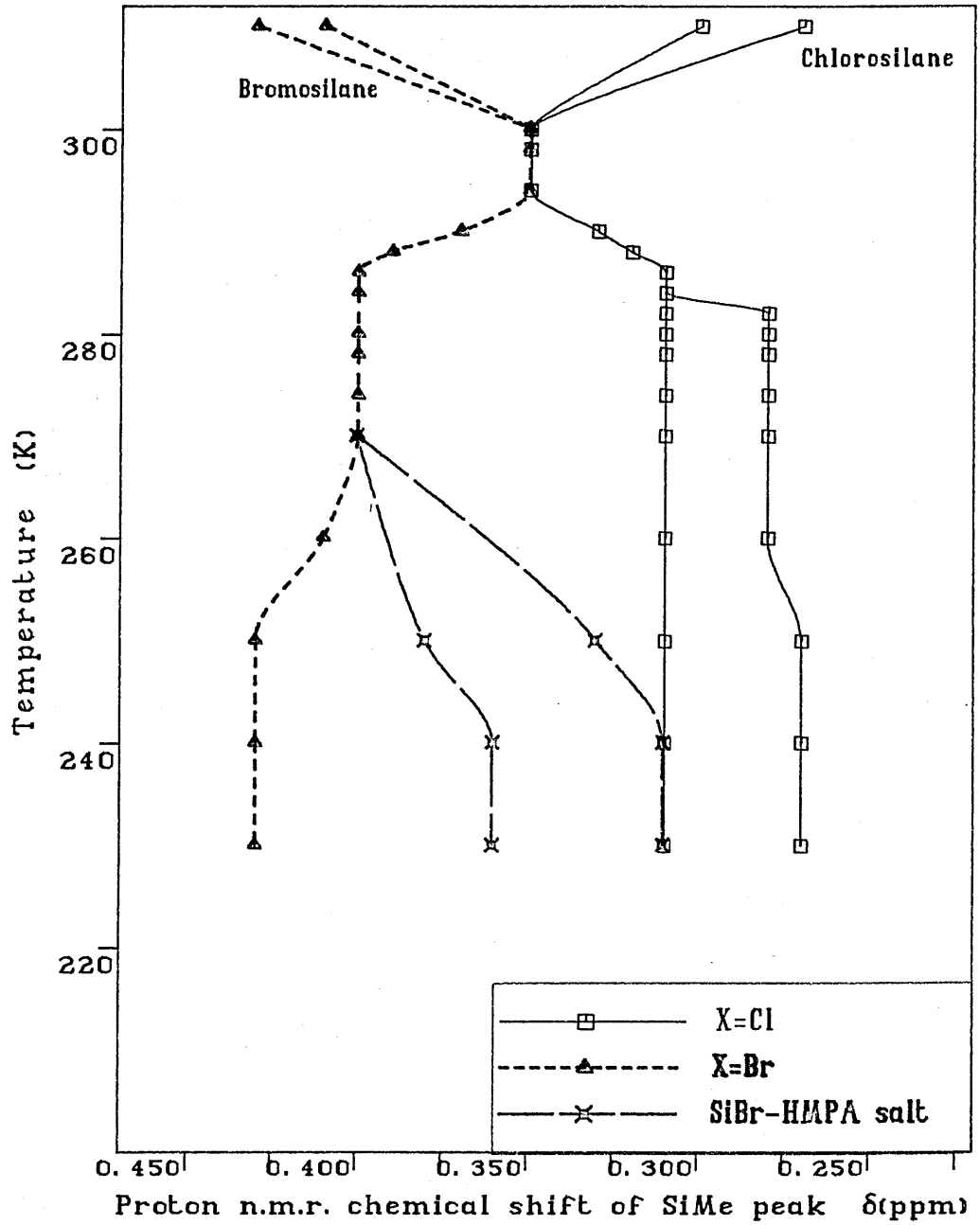

2.10 Interactions of chloromethylphenylsilane (PhMeHSiCl) with nucleophiles (NMI, HMPA, DMF)

In contrast to the diastereotopic silyl systems, evidence for five coordination has been provided by the chemical shift trends of the interaction between methylphenylsilyl triflate ($PhMeHSiOSO_2CF_3$) with N-methylimidazole.[74] Therefore it is interesting to investigate whether an analogous pentacoordinate complex is produced by varying the leaving group from triflate to chloride. The titrations of nucleophiles (NMI, HMPA, DMF) with PhMeHSiCl were monitored by proton, carbon-13 and silicon-29 n.m.r. spectroscopy. All the spectral results are shown in the experimental section. The chemical shift changes in the SiMe moiety are illustrated in the accompanying figures.

2.10.1 Interaction of PhMeHSiCl with 1-methylimidazole (NMI)

Successive additions of aliquots of NMI to PhMeHSiCl, until a 1:3 ratio of PhMeHSiCl to NMI was reached, resulted in a steady and marked low frequency shift of 88 ppm in the silicon-29 spectra, from an initial value of 5.2 ppm. This behaviour is accompanied by a slight broadening of the silicon line shapes, indicating that the silicon species are exchanging with each other. Thus the shape of the titration curve and the exchange behaviour at low ratios of PhMeHSiCl to NMI are consistent with the formation of a pentacoordinate PhMeHSiCl-$(NMI)_2$ complex, which is undergoing fast exchange with the four coordinate 1:1 PhMeHSiCl-NMI complex. This four coordinate adduct in turn exchanges relatively slowly, on the silicon-29 n.m.r. time scale, with the uncomplexed PhMeHSiCl as evidenced by the broad signals, until a 2 molar excess of NMI was present.

The silane resonances experience a small down frequency change in the proton and carbon-13 n.m.r. spectra, except for the carbon-13 SiMe signal which moves downfield with increasing concentration of NMI. On silylation, deshielding of the NMI resonances results which is manifested

by the high frequency chemical shift changes, particularly at the imidazolium C_2-H proton.

The chemical shift trends in the silicon-29 n.m.r. spectra of PhMeHSiCl are similar to those of $PhMeHSiOSO_2CF_3$, indicating that an analogous complex is formed irrespective of counterion. Thus the observations are in accord with a comparable reaction scheme.

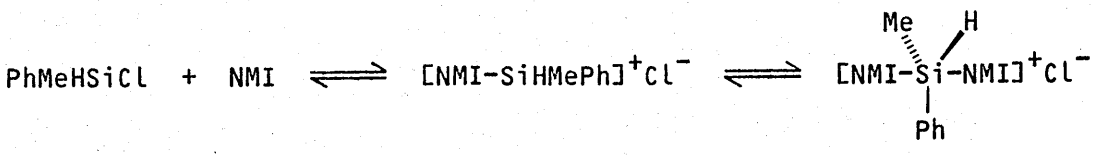

Scheme 2.10.1

The five coordinate solid adduct, hydridomethylphenyl-bis-(3-methyl-1-imidazolium) silicon (IV) chloride $[PhMeHSi-(NMI)_2]^+Cl^-$, has been synthesed. Its n.m.r. spectral data in solution, especially the broadened silicon-29 chemical shift at -50 ppm, strongly imply the presence of a five coordinate complex and that dissociation of the adduct into its components is not substantial.

2.10.2 Interaction of PhMeHSiCl with N,N-dimethylformamide (DMF)

The proton and carbon-13 chemical shift titration of PhMeHSiCl with DMF failed to show any significant changes attributable to adduct formation, since the spectral data remained essentially the same even in a four molar excess of DMF. However, the 2 ppm upfield shift of the silicon-29 signal was accompanied by intense broadening, which was indicative of a very slow exchange.

Furthermore, an interesting feature was noted in the proton NMe resonances of DMF. The chemical shift separation between the two NMe peaks reduced by 5Hz from an initial value of 7.8Hz, when the ratio of PhMeHSiCl to DMF reached 1:0.8. A gradual increase in the chemical shift

difference between these two signals was observed upon further addition of DMF. This anomalous behaviour was also exhibited in the silylation of DMF by chlorodimethylphenylsilane, $PhMe_2SiCl$. Thus these two systems were further investigated and a detailed rationalization of the results will be discussed in the following section.

The insignificant adduct formation may be due to a very small equilibrium constant for complexation at ambient temperatures, therefore a low temperature silicon-29 n.m.r. study was undertaken for 1:3 mixture of PhMeHSiCl and DMF. Cooling the solution mixture down to 200K induced a low frequency shift of 3 ppm from a value of 3 ppm for the uncomplexed PhMeHSiCl, and a pronounced reduction in peak intensity due to exchange broadening. Enhanced complex formation is not apparent even at low temperatures. Nevertheless, these two trends are fully consistent with a slight shift towards complex formation.

2.10.3 Interaction of PhMeHSiCl with hexamethylphosphoramide (HMPA)

HMPA is a more efficient oxygen donor than DMF therefore it is expected to behave differently with PhMeHSiCl. Titration of HMPA against PhMeHSiCl caused the n.m.r. resonances of all three nuclei to move steadily upfield. The shape of the proton titration curve for the SiMe signal is analogous to that observed in the NMI system. This clearly implies that the interaction with HMPA follows a similar reaction pathway to that with NMI. When the silane and HMPA mixture reached a 1:1 stoicheiometry, sharp points of inflexion occurred in both the proton and carbon-13 titration curves, which can be rationalized by the formation of a second type of complex.

Nevertheless, such adduct formation is not reflected to a great extent in the silicon-29 spectra. Furthermore, the silicon-29 titration curve exhibits completely different behaviour to that observed for the titration of NMI. With a five fold excess of HMPA, the silicon-29 signal

Figure 2.10.1
Proton n.m.r. titration studies of PhMeHSiCl against nucleophiles (NMI, HMPA, DMF).

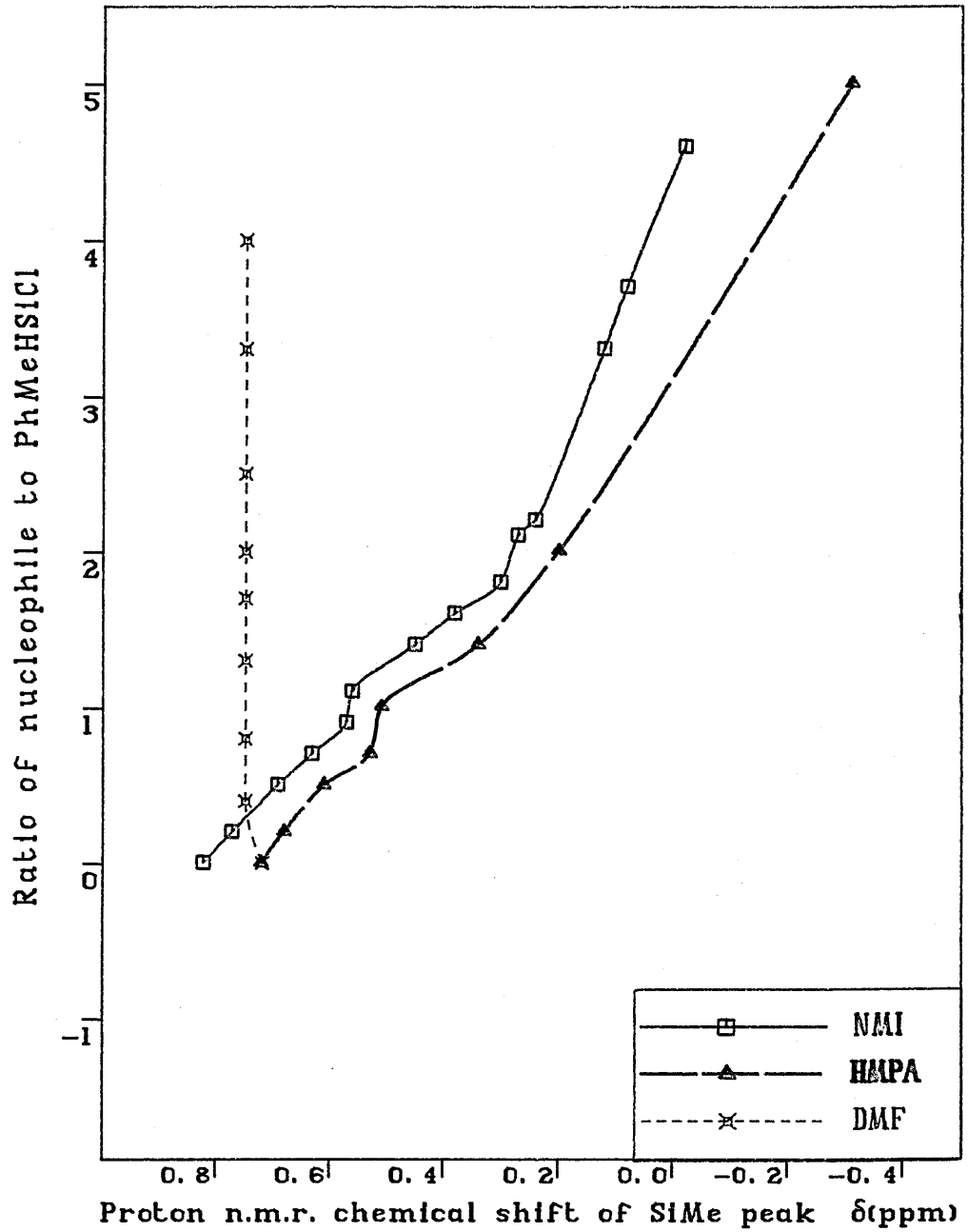

Figure 2.10.2
Carbon-13 n.m.r. titration studies of PhMeHSiCl against nucleophiles (NMI, HMPA, DMF).

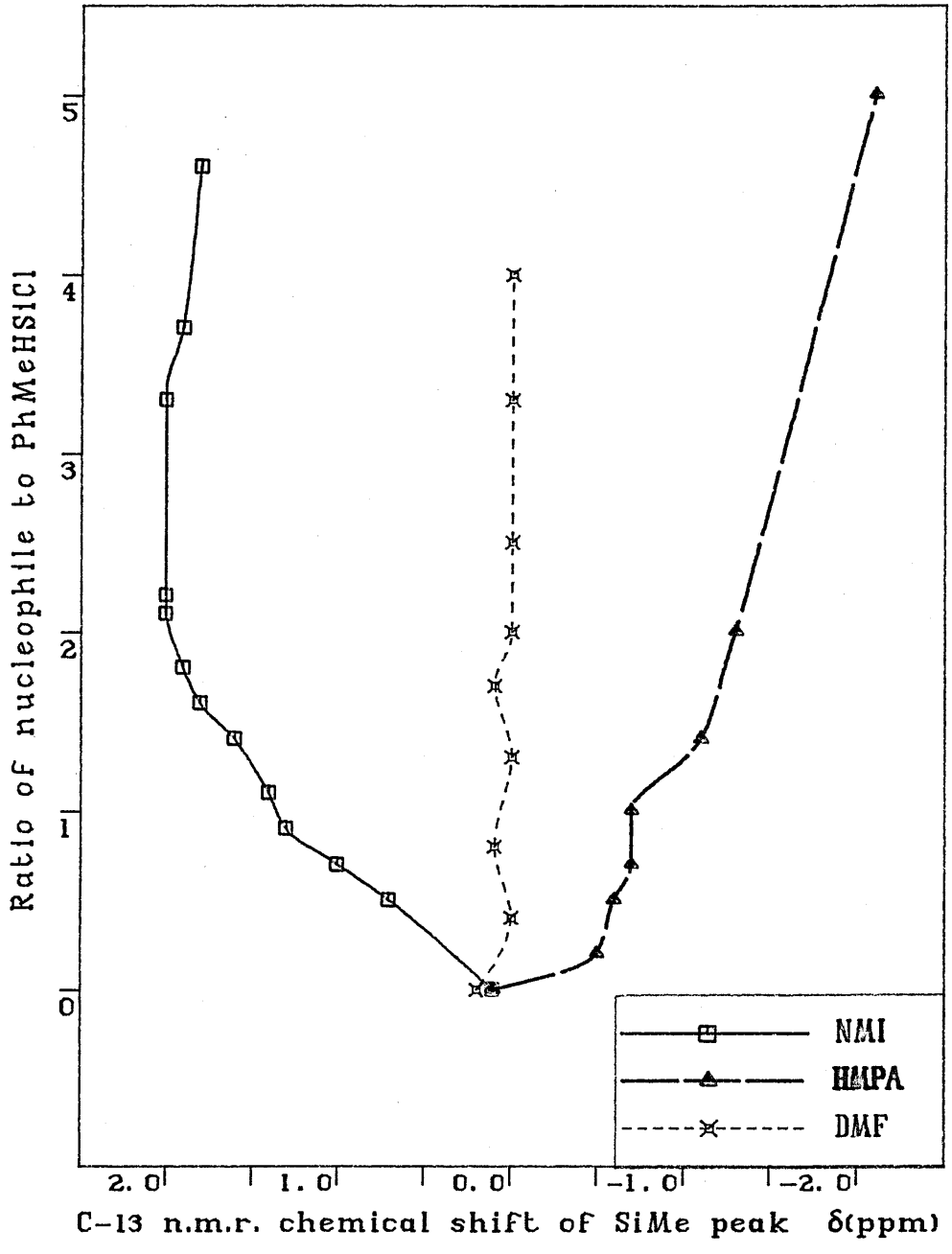

Figure 2.10.3
Silicon-29 n.m.r. titration studies of PhMeHSiCl against nucleophiles (NMI, HMPA, DMF).

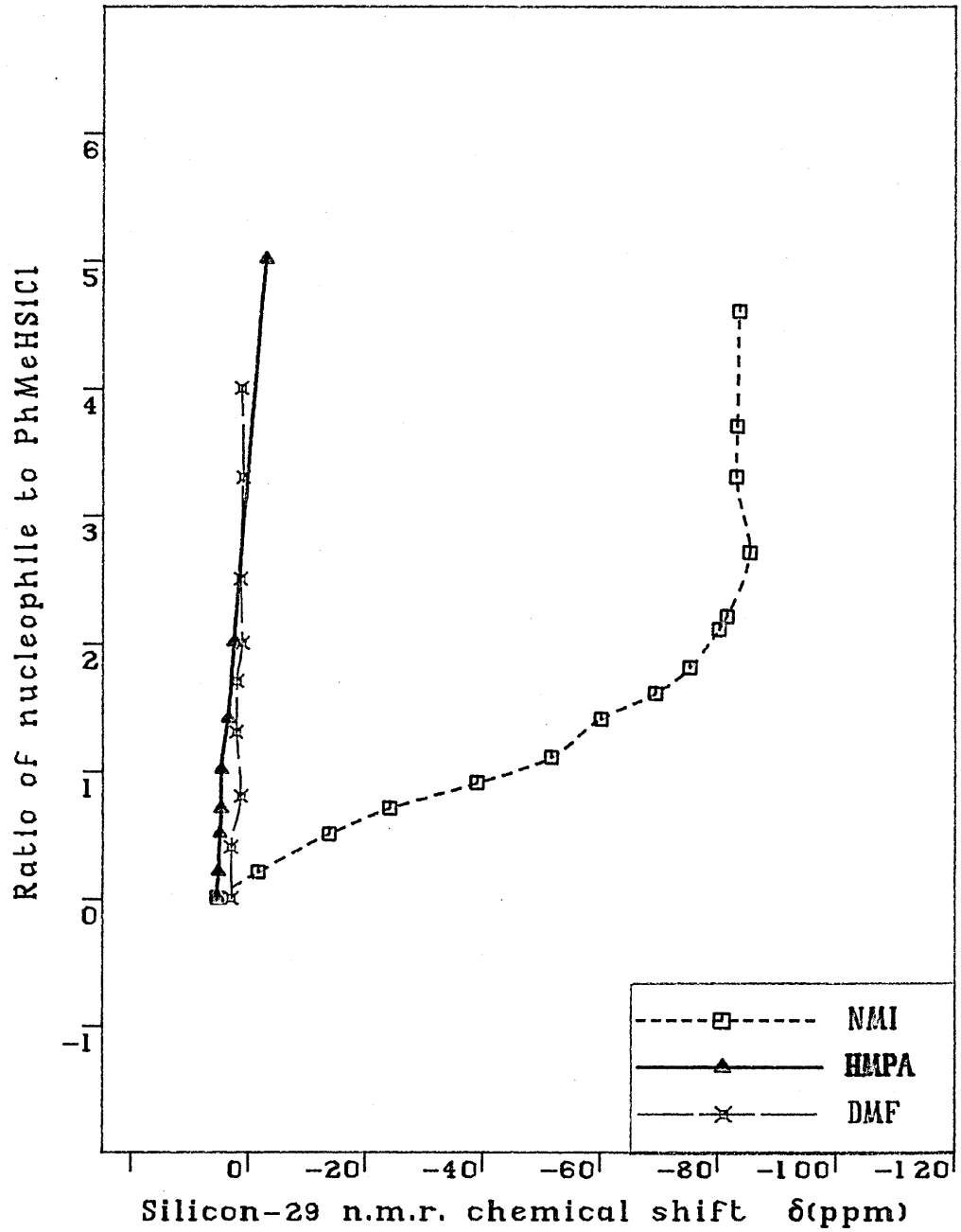

only shifted 8 ppm upfield from a value of 5.3 ppm for the uncomplexed silane. A low equilibrium constant for complex formation at ambient temperature may be responsible for this observation and the unsuccessful synthesis of the solid five coordinate $[PhMeHSi\text{-}(HMPA)_2]^+Cl^-$ adduct.

To clarify the difference in the results found in the silicon-29 spectra, a variable temperature silicon-29 n.m.r. study was performed on a 1:3 mixture of PhMeHSiCl and HMPA. Lowering the temperature to 200K caused a down frequency shift to -59.5 ppm together with intense broadening of the resonance, characteristic of five coordinate silicon and chemical exchange.

2.10.4 Summary

It can be concluded that both HMPA and NMI interact with PhMeHSiCl via a similar route forming pentacoordinate ionic $[PhMeHSi\text{-}(Nu)_2]^+Cl^-$ complexes, as described by the following scheme. However the silane-oxygen donor adduct can only be observed readily at low temperatures, owing to the low equilibrium constant for such complex formation. The ease of pentacoordination at silicon for PhMeHSiCl increases with nucleophiles in the sequence Nu=DMF < HMPA < NMI.

$$PhMeHSiCl + Nu \rightleftharpoons [PhMeHSi\text{-}Nu]^+Cl^- \rightleftharpoons [PhMeHSi\text{-}(Nu)_2]^+Cl^-$$

Scheme 2.10.2

2.11 Interaction of PhMeRSiCl (R=H, Me) with DMF

N,N-Dimethylformamide (DMF) and amides in general possess two potential donor sites, the oxygen and the nitrogen atoms. This dual nature of the amides is often referred to as ambidentate nucleophilicity. Extensive studies have been carried out concerning the site of protonation in these species, which has been the subject of considerable controversy. A

detailed account of the arguments regarding the site of protonation has been presented by Homer and Johnson.[75]

The greater basicity of nitrogen nucleophiles suggests intuitively that this is the preferred donor site. However n.m.r. studies in concentrated acids[76] provide convincing evidence that the oxygen atom is the predominant site of protonation. This can be rationalized by the extra stability conferred on the O-protonated species by resonance, as depicted in the following scheme. Delocalization of the resulting positive charge on the oxygen, carbon and particularly nitrogen is not possible with protonation on nitrogen.

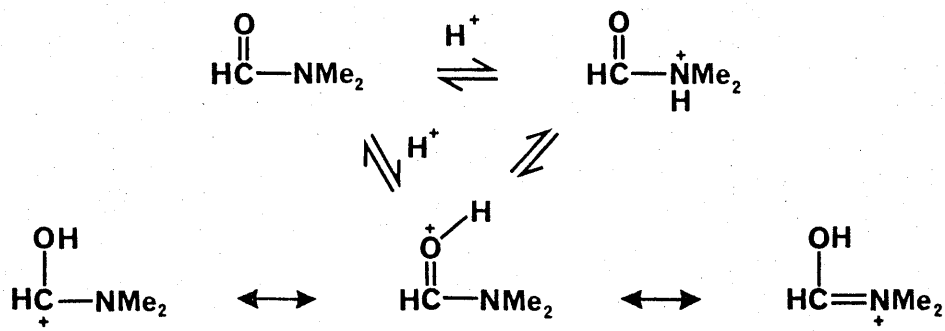

Scheme 2.11.1 Resonance structures of DMF

The magnetic non-equivalence of the two methyl groups attached to the nitrogen atom can be partly accounted for by differential shielding of the adjacent carbonyl group. Total line shape analysis of variable temperature n.m.r. data provides an estimate for the barrier to rotation for the (O)C—N bond in DMF, which is approximately 80 $kJmol^{-1}$.[33] As a consequence of the hindered rotation about this bond, two singlets for the N-methyl proton and carbon atoms are observed in the proton and carbon-13 n.m.r. spectra respectively. This is attributed to partial double bond character derived from the delocalization of electron density over the three atoms, oxygen, carbon and nitrogen, which also results from the silylation or protonation on the oxygen atom.

Restricted rotation due to the additional steric bulk created on nitrogen as a result of silylation has been disputed by Yoder and Hausman.[77] Their studies on the structure and dynamics of N-methyl and N-tert-butyldimethylsilyl amides provided evidence that the barriers to rotation about the (O)C—N bond are lower in those species with highly hindered nitrogen, compared with the analogous N-trimethylsilyl derivatives. Free rotation of the (O)C—N bond results when protonation or silylation takes place at the nitrogen atom, destroying the anisochrony of the two N-methyl resonances.

2.11.1 Interaction of PhMeHSiCl with DMF

In the preceding discussion on the interaction of PhMeHSiCl with DMF, a brief account was provided on the interesting changes in the chemical shift separation of the two N-methyl peaks of DMF. The variation in the chemical shift difference between the two proton N-methyl signals depends upon the concentration of DMF in the system.

The relative shieldings of these two methyl groups are greatly affected by solvent. The solvent effect was investigated by repeating the experiment in the absence of the silane; successive aliquots of DMF were added to a similar quantity of chloroform-d_1. The separation between the two methyl peaks remained essentially constant except at very high concentrations of DMF, in which cases the solution behaved virtually as neat DMF. Therefore, solvent effect is unlikely to be responsible for such a change in the chemical shift difference.

The merging of the two methyl resonances implies that the nitrogen atom may be protonated or silylated. In order to distinguish between these two processes, the reaction was further studied in the presence of a base to remove the acid impurity, hydrogen chloride. Pyridine and triethylamine were used as acid scavengers in the preliminary studies, however the same feature was still observed as the PhMeHSiCl was titrated against DMF.

To confirm that this variation in the peak separation was not induced by protonation, the titration was performed with equimolar quantities of PhMeHSiCl and the sterically hindered 2,6-di-tert-butylpyridine (2,6DBP), which has a very large pKa value. All the n.m.r. data for the interactions of PhMeRSiCl (R=H, Me) with DMF are listed in the tables provided in the experimental chapter. The changes in the chemical shift of the two N-methyl signals are presented in the accompanying figures.

No apparent changes in the chemical shifts of the silane were detected in the proton, carbon-13 and silicon-29 n.m.r. spectra, implying that adduct formation was insignificant. However line broadening of the proton and silicon-29 SiMe peaks was observed, which was indicative of a slow exchange between the uncomplexed silane and its DMF adduct. The two carbon-13 N-methyl resonances of DMF remained unaltered even with a five molar equivalence of DMF. Nevertheless, only a singlet at 2.80 ppm was recorded in the proton spectra for the two N-methyl entities, until a 1:0.6 ratio of PhMeHSiCl to DMF was reached. The chemical shift separation between these two proton signals then increased gradually from 1.1 to 7.7 Hz, when DMF was in five fold excess.

This anomalous behaviour can be taken as evidence for N-silylation at low concentrations of DMF since differential deshielding of the N-methyls is not observed under this condition. Furthermore, the small upfield shift of the proton N-Me resonances is consistent with the studies of Pugmire and Grant.[68] They reported that direct protonation on nitrogen caused low frequency shifts in the attached methyl groups. This feature is not exhibited in the silylations of DMF by halotrimethylsilanes (Me_3SiX; X=Cl, Br), bromomethyldiphenylsilane ($Ph_2MeSiBr$) or the diastereotopic $PhCHMeSiMe_2Cl$, but, surprisingly, it is observed with chlorodimethylphenylsilane ($PhMe_2SiCl$).

2.11.2 Interaction of $PhMe_2SiCl$ with DMF

As with PhMeHSiCl, the titration studies were carried out in the presence and the absence of 2,6DBP. In both cases, the results are comparable to those observed in the corresponding silylation by PhMeHSiCl. Changes in the chemical shifts and the line shapes of the silane resonances were not noted in the proton, carbon-13 and silicon-29 n.m.r. spectra, indicating that adduct formation between $PhMe_2SiCl$ and DMF was insignificant. The collapse and the subsequent divergence of the two proton N-methyl peaks of DMF occur at a similar silane to DMF ratio and share the same trend as in the case of PhMeHSiCl. The magnitude of the chemical shift difference between these two signals also varies in an analogous pattern relative to that of PhMeHSiCl, with increasing proportion of DMF.

Based upon the rationalization for the PhMeHSiCl system, the collapse of these two peaks can also be explained by N-silylation of DMF by $PhMe_2SiCl$. However, silylation at the oxygen atom of DMF is generally the much preferred and dominant route. In order to clarify the situation, the interaction of $PhMe_2SiCl$ with DMF was further investigated using oxygen-17 n.m.r. spectroscopy.

In comparison with the silicon-29 nucleus, oxygen-17 nucleus is more difficult to observe owing to its low receptivity, although the relaxation time is normally very fast. Using water as the reference standard, the range of chemical shifts for the majority of oxygen-17 species spans from +900 to -50 ppm, with the highly deshielded species at higher frequencies.[78] The carbonyl group (C=O) is considerably deshielded with respect to C—O-, thus an upfield shift is expected on O-silylation due to an increase in shielding induced by silicon.

In the oxygen-17 n.m.r. chemical shift titration of $PhMe_2SiCl$ against DMF, no pronounced changes in the oxygen-17 signal of the carbonyl group of DMF were noted. This indicates either the absence of O-silylation of DMF by $PhMe_2SiCl$ or, more likely, a low equilibrium constant for adduct formation.

Figure 2.11.1

Proton n.m.r. titration studies of PhMeRSiCl (R=H, Me) against DMF in the presence of 2,6DBP.

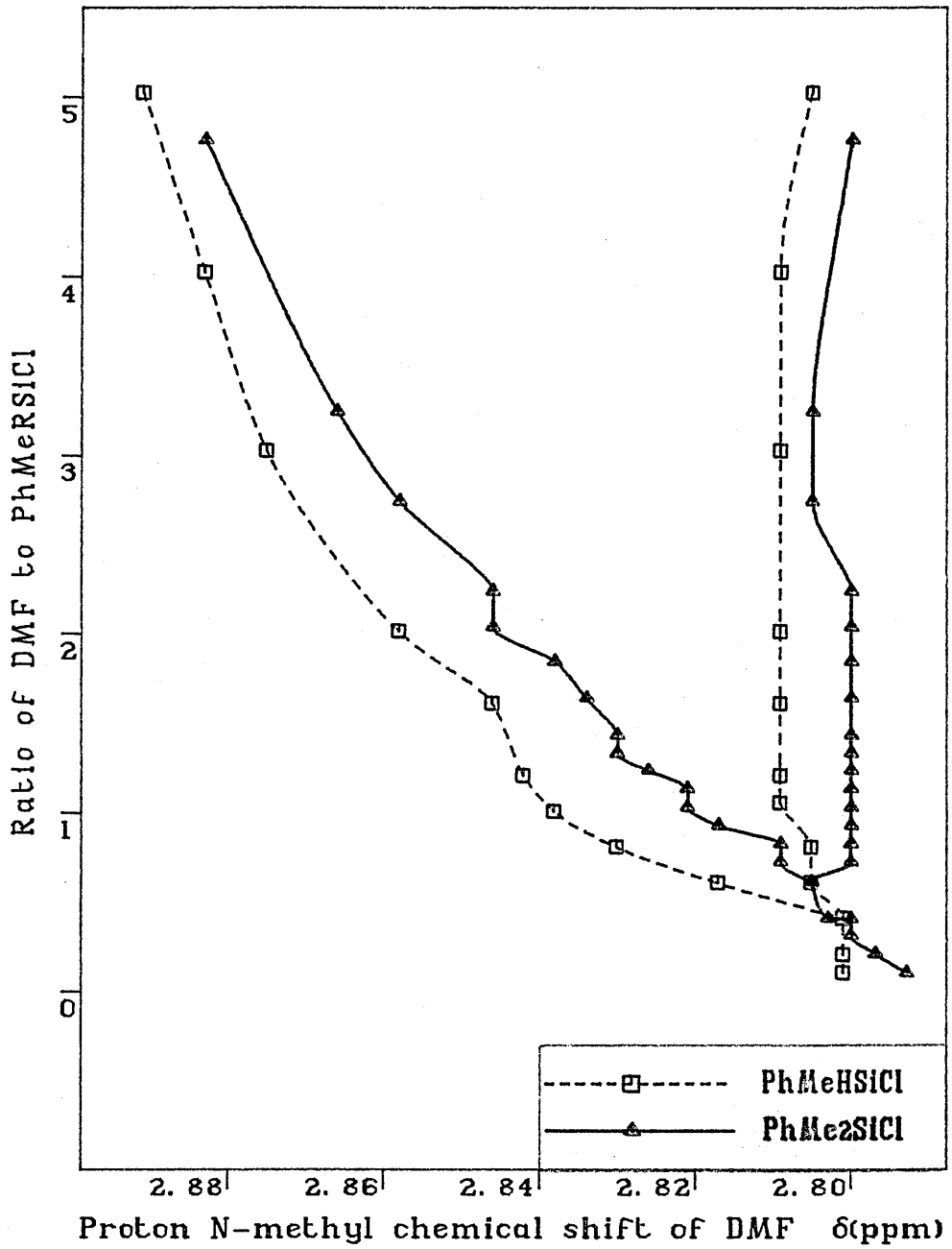

Figure 2.11.2
Separation between N-Me peaks of DMF in proton n.m.r. titration studies of PhMeRSiCl (R=H, Me) against DMF.

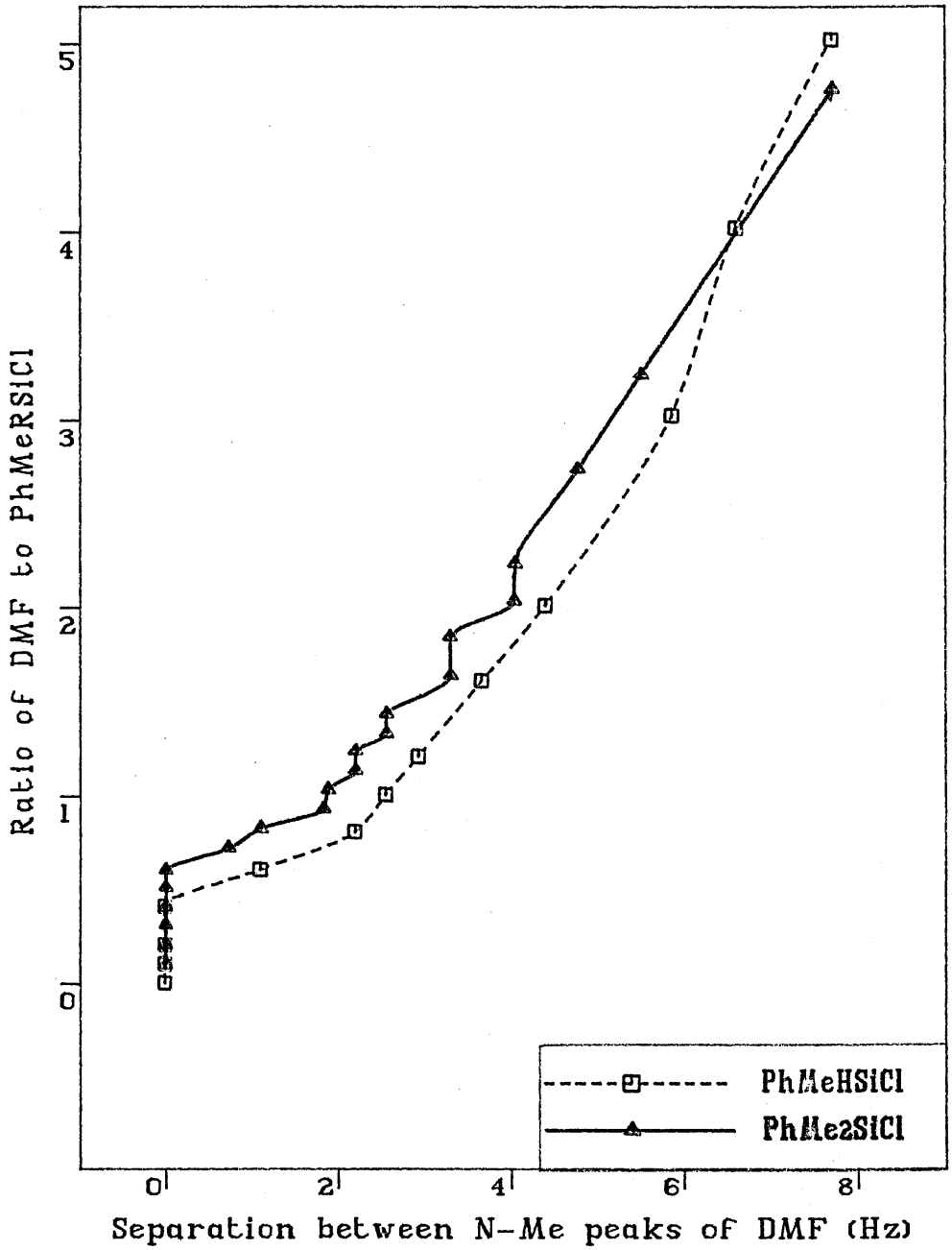

2.11.3 Interpretation of results

The titration studies on these two silyl systems (PhMeRSiCl; R=H, Me) provide some evidence for N-silylation of DMF. However further detailed investigations on these systems are required for definite conclusions to be drawn and to explain why this phenomenon only occurs under certain conditions. The collapse is not detected in the carbon-13 n.m.r. spectra owing to the different time scale of the carbon-13 nuclei compared with the proton nuclei.

At low concentrations of DMF, silylation at nitrogen of DMF may take place leading to free and rapid rotation of the (O)C—N bond, giving an average N-methyl signal on the proton n.m.r. time scale. With increasing proportion of DMF, O-silylation may be more favourable and dominates. Delocalization of the positive charge on the three nuclei:- oxygen, carbon and nitrogen, restricts the rotation of the bond by raising the energy barrier, thus two separate methyl resonances result.

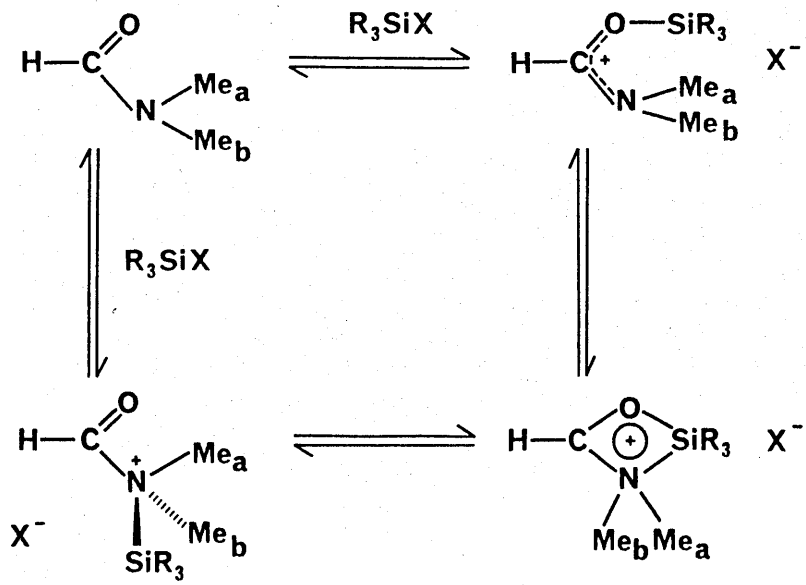

Scheme 2.11.2 O- and N-silylations of DMF

2.12 General summary

The conclusion inferred from the accumulated results strongly indicate that [silane-nucleophile]$^+X^-$ ionic adducts are formed as a consequence of the interactions between nucleophiles and highly electrophilic silicon species. For the diastereotopic silyl systems, $PhCHMeSiMe_2X$ (X=Cl, Br, OSO_2CF_3), the four coordinate [$PhCHMeSiMe_2$-nucleophile]$^+X^-$ ionic complexes with a 1:1 stoicheiometry are the dominant species present in the silylating mixture in solution. Conversely with PhMeHSiCl, the four coordinate ionic salts are susceptible to further attack by a second molecule of nucleophile, yielding five coordinate [PhMeHSi-$(Nu)_2$]$^+Cl^-$ ionic complexes.

The stability of silane-nucleophile adducts is controlled by a combination of structural and electronic factors. For a given silane, the equilibrium constant for the formation of such complexes depends upon the electron donating ability of the attacking nucleophile. Thus stronger donors, for instance N-methylimidazole and hexamethylphosphoramide, should be more efficient at forming stable complexes accompanied by a higher equilibrium constant.

Furthermore, the silane-nucleophile complexes undergo chemical exchanges with other nucleophiles and with their parent silanes at a rate controlled by the initial dissociation of the complex into its individual components. The rate of this dissociation is governed by the nucleophilicity and the solvation of the counterion, as well as the ion pairing of the complex, which decreases in the following sequence X=Cl > Br > OSO_2CF_3.

More importantly, the halide counterion of the adduct is found to induce rapid racemization of halosilane, which supports the finding by Prince[71] on the chloride exchange reaction of triphenylchlorosilane, Ph_3SiCl, with radioactive labelled tetrabutylammonium chloride. In addition, the facile exchange between the four and five coordinate PhMeHSiCl-nucleophile adducts illustrates that racemization of this

silane by nucleophiles can take place without involving a six coordinate silicon intermediate.

Chapter 3 Kinetic studies on the racemization of diastereotopic silanes

3.1 Introduction

Having established the nature of the major species present in silylation reactions, the mechanism of nucleophilic substitution at silicon can be further elucidated by investigating the kinetic aspects of the interactions of silanes with nucleophiles. An advantage of utilizing the diastereotopic silanes, $PhCHMeSiMe_2X$ (X=Cl, Br, OSO_2CF_3), for kinetic studies is the anisochrony of the two diastereotopic SiMe n.m.r. peaks. This approach is very common and has been widely exploited in other areas of chemistry, such as the evaluation of the activation energy barriers to hindered rotation.[79]

Nucleophilic attack at the diastereotopic silanes, $PhCHMeSiMe_2X$ (X=Cl, Br) may induce inversion of configuration at silicon. Consequently, a dynamic equilibrium is established between the silicon species and its inverted isomer. If the exchange is fast on the n.m.r. time scale, chemical shift non-equivalence is destroyed and coalescence of the two diastereotopic SiMe signals results. The rate of exchange at coalescence reflects the rate of racemization of the silane under investigation. Therefore, kinetic information on the racemization processes at silicon can be assessed by monitoring the changes in the line shape of the diastereotopic SiMe resonances using n.m.r. spectroscopy. This technique is known as dynamic n.m.r. spectroscopy (DNMR); it requires an appreciable chemical shift separation between the two diastereotopic peaks for accurate rate constants to be evaluated. Only the carbon-13 diastereotopic SiMe resonances of $PhCHMeSiMe_2X$ (X=Cl, Br, OSO_2CF_3) show sufficient chemical shift differences, thus the kinetic studies were performed solely on these systems.

The racemization processes of the diastereotopic silanes, $PhCHMeSiMe_2X$ (X=Cl, Br) were examined in detail with a diverse range of nucleophiles, in various solvents and at different concentrations. Successive aliquots of a nucleophile were syringed into a silane solution; the two carbon-13 diastereotopic SiMe resonances were recorded after each addition of

nucleophile until the two peaks coalesced. Complete line shape analysis was carried out for each silane-nucleophile interaction using a modified version of the DNMR4 program from the Quantum Chemistry Program Exchange.[80] It is essential to have good quality spectra for line shape comparison. Thus the n.m.r. spectra were recorded with optimal resolution, correct phase setting and a reasonably long scanning period to maximise the signal-to-noise ratio. The rate constants calculated by computer simulation, the reaction conditions and the variations in the concentrations of both silane and nucleophile are tabulated in the experimental section for each reaction.

3.2 Mechanistic proposals

By inference from the findings in the preceding chapter, two mechanisms for the racemization of halosilanes can be postulated to accommodate different equilibrium constants (K_{eq}) for adduct formation, which are governed by the nature of the counterion and the donor strength of the attacking nucleophile.

3.2.1 The first mechanism

In the cases where low equilibrium constants are observed, for instance when X=Cl with most nucleophiles or X=Br with weak nucleophiles, the racemization of halosilanes may proceed via the following pathway. Salt formation between the silane and nucleophile is assumed to be minimal, possibly with NMI and HMPA as the only exceptions. Hence the concentration of the counterion, $[X^-]$, will be extremely small and the proportion of free nucleophile in solution, $[Nu_f]$, will be essentially equal to the quantity added, $[Nu_o]$.

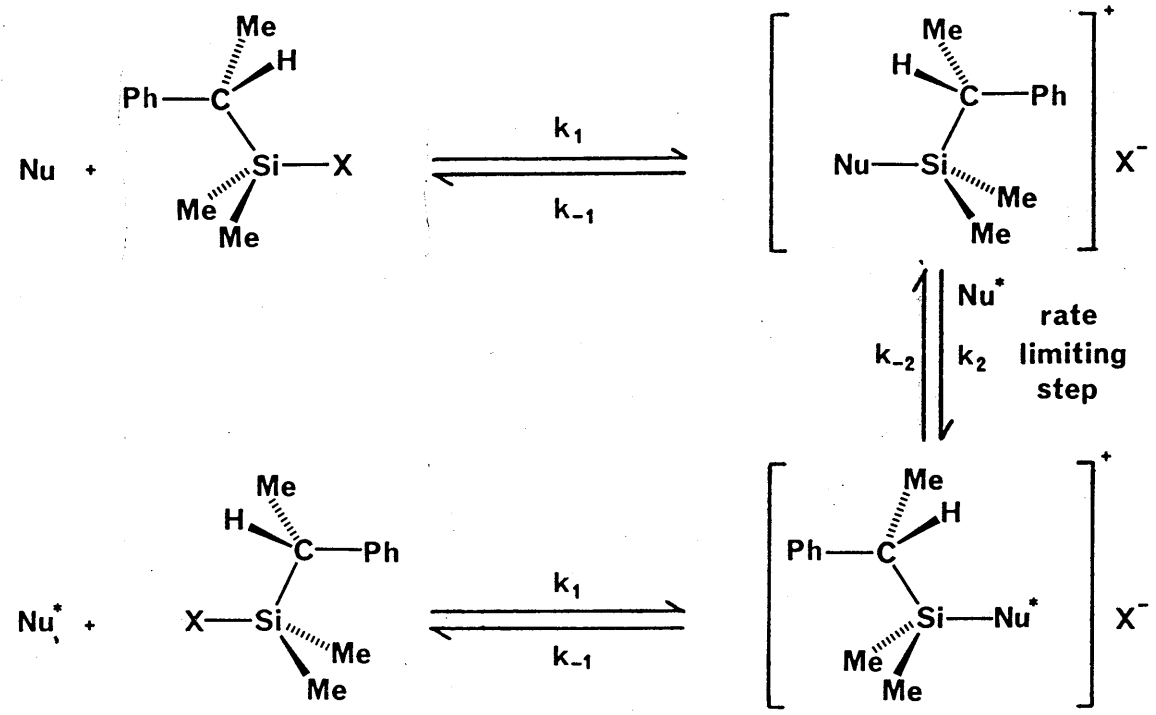

The first mechanism

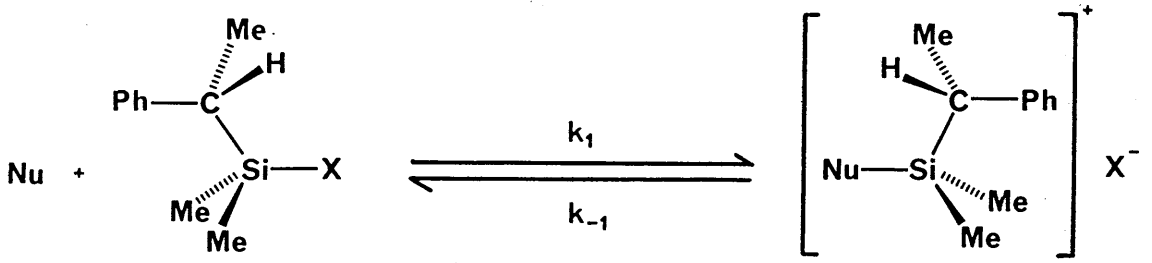

$k_1 \gg k_{-1}$

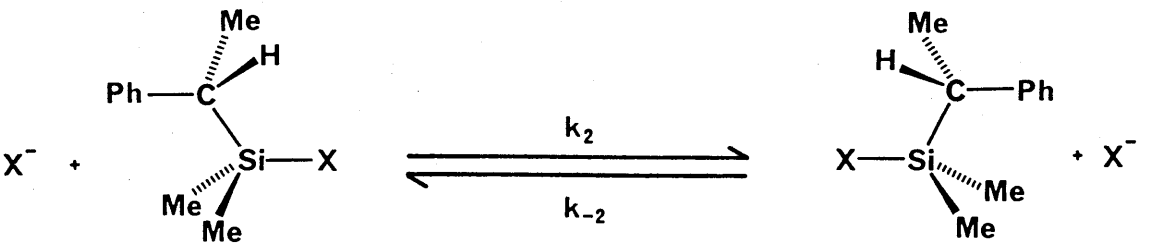

The second mechanism

Scheme 3.2.1 Proposed mechanisms

$$PhCHMeSiMe_2X + Nu \rightleftharpoons PhCHMeSiMe_2Nu^+X^-$$

$$PhCHMeSiMe_2Nu^+X^- + Nu^* \rightleftharpoons PhCHMeSiMe_2Nu^{*+}X^- + Nu$$

Rate determining step

Scheme 3.2.2

Assuming that the attack of a second molecule of nucleophile at a silane-nucleophile adduct is the rate determining step, the silane-nucleophile complex is ion-paired and the equilibrium constant for ion-pair dissociation (K_d) is zero, the rate of racemization can be expressed by equation 3.2.1.

$$\text{Rate} = k_2[PhCHMeSiMe_2Nu^+ X^-][Nu^*] \qquad \textbf{Equation 3.2.1}$$

However the equilibrium constant for complex formation (K_{eq}) is related to $[PhCHMeSiMe_2Nu^+ X^-]$ by the following equation.

$$K_{eq} = \frac{k_1}{k_{-1}} = \frac{[PhCHMeSiMe_2Nu^+ X^-]}{[PhCHMeSiMe_2X]\,[Nu]} \qquad \textbf{Equation 3.2.2}$$

Therefore $[PhCHMeSiMe_2Nu^+ X^-] = K_{eq}[PhCHMeSiMe_2X][Nu]$ and since Nu is the same as Nu^*, the overall racemization rate law can be rewritten as follows:-

$$\text{Rate} = k_2K_{eq}[PhCHMeSiMe_2X][Nu_o]^2 \qquad \textbf{Equation 3.2.3}$$

Nevertheless, if the silane-nucleophile adduct is not completely ion-paired, the $[PhCHMeSiMe_2Nu^+ X^-]$ term in equation 3.2.1 is replaced by $[PhCHMeSiMe_2Nu^+]$ and the rate of racemization becomes

$$\text{Rate} = k_2[PhCHMeSiMe_2Nu^+][Nu^*] \qquad \textbf{Equation 3.2.4}$$

The concentration of $PhCHMeSiMe_2Nu^+$ depends upon the extent of dissociation of the complex which can be described by the following scheme.

$$PhCHMeSiMe_2Nu^+ X^- \overset{K_d}{\rightleftharpoons} PhCHMeSiMe_2Nu^+ + X^-$$

Scheme 3.2.3

$$K_d = \frac{[PhCHMeSiMe_2Nu^+]\,[X^-]}{[PhCHMeSiMe_2Nu^+\ X^-]} \qquad \textbf{Equation 3.2.5}$$

$$[PhCHMeSiMe_2Nu^+][X^-] = K_d[PhCHMeSiMe_2Nu^+\ X^-]$$

In the absence of added X^-, the concentration of X^- is equal to that of $PhCHMeSiMe_2Nu^+$ ($[X^-] = [PhCHMeSiMe_2Nu^+]$), therefore

$$[PhCHMeSiMe_2Nu^+] = K_d^{0.5}[PhCHMeSiMe_2Nu^+\ X^-]^{0.5} \qquad \textbf{Equation 3.2.6}$$

The rate equation can be modified to

$$\text{Rate} = k_2K_d^{0.5}[PhCHMeSiMe_2Nu^+\ X^-]^{0.5}[Nu^*] \qquad \textbf{Equation 3.2.7}$$

However, $[PhCHMeSiMe_2Nu^+\ X^-] = K_{eq}\,[PhCHMeSiMe_2X]\,[Nu]$, thus substituting this into equation 3.2.7 yields the overall racemization rate law which can be expressed as

$$\text{Rate} = k_2K_{eq}^{0.5}K_d^{0.5}[Nu^*][PhCHMeSiMe_2X]^{0.5}[Nu]^{0.5} \qquad \textbf{Equation 3.2.8}$$

The above equation can be simplified to give the following equation.

$$\text{Rate} = k_2K_{eq}^{0.5}K_d^{0.5}[PhCHMeSiMe_2X]^{0.5}[Nu_o]^{1.5} \qquad \textbf{Equation 3.2.9}$$

The presence of the K_d term indicates that the rate of racemization is governed by the extent of ion-pair dissociation (K_d) in this situation. However the overall rate equation is different from equation 3.2.3. Furthermore, direct substitution of equation 3.2.2 into equation 3.2.5 also produces the same result (equation 3.2.9).

To account for all possibilities, the overall rate equation for this mechanism can be expressed in the following form.

$$\text{Rate} = P_A\{k_2K_{eq}[PhCHMeSiMe_2X][Nu_o]^2\} + P_B\{k_2'K_{eq}^{0.5}K_d^{0.5}[PhCHMeSiMe_2X]^{0.5}[Nu_o]^{1.5} \quad \text{Equation 3.2.10}$$

where P_A and P_B are the proportionality factors

3.2.2 The second mechanism

When X=Br with strong nucleophiles or when $X=OSO_2CF_3$ with moderately strong donor species, the silane-nucleophile complexes are formed readily and are more stable with larger equilibrium constants for adduct formation. Under these conditions, the following mechanism may hold and the concentration of free nucleophile, $[Nu_f]$, in solution will be insignificant. Assuming that $PhCHMeSiMe_2X$ is present in excess and the adduct is not ion-paired i.e. dissociated, the concentrations of X^- will be relatively high. In extreme cases, it can be assumed that salt formation may account for almost all the added nucleophile, which is fully supported by the n.m.r. chemical shift titration results in the previous chapter. If this is the case, the concentration of nucleophile added ($[Nu_o]$) should be approximately equal to the concentration of X^- ($[X^-]$) as illustrated by the following equations.

$$K_{eq} = \frac{[PhCHMeSiMe_2Nu^+]\,[X^-]}{[PhCHMeSiMe_2X]\,[Nu]} \qquad \text{Equation 3.2.11}$$

$[PhCHMeSiMe_2Nu^+] = [X^-]$, therefore the above equation can be rewritten as:-

$$[X^-]^2 = K_{eq}\,[PhCHMeSiMe_2X]\,[Nu_f] \qquad \textbf{Equation 3.2.12}$$

$$[Nu_o] = [X^-] + [Nu_f] \qquad \textbf{Equation 3.2.13}$$

$$[X^-] = \{K_{eq}\,([Nu_o] - [X^-])\,[PhCHMeSiMe_2X]\}^{0.5} \qquad \textbf{Equation 3.2.14}$$

$$[X^-]^2 = K_{eq}\,[Nu_o]\,[PhCHMeSiMe_2X] - K_{eq}\,[X^-]\,[PhCHMeSiMe_2X] \qquad \textbf{Equation 3.2.15}$$

$$[X^-]^2 + K_{eq}[Nu_o][PhCHMeSiMe_2X] - K_{eq}[X^-][PhCHMeSiMe_2X] = 0 \qquad \textbf{Equation 3.2.16}$$

If K_{eq} is very large the second and third term will dominate, then the rate expression becomes

$$K_{eq}\,[PhCHMeSiMe_2X]\,[X^-] - K_{eq}\,[PhCHMeSiMe_2X]\,[Nu_o] = 0 \qquad \textbf{Equation 3.2.17}$$

Thus $[X^-]$ is equal to $[Nu_o]$ under this condition.

If the formation of the silane-nucleophile adduct is the rate determining step, then the rate law for the racemization rate is

$$\textbf{Rate} = k_1[PhCHMeSiMe_2X][Nu_o] \qquad \textbf{Equation 3.2.18}$$

However if the halide exchange is the rate limiting process, the rate expression becomes

$$\text{Rate} = k_2[PhCHMeSiMe_2X][X^-] \qquad \textbf{Equation 3.2.19}$$

The concentration of free X^- depends upon the equilibrium constant for ion-pair dissociation (K_d), which is related to the equilibrium constant for complex formation (K_{eq}). As illustrated in the last section, the equilibrium constants for adduct formation (K_{eq}) and ion-pair dissociation (K_d) can be described by the following equations.

$$K_{eq} = \frac{[PhCHMeSiMe_2Nu^+\ X^-]}{[PhCHMeSiMe_2X]\ [Nu]} \quad \text{and} \quad K_d = \frac{[PhCHMeSiMe_2Nu^+]\ [X^-]}{[PhCHMeSiMe_2Nu^+\ X^-]}$$

These two equations can be rearranged to give

$$[PhCHMeSiMe_2Nu^+\ X^-] = K_{eq}\ [PhCHMeSiMe_2X]\ [Nu]$$

$$[X^-] = [PhCHMeSiMe_2Nu^+] = K_d^{0.5}\ [PhCHMeSiMe_2Nu^+\ X^-]^{0.5}$$

From equation 3.2.19, the rate of racemization can be expressed as

$$\text{Rate} = k_2\ [PhCHMeSiMe_2X]\ [X^-]$$

However $[X^-]$ is governed by K_d which is related to K_{eq}, the rate equation can therefore be modified.

$$\text{Rate} = k_2\ [PhCHMeSiMe_2X]\ K_d^{0.5}\ [PhCHMeSiMe_2Nu^+\ X^-]^{0.5}$$

$$\text{Rate} = k_2\ [PhCHMeSiMe_2X]\ K_d^{0.5}\ K_{eq}^{0.5}\ [PhCHMeSiMe_2X]^{0.5}\ [Nu]^{0.5}$$

Thus the overall racemization rate expression can be rewritten as

$$\text{Rate} = k_2K_{eq}^{0.5}K_d^{0.5}[PhCHMeSiMe_2X]^{1.5}[Nu_f]^{0.5} \qquad \text{Equation 3.2.20}$$

A. small K_{eq} and small K_d

If K_{eq} and K_d both lie towards the left, the concentration of free nucleophile in solution, $[Nu_f]$, will be similar to the quantity of added nucleophile, $[Nu_o]$. The rate equation for racemization becomes

$$[Nu_f] = [Nu_o]$$

$$\text{Rate} = k_2 K_{eq}^{0.5} K_d^{0.5} [PhCHMeSiMe_2X]^{1.5} [Nu_o]^{0.5} \quad \text{Equation 3.2.21}$$

B. large K_{eq} and small K_d

If K_{eq} lies towards salt formation and K_d lies towards the ion-pair, the concentration of the ion-pair, $PhCHMeSiMe_2Nu^+ X^-$, will be approximately equal to that of the added nucleophile, $[Nu_o]$. The rate law can be expressed in the following form.

$$[PhCHMeSiMe_2Nu^+ X^-] = [Nu_o]$$

$$\text{Rate} = k_2 [PhCHMeSiMe_2X] K_d^{0.5} [PhCHMeSiMe_2Nu^+ X^-]^{0.5}$$

$$\text{Rate} = k_2 K_d^{0.5} [PhCHMeSiMe_2X] [Nu_o]^{0.5} \quad \text{Equation 3.2.22}$$

C. large K_{eq} and large K_d

If the equilibrium constant lies towards the formation of the adduct, which dissociates readily into its separate ions, the concentration of free X^- will be essentially the same as that of the added nucleophile, $[Nu_o]$. The rate equation can be modified to

$$[X^-] = [Nu_o]$$

$$\text{Rate} = k_2 [PhCHMeSiMe_2X] [Nu_o] \quad \text{Equation 3.2.23}$$

A charged halide ion is, in principle, more nucleophilic than a neutral nucleophile molecule. Thus, for a given halosilane, the attack by a halide ion at the halosilane should take place more readily than that by a neutral nucleophile molecule. Furthermore, owing to a lesser degree of steric hindrance and greater nucleophilicity of the halide anion over the uncharged donor molecule, the pentavalent transition state formed as a consequence of the attack by the halide ion at the halosilane should be more stable compared with that produced by the corresponding attack of

the nucleophile molecule. Therefore, on the basis of these kinetic and thermodynamic factors, it is more likely for the initial formation of the silane-nucleophile complex to be the rate determining process in this mechanism until the system is in dynamic equilibrium. Once the equilibrium is reached and a steady state is established, then the concentration of free X^- depends only on the equilibrium constant (K_{eq}) and not on the rate of adduct formation. Thus the halide exchange may become the rate limiting step under these conditions.

Disregarding the mechanistic pathway chosen and the various conditions imposed, the rate expression for the nucleophile catalysed racemization of $PhCHMeSiMe_2X$ (X=Cl or Br) can be generalized by the following simplified equation.

$$\text{Rate} = \frac{d[PhCHMeSiMe_2X^*]}{dt} = k[PhCHMeSiMe_2X]^m[Nu]^n \qquad \text{Equation 3.2.24}$$

where k is an overall rate constant including the term for the equilibrium constant for adduct formation (K_{eq}). The [Nu] term in the above expression (equation 3.2.24) is regarded as the concentration of added nucleophile, which is the basic assumption for the interpretations of the results from the kinetic and variable temperature titration studies.

$$\frac{\text{Rate}}{[PhCHMeSiMe_2X]} = \frac{d[PhCHMeSiMe_2X^*]}{dt\ [PhCHMeSiMe_2X]} = k_{obs} = \tau^{-1}$$

where τ is the life time of activated $PhCHMeSiMe_2X$, $PhCHMeSiMe_2X^*$, and k_{obs} is a pseudo-first order rate constant at a particular concentration of nucleophile calculated using the DNMR4 program. Therefore equation 3.2.24 can be modified to

$$k_{obs} = \tau^{-1} = k\ [PhCHMeSiMe_2X]^{m-1}\ [Nu]^n$$

Assuming that the concentration of free silane remains virtually unaltered throughout the experiment on addition of nucleophile or m equals to 1, the observed rate constant (k_{obs}) depends mainly upon the k $[Nu]^n$ term. The theoretical line shape at a particular observed rate constant is simulated and compared with the experimentally measured result using total line shape analysis as illustrated in Figure 3.2.1. Taking the natural logarithm of the above equation yields the following expression.

$$\ln k_{obs} = n \ln [Nu] + \ln k + (m-1) \ln [PhCHMeSiMe_2X] \quad \textbf{Equation 3.2.25}$$

Therefore by plotting the observed pseudo-first order rate constants ($\ln k_{obs}$) against the corresponding concentration of the added nucleophile ($\ln [Nu]$), the order with respect to the nucleophile (n) can be obtained from the gradient of the straight line kinetic plot. The order in nucleophile can be used to verify the various rate laws and the validity of the assumptions as well as serving as an useful tool in the elucidation of reaction mechanism. Hence it may be possible to distinguish between the two postulated mechanisms for the racemization of a given silane and nucleophile.

Kinetic plots for each silane-nucleophile interaction are shown in the accompanying figures. The rate of racemization of halosilanes is controlled by the nature of the leaving group of the silane, the strength of the nucleophile, the solvent and the concentration. A detailed interpretation of the results is therefore based on these governing factors and is provided in the subsequent sections.

3.3 The effect of leaving group

With a concentrated silane solution, a smaller amount of nucleophile is required to induce racemization, thus significant medium effect due to the presence of large quantities of nucleophile can be minimised. Furthermore, a high concentration of silane is compatible with the

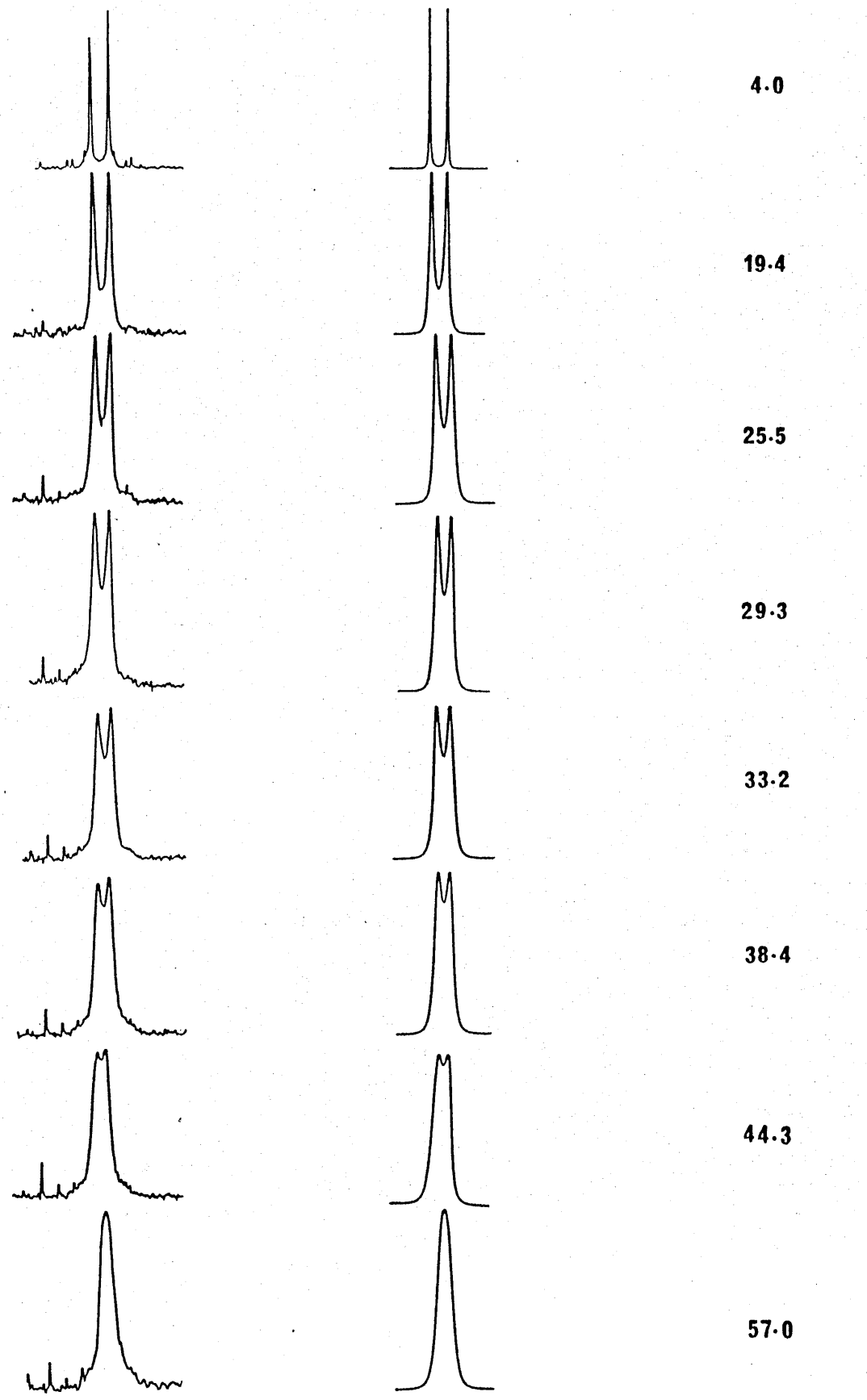

Figure 3.2.1 Comparison of the theoretical and calculated line shapes

necessary signal-to-noise ratio. Thus the nucleophile assisted racemization reactions of $PhCHMeSiMe_2X$ (X=H, Cl, Br, OSO_2CF_3) were normally studied in the presence of 9% (0.2 ml) benzene-d_6 to make meaningful comparisons of the results.

3.3.1 Racemization of $PhCHMeSiMe_2H$

With a four fold excess of HMPA, the observed line shapes of the two carbon-13 diastereotopic SiMe peaks for $PhCHMeSiMe_2H$ remained unchanged. However the chemical shift separation reduced slightly from 6 to 4 Hz, which could be attributable to a medium effect. This implies that either the racemization of $PhCHMeSiMe_2H$ is extremely slow and cannot be registered by the n.m.r. spectrometer, or the nucleophilic attack of HMPA at the silane occurs with retention of configuration at silicon.

Poor leaving groups such as the hydride atom almost always undergo nucleophilic substitution with retention, which should not result in racemization. Nevertheless if the silane does exchange slowly with the inverted isomer, it is very unlikely for the racemization process to proceed via either of the two proposed mechanistic pathways described above. This is simply because the formation of the hydride counterion is highly unfavourable. Therefore, for silanes with very poor leaving groups undergoing racemization, an alternative mechanism may be in operation involving molecular intermediates with expansion of coordination at silicon, as suggested by Corriu.[8] However no evidence for the operation of such a mechanism was found in this study.

$$R_3SiX + Nu \rightleftharpoons \underset{\text{5 coordinate}}{R_3SiNuX} \rightleftharpoons \underset{\text{6 coordinate}}{R_3SiNu_2X}$$

(X = poor leaving group)

Scheme 3.3.4

3.3.2 Racemization of $PhCHMeSiMe_2X$ (X=Cl, Br, OSO_2CF_3)

Pyridine is considered to be a comparatively weak nucleophile, though surprisingly only a 0.008 molar equivalent of pyridine is sufficient to induce coalescence of the two diastereotopic SiMe resonances of $PhCHMeSiMe_2OSO_2CF_3$, giving a sharp singlet with a normal linewidth. The reaction rate is much too rapid to be measured accurately with such a concentrated silane solution, however the higher the proportion of solvent the more pronounced the solvent effect. Under identical reaction conditions, an equimolar quantity of pyridine was required for the collapse of the two SiMe peaks for $PhCHMeSiMe_2Br$, whereas those for the analogous chlorosilane were only near the point of coalescence with a ten fold excess of pyridine.

Therefore it can be generalized that for a given nucleophile at ambient temperature, the relative rate of racemization of $PhCHMeSiMe_2X$ (X=Cl, Br, OSO_2CF_3) decreases with counterion in the following sequence $X=OSO_2CF_3$ > Br > Cl. The results obtained for a series of interactions between $PhCHMeSiMe_2X$ (X=Cl, Br) and a wide range of nucleophiles are also in accordance with this trend.

The rationale behind these observations lies in the nature of the counterion, which can be categorized by its leaving group ability, its nucleophilicity and its facility to be solvated. In comparisons with the bromide and triflate anion, the chloride ion is a relatively poor leaving group and is less easily solvated but it is a good nucleophile. These combining factors contribute to the unfavourable formation of the $[PhCHMeSiMe_2Nu]^+Cl^-$ ionic complex, and consequently the slower racemization of $PhCHMeSiMe_2Cl$. This is because the silane-nucleophile salt plays a determining role in the reaction pathway, as indicated in the derivation of the rate expressions.

Because the triflate anion is a comparatively poor nucleophile, the attack by the triflate anion at the silicon atom of $PhCHMeSiMe_2OSO_2CF_3$

Figure 3.3.1
A kinetic plot for the racemization of PhCHMeSiMe2Cl catalysed by HMPA.

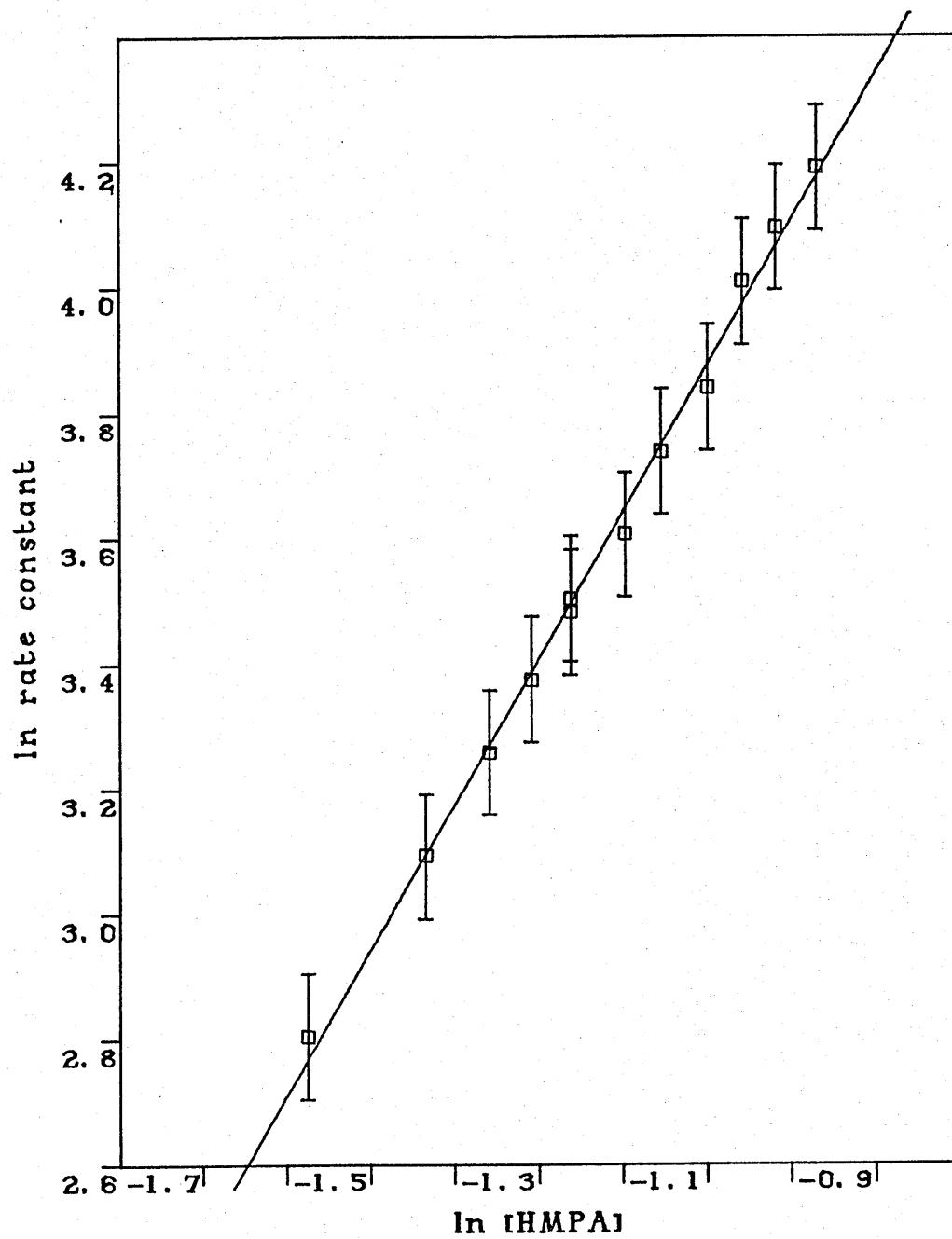

ln kobs = 2.329 (s.d. 0.044) ln [HMPA] + 6.436 (s.d. 0.054)

solvent: 9% Benzene-d6 (0.2 ml)

Figure 3.3.2

The effect of leaving group on the racemization of PhCHMeSiMe2X (X=Cl, Br) catalysed by NMI.

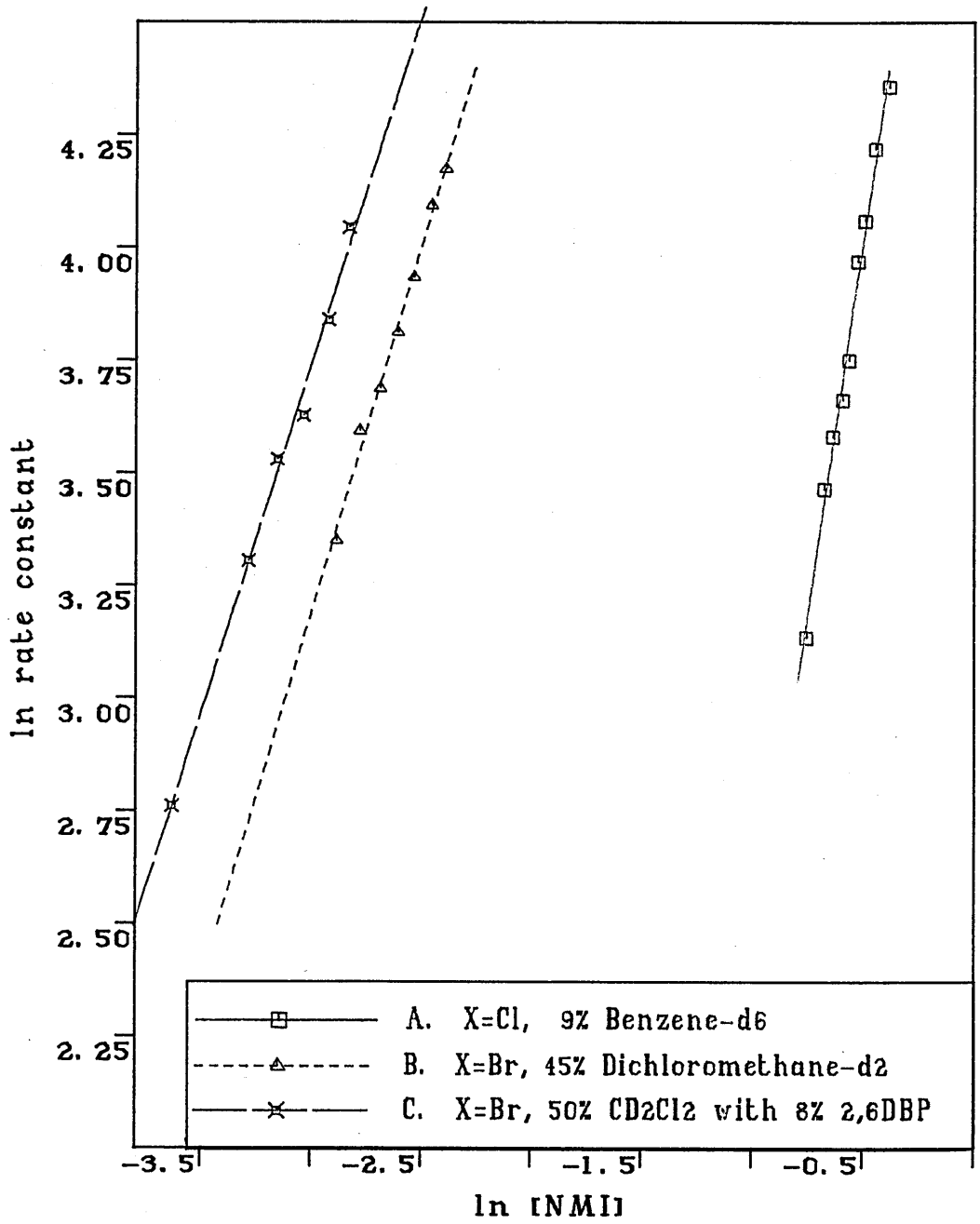

A. ln kobs = 3.367 (s.d. 0.13) ln [NMI] + 5.730 (s.d. 0.07)

B. ln kobs = 1.635 (s.d. 0.06) ln [NMI] + 8.101 (s.d. 0.15)

C. ln kobs = 1.549 (s.d. 0.05) ln [NMI] + 8.384 (s.d. 0.17)

Figure 3.3.3

The effect of leaving group on the racemization of PhCHMeSiMe2X (X=Cl, Br) catalysed by DMPU.

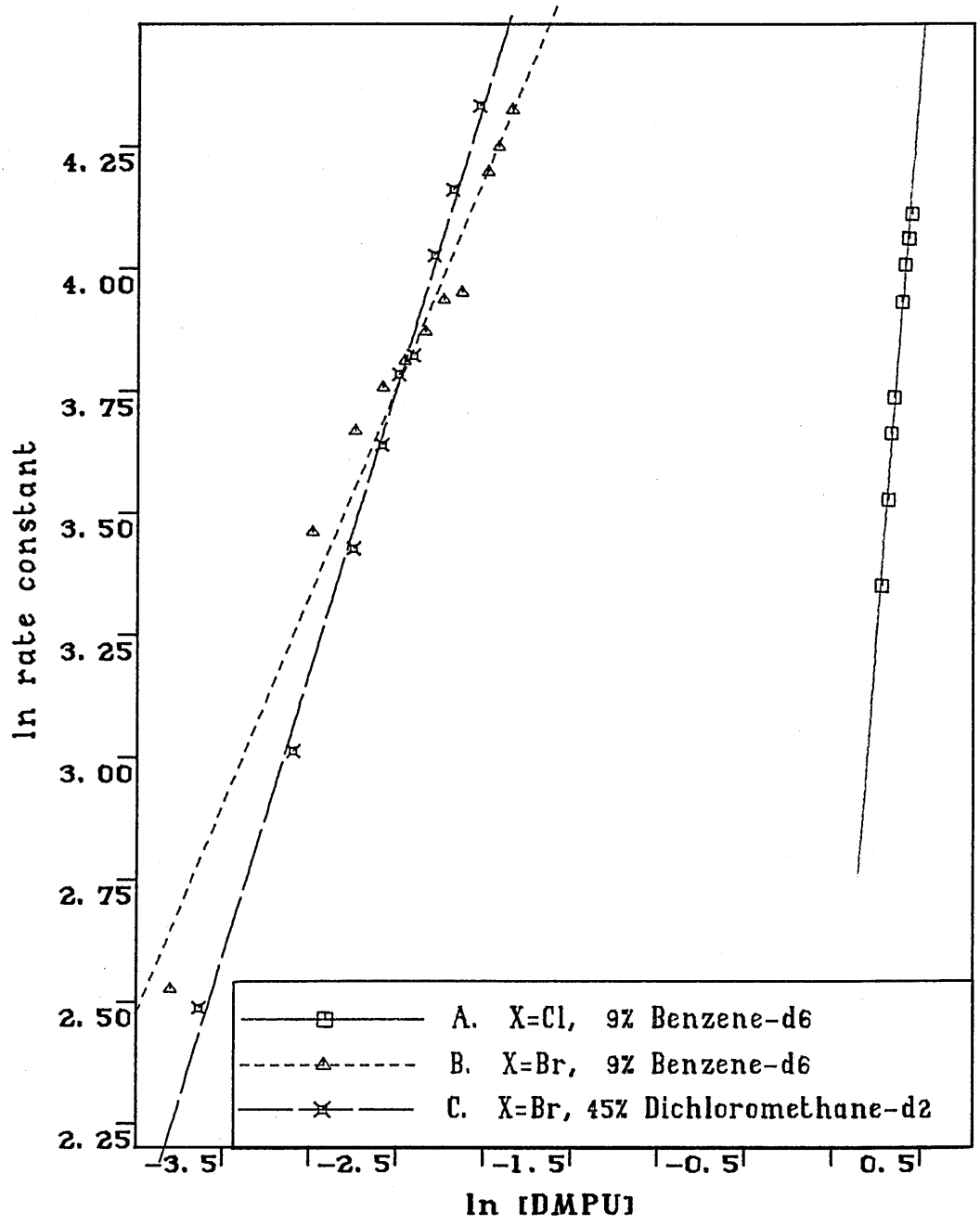

A. ln kobs = 4.738 (s.d. 0.22) ln [DMPU] + 2.108 (s.d. 0.08)

B. ln kobs = 0.858 (s.d. 0.04) ln [DMPU] + 5.912 (s.d. 0.11)

C. ln kobs = 1.174 (s.d. 0.03) ln [DMPU] + 6.694 (s.d. 0.07)

Figure 3.3.4

The effect of leaving group on the racemization of PhCHMeSiMe2X (X=Cl, Br) catalysed by DMEU.

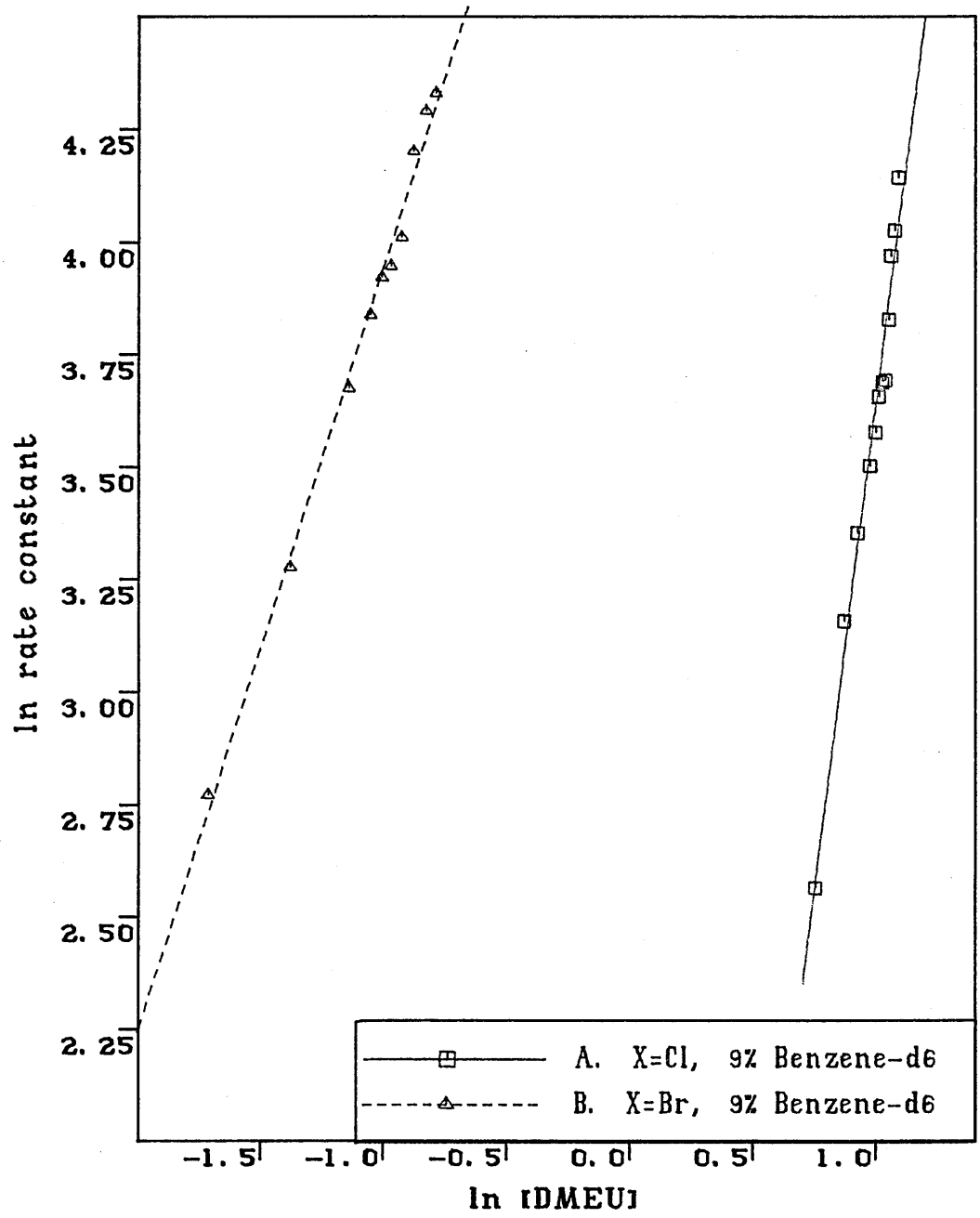

A. ln kobs = 4.379 (s.d. 0.20) ln [DMEU] - 0.708 (s.d. 0.20)

B. ln kobs = 1.697 (s.d. 0.05) ln [DMEU] + 5.644 (s.d. 0.05)

Figure 3.3.5

The effect of leaving group on the racemization of PhCHMeSiMe2X (X=Cl, Br) catalysed by TMU.

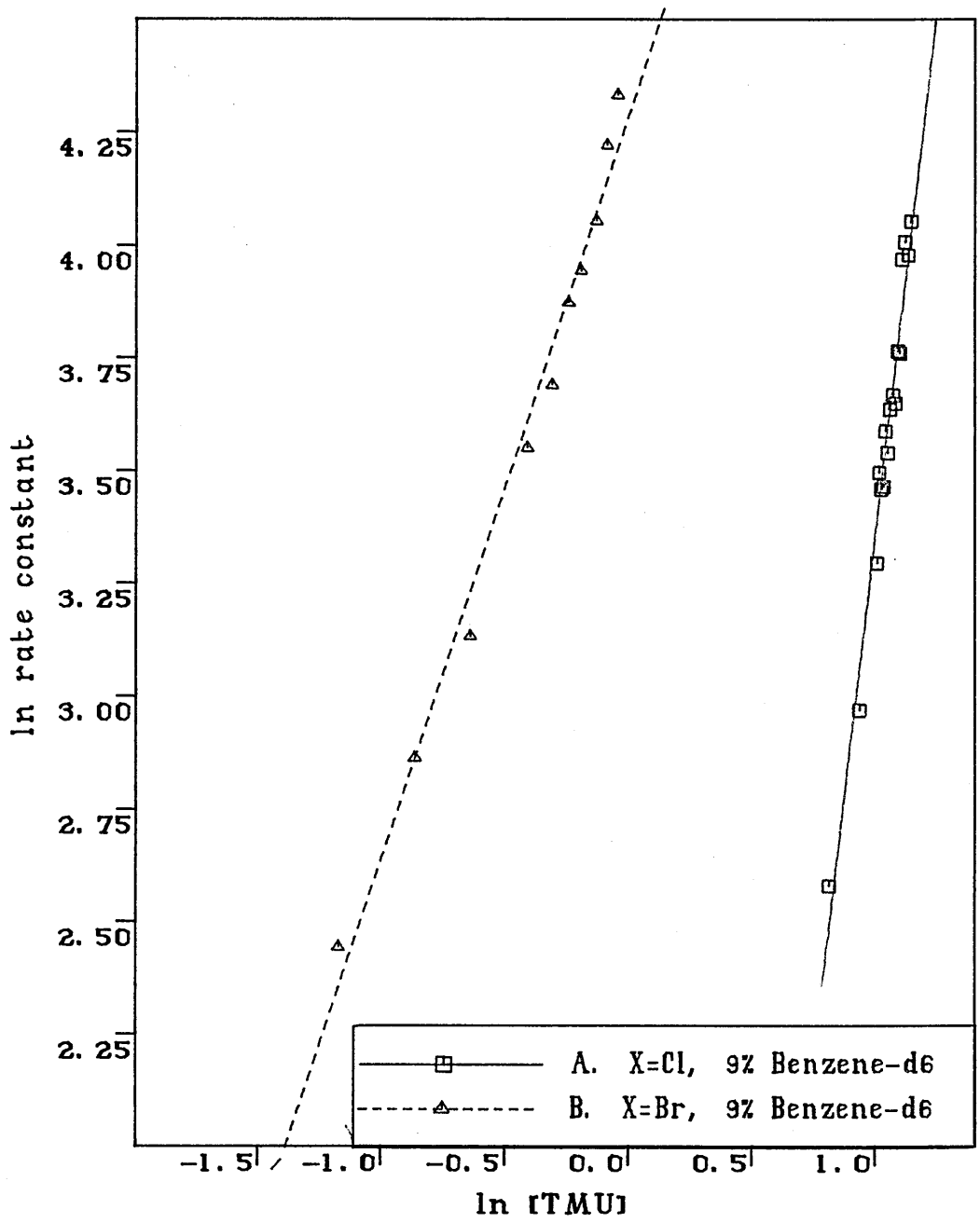

A. ln kobs = 4.692 (s.d. 0.20) ln [TMU] - 1.337 (s.d. 0.22)

B. ln kobs = 1.649 (s.d. 0.07) ln [TMU] + 4.273 (s.d. 0.04)

Figure 3.3.6

The effect of leaving group on the racemization of PhCHMeSiMe2X (X=Cl, Br) catalysed by NMPO.

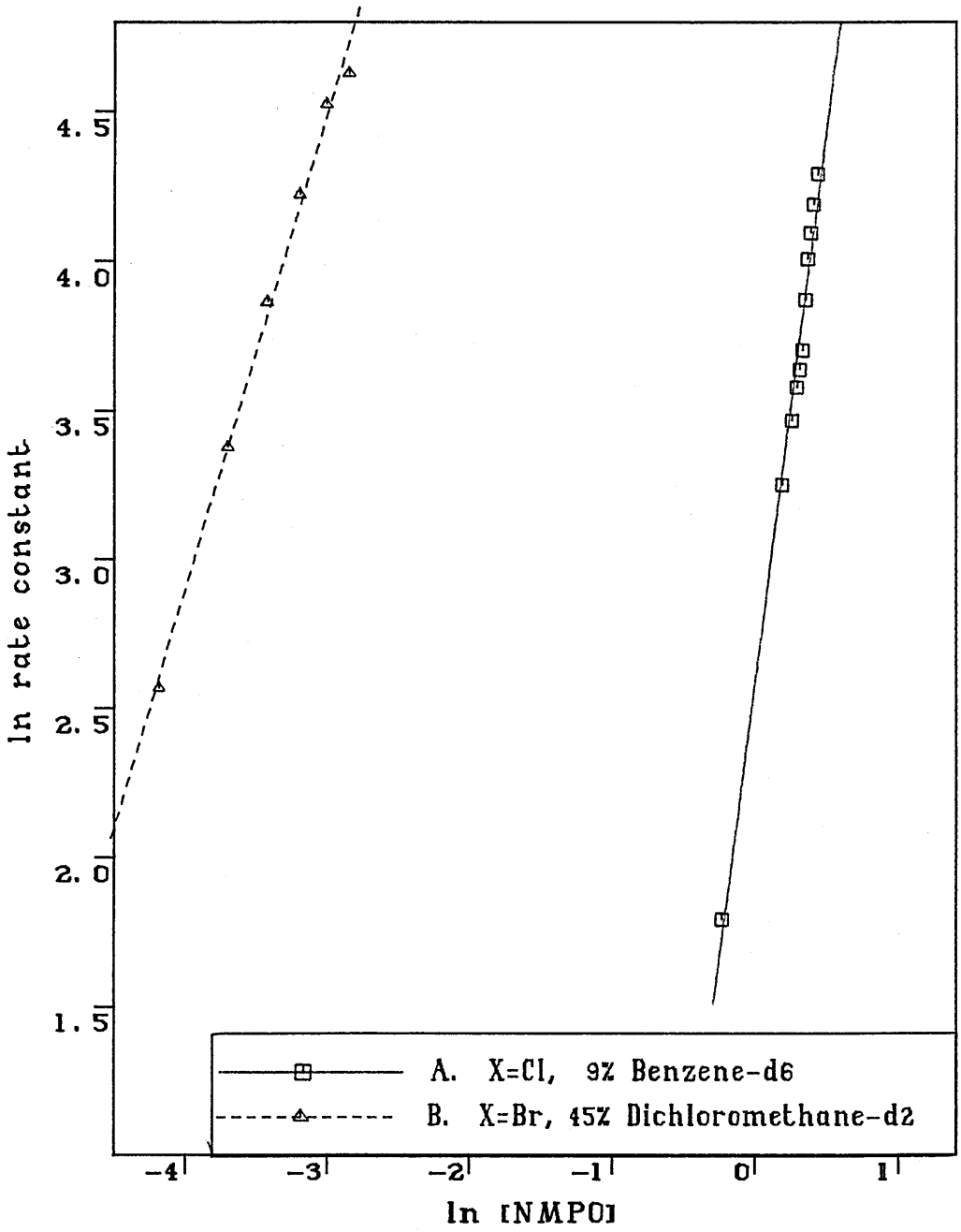

A. ln kobs = 3.739 (s.d. 0.14) ln [NMPO] + 2.606 (s.d. 0.05)

B. ln kobs = 1.600 (s.d. 0.05) ln [NMPO] + 9.271 (s.d. 0.19)

Figure 3.3.7
The effect of leaving group on the racemization of PhCHMeSiMe2X (X=Cl, Br) catalysed by NMP.

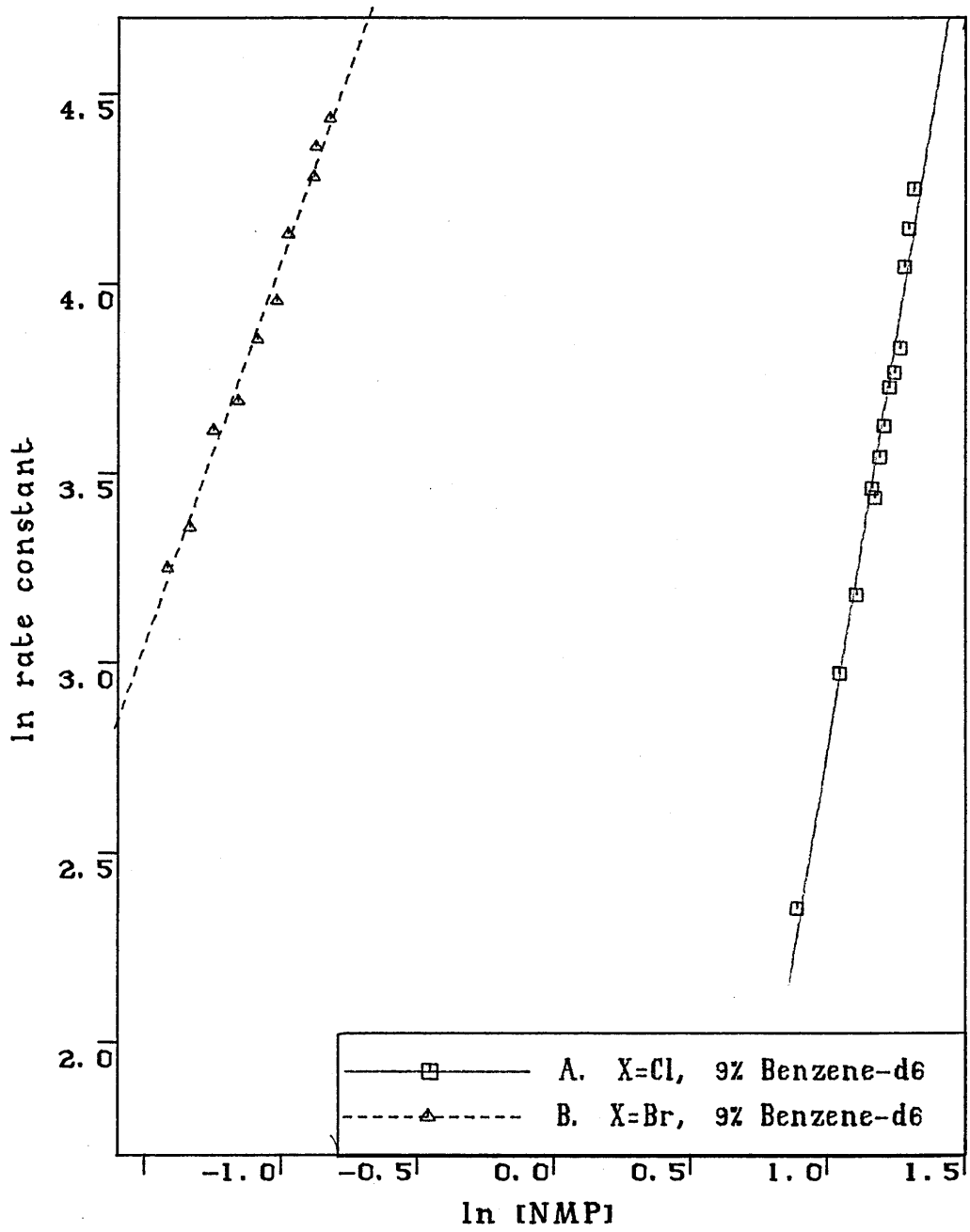

A. ln kobs = 4.395 (s.d. 0.17) ln [NMP] - 1.629 (s.d. 0.21)

B. ln kobs = 2.022 (s.d. 0.07) ln [NMP] + 6.066 (s.d. 0.08)

Figure 3.3.8
The effect of leaving group on the racemization of PhCHMeSiMe2X (X=Cl, Br) catalysed by DMF.

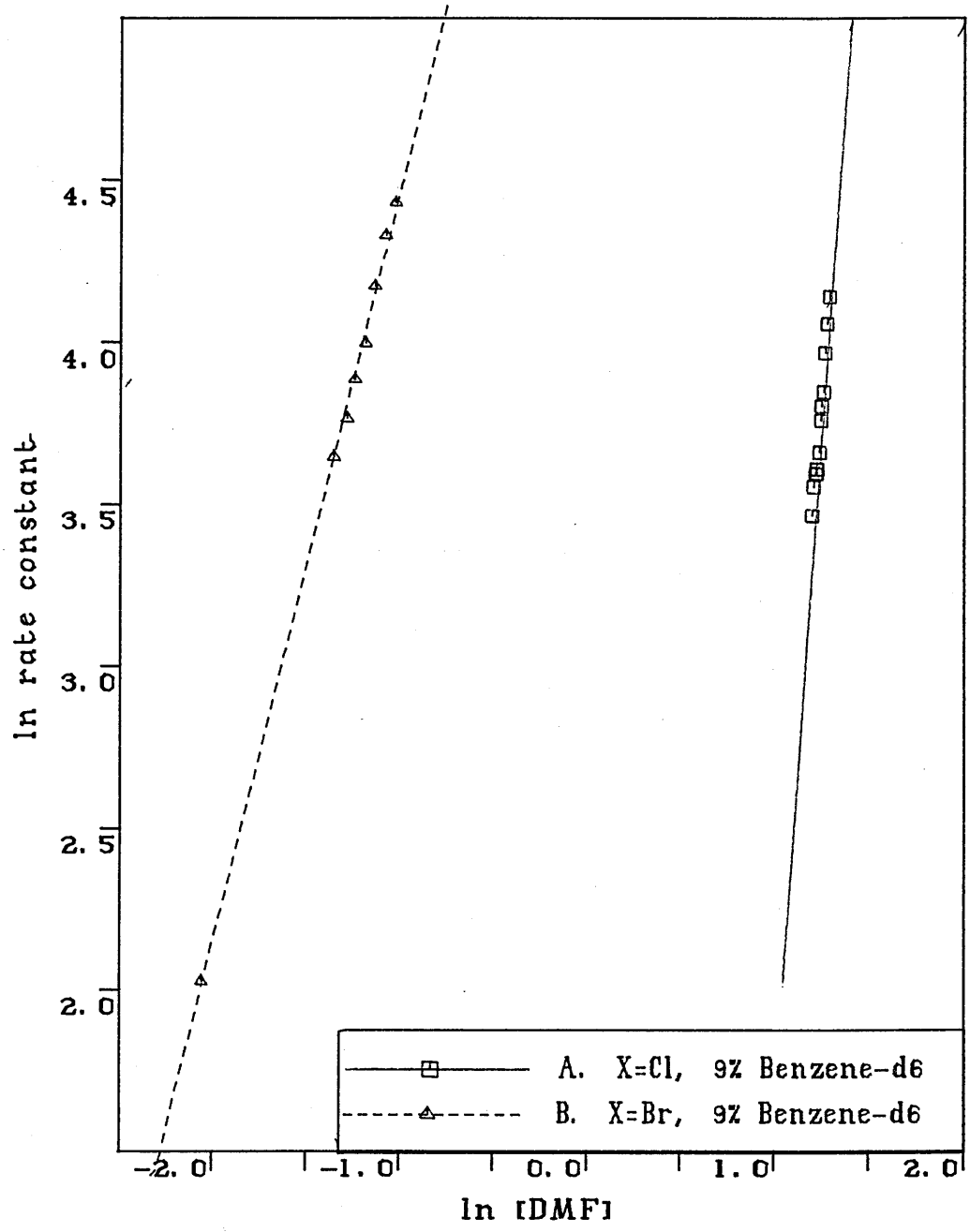

A. ln kobs = 7.575 (s.d. 0.29) ln [DMF] - 5.607 (s.d. 0.36)

B. ln kobs = 2.325 (s.d. 0.04) ln [DMF] + 6.776 (s.d. 0.05)

Figure 3.3.9

The effect of leaving group on the racemization of PhCHMeSiMe2X (X=Cl, Br) catalysed by pyridine (py).

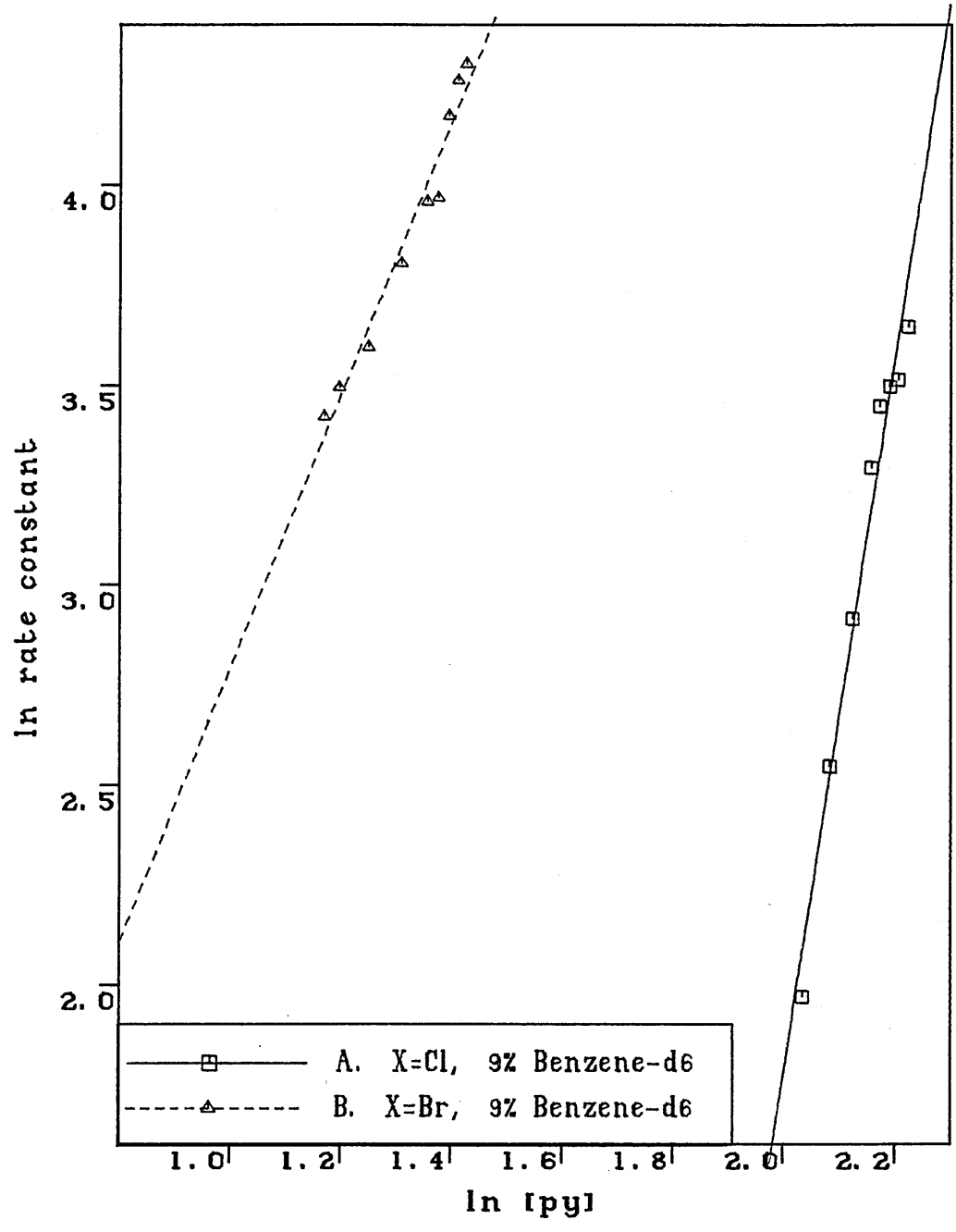

A. ln kobs = 8.982 (s.d. 0.58) ln [py] - 16.157 (s.d. 1.24)

B. ln kobs = 3.422 (s.d. 0.23) ln [py] - 0.624 (s.d. 0.30)

Figure 3.3.10
The effect of leaving group on the racemization of PhCHMeSiMe2X (X=Cl, Br) catalysed by 3,5DMP.

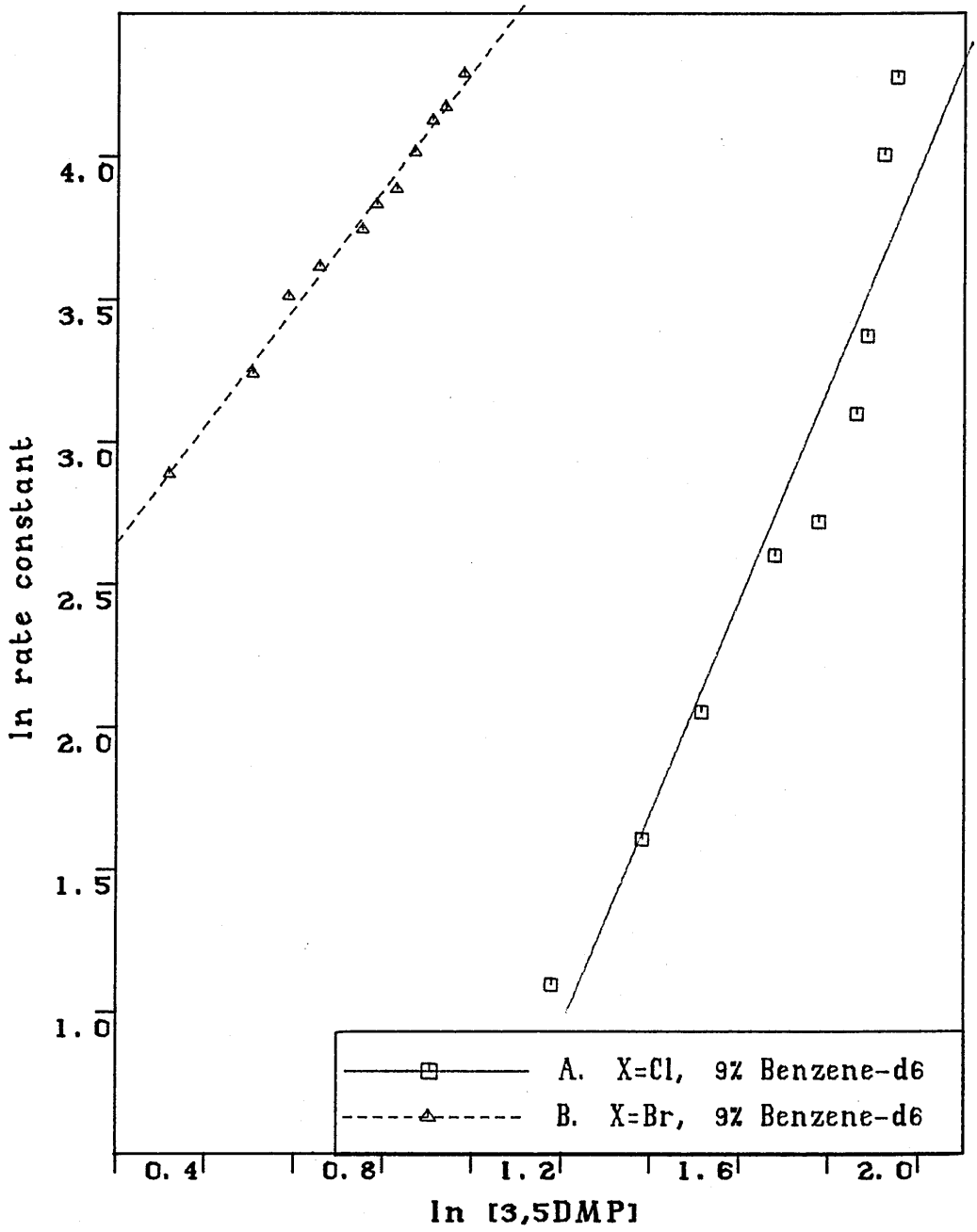

A. ln kobs = 3.758 (s.d. 0.40) ln [3,5DMP] - 3.544 (s.d. 0.68)

B. ln kobs = 2.071 (s.d. 0.06) ln [3,5DMP] + 2.238 (s.d. 0.04)

Figure 3.3.11
A kinetic plot for the racemization of PhCHMeSiMe2Br catalysed by 2,4DMP.

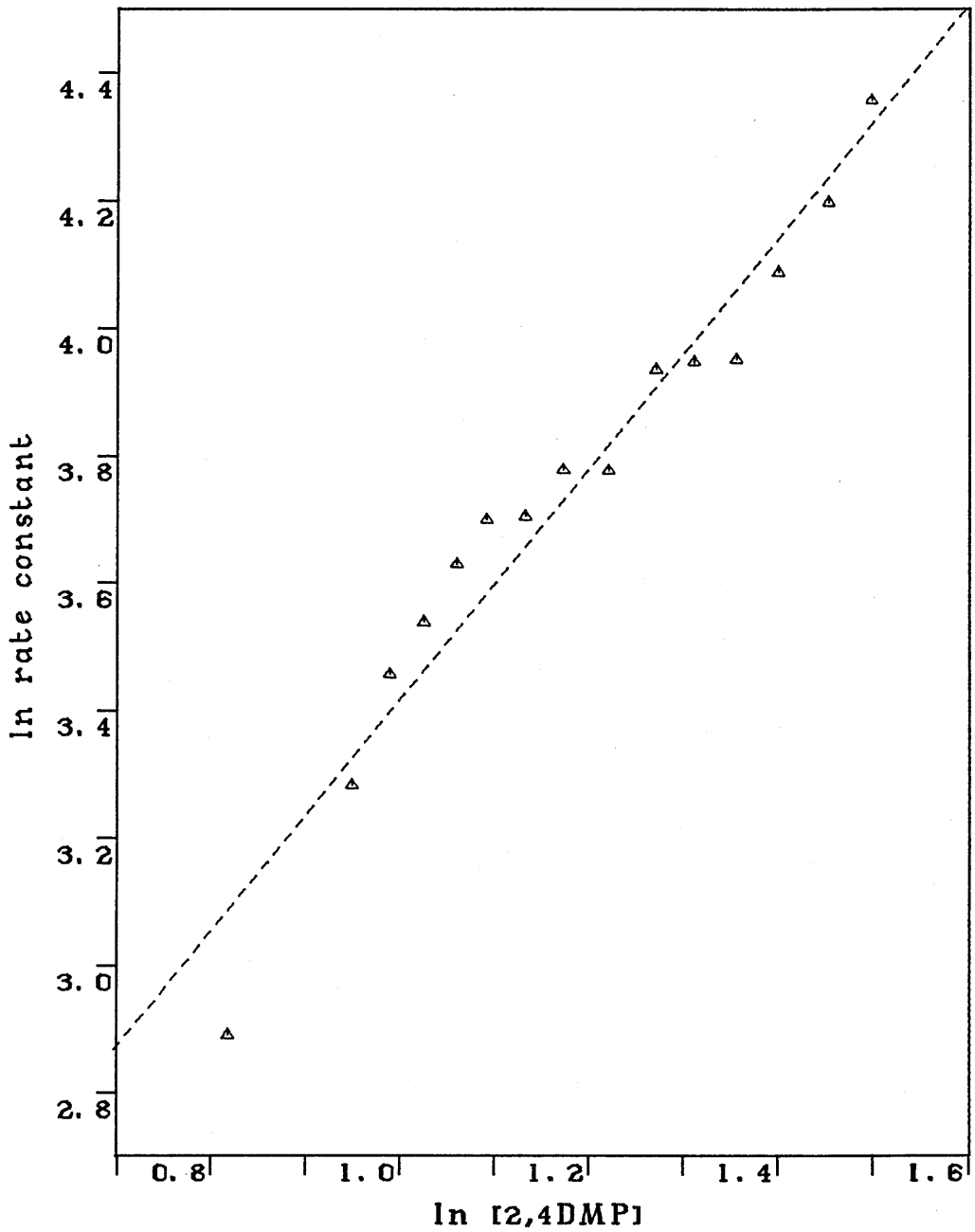

ln kobs = 1.812 (s.d. 0.114) ln [2,4DMP] + 1.603 (s.d. 0.137)
solvent: 9% Benzene-d6 (0.2 ml)

should be slower with respect to the analogous bromide exchange of the bromosilane. Therefore, if the attack by the counterion of a silane-nucleophile adduct at the uncomplexed silane is rate determining, the relative rate of racemization should decrease with counterion in the following order X=Br > OSO_2CF_3. Nevertheless, for a given nucleophile, the rate of racemization of $PhCHMeSiMe_2OSO_2CF_3$ was immeasurably fast relative to the bromosilane. This apparent contradiction can be rationalized by the greater leaving group ability of the triflate anion compared with the bromide analogue. Furthermore, the larger equilibrium constant for adduct formation in the case of silyl triflate as well as the greater ability of the counterion to be solvated lead to a higher concentration of triflate anion in solution.

3.4 The effect of nucleophile

Owing to their catalytic behaviour in silylation reactions, nucleophiles are frequently used in conjunction with silicon reagents. The nature of nucleophile is therefore crucial in governing the outcome of nucleophilic substitution at silicon. Detailed studies were performed on the interactions of $PhCHMeSiMe_2X$ (X=Cl, Br), usually in 9% (0.2 ml) benzene-d_6, with five different classes of donor species. These categories consisted of amides (NMPO, NMP and DMF), ureas (DMPU, DMEU and TMU), pyridine as well as the substituted pyridines (2,4DMP, 3,5DMP and 2,6DMP), amines including imidazole (Et_3N and NMI) and lastly the phosphine oxide, HMPA. Reproducibility was checked by repeating the reaction of $PhCHMeSiMe_2Cl$ with HMPA in 9% benzene-d_6.

Less concentrated $PhCHMeSiMe_2Br$ solutions in the more polar dichloromethane-d_2 were used for the reactions with strong nucleophiles. A five fold dilution containing 1.8 ml dichloromethane-d_2 was required for monitoring the HMPA activated racemization of $PhCHMeSiMe_2Br$, otherwise the reaction rate was too rapid to be measured accurately and salt precipitation was also observed. Instantaneous precipitation of the adduct was noted when NMI or NMPO was added to a bromosilane solution in

Table 3.4.1
Summary of the kinetic results for the nucleophile assisted racemizations of $PhCHMeSiMe_2X$ (X=Cl, Br)

Nucleophile	Molar ratio of silane : Nu at coalescence X=Cl	X=Br	Order in Nu X=Cl	X=Br
HMPA	1.0 : 0.08	instant precipitation immeasurably fast[c]	2.33	-
		1.0 : 0.02[a]	-	1.48
		1.0 : 0.01[a,b]	-	1.34
NMI	1.0 : 0.13	instant precipitation	3.37	-
		1.0 : 0.035[c]	-	1.64
		1.0 : 0.027[b,c]	-	1.55
NMPO	1.0 : 0.34	instant precipitation	3.74	-
		1.0 : 0.02[c]	-	1.60
DMPU	1.0 : 0.37	1.0 : 0.03	4.74	0.86
		1.0 : 0.05[c]	-	1.17
DMEU	1.0 : 0.86	1.0 : 0.10	4.38	1.70
DMF	1.0 : 1.00	1.0 : 0.07	7.58	2.33
NMP	1.0 : 1.18	1.0 : 0.09	4.40	2.02
TMU	1.0 : 1.02	1.0 : 0.22	4.69	1.65
3,5DMP	1.0 : 6.23	1.0 : 0.76	3.76	2.07
py	1.0 : 9.87[d]	1.0 : 1.31	8.98	3.42
2,4DMP	1.0 : 6.38[e]	1.0 : 1.68	-	1.81
2,6DMP	no	no	-	-
Et_3N	no	no	-	-

Quantities used: silane 2.0 ml
solvent 0.2 ml benzene-d_6

a 0.4 ml silane in 1.8 ml dichloromethane-d_2
b in the presence of 2,6DBP
c 1.0 ml silane in 1.2 ml dichloromethane-d_2
d near coalescence
e only broadened
no not observed
The rate of exchange between $PhCHMeSiMe_2OSO_2CF_3$ and py was very rapid and immeasurable.

9% benzene-d_6. Therefore the interactions with NMI, NMPO and DMPU were carried out with dichloromethane-d_2 as the solvent; the silane solutions were diluted two fold with 1.0 ml of silane dissolved in 1.2 ml of solvent. DMPU was also studied in this solvent to enable comparison of the results to be made with the 9% benzene-d_6 solution.

For each silane-nucleophile interaction, the gradual broadening and the subsequent coalescence of the two diastereotopic carbon-13 SiMe signals were followed with increasing concentration of nucleophile. The kinetic plots of ln rate constant versus ln [Nu] for $PhCHMeSiMe_2X$ (X=Cl, Br) with a particular nucleophile are provided in the appropriate figures. A summary of the calculated orders in nucleophile and the ratios of silane to nucleophile at coalescence for a given silane is shown in Table 3.4.1.

3.4.1 Nucleophile assisted racemization of $PhCHMeSiMe_2Cl$

Inspection of the results indicates that the variations in the quantity of nucleophile needed for coalescence to occur share the same trend as the orders in nucleophile, which reflects the nucleophilicity of the donor species. With increasing donor strength, a larger ratio of silane to nucleophile was observed since the merging of the two peaks occurred more readily in the presence of a reduced amount of nucleophile. An approximate second order with respect to HMPA was observed for the racemization of $PhCHMeSiMe_2Cl$, which is fully consistent with the first proposed mechanistic route involving two consecutive nucleophilic attacks as illustrated in Scheme 3.2.1.

The racemization of the chlorosilane should proceed via the same mechanism for all nucleophiles. Surprisingly, high orders in nucleophile were noted especially in the cases of DMF and pyridine, with orders of 7.58 and 8.98 respectively. These unexpected results can be attributed to two factors. Firstly, the polarity of the medium changes with increasing concentration of nucleophile favouring the formation of salt

and secondly the aggregation of nucleophile molecules, which can be represented mathematically by the following scheme and rate equations.

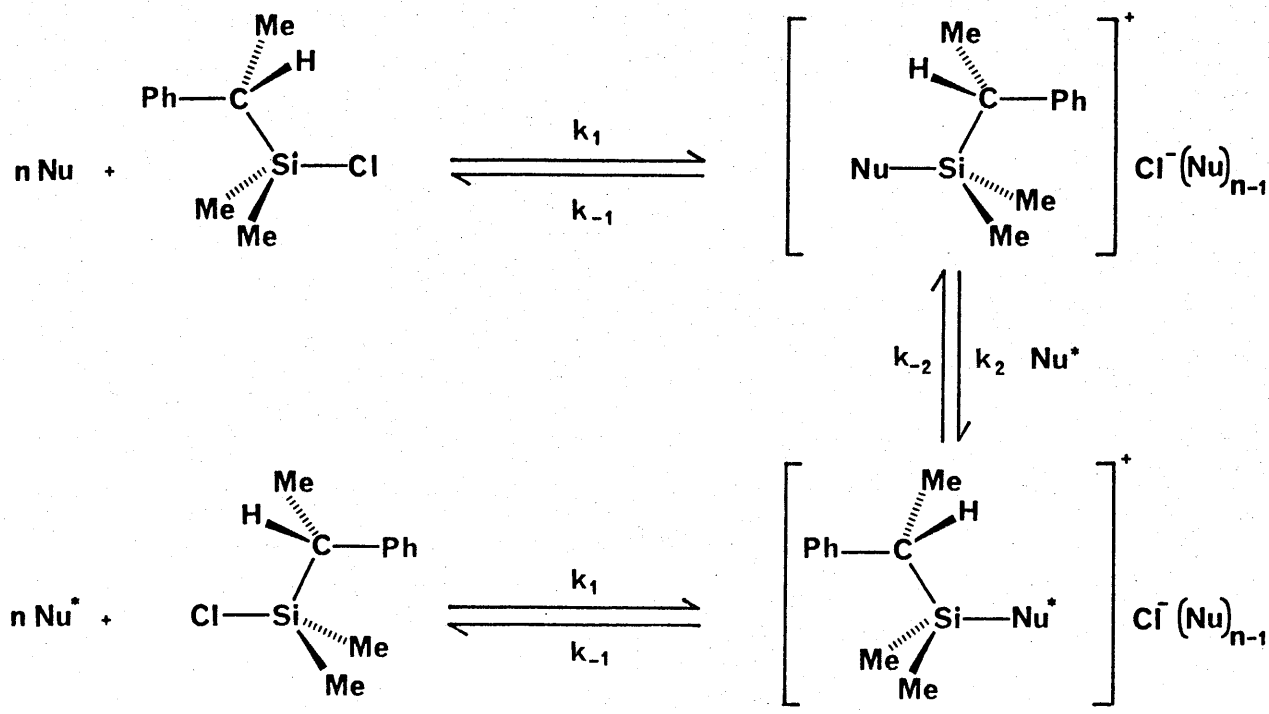

n is the number of aggregated nucleophile molecules

Scheme 3.4.1 Aggregation of Nu molecules in $PhCHMeSiMe_2Cl$ racemization

It is assumed that the attack of a second molecule of nucleophile at the silicon atom of the silane-nucleophile adduct is the rate determining step of the process. If the silane-nucleophile complex is ion-paired, no ion-pair dissociation takes place and the racemization can be expressed by the following rate law.

$$\text{Rate} = k_2[PhCHMeSiMe_2Nu^+ X^-(Nu)_{n-1}][Nu^*] \qquad \textbf{Equation 3.4.1}$$

However the equilibrium constant for complex formation (K_{eq}) is related to the concentration of the adduct.

$$K_{eq} = \frac{k_1}{k_{-1}} = \frac{[PhCHMeSiMe_2Nu^+ X^-(Nu)_{n-1}]}{[PhCHMeSiMe_2X]\,[Nu]^n} \qquad \text{Equation 3.4.2}$$

$$[PhCHMeSiMe_2Nu^+ X^-(Nu)_{n-1}] = K_{eq}[PhCHMeSiMe_2X][Nu]^n$$

Substituting the above expression into the equation 3.4.1 yields an overall rate law for the racemization of the chlorosilane since Nu is the same as Nu^*.

$$\text{Rate} = k_2K_{eq}[PhCHMeSiMe_2X][Nu]^{n+1} \qquad \text{Equation 3.4.3}$$

Nevertheless if the adduct dissociates into separate ions, the rate expression for the racemization can be written in the following form.

$$\text{Rate} = k_2[PhCHMeSiMe_2Nu^+][Nu^*] \qquad \text{Equation 3.4.4}$$

$$K_{eq} = \frac{k_1}{k_{-1}} = \frac{[PhCHMeSiMe_2Nu^+ X^-(Nu)_{n-1}]}{[PhCHMeSiMe_2X\ ]\,[Nu]^n} \qquad \text{Equation 3.4.5}$$

$$K_{eq}\,[PhCHMeSiMe_2X]\,[Nu]^n = [PhCHMeSiMe_2Nu^+ X^-(Nu)_{n-1}]$$

$$PhCHMeSiMe_2Nu^+X^-(Nu)_{n-1} \overset{K_d}{\rightleftharpoons} PhCHMeSiMe_2Nu^+ + X^-(Nu)_{n-1}$$

Scheme 3.4.2

The equilibrium constant for ion-pair dissociation (K_d) can be expressed as follows:-

$$K_d = \frac{[PhCHMeSiMe_2Nu^+]\,[X^-(Nu)_{n-1}]}{[PhCHMeSiMe_2Nu^+ X^-(Nu)_{n-1}]} \qquad \text{Equation 3.4.6}$$

Combining equations 3.4.5 and 3.4.6 gives the following expression.

$$[PhCHMeSiMe_2Nu^+][X^-(Nu)_{n-1}] = K_d[PhCHMeSiMe_2Nu^+X^-(Nu)_{n-1}]$$

Equation 3.4.7

$[PhCHMeSiMe_2Nu^+] = [X^-(Nu)_{n-1}]$, therefore the above equation can be rewritten as

$$[PhCHMeSiMe_2Nu^+] = K_d^{0.5}[PhCHMeSiMe_2Nu^+X^-(Nu)_{n-1}]^{0.5}$$

Substituting this equation into the overall rate expression produces the following rate law.

$$\text{Rate} = k_2K_d^{0.5}[PhCHMeSiMe_2Nu^+\ X^-(Nu)_{n-1}]^{0.5}[Nu^*] \quad \textbf{Equation 3.4.8}$$

But from equation 3.4.5

$$[PhCHMeSiMe_2Nu^+\ X^-(Nu)_{n-1}] = K_{eq}\ [PhCHMeSiMe_2X]\ [Nu]^n$$

Hence the overall rate equation for the racemization of chlorosilane can be reduced to

$$\textbf{Rate} = k_2K_{eq}^{0.5}K_d^{0.5}[PhCHMeSiMe_2X]^{0.5}[Nu]^{(n+2)/2} \quad \textbf{Equation 3.4.9}$$

Furthermore, with a weak donor species for instance pyridine, a large quantity of nucleophile is necessary for coalescence of the two diastereotopic SiMe signals. In this case, the nucleophile becomes the solvent giving rise to a pronounced medium effect stabilizing the salt. Apart from aggregation of molecules through hydrogen bonding, complex formation between DMF and aromatic solvents, such as benzene, has been proposed.[81] The preferred geometrical arrangement of the DMF-benzene complex is shown in the figure below. The nitrogen atom, with its fractional positive charge, is located above the centre of the benzene ring. The carbonyl group tends to be as far away from the centre as

possible with the amide and benzene planes remaining approximately parallel.

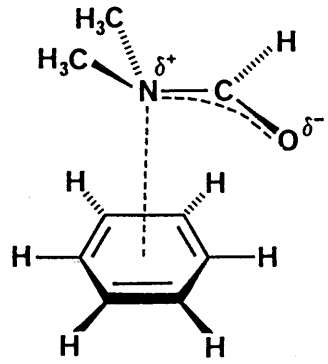

Figure 3.4.1 DMF-benzene complex

3.4.2 Nucleophile promoted racemization of $PhCHMeSiMe_2Br$

Due to precipitation of silane-nucleophile adduct, the interactions with strong donors were performed in dichloromethane-d_2 at different concentrations. Therefore the results are divided into two groups according to the concentration of the silane and the solvent used. Thus the reactions in 9% (0.2 ml) benzene-d_6 are considered separately to those in dichloromethane-d_2.

The changes in the quantity of nucleophile utilized for inducing racemization and the orders in nucleophile follow similar trends to those observed for the corresponding racemization of $PhCHMeSiMe_2Cl$. However in contrast to the analogous chlorosilane, the orders in nucleophile for the $PhCHMeSiMe_2Br$ series are much smaller and lie between 1 to 3 approximately. Furthermore, the amount of nucleophile required for the coalescence of the two SiMe signals was five to ten fold less than that for the chlorosilane racemizations, hence the ratios of silane to nucleophile at coalescence were considerably larger for the bromosilane.

Similar to the $PhCHMeSiMe_2Cl$ series, DMF and pyridine again yield the highest orders for the bromosilane racemization, which are 2.326 and

3.422 respectively. No significant broadening of the two diastereotopic SiMe resonances could be detected for either of the silanes, $PhCHMeSiMe_2X$ (X=Cl, Br), even in five to seven fold excess of 2,6-dimethylpyridine (2,6DMP) or triethylamine (Et_3N). With successive additions of 2,4-dimethylpyridine (2,4DMP) to the $PhCHMeSiMe_2Cl$ solution, slight changes in the line shapes of the two peaks were noted, though merging of the signals were not observed even with a six molar excess of the nucleophile.

The lack of reactivity in these two substituted pyridines, particularly 2,6DMP, is quite surprising in view of the 3,5DMP results. The similarity between the donor properties of the three methyl substituted pyridines (pKa = 6.77, 6.72 and 6.14; Taft's scale of nucleophilicity[41] or Beta = 0.76, 0.74 and 0.70 for 2,6DMP, 2,4DMP and 3,5DMP respectively) strongly implies that the effect is largely steric in origin for 2,6DMP. Nevertheless the extremely hindered nature of 2,6-di-tert-butyl-4-methylpyridine did not prevent its interaction with tert-butyldimethylsilyl perchlorate as reported by Barton and Tully,[82] although no supporting data for complex formation was provided. Such adduct formation is not entirely unexpected since silyl perchlorates are more effective complexing agents than the commonly employed silylating species, for example trimethylsilyl triflate. This steric explanation can also be advanced to account for the results with Et_3N. However the major contributing factor is more likely to be its comparatively weak donor strength.

With increasing nucleophilicity of the donor, the gradual reduction in the orders with respect to nucleophile strongly indicates a change in the reaction pathway. Second orders are observed with nucleophiles, such as NMP and 3,5DMP, which are in accord with the mechanism in section 3.2.1, where two molecules of nucleophile attack consecutively at silicon. The observation of an approximately first order with respect to DMPU, a relatively powerful nucleophile, implies that the mechanism postulated in section 3.2.2 is operating. Fractional orders between 1 and 2 for nucleophiles with intermediate strength, for instance DMEU and TMU, can

Figure 3.4.2

The effect of nucleophile on the racemization of PhCHMeSiMe2Cl in the presence of 2,6DBP in dichloromethane-d2.

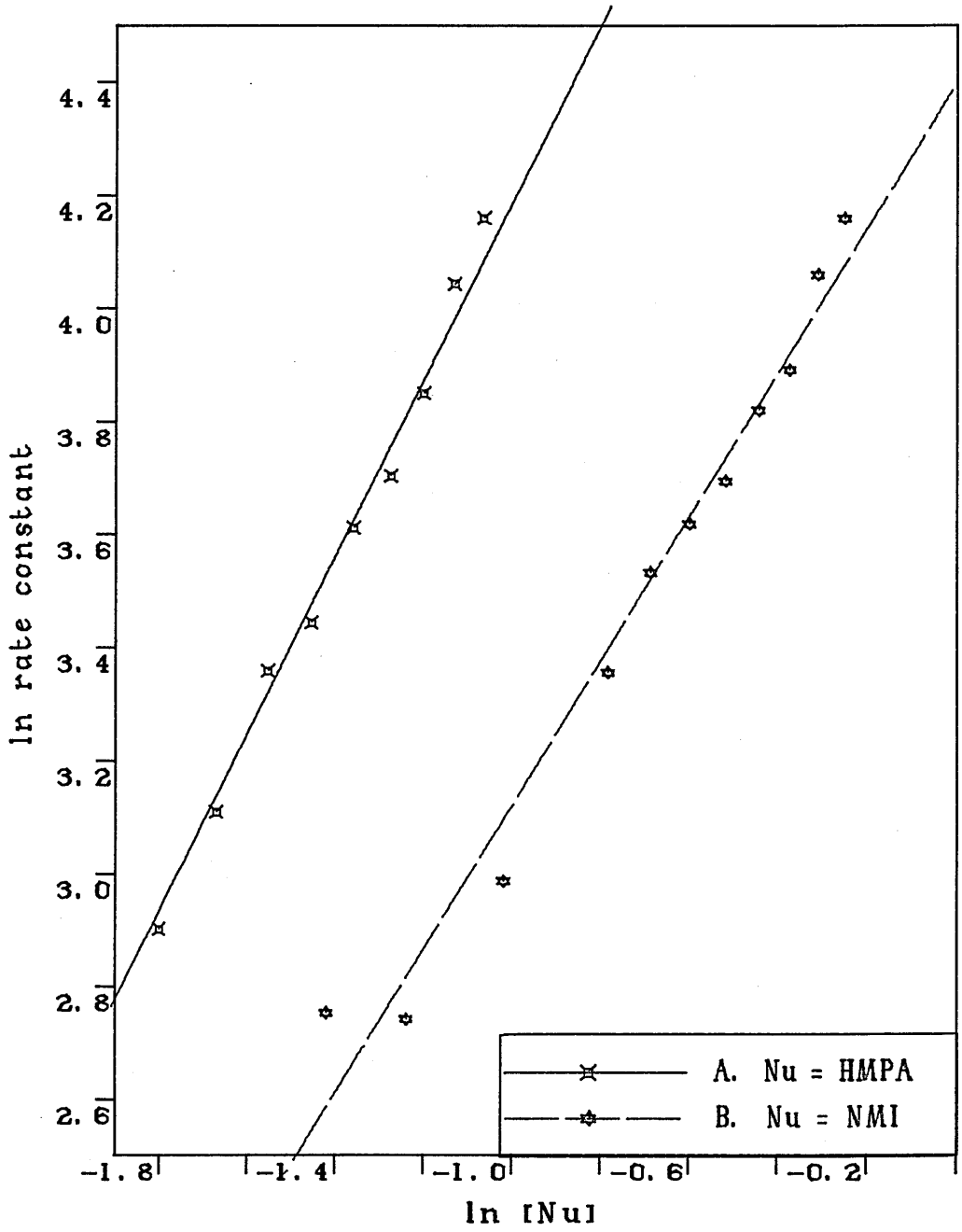

A. ln kobs = 1.569 (s.d. 0.05) ln [HMPA] + 5.748 (s.d. 0.08)

B. ln kobs = 1.277 (s.d. 0.06) ln [NMI] + 4.392 (s.d. 0.05)

be rationalized either by the operation of the first mechanism (Scheme 3.2.1) under the conditions of ion-pair dissociation or alternatively by a combination of the two mechanistic routes.

The formation of a silane-nucleophile adduct was clearly demonstrated by the precipitation of salts, when strong donor species (HMPA, NMI or NMPO) were added to $PhCHMeSiMe_2Br$ solutions in the relatively non-polar benzene-d_6. HMPA proved to be an extremely efficient nucleophile since the racemization of $PhCHMeSiMe_2Br$ was very rapid even with a five times less concentrated silane solution in 1.8 ml dichloromethane-d_2. Hence, only three data points were recorded but they produced a linear regression line without appreciable scatter. The orders in these nucleophiles (HMPA, NMI, NMPO and DMPU) are similar to that observed by Cartledge[72,73] on halide exchanges and the order of 1.6 in chloride ion reported by Prince[71] on halide exchange of Ph_3SiCl. However, for (-)1-NpPhMeSiCl, orders of 0.5 and 1.5 were observed for racemisation and exchange respectively. These different orders resulted from a combination of retention and inversion at silicon.

3.5 The effect of solvent

The nature of solvent is expected to play a key role in governing the rate of racemization since ionic intermediates are involved in the two postulated mechanisms. Changes in the medium will affect the stabilization of the ionic charges and hence alter the reaction rate. The influence of solvent on the rate of racemization of a halosilane was examined in detail by studying the interactions of $PhCHMeSiMe_2Cl$ with nucleophiles (NMI, HMPA) in 9% (0.2 ml) in different solvents. The results together with the physical constants of the various solvents used are outlined in the following table.

Table 3.5.1 Solvent effect on the racemization of $PhCHMeSiMe_2Cl$ catalysed by nucleophiles (NMI, HMPA)

Solvent	Polarity (E_T)	Dielectric constant (ϵ)	Ratio silane:Nu		Order in Nu	
			HMPA	NMI	HMPA	NMI
$C_6D_6.CD_3$	33.9	2.4	1:0.080	1:0.129	2.995	2.557
C_6D_6	34.5	2.3	1:0.075	1:0.126	2.329	3.367
CD_2Cl_2	41.1	8.9	1:0.052	1:0.077	1.745	1.921
CD_3NO_2	46.3	35.9	1:0.012	1:0.031	1.256	1.141

The quantity of nucleophile required for coalescence follows a similar trend to the order with respect to the nucleophile, which is directly related to the observed rate of racemization of the silane. The results above can be rationalized in terms of the physical properties of the solvent. Generally, in solvents with analogous properties, the two diastereotopic SiMe resonances collapse at a similar rate for a particular silane and nucleophile. The comparatively non-polar solvents, toluene-d_8 and benzene-d_6, require a higher proportion of nucleophile to induce coalescence. The orders in the nucleophile for the racemization reaction are between 2 to 3. With more polar solvents, such as nitromethane-d_3, the order is closer to unity and a smaller quantity of nucleophile is needed for racemization.

This strongly suggests that different mechanisms are adopted for solvents with different polarities and dielectric constants. The higher orders with respect to nucleophile in relatively non-polar solvents are consistent with the first mechanistic route in Scheme 3.2.1, where two molecules of nucleophiles are involved, corresponding to a second order in nucleophile. Similarly, when the racemization takes place in polar media, it probably follows the second pathway as depicted in Scheme 3.2.1, resulting in an approximate first order in the nucleophile.

The stabilization of the counterion Cl^- offered by the solvent can account for such a change-over in the reaction mechanism. The formation

Figure 3.5.1
The effect of solvent on the racemization of PhCHMeSiMe2Cl catalysed by HMPA.

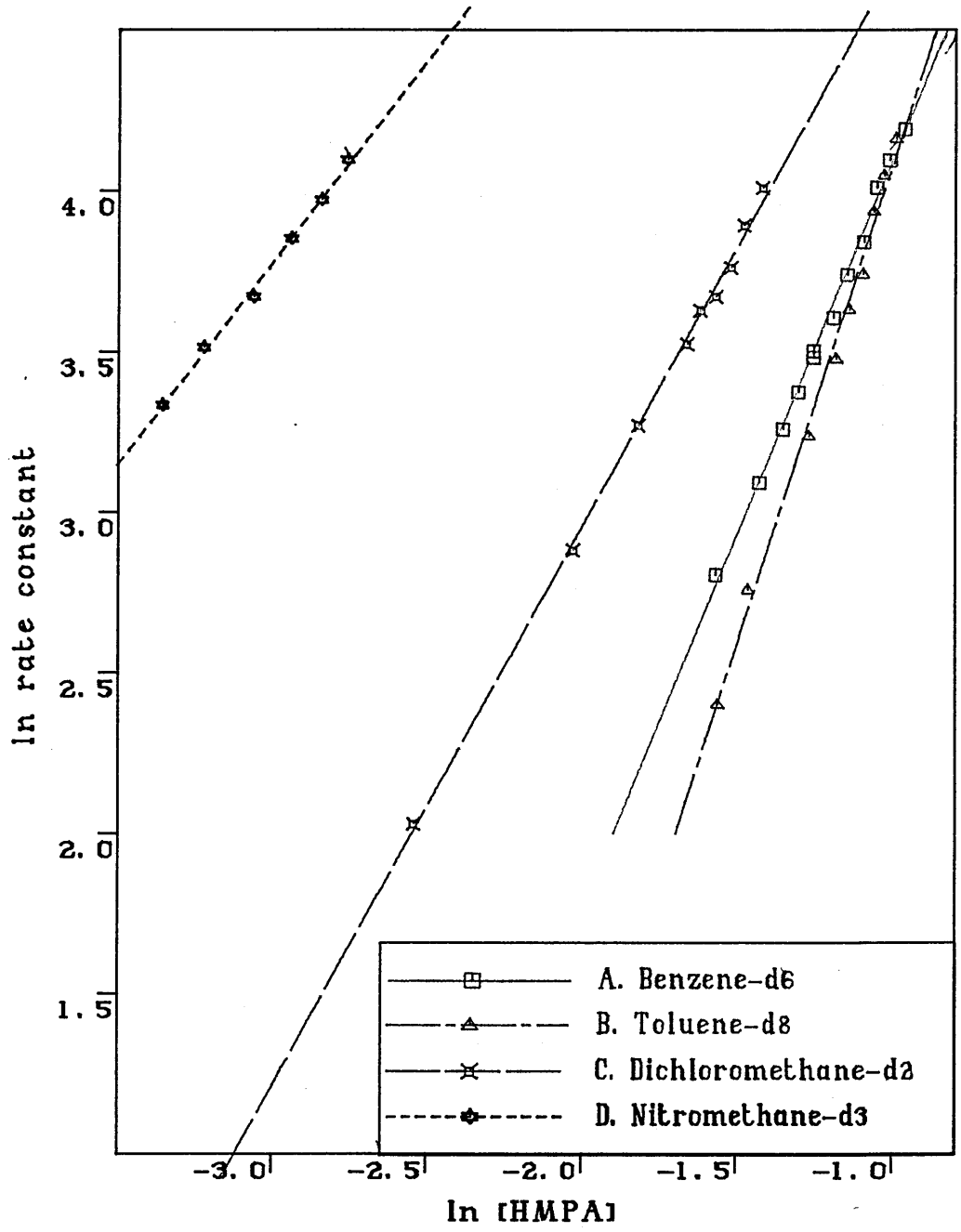

A. ln kobs = 2.329 (s.d. 0.04) ln [HMPA] + 6.436 (s.d. 0.05)
B. ln kobs = 2.995 (s.d. 0.09) ln [HMPA] + 7.076 (s.d. 0.11)
C. ln kobs = 1.745 (s.d. 0.03) ln [HMPA] + 6.440 (s.d. 0.05)
D. ln kobs = 1.256 (s.d. 0.03) ln [HMPA] + 7.547 (s.d. 0.01)

Figure 3.5.2
The effect of solvent on the racemization of PhCHMeSiMe2Cl catalysed by NMI.

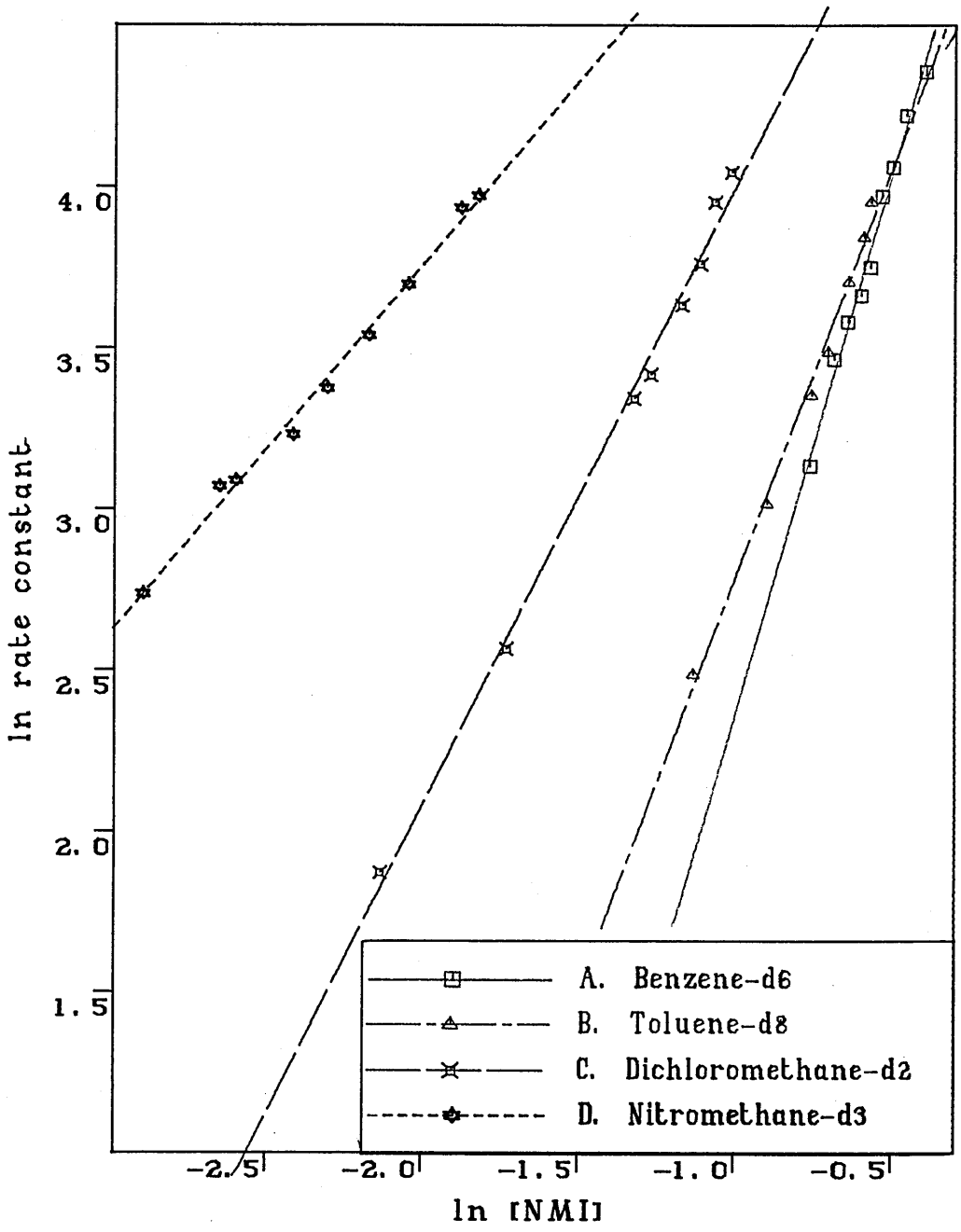

A. ln kobs = 3.367 (s.d. 0.13) ln [NMI] + 5.730 (s.d. 0.07)
B. ln kobs = 2.557 (s.d. 0.93) ln [NMI] + 5.323 (s.d. 0.72)
C. ln kobs = 1.921 (s.d. 0.06) ln [NMI] + 5.911 (s.d. 0.08)
D. ln kobs = 1.141 (s.d. 0.03) ln [NMI] + 6.042 (s.d. 0.07)

and the subsequent ion dissociation of the ionic salt, $[PhCHMeSiMe_2Nu]^+Cl^-$, are favoured as the medium becomes more polar. Solvents with large polarities and dielectric constants stabilize ionic charges and enhance dissociation of the $[PhCHMeSiMe_2Nu]^+Cl^-$ complex into its separate ions by solvation. As concluded in the preceding chapter, the counterion, Cl^-, may attack the silicon atom of $PhCHMeSiMe_2Cl$ inducing racemization of the silane.

3.6 The effect of concentration

An initial qualitative study on the effect of dilution on the rate of racemization of a halosilane was carried out by syringing successive aliquots of dichloromethane-d_2 into a coalesced mixture of $PhCHMeSiMe_2X$ (X=Cl or Br) and HMPA. The changes in the line shape of the coalesced broad SiMe peak were examined as the concentrations of silane and HMPA were altered.

Dilution with dichloromethane-d_2 causes an initial sharpening of the broad SiMe resonance of $PhCHMeSiMe_2Cl$, indicating an increase in the racemization rate. Rate retardation was observed after a certain limit was reached, accompanied by line broadening of the sharp signal. However additions of dichloromethane-d_2 to the reaction mixture of the corresponding bromosilane and HMPA only induced deceleration of the racemization rate.

The above rationalization for the acceleration of the racemization rate with increasing polarities and dielectric constants of solvents can also be applied to explain the initial rise in the racemization rate of $PhCHMeSiMe_2Cl$ in this case. The rate expressions in section 3.2 clearly demonstrate that the rate of racemization of $PhCHMeSiMe_2X$ (X=Cl, Br) is directly proportional to and controlled by the equilibrium constant for adduct formation (K_{eq}) as well as the concentrations of the silane and nucleophile, i.e. rate α $K_{eq}[PhCHMeSiMe_2X][Nu]$. Variations in K_{eq} or the concentrations of the reacting species will lead to changes in the

reaction rate. Thus the racemization rate is governed by a delicate balance between the equilibrium constant and the concentrations of the substrates.

Owing to the introduction of dichloromethane-d_2, the medium becomes more polar, facilitating the solvation and hence stabilization of the ionic $[PhCHMeSiMe_2\text{-}HMPA]^+Cl^-$ intermediate, thus a larger equilibrium constant for such adduct formation results. Nevertheless, an increasing proportion of solvent reduces the concentrations of the silane and nucleophile. The increase in the equilibrium constant probably offsets the decrease in the concentrations yielding an overall acceleration in the racemization rate of $PhCHMeSiMe_2Cl$ at the beginning of the dilution process.

As the additions of dichloromethane-d_2 continue, the dilution effect dominates leading to rate deceleration. This explanation can also be responsible for the decrease in the racemization rate of the analogous bromosilane. The $[PhCHMeSiMe_2\text{-}HMPA]^+Br^-$ salt is formed readily and is more easily solvated than its chloride counterpart. Therefore increasing the polarity of the medium will offer a comparatively small stabilizing effect on the adduct; the equilibrium constant will not be affected significantly. Thus the decrease in the rate of racemization of $PhCHMeSiMe_2Br$ is mainly due to the lowering of concentrations of the reactants.

The influence of concentration on the rate of HMPA catalysed racemization was investigated in detail by following the rate at which the two diastereotopic SiMe peaks of $PhCHMeSiMe_2Cl$ coalesce, at four different silane concentrations in either benzene-d_6 or dichloromethane-d_2 as listed below. The experimental results are summarized in the following table and are presented in the figures provided.

A. 2.0 ml of silane in 0.2 ml solvent (standard 9%)

B. 1.0 ml of silane in 1.2 ml solvent (two fold dilution)

C. 0.4 ml of silane in 1.8 ml solvent (five fold dilution)

D. 0.2 ml of silane in 2.0 ml solvent (ten fold dilution)

Table 3.6.1 Concentration effect of on the racemization of $PhCHMeSiMe_2Cl$

Concentration	Ratio of $PhCHMeSiMe_2Cl$: HMPA at coalescence	Order in Nu
9% benzene-d_6 (0.2 ml)	1.0 : 0.075	2.329
Two fold C_6D_6 (1.2 ml)	1.0 : 0.248	4.210
Five fold C_6D_6 (1.8 ml)	1.0 : 0.984	7.664
Ten fold C_6D_6 (2.0 ml)	1.0 : 2.559	3.504 (53.127)
9% CD_2Cl_2 (0.2 ml)	1.0 : 0.052	1.745
Two fold CD_2Cl_2 (1.2 ml)	1.0 : 0.038	1.244
Five fold CD_2Cl_2 (1.8 ml)	1.0 : 0.079	0.961
Ten fold CD_2Cl_2 (2.0 ml)	1.0 : 0.153	1.282

In each dilution series, the relative quantity of HMPA required to induce coalescence of the two diastereotopic SiMe peaks is inversely proportional to the silane concentration. The higher the proportion of solvent the more dilute the silane solution, and the larger the relative amount of HMPA needed to promote racemization of $PhCHMeSiMe_2Cl$. However, dilution with the relatively non-polar benzene-d_6 produces an opposite trend to that observed with dichloromethane-d_2 for the order with respect to HMPA.

The order in HMPA tends towards unity as the silane solution in the polar dichloromethane-d_2 becomes increasingly dilute. In the presence of 9% (0.2 ml) dichloromethane-d_2, an order of 1.74 in HMPA was evaluated for the $PhCHMeSiMe_2Cl$ racemization. However, on five fold dilution with 0.4 ml of chlorosilane in 1.8 ml dichloromethane-d_2, an approximate first order in the nucleophile was recorded. The small but significant reduction in the order with respect to HMPA is consistent with a change in the reaction mechanism, from one involving two molecules of nucleophile to a pathway consisting of only one molecule of HMPA as described in section 3.2. Again, the stabilization of the ionic

$[PhCHMeSiMe_2\text{-}HMPA]^+Cl^-$ salt by solvation plays a determining role in the choice of mechanism.

Owing to the rapid dissociation of the ionic complex into its individual components, the $[PhCHMeSiMe_2\text{-}HMPA]^+Cl^-$ species is rather short-lived in the absence of solvent stabilization. As a consequence of increasing solvation of the small, hard chloride ion in a more polar medium, the equilibrium is pushed towards complex formation and dissociation of the adduct becomes insignificant. Thus the racemization of $PhCHMeSiMe_2Cl$, catalysed by nucleophilic attack of the counterion at the silane, will be more favourable under these conditions.

Interestingly, with the relatively non-polar benzene-d_6 as the solvent, the analogous racemization of $PhCHMeSiMe_2Cl$ exhibited completely different behaviour regarding the order with respect to the nucleophile. The second order in HMPA observed for the racemization in 9% (0.2 ml) benzene-d_6 strongly implies that the reaction proceeds via the mechanism involving two consecutive nucleophilic attacks at silicon. This is in good agreement with the results obtained from the preceding sections. The unexpected increase in the orders with respect to HMPA, in dilute silane solutions in benzene-d_6, can be accounted for by aggregation of polar molecules of nucleophile in the comparatively non-polar medium. In a ten fold diluted silane solution, only 0.2 ml of $PhCHMeSiMe_2Cl$ is present in 2.0 ml benzene-d_6. The large medium effect is manifested by the scatter of the data points around the linear regression line. Thus the order of 3.504 in HMPA calculated for this system may not be valid. When only the last four data points at high concentrations of HMPA are considered, the kinetic plot yields an order in HMPA of 53.127 which is extremely unlikely.

Figure 3.6.1

The effect of concentration on the racemization of PhCHMeSiMe2Cl catalysed by HMPA in benzene-d6.

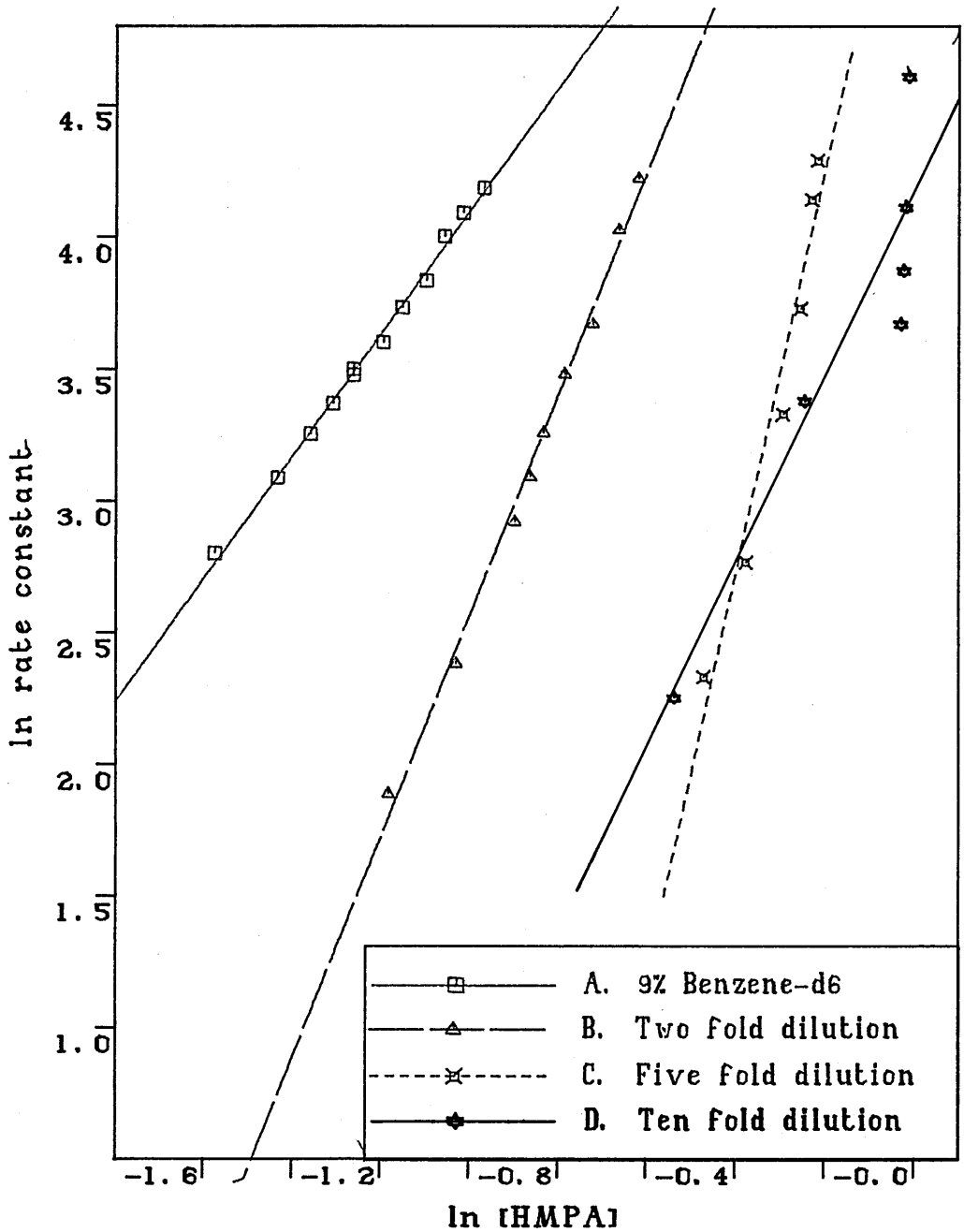

A. ln kobs = 2.329 (s.d. 0.04) ln [HMPA] + 6.436 (s.d. 0.05)

B. ln kobs = 4.210 (s.d. 0.12) ln [HMPA] + 6.751 (s.d. 0.10)

C. ln kobs = 7.664 (s.d. 0.75) ln [HMPA] + 5.767 (s.d. 0.24)

D. ln kobs = 3.504 (s.d. 0.62) ln [HMPA] + 4.159 (s.d. 0.15)

Figure 3.6.2

The effect of concentration on the racemization of PhCHMeSiMe2Cl catalysed by HMPA in dichloromethane-d2.

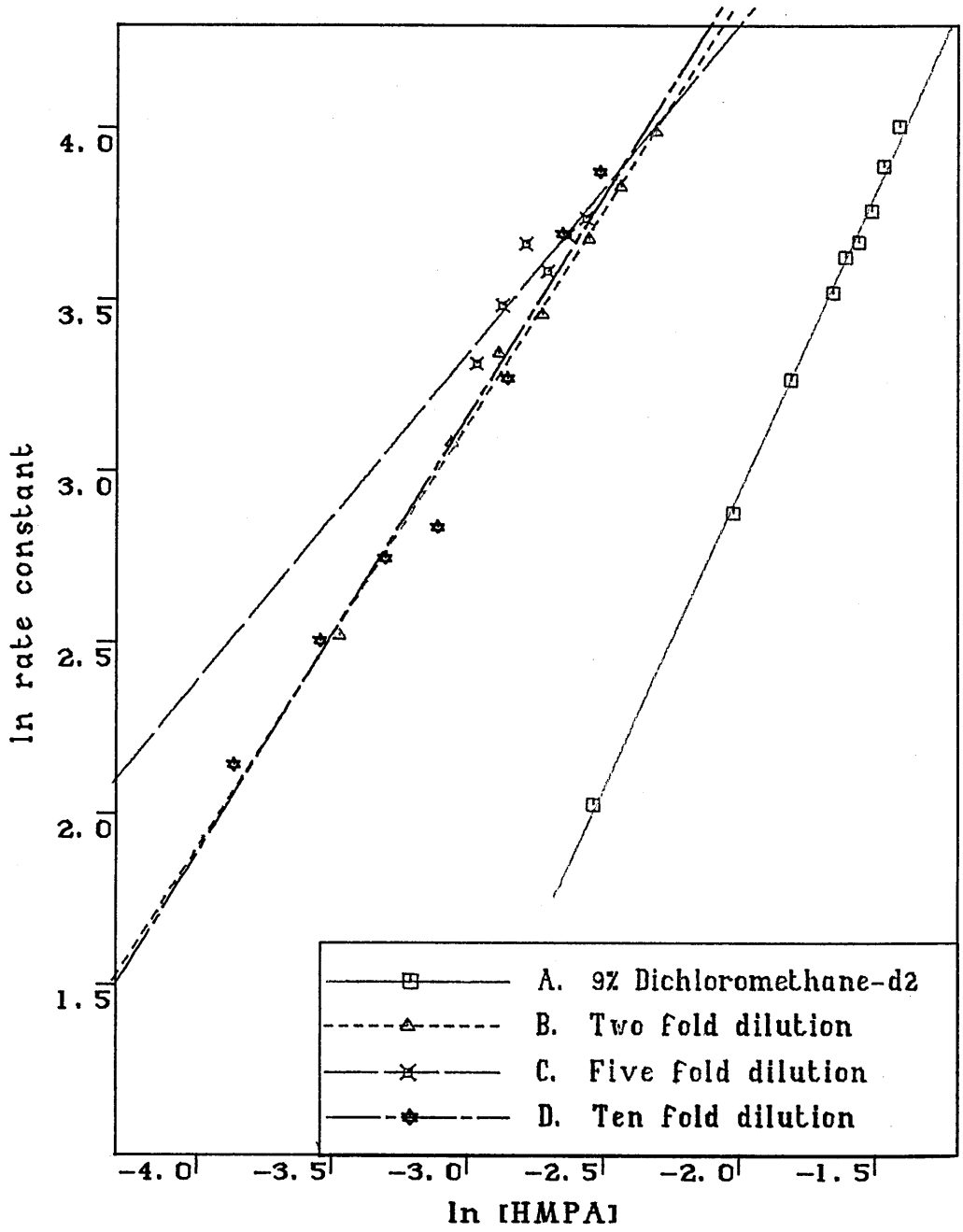

A. ln kobs = 1.745 (s.d. 0.03) ln [HMPA] + 6.440 (s.d. 0.05)

B. ln kobs = 1.244 (s.d. 0.03) ln [HMPA] + 6.864 (s.d. 0.09)

C. ln kobs = 0.961 (s.d. 0.19) ln [HMPA] + 6.223 (s.d. 0.51)

D. ln kobs = 1.282 (s.d. 0.09) ln [HMPA] + 7.012 (s.d. 0.28)

3.7 The effect of hydrolysis

Extreme care was exercised to ensure that all reactions were studied under comparatively moisture-free conditions, though trace amounts of hydrolysis cannot be ruled out. Nonetheless, in order to confirm that the racemization of $PhCHMeSiMe_2X$ (X=Cl, Br) was indeed promoted by the added nucleophile and not by the hydrolysed product HX, a sterically bulky base was introduced to remove any traces of acid impurity. Based upon the 2,6DMP results in section 3.4, the formation of silane-nucleophile complexes is dependent on steric factors. Therefore being an extremely weak nucleophile, this base should not affect the racemization of silane and merely function as an acid scavenger.

Thus the nucleophile (NMI, HMPA) enhanced racemizations of $PhCHMeSiMe_2X$ (X=Cl, Br) were examined in the presence of 8% (0.2 ml) of the sterically hindered 2,6-di-tert-butylpyridine (2,6DBP) in 84%, two and five fold diluted silane solutions in dichloromethane-d_2. The results are outlined in Table 3.7.1 and are presented in the accompanying graphs.

Analogous orders with respect to a given nucleophile are obtained for a given silane except in the case of $PhCHMeSiMe_2Cl$ with NMI, which implies that the percentage of hydrolysis in the reaction mixtures is indeed insubstantial. Nevertheless, the quantity of nucleophile required for racemization is affected by the presence of 2,6DBP. In the absence of the strong base, the added nucleophile will first remove the acid impurity by complexation yielding NuH^+X^- adduct, prior to attacking the silicon species. No such complexation takes place if the hydrolysed impurity is already consumed by the base before the introduction of nucleophile. Thus for a given silane, when a strong base is utilized as an acid acceptor, racemization should occur with a reduced amount of added donor species as is indeed observed for the racemization of $PhCHMeSiMe_2Br$. Surprisingly, a greater quantity of nucleophile is needed to cause racemization of the chloride counterpart. Medium effects may be a contributing factor to this unexpected finding.

Figure 3.7.1
The effect of hydrolysis on the racemization of PhCHMeSiMe2Br with five fold dilution in dichloromethane-d2.

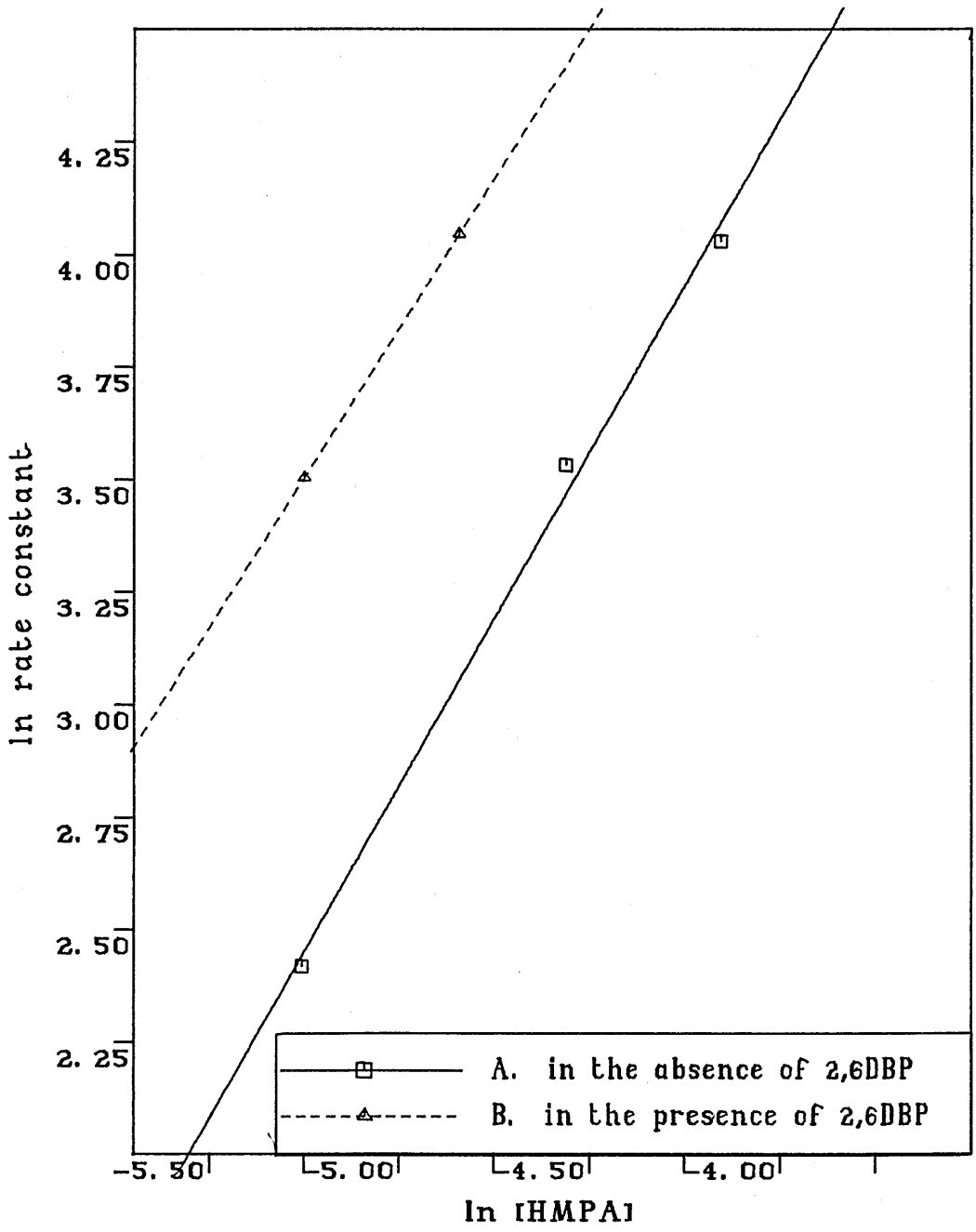

A. ln kobs = 1.483 (s.d. 0.07) ln [HMPA] + 10.223 (s.d. 0.33)

B. ln kobs = 1.335 ln [HMPA] + 10.503

Table 3.7.1 The effect of hydrolysis on the nucleophile (NMI, HMPA) assisted racemization of $PhCHMeSiMe_2X$ (X=Cl, Br)

Nucleophile (Nu)	Ratio of $PhCHMeSiMe_2X$: Nu at coalescence X=Cl[a]	X=Br	Order in Nu X=Cl	X=Br
HMPA	1.0 : 0.052	1.0 : 0.017[b]	1.74	1.48
	1.0 : 0.076[c]	1.0 : 0.009[b,c]	1.57	1.34
NMI	1.0 : 0.077	1.0 : 0.035[d]	1.92	1.64
	1.0 : 0.174[c]	1.0 : 0.027[c,d]	1.28	1.55

a 9% dichloromethane-d_2 (0.2 ml)

b Five fold dilution with 0.4 ml silane in 1.8 ml CD_2Cl_2

c in the presence of 2,6DBP

d Two fold dilution with 1.0 ml in 1.2 ml CD_2Cl_2

3.8 Correlations between observed rate constant and the parameters: nucleophilicity,[41] relative equilibrium constant[63] and rate of alcoholysis[57]

The results described above manifest that racemization of silanes occurs as a consequence of nucleophilic attacks at silicon. Thus the nucleophilicity of a donor species should be an important factor governing the order of reaction with respect to nucleophile, and hence the reaction rate. This hypothesis can be verified by correlating the kinetic results with the Beta scale of nucleophilicity derived by Taft. It is also interesting to compare the results for the diastereotopic $PhCHMeSiMe_2X$ (X=Cl, Br) system with those found for the interactions between other silanes and the analogous nucleophiles.

The product of the order in nucleophile (n) and the natural logarithm of the concentration of nucleophile at coalescence (ln [Nu]) was used for these correlations. One reason for selecting this n ln [Nu] term is because it depends on the nature of nucleophile. Furthermore, it is the

major variable controlling the magnitude of the observed rate constant (k_{obs}), which in turn governs the rate of racemization as shown in section 3.2. For a particular nucleophile at the point of coalescence, this term can be evaluated from the following expression (equation 3.2.25), which can be determined experimentally from the kinetic plots.

$$\ln k_{obs} = n \ln [Nu] + \text{constant} \qquad \text{Equation 3.8.1}$$

The observed rate constant at coalescence cannot be extrapolated experimentally in all cases. Therefore it is calculated using the expression for coalescence based on the peak separation (δv) of the two exchanging entities, $k = \frac{\pi \delta v}{\sqrt{2}}$. Substituting these calculated values of k_{obs} into the above regression equation gives the values of n ln [Nu] for the racemizations of $PhCHMeSiMe_2X$ (X=Cl, Br) for individual nucleophiles, which are subsequently used for the correlations. The n ln [Nu], Beta, ln K_{rel} together with Frye's ln k_1 values are shown in the table below. The correlations of n ln [Nu] with the various parameters are presented in the appropriate graphs.

Table 3.8.1

Correlation of the kinetic results with Taft's Beta, ln K_{rel} and Frye's ln k_1 values

Nucleophile (Nu)	Order in Nu x ln [Nu] at coalescence[a] $PhCHMeSiMe_2Cl$	$PhCHMeSiMe_2Br$	Beta	ln K_{rel}	ln k_1
HMPA	-2.384	-	1.05	9.2	6.908
NMI	-1.679	-	0.82	10.4	-
NMPO	1.446	-	0.78	5.2	-
DMPU	1.943	-1.678	0.79	2.2	-
DMEU	4.760	-1.410	0.75	-2.2	-
DMF	9.658	-2.542	0.69	-0.2	-
NMP	5.681	-1.832	0.77	0.0	-
TMU	5.389	-0.039	0.78	-	-
3,5DMP	7.595	1.996	0.70	-0.6	5.703
py	20.208	4.858	0.64	-	4.605
2,4DMP	-	2.631	0.74	-	-

[a] Calculated from the plot of ln k_{obs} versus ln [Nu] by inputing the theoretical k_{obs} at coalescence into the equation

ln k_{obs} = order in Nu x ln [Nu] + constant

3.8.1 Correlation of n ln [Nu] with Taft's Beta values

The plot of n ln [Nu] for the nucleophile catalysed racemization of $PhCHMeSiMe_2Cl$ in 9% benzene-d_6 against Taft's Beta values, for each nucleophile used in this study, shows a good correlation between the rate of racemization and the nucleophilicity of the donor species, although the point for HMPA deviates from the main trend. The correlation with the analogous bromosilane series is not as satisfactory as with the chloride counterpart, however a general trend is still significant although the point for DMF lies slightly outside the main trend.

Figure 3.8.1
Correlation of n ln [Nu] with Beta values for the racemization of PhCHMeSiMe2X (X=Cl, Br).

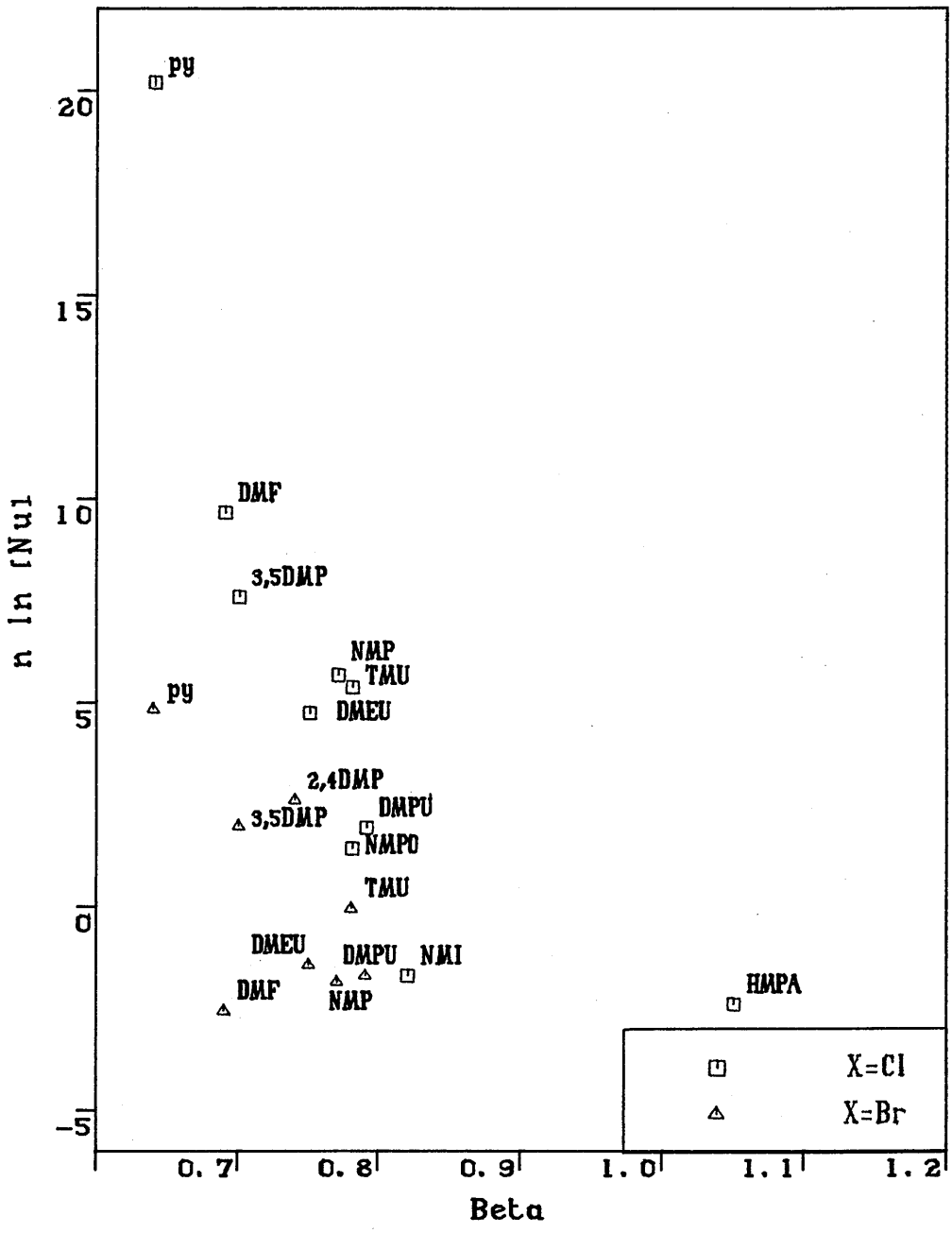

3.8.2 Correlation of n ln [Nu] with ln K_{rel} values

Silicon-29 n.m.r. chemical shifts of silane-nucleophile adducts were the basis for the determination of the relative equilibrium constants (K_{rel}).[63] Choosing NMP as the arbitrary reference point, the ratio of the silicon-29 chemical shift of a particular silane-nucleophile adduct to that of the $[Me_3Si\text{-}NMP]^+OSO_2CF_3^-$ complex produces a K_{rel} value for the nucleophile under study, as illustrated by the following reaction schemes and equations.

$$NMP + Me_3SiOSO_2CF_3 \overset{K_{NMP}}{\rightleftharpoons} (Me_3Si\text{-}NMP)^+OSO_2CF_3^- \qquad \text{Scheme 3.8.1}$$

$$K_{NMP} = \frac{[(Me_3Si\text{-}NMP)^+OSO_2CF_3^-]}{[Me_3SiOSO_2CF_3]\,[NMP]} \qquad \text{Equation 3.8.1}$$

$$Nu + Me_3SiOSO_2CF_3 \overset{K_{Nu}}{\rightleftharpoons} (Me_3Si\text{-}Nu)^+OSO_2CF_3^- \qquad \text{Scheme 3.8.2}$$

$$K_{Nu} = \frac{[(Me_3Si\text{-}Nu)^+OSO_2CF_3^-]}{[Me_3SiOSO_2CF_3]\,[Nu]} \qquad \text{Equation 3.8.2}$$

K_{rel} is related to the two equilibrium constants, K_{NMP} and K_{Nu}, by the following expression.

$$K_{rel} = \frac{K_{Nu}}{K_{NMP}} = \frac{[(Me_3SiNu)^+OSO_2CF_3^-][Me_3SiOSO_2CF_3][NMP]}{[Me_3SiOSO_2CF_3][Nu][(Me_3SiNMP)^+OSO_2CF_3^-]} \qquad \text{Equation 3.8.3}$$

The equation can be simplified to

$$K_{rel} = \frac{[(Me_3SiNu)^+OSO_2CF_3^-][NMP]}{[(Me_3SiNMP)^+OSO_2CF_3^-][Nu]} \qquad \text{Equation 3.8.4}$$

Thus the K_{rel} values are a measure of the equilibrium constants for the interactions of the $(Me_3Si\text{-}NMP)^+OSO_2CF_3^-$ salt with different nucleophiles.

$$Nu + (Me_3Si\text{-}NMP)^+OSO_2CF_3^- \overset{K_{rel}}{\rightleftharpoons} (Me_3Si\text{-}Nu)^+OSO_2CF_3^- + NMP$$

Scheme 3.8.3

The above kinetic data provide evidence that the attack of a second molecule of nucleophile at the silicon atom of the silane-nucleophile complex is the crucial process in the racemizations of $PhCHMeSiMe_2Cl$ and, in certain cases, $PhCHMeSiMe_2Br$.

$$Nu + PhCHMeSiMe_2X \overset{K_{eq}}{\rightleftharpoons} [PhCHMeSiMe_2\text{-}Nu]^+X^-$$

$$Nu + [PhCHMeSiMe_2\text{-}Nu]^+X^- \underset{k_{-2}}{\overset{k_2}{\rightleftharpoons}} [PhCHMeSiMe_2\text{-}Nu]^+X^- + Nu$$

In the detailed discussion in section 3.2.1, two rate equations were derived for this mechanistic pathway, depending upon the degree of ion-pair dissociation of the silane-nucleophile adduct.

$$Rate = k_2K_{eq}[PhCHMeSiMe_2X][Nu]^2 \qquad \text{no dissociation}$$

$$Rate = k_2K_{eq}^{0.5}[PhCHMeSiMe_2X]^{0.5}[Nu]^{1.5} \qquad \text{ion-pair dissociation}$$

These two rate expressions can be generalized by the following equation.

$$Rate = k\,[PhCHMeSiMe_2X]^m\,[Nu]^n \qquad \textbf{Equation 3.8.5}$$

$$\frac{Rate}{[PhCHMeSiMe_2X]} = k\,[PhCHMeSiMe_2X]^{m-1}\,[Nu]^n$$

where k is an overall constant, m can be either 1 or 0.5 and n is the order in nucleophile with a value of either 2 or 1.5.

Taking the natural logarithm of the above expression produces the following equation.

$$\ln \left(\frac{\text{Rate}}{[PhCHMeSiMe_2X]}\right) = \ln k + (m-1) \ln [PhCHMeSiMe_2X] + n \ln [Nu]$$

This expression can be simplified to give the equation below.

$$\ln k = -n \ln [Nu] + c$$

$$\text{where } c = \ln \left(\frac{\text{Rate}}{[PhCHMeSiMe_2X]}\right) + (m-1) \ln [PhCHMeSiMe_2X]$$

The plot of n ln [Nu] versus K_{rel} essentially reflects a plot of ln k against K_{rel}. The correlations of the ln K_{rel} values with n ln [Nu] for the racemizations of $PhCHMeSiMe_2X$ (X=Cl, Br) are not satisfactory with considerable scatter, particularly in the case of the bromosilane; although they each produce a noticeable general trend. The discrepancy is partly due to systematic errors; different silanes and unrelated techniques are used for the generation and the evaluation of the ln K_{rel} and n ln [Nu] values. A K_{rel} value effectively describes the thermodynamic equilibrium of a nucleophilic attack at the silicon atom of a silane-nucleophile complex, which may not apply to the racemizations of $PhCHMeSiMe_2Br$ promoted by strong nucleophiles such as DMPU and DMEU. This could account for the poor correlation observed for the racemization of $PhCHMeSiMe_2Br$.

Furthermore the quantity of nucleophile used varies in each case, therefore changes in the polarity of the medium induced by the presence of polar nucleophile will be different in each system. Hence, it may not be valid to assume that the concentration of $PhCHMeSiMe_2X$ remains

Figure 3.8.2
Correlation of n ln [Nu] with ln Krel values for the racemization of PhCHMeSiMe2X (X=Cl, Br).

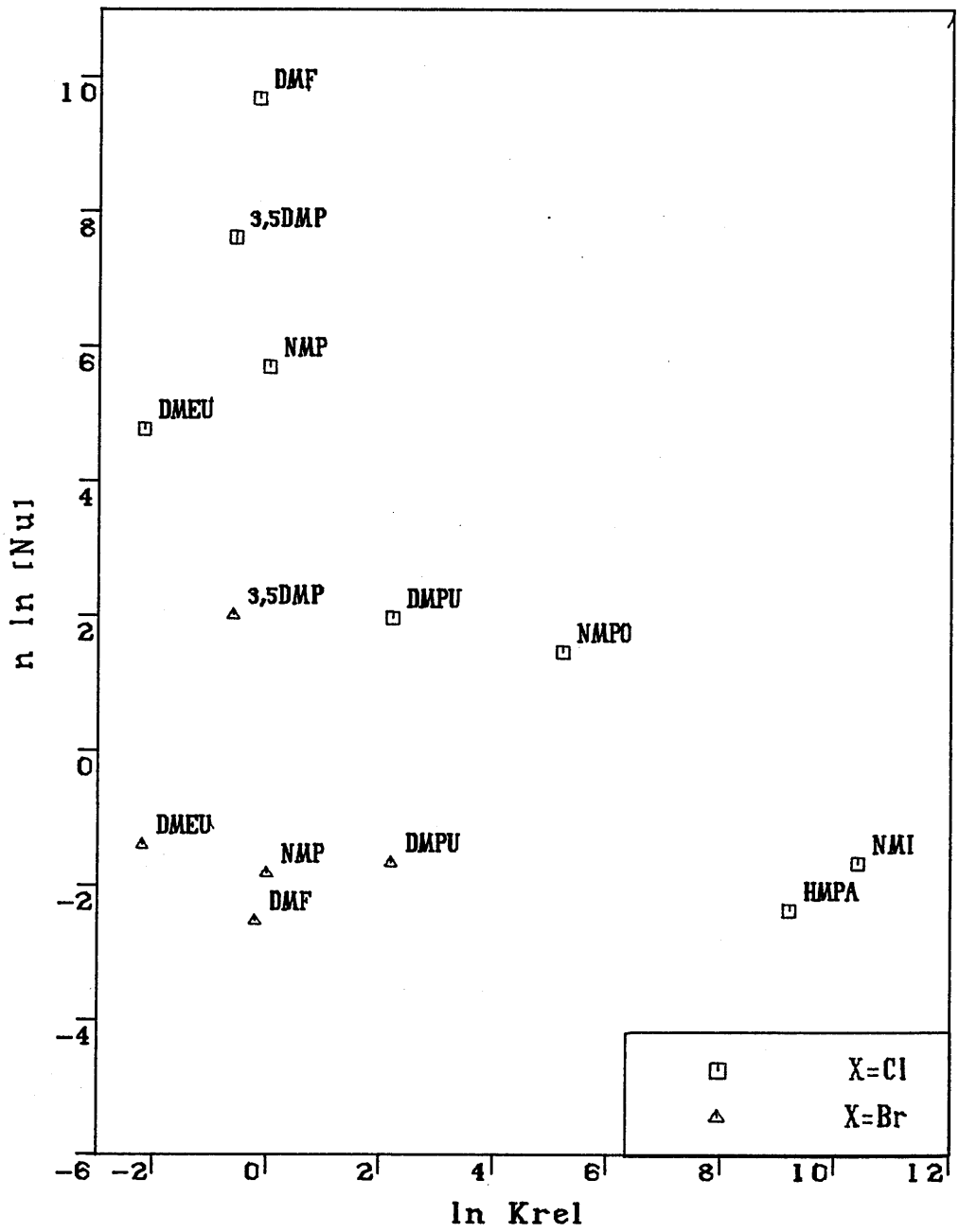

appreciably unchanged throughout the experiment when large quantities of nucleophile are added. The rate of reaction is a function of both the equilibrium constant for salt formation (K_{eq}) and the rate constant (k), which is related to the nucleophilicity of the donor species; k is therefore different for different nucleophiles. The assumption that k, and hence the rate, is a constant for all cases will inevitably lead to some scatter in the correlation plot.

3.8.3 Correlation of n ln [Nu] with Frye's ln k_1 values

In a recent publication,[57] Frye et al. reported a detailed kinetic study on the nucleophile enhanced tertiary alcoholysis of dichlorodiphenylsilane (Ph_2SiCl_2). On the basis of the kinetic results, they supported the mechanism postulated by Chojnowski.[9] A four coordinate ionic silane-nucleophile adduct was formed in the initial, rapid pre-equilibrium step, which is followed by the rate determining alcoholysis as shown in the scheme below. The overall rate (k_1) of the process was monitored in the presence of a range of nucleophiles.

$$Nu + Ph_2SiCl_2 \rightleftharpoons [Ph_2ClSi\text{-}Nu]^+Cl^- \xrightarrow{ROH} Ph_2ClSiOR + HCl$$

Scheme 3.8.4

A plot of n ln [Nu] for the racemization of $PhCHMeSiMe_2Cl$ versus the ln k_1 values yields an excellent correlation, though it only consists of three data points. It is not possible to perform a similar comparison for the corresponding $PhCHMeSiMe_2Br$ due to insufficient data. The implications of this correlation are very important. The n ln [Nu] values represent the observed rate constants for the racemization of $PhCHMeSiMe_2Cl$ at particular concentrations of a nucleophile, whereas the ln k_1 measurements are the relative rates for the alcoholysis of Ph_2SiCl_2.

Figure 3.8.3
Correlation of n ln [Nu] with Frye's ln k1 values for the racemization of PhCHMeSiMe2X (X=Cl, Br).

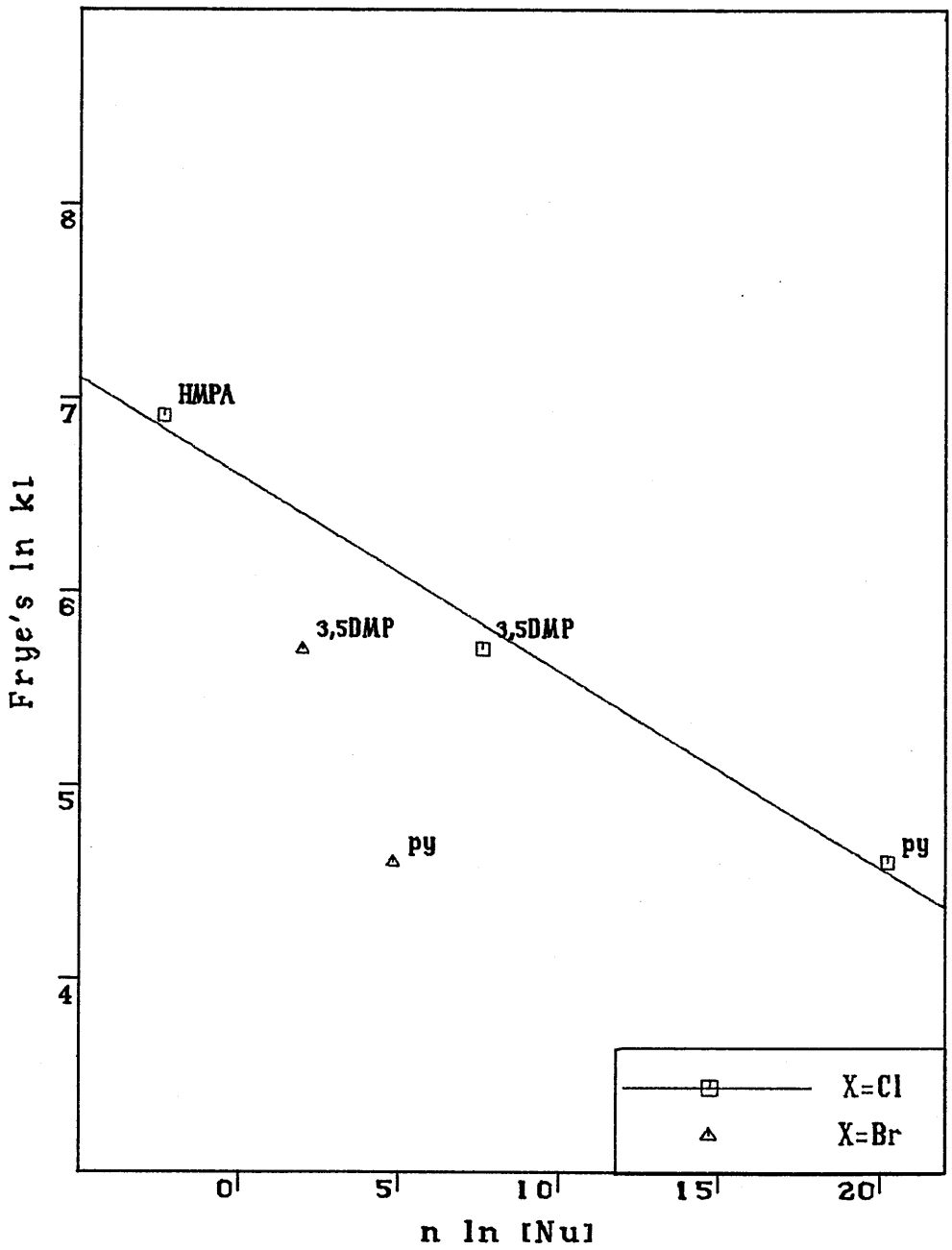

The initial step in the racemization process proposed in section 3.2.1 is the same as that in the mechanism of alcoholysis proposed by Frye.[57] These two pathways differ in the nature of the second step; racemization occurs via the attack of a second molecule of nucleophile whereas alcoholysis involves nucleophilic attack by an alcohol molecule. Therefore, in both mechanisms, the overall rate should be proportional to the equilibrium constant for formation of the silane-nucleophile adduct in an initial pre-equilibrium step. Thus the good correlation between these overall rates provides further support for the hypothesis that the initial process is common in both reactions. Furthermore, the essentially zero rate increase observed by Frye for 2,6-dimethylpyridine (2,6DMP) and triethylamine (Et_3N) is consistent with the non-observable racemization of $PhCHMeSiMe_2Cl$ in the presence of these species in this study.

3.9 Analysis of errors

The major sources of error in the evaluation of the order in nucleophile lie in the concentrations of added nucleophile and the computer simulation of the observed rate constants (k_{obs}), which is approximately $\pm 0.5\ s^{-1}$. For each experiment, the quantities of silane, solvent and nucleophile are measured as accurately as possible using gas-tight syringes and are weighed to four decimal places, with an error limit of ± 0.0005 g. Therefore the total percentage error in each data point is estimated to be 2%.

The evaluation of the orders in nucleophile is based upon an important assumption that the concentration of free nucleophile in solution is approximately equal to the concentration of added nucleophile. This can partly account for the discrepancy between the calculated orders in nucleophile and the theoretical values according to the rate expressions.

3.10 General summary

The evidence provided in this chapter has been interpreted in terms of two mechanisms. The choice of mechanistic route for a particular set of reaction condition depends mainly on the stability of the silane-nucleophile adduct. Further support for this hypothesis comes from the good correlation between the results presented above and those of Frye on the alcoholysis of Ph_2SiCl_2.

Racemization involving less stable silane-nucleophile complexes is more likely to proceed via the mechanism in section 3.2.1, where two molecules of nucleophile are utilized resulting in either a second order or an order of 1.5 in nucleophile. Conversely, if the salt is stable, the halide exchange pathway depicted in section 3.2.2 will be responsible for the racemization process, which only requires one molecule of nucleophile corresponding to a first or a half order with respect to nucleophile.

On the basis of the kinetic data, it is not feasible to determine whether the silane-nucleophile adduct is ion-paired. However, the n.m.r. chemical shift titration results in the previous chapter and the interpretation of the conductivity measurements[9,70] strongly imply a tighter ion-pairing when the counterion is the hard and small chloride ion than in the case of the bromide or triflate anion.

The leaving group of a silane, the concentration of the system under investigation, the nature of nucleophile and solvent are the major contributing factors governing the stability of a silane-nucleophile adduct. The relative rate of racemization of $PhCHMeSiMe_2X$ (X=Cl, Br, OSO_2CF_3) decreases with varying leaving group or counterion in the following sequence OSO_2CF_3 > Br > Cl. In comparison with the bromide and triflate analogues, the $[PhCHMeSiMe_2\text{-}Nu]^+Cl^-$ salts are thermodynamically less stable. This is partly due to the greater difficulty encountered in solvating the hard and small chloride ion, in contrast to the bromide and triflate anions. Dissociation of the $[PhCHMeSiMe_2\text{-}Nu]^+Cl^-$ adduct into

its components, the uncomplexed silane and nucleophile, is also facilitated by the greater nucleophilicity of the chloride ion.

The effect of solvent is fundamentally related to that of concentration, enhancement of stabilization results as the medium becomes more polar, which can be induced either by altering the nature of the solvent or by diluting a silane solution with a polar solvent. The order of reaction in nucleophile and hence the rate of racemization are shown to be controlled by the nucleophilicity of the attacking donor species. This finding is evidenced by the good correlation of the results of racemizations of $PhCHMeSiMe_2X$ (X=Cl, Br) with the Beta values assigned by Taft.

Analysis of these kinetic data enables the two proposed mechanisms to be distinguished for individual systems. Thus $PhCHMeSiMe_2X$ (X=Cl, Br) racemizes via the first mechanism (Scheme 3.2.1) resulting in an approximate second order in nucleophile when X=Cl with strong nucleophiles or when X=Br with weak donor species. This is consistent with the second order in nucleophile reported by Corriu.[8,35] The halide exchange process becomes the preferred mechanistic pathway for the racemization of $PhCHMeSiMe_2Br$ in the presence of strong nucleophiles, with an order in nucleophile close to unity. The surprising fractional orders in nucleophile recorded in this study are in accord with the observations by Cartledge[72,73] and Prince.[71] From their kinetic studies on halide exchanges, they both independently produced orders in nucleophile similar in magnitude to those evaluated for the diastereotopic bromosilane. A change-over in the reaction mechanism is detected, accompanied by a reduction in the order with respect to nucleophile, with increasing stability of the silane-nucleophile adduct.

The possibility of acid catalysed racemization can be eliminated on the basis of the similarity between the kinetic results in the presence and absence of the sterically hindered strong base, 2,6DBP. Furthermore, the percentage of hydrolysis in silane solutions was found to be insignificant.

Chapter 4 Thermodynamic studies on the racemization of diastereotopic silanes

4.1 Introduction

On the basis of the findings from the n.m.r. chemical shift titration and kinetic studies, two mechanisms for the racemizations of $PhCHMeSiMe_2X$ (X=Cl, Br) have been postulated and verified in the preceding chapter. These verifications are further validated by examining the thermodynamic aspects of the racemizations of the diastereotopic silanes, $PhCHMeSiMe_2X$ (X=Cl, Br).

The rate of a chemical reaction can be defined by the following fundamental expression.

$$\text{Reaction rate} = \text{rate constant} \times (\text{reactant concentration})^n$$

Varying the temperature will not alter the reaction order unless there is a change in the mechanism, in which case the reaction is no longer the same. Similarly, the reactant concentration is essentially unaffected by temperature. However, the rate constant is a temperature-dependent term, which explains the critical effect of temperature on the rate of reaction. This is the underlying principle of the Arrhenius activation theory and the Eyring absolute rate theory for the evaluation of activation parameters.

The Arrhenius activation theory is based on the assumption that the reactant molecules must overcome a certain potential energy barrier known as the activation energy (E_a), corresponding to the energy of a transition state or an activated complex, prior to transforming into the products.[83] A dynamic equilibrium is established between the activated and unactivated molecules. This concept can be summarized mathematically by the equation $k = A\, e^{-E_a/RT}$, which is derived by applying the van't Hoff isochore to the equilibrium.

The pre-exponential or frequency factor (A) has been interpreted as the number of effective collisions per unit volume and unit time, leading to

product formation. The exponential term ($e^{-E_a/RT}$) gives the fraction of molecules which possess the activation energy (E_a). This can be experimentally measured from the slope of a linear plot of ln k versus 1/T. The Arrhenius parameters, E_a and A, are assumed to be temperature independent over the narrow range of temperature studied and are related to the activation parameters, the enthalpy ($\Delta H^{\ddagger}$) and entropy ($\Delta S^{\ddagger}$) of activation, at a given temperature.

$$\Delta H^{\ddagger} = E_a - RT \qquad \text{and} \qquad \Delta S^{\ddagger} = R\left(\ln A - \ln \frac{k_B T}{h}\right)$$

R is the gas constant, h is the Planck constant and k_B is the Boltzmann constant which is the ratio of the gas constant (R) to the Avogadro number (N).

The absolute reaction rate theory developed by Eyring is a transition state treatment based on statistical thermodynamics.[83] This hypothesis is somewhat complicated and will not be discussed in great depth, however a brief description is outlined below. An essential feature of the Eyring formulation of reaction rate is that all chemical reactions are assumed to proceed via a transition state or an activated complex, which is in thermodynamic equilibrium with the reactants, even though the overall chemical reaction may be irreversible. This method offers an accurate treatment of the reaction rate especially when a dynamic equilibrium is established between the reactants and products.

$$\underset{\text{reactants}}{A + B} \rightleftharpoons \underset{\text{transition state}}{C^{\ddagger}}$$

The equilibrium constant for the formation of transition state ($K^{\ddagger}$) can be expressed in terms of the concentrations of A, B and $C^{\ddagger}$ at a particular time t.

$$K^{\ddagger} = \frac{[C^{\ddagger}]}{[A]\,[B]} \qquad \text{Equation 4.1.1}$$

The transition complex ($C^{\ddagger}$) is a highly strained state between bond forming and bond breaking. It can be regarded as a normal molecule except that one of its vibrational modes is equivalent to a translational degree of freedom which leads to the formation of products. Treating this degree of freedom as a classical vibration gives the following expression for its frequency (v) at temperature T.

$$h\nu = k_B T \qquad \textbf{Equation 4.1.2}$$

According to this model, the rate of reaction is equal to the concentration of the activated molecule ($C^{\ddagger}$) multiplied by the frequency of vibration (v) of the bond about to break and dissociate into the products.

$$\text{Rate} = \nu\,[C^{\ddagger}] \qquad \textbf{Equation 4.1.3}$$

This rate equation can be modified by substituting the frequency term with equation 4.1.2.

$$\text{Rate} = \frac{k_B T}{h}\,[C^{\ddagger}] \qquad \textbf{Equation 4.1.4}$$

$[C^{\ddagger}]$ is governed by the law of chemical equilibrium as illustrated by equation 4.1.1.

$$\text{Rate} = \frac{k_B T}{h}\,K^{\ddagger}\,[A]\,[B] \qquad \textbf{Equation 4.1.5}$$

However, by definition, the rate can be alternatively expressed by the following equation.

$$\text{Rate} = k\,[A]\,[B] \qquad \textbf{Equation 4.1.6}$$

Combining equations 4.1.5 and 4.1.6 yields an expression for the rate constant (k).

$$k\,[A]\,[B] = \frac{k_B T}{h} K^{\ddagger}\,[A]\,[B]$$

$$k = \frac{k_B T}{h} K^{\ddagger} \qquad \text{Equation 4.1.7}$$

Like any other equilibrium constant, $K^{\ddagger}$ is proportional to the standard free energy change of formation of the transition state ($\Delta G^{\ddagger}$) as described by the van't Hoff isotherm.

$$\Delta G^{\ddagger} = -R\,T\,\ln K^{\ddagger} \quad \text{or} \quad K^{\ddagger} = e^{-\Delta G^{\ddagger}/RT} \qquad \text{Equation 4.1.8}$$

Thus the rate of reaction is controlled by the free energy of activation ($\Delta G^{\ddagger}$).

$$k = \frac{k_B T}{h} e^{-\Delta G^{\ddagger}/RT} \qquad \text{Equation 4.1.9}$$

However, $\Delta G^{\ddagger}$ is related to the standard enthalpy change ($\Delta H^{\ddagger}$) and the standard entropy change ($\Delta S^{\ddagger}$) of formation of the activated complex by the following thermodynamic relationship.

$$\Delta G^{\ddagger} = \Delta H^{\ddagger} - T\Delta S^{\ddagger} \qquad \text{Equation 4.1.10}$$

Hence, the fundamental Eyring equation can be rewritten to produce equation 4.1.11.

$$k = \frac{k_B T}{h} e^{-\Delta H^{\ddagger}/RT}\, e^{\Delta S^{\ddagger}/R} \qquad \text{Equation 4.1.11}$$

To allow for the possibility that not every activated complex is converted into the reaction products, a transmission coefficient (K) is introduced into the above equation. This transmission coefficient is

normally equal to unity for most chemical reactions, indicating complete transformation of activated molecules into products.

$$k = \frac{K\, k_B T}{h}\, e^{-\Delta H^{\ddagger}/RT}\, e^{\Delta S^{\ddagger}/R} \qquad \text{Equation 4.1.12}$$

Equation 4.1.11 can be rearranged to give

$$\frac{k}{T} = \frac{k_B}{h}\, e^{-\Delta H^{\ddagger}/RT}\, e^{\Delta S^{\ddagger}/R} \qquad \text{Equation 4.1.13}$$

The natural logarithm (ln) form of the above expression yields the following equation.

$$\ln\left(\frac{k}{T}\right) = \frac{-\Delta H^{\ddagger}}{RT} + \ln\frac{k_B}{h} + \frac{\Delta S^{\ddagger}}{R} \qquad \text{Equation 4.1.14}$$

In this transition state approach, the activation parameters, $\Delta H^{\ddagger}$ and $\Delta S^{\ddagger}$, are assumed to be independent of temperature. A straight line plot of ln (k/T) versus 1/T produces a gradient of $-\Delta H^{\ddagger}/R$ and an intercept of ln (k_B/h) + $\Delta S^{\ddagger}/R$; the activation parameters can therefore be evaluated.

4.2 Thermodynamic studies on the racemizations of $PhCHMeSiMe_2X$ (X=Cl, Br)

The thermodynamic aspects of the nucleophile assisted racemizations of $PhCHMeSiMe_2X$ (X=Cl, Br) were investigated by varying the temperature of a mixture of silane and nucleophile (NMI or HMPA) in dichloromethane-d_2. Initially, an aliquot of a nucleophile was added to a solution of silane (2.0 ml) in 9% dichloromethane-d_2 until the two carbon-13 diastereotopic SiMe resonances of $PhCHMeSiMe_2X$ (X=Cl, Br) coalesced, giving a broadened singlet. However, owing to the precipitation of $[PhCHMeSiMe_2\text{-}NMI]^+Cl^-$ ionic adduct at low temperatures, the reaction conditions were altered by

using a less concentrated silane solution, with 1.0 ml of silane in 1.2 ml dichloromethane-d_2, prior to the addition of nucleophile.

In certain cases, the experiments were repeated in the presence of 8% (0.2 ml) 2,6-di-tert-butylpyridine (2,6DBP) to examine the effect of hydrolysis. On progressive cooling, carbon-13 n.m.r. spectra were recorded until two well-separated diastereotopic SiMe resonances were observed. The reversibility was confirmed when an analogous carbon-13 n.m.r. spectrum was taken on warming back to ambient temperature. Similar to the kinetic studies, theoretical line shapes of the diastereotopic SiMe peaks at particular rate constants were simulated and compared with the experimental results at various temperatures by total line shape analysis.

The reaction conditions, the spectral data for the diastereotopic SiMe signals and the observed rate constants at a series of temperatures are tabulated in the experimental section. The activation parameters are calculated according to the Eyring as well as the Arrhenius equations, and are shown in the accompanying tables for comparison. The Eyring plots are identical to those of Arrhenius, therefore only the Eyring plots are provided here. Analysis of the results focuses on the effects of the leaving group on silane, the nature of nucleophile, the concentration of the system and hydrolysis on the thermodynamic behaviour of racemization at silicon.

4.2.1 Evaluation and comparisons of activation parameters from the Arrhenius and Eyring plots

The detailed discussion in the preceding section has illustrated two approaches for the evaluation of activation parameters, $\Delta H^{\ddagger}$ and $\Delta S^{\ddagger}$. In the first method, the activation parameters are calculated from the Arrhenius parameters, E_a and A, which can be obtained from the slope and intercept of a linear plot of the observed rate constants ($\ln k_{obs}$) against the reciprocals of temperature (1/T). Conversely, the gradient

Table 4.2.1

Evaluation of enthalpy and entropy values from Arrhenius parameters for nucleophile (HMPA, NMI) catalysed racemization of $PhCHMeSiMe_2X$ (X=Cl, Br) at 20°C (293K)

System	E_a ($kJmol^{-1}$)	$\Delta H^{\ddagger}$ ($kJmol^{-1}$)	A (s^{-1})	$\Delta S^{\ddagger}$ ($JK^{-1}mol^{-1}$)
X=Br Nu=HMPA with 2,6DBP	47.505±1.33	45.069±1.33	$1.29\pm0.95\times10^{10}$	-51.258±4.60
X=Br Nu=NMI with 2,6DBP	41.452±2.43	39.016±2.43	$1.25\pm2.21\times10^{9}$	-70.698±8.48
X=Br Nu=NMI	47.480±0.90	45.044±0.90	$1.47\pm0.68\times10^{10}$	-50.201±3.16
X=Cl Nu=HMPA 9% solvent	12.525±0.65	10.089±0.65	$1.28\pm0.45\times10^{4}$	-166.171±2.51
X=Cl Nu=HMPA	12.590±0.66	10.154±0.66	$9.21\pm3.34\times10^{3}$	-168.941±2.57
X=Cl Nu=HMPA with 2,6DBP	11.034±0.50	8.598±0.50	$4.63\pm1.22\times10^{3}$	-174.669±1.95
X=Cl Nu=NMI	46.678±3.46	44.242±3.46	$1.01\pm5.18\times10^{12}$	-14.997±1.95

Table 4.2.2

Evaluation of enthalpy and entropy values from Eyring plots and comparison with the Arrhenius results

System	Eyring $\Delta H^{\ddagger}$	Arrhenius $\Delta H^{\ddagger}$	Eyring $\Delta S^{\ddagger}$	Arrhenius $\Delta S^{\ddagger}$
X=Br Nu=HMPA with 2,6DBP	45.098±1.32	45.069±1.33	-59.418±4.57	-51.258±4.60
X=Br Nu=NMI with 2,6DBP	39.059±2.44	39.016±2.43	-78.805±8.56	-70.698±8.48
X=Br Nu=NMI	45.115±0.90	45.044±0.90	-58.211±3.15	-50.201±3.16
X=Cl Nu=HMPA 9 % solvent	10.370±0.67	10.089±0.65	-173.432±2.59	-166.171±2.51
X=Cl Nu=HMPA	10.444±0.69	10.154±0.66	-176.177±2.67	-168.941±2.57
X=Cl Nu=HMPA with 2,6DBP	8.896±0.52	8.598±0.50	-181.873±2.05	-174.669±1.95
X=Cl Nu=NMI	45.010±3.42	44.242±3.46	-21.158±14.88	-14.997±0.05

and intercept of a Eyring plot of ln (k_{obs}/T) versus 1/T provide direct information on the activation parameters.

The enthalpy and entropy of activation are assumed to be independent of temperature in the Eyring treatment, a temperature term is not involved in calculating these activation parameters. However, the temperature (T) is taken to be 20°C (293K) in the evaluation of $\Delta H^{\ddagger}$ and $\Delta S^{\ddagger}$ from the Arrhenius parameters. The values of $\Delta H^{\ddagger}$ evaluated according to the Eyring equation are essentially identical to that obtained from the Arrhenius activation energy (E_a). This indicates that $\Delta H^{\ddagger}$ is unaffected by temperature for this diastereotopic system. However, the two sets of $\Delta S^{\ddagger}$ values differ by a constant factor of 8 $JK^{-1}mol^{-1}$. The discrepancy may be due to the temperature dependence of the $\Delta S^{\ddagger}$ in the Arrhenius approach; the natural logarithm of temperature, ln T, where T is 293K gives a value of approximately 6 $JK^{-1}mol^{-1}$.

4.2.2 The effect of hydrolysis

In the variable temperature study on the HMPA catalysed racemization of $PhCHMeSiMe_2Br$, a 0.0048 molar equivalent (4.17 μl) of HMPA was adequate to induce coalescence of the two diastereotopic SiMe peaks. However the presence of a minute quantity of acid impurity, HBr, in the system will be sufficient to remove such an insignificant amount of HMPA, forming the $HMPAH^{+}Br^{-}$ complex and causing the two resonances to reappear.

Thus the two diastereotopic SiMe signals observed, on lowering the temperature of the reaction mixture, may not be entirely due to the deceleration of the rate of racemization of $PhCHMeSiMe_2Br$. The removal of HMPA by HBr was confirmed by the irreversibility of the coalescing process on returning to ambient temperature. Furthermore, when a small amount of 2,6DBP was introduced to the mixture at room temperature, coalescence of the two peaks was re-observed.

Figure 4.2.1
Variable temperature studies on nucleophile assisted racemization of PhCHMeSiMe2X (X=Cl, Br) in the presence of 2,6DBP.

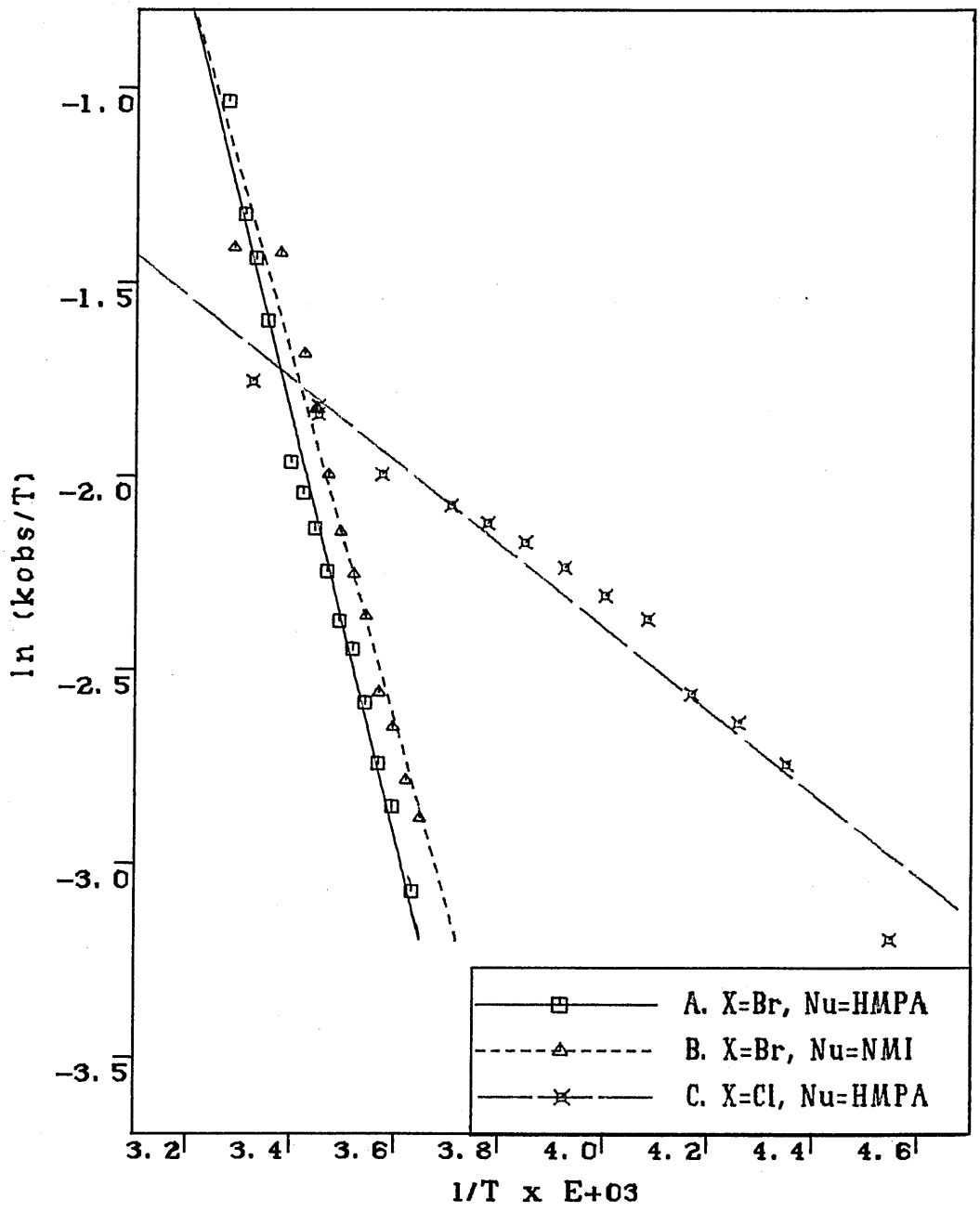

A. ln (kobs/T) = -5424.1 (s.d. 1590) 1/T + 16.613 (s.d. 0.55)
B. ln (kobs/T) = -4697.8 (s.d. 2930) 1/T + 14.282 (s.d. 1.03)
C. ln (kobs/T) = -1070.0 (s.d. 63) 1/T + 1.885 (s.d. 0.25)

Thus this experiment had to be conducted in the presence of 2,6DBP to eliminate undesirable side reactions with the acid impurity. In order to make valid comparisons with the other systems, the NMI assisted racemization of $PhCHMeSiMe_2Br$ and the HMPA catalysed racemization of $PhCHMeSiMe_2Cl$ were also studied under identical conditions with 8% 2,6DBP. The presence of the strong base causes a small decrease in the enthalpies and entropies of activation for both $PhCHMeSiMe_2X$ (X=Cl, Br). The greater negativity of the $\Delta S^{\ddagger}$ values can be explained by the increasing order in the system induced by 2,6DBP.

4.2.3 The effect of concentration

Variable temperature studies on the HMPA catalysed racemization of $PhCHMeSiMe_2Cl$ were performed in both 9% (0.2 ml) and 45% (1.2 ml) of dichloromethane-d_2. The influence of concentration was therefore examined by comparing the activation parameters evaluated for both systems. Varying the medium causes no apparent changes in either the enthalpy or the entropy of activation; the $\Delta H^{\ddagger}$ and $\Delta S^{\ddagger}$ values remain essentially the same on dilution.

4.2.4 The effect of nucleophile

The $[PhCHMeSiMe_2\text{-}NMI]^+Cl^-$ ionic adduct precipitates out of solution much more readily than its HMPA counterpart, as discussed earlier. On lowering the temperature of the less concentrated mixture of $PhCHMeSiMe_2Cl$ and NMI in 1.2 ml dichloromethane-d_2, two asymmetric diastereotopic SiMe signals were observed with the intensity of one of the peaks remaining unaltered. However the racemization process was proved to be reversible on warming back to ambient temperature. A possible rationalization for this peculiar observation is the precipitation of the $[PhCHMeSiMe_2\text{-}NMI]^+Cl^-$ complex, possibly as an immiscible oily layer, with decreasing temperature.

Figure 4.2.2

The effect of concentration on variable temperature studies of racemization of PhCHMeSiMe2Cl catalysed by HMPA.

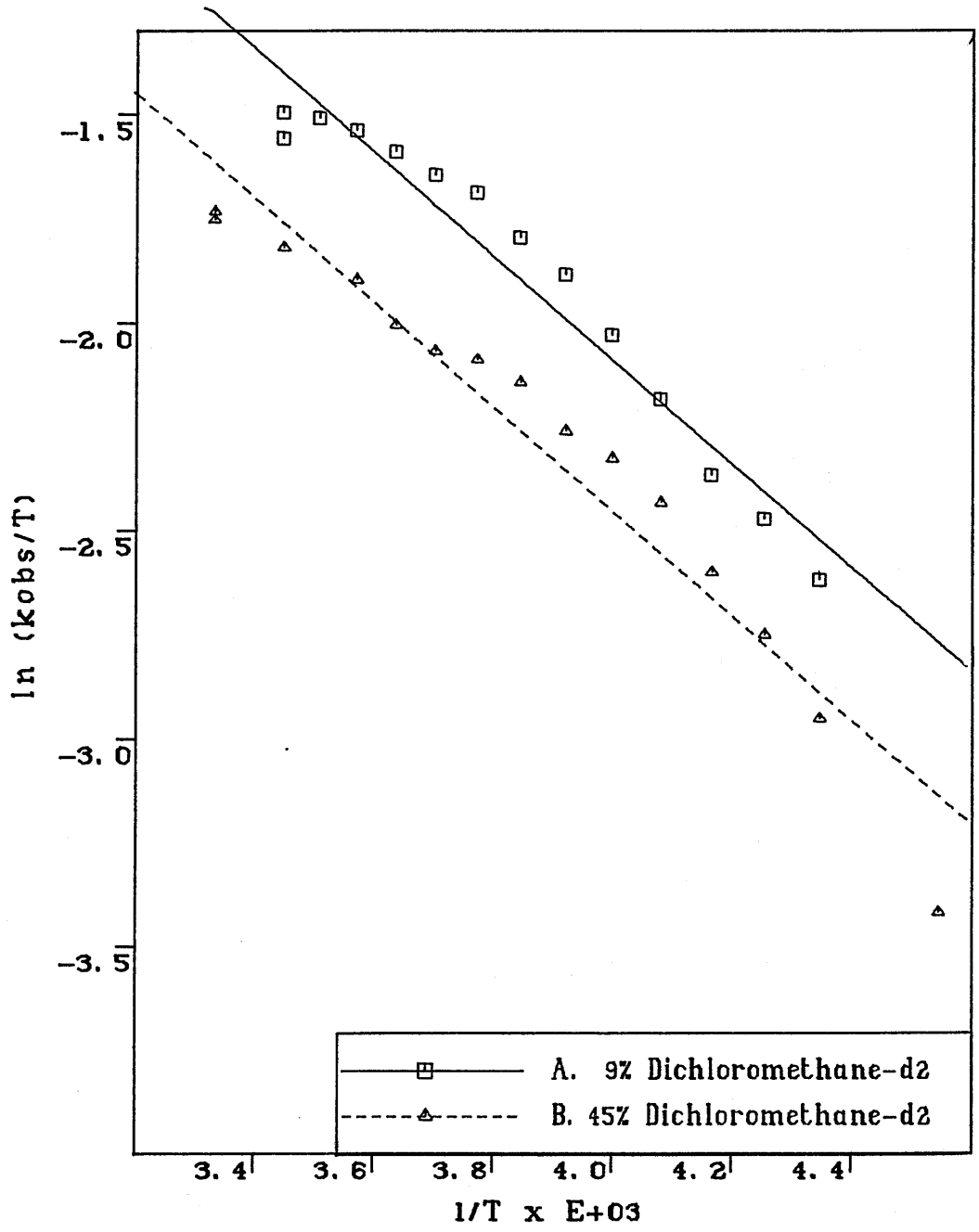

A. ln (kobs/T) = -1247.3 (s.d. 80.7) 1/T + 2.900 (s.d. 0.31)

B. ln (kobs/T) = -1256.1 (s.d. 83.0) 1/T + 2.570 (s.d. 0.32)

Owing to the asymmetry in the line shapes of the two SiMe signals, it is difficult to use total line shape analysis for the evaluation of observed rate constants. Complete bandshape calculations were based solely on the line shape of the SiMe resonance which was affected by the lowering of temperature. Thus even if the results are valid, they are expected to bear significant errors. It is therefore not feasible to compare the thermodynamic behaviour of NMI enhanced racemization of $PhCHMeSiMe_2Cl$ with that promoted by HMPA and the analogous racemization of $PhCHMeSiMe_2Br$.

In contrast to the $PhCHMeSiMe_2Cl$, salt precipitation is not encountered with the corresponding bromosilane under these conditions. The activation parameters for the racemization of $PhCHMeSiMe_2Br$ catalysed by NMI in the presence of 2,6DBP are compared with those obtained for the analogous HMPA enhanced process. The activation enthalpy for NMI is only 6 $kJmol^{-1}$ lower than that for HMPA, whereas the activation entropy is 20 $JK^{-1}mol^{-1}$ more negative in the case of NMI relative to HMPA. Nevertheless, it is not possible to provide a general conclusion on the influence of nucleophile merely on the basis of these findings.

4.2.5 The effect of leaving group

Under identical reaction conditions with a given nucleophile as the catalyst, the activation enthalpy for the racemization of $PhCHMeSiMe_2Br$ is approximately four times greater than that of the corresponding chlorosilane. Similarly, the activation entropy for the $PhCHMeSiMe_2Br$ racemization is about three fold more positive with respect to the chloride analogue, indicating a more ordered transition state in the case of the chlorosilane although solvent ordering may also be important. The influence of counterion on the activation parameters will be further discussed in the following section.

Figure 4.2.3

The effect of leaving group on variable temperature studies of racemization of PhCHMeSiMe2X (X=Cl, Br) catalysed by NMI.

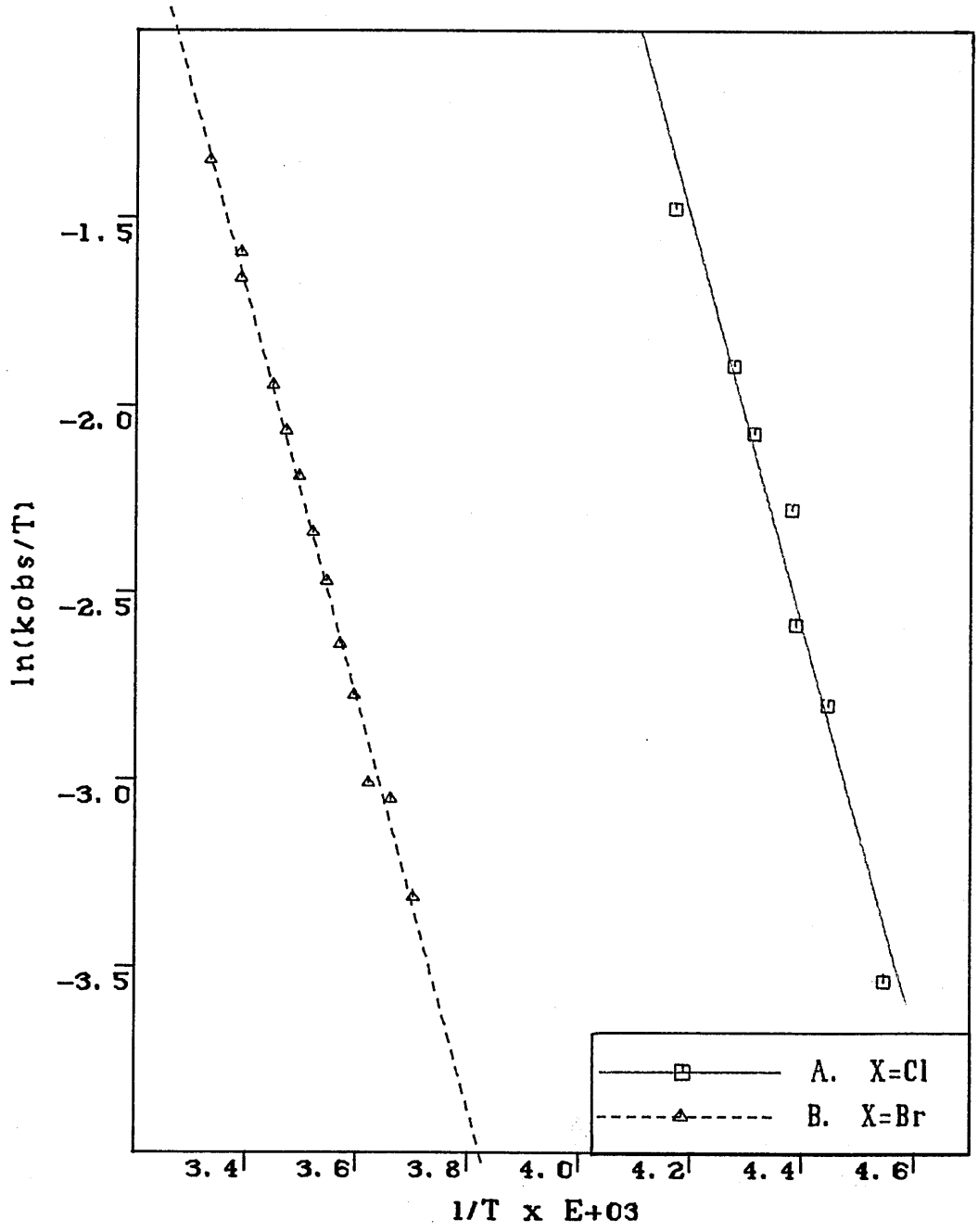

A. ln (kobs/T) = -5413.6 (s.d. 41) 1/T + 21.215 (s.d. 1.79)

B. ln (kobs/T) = -5426.2 (s.d. 108) 1/T + 16.759 (s.d. 0.38)

4.3 Analysis of results

4.3.1 Racemization of $PhCHMeSiMe_2Br$

The extremely exothermic nature of the formation of four coordinate 1:1 ionic $PhCHMeSiMe_2Br$-nucleophile adducts demonstrates that the complexation process is accompanied by a large and negative enthalpy of reaction. Thus the silane-nucleophile complex will be lower in energy relative to the uncomplexed silane. Based upon the n.m.r. chemical shift titration results and the n.m.r. data for the solid adduct synthesised, it can be concluded that $PhCHMeSiMe_2Br$ forms comparatively stable four coordinate ionic adducts with strong nucleophiles. Therefore a relatively high energy barrier is predicted for the dissociation of the bromosilane-nucleophile adduct into its individual components.

Furthermore, the attack by nucleophiles at the $[PhCHMeSiMe_2\text{-}Nu]^+Br^-$ complex may be facilitated, with respect to the uncomplexed silane, because the nucleophile in a silane-nucleophile adduct is an excellent, neutral, leaving group. Hence, the activation enthalpy required for the nucleophilic attack at a silane-nucleophile salt should be less than that at the corresponding uncomplexed silane. However the concentrations of the reacting species are also important in governing the rate of reaction. In addition, the failure to observe any evidence for five coordinate acyclic $PhCHMeSiMe_2Br$-nucleophile adducts indicates that the stability of $[PhCHMeSiMe_2\text{-}(Nu)_2]^+Br^-$ intermediate is low, if it exists at all.

4.3.2 Racemization of $PhCHMeSiMe_2Cl$

As a consequence of nucleophilic attack at $PhCHMeSiMe_2Cl$, a dynamic equilibrium is established between the uncomplexed silane and the $[PhCHMeSiMe_2\text{-}Nu]^+Cl^-$ adduct. The evidence from the n.m.r. chemical shift studies in chapter 2 shows that these two silicon species exchange rapidly with each other. This is partly due to the instability and hence

the ready decomposition of chlorosilane-nucleophile complex, which is strongly supported by the n.m.r. data of the solid adducts in solution. The formation of $[PhCHMeSiMe_2\text{-}Nu]^+Cl^-$ adducts is not so exothermic as that of the bromide analogue. This indicates that the energy difference between the uncomplexed $PhCHMeSiMe_2Cl$ and its nucleophile salt is not very large, which is in accordance with the rapid dissociation of $[PhCHMeSiMe_2\text{-}Nu]^+Cl^-$ complexes. Thus the energy barrier for the formation or the dissociation of $PhCHMeSiMe_2Cl$-nucleophile adduct should be relatively small.

Therefore, the rate of racemization of $PhCHMeSiMe_2Cl$ is more likely to be controlled by the second nucleophilic attack at the silicon atom of the $[PhCHMeSiMe_2\text{-}Nu]^+Cl^-$ salt. This is in good agreement with the postulated mechanistic route depicted in Scheme 3.2.2. The same type of bond is being broken and formed in the transition state of this process, namely, the Si—Nu bond without the involvement of the counterion. Hence, the energy needed for this nucleophilic substitution step is the same for both chloro- and bromosilanes, irrespective of the counterion.

The greater scatter observed in the Eyring plot for the HMPA assisted racemization of $PhCHMeSiMe_2Cl$ may be due to the wider temperature range studied leading to more significant changes in the viscosity of the medium. In addition, salt formation is enhanced at lower temperatures which may result in a change in the reaction mechanism. Thus racemization induced by the attack of chloride ion at the silicon atom of the chlorosilane is facilitated.

4.3.3 Comparison of the two racemization processes

Four coordinate 1:1 ionic $[PhCHMeSiMe_2\text{-nucleophile}]^+X^-$ adducts are postulated to be the intermediates involved in the mechanisms for the racemization at silicon. The overall rate of reaction is dependent on the concentration of the adduct, which is governed by the equilibrium constant for adduct formation. Silane-nucleophile adduct formation is

found to be an exothermic process for both silanes, $PhCHMeSiMe_2X$ (X=Cl, Br). Therefore, cooling a mixture of silane and nucleophile will shift the equilibrium towards adduct formation with a corresponding increase in the overall rate. Thus an apparent negative activation enthalpy may result due to an increase in the overall rate with decreasing temperature. Nevertheless, this trend may be offset by the decrease in reaction rate as expected from the energy Maxwell-Boltzmann distribution.

In the case of the bromosilane with good nucleophiles, $[PhCHMeSiMe_2$-nucleophile$]^+Br^-$ complexes are essentially fully formed at ambient temperatures. Lowering the temperature will only induce a relatively small increase in the equilibrium constant. In contrast, the chlorosilane-nucleophile adduct formation is accompanied with a low equilibrium constant at ambient temperatures. Thus on cooling a mixture of chlorosilane and nucleophile, adduct formation is greatly favoured and a comparatively larger equilibrium constant results. Hence, the chlorosilane-nucleophile system will experience a more negative activation enthalpy compared with the bromosilane analogue.

The activation enthalpies are derived by monitoring the rate of reaction with variations in the temperature of the system under investigation. Thus, the difference in the activation energies found for the chloro- and bromosilanes may be an artefact arising from the method used for the evaluation of these values and may not reflect the true energy barriers between the various species involved.

The increase in the negativity of the activation entropy of the chlorosilane relative to its bromide analogue may be accounted for by a steric effect. The $[PhCHMeSiMe_2$-$Nu]^+Cl^-$ adduct may be more sterically hindered with respect to the uncomplexed bromosilane, therefore a greater degree of rearrangement may be required as a result of nucleophilic attack. The enthalpy and entropy values are also influenced considerably by solvation. Stabilization of the ionic intermediate has a more pronounced effect on the $[PhCHMeSiMe_2$-$Nu]^+Cl^-$ salt, resulting in a lowering of its energy barrier for reaction. However, solvation of the

ionic charges by the medium induces order in the system. Thus the racemization of chlorosilane is accompanied by a low activation enthalpy but a large and negative activation entropy.

4.4 Analysis of errors

The most significant sources of error in the thermochemical data, calculated from variable temperature n.m.r. studies, are the temperatures of the system under investigation and the observed rate constants (k_{obs}). Calibration of the temperature control unit indicates that the temperature accuracy is $\pm 2^{o}C$. The computer simulation of the observed rate constants using total line shape analysis gives an error limit of $\pm 0.5\ s^{-1}$. Other contributing factors include the measurements in the quantities of silane, solvent and nucleophile used in each experiment, each of which has an accuracy of ± 0.0005 g.

Chapter 5 Conclusion

5.1 Introduction

During the past four decades, numerous kinetic studies on nucleophilic substitution reactions at silicon have been performed in an attempt to deduce the mechanistic details from structure-reactivity correlations, solvent effects and dynamic stereochemical behaviour. The preliminary work was carried out by Allen, Modena and Eaborn,[36] who studied the solvolysis of hindered triorganochlorosilanes in various solvents and suggested an S_N2 mechanism for such process. Using optically active silanes, Sommer et al.[44] demonstrated that nucleophilic displacements at silicon are highly stereospecific and often proceed with retention.

More recently, an important finding by Corriu[8] showed that these processes were enhanced substantially and the stereochemical pathways were completely reversed by the presence of catalytic quantities of nucleophiles such as HMPA. He further proposed the involvement of penta- and hexacoordinate intermediates. Based on the kinetics of isomerization and ligand exchange reactions of cyclic silicon compounds, Cartledge et al.[72,73] believed that these processes took place via pseudorotation with an ionic pentacoordinate siliconium species as the intermediate, which was similar to that proposed by Corriu. This argument is supported by Martin,[52,53] who used the pseudorotation phenomenon to rationalize the nucleophile assisted racemization of a novel spirocyclic silicon complex.

However, Chojnowski[9] postulated an alternative mechanistic route with four coordinate 1:1 ionic silane-nucleophile adducts as intermediates. This pathway has received additional support from Bassindale and Stout[56] as well as Frye et al..[57] By examining the kinetic and the thermodynamic behaviour of racemization reactions of $PhCHMeSiMe_2X$ (X=Cl, Br), this project provides a more thorough understanding of the nature of the transient species, and hence helps to elucidate the mechanistic pathways involved in these processes.

5.2 The interactions of diastereotopic silanes with nucleophiles

As a consequence of the interactions between the highly electrophilic $PhCHMeSiMe_2X$ (X=Cl, Br, OSO_2CF_3) compounds with nucleophiles (HMPA, NMI), four coordinate ionic $[PhCHMeSiMe_2\text{-nucleophile}]^+X^-$ adducts with a 1:1 stoicheiometry are shown to be the dominant species present in silylating mixtures in solution. The stability of these $[PhCHMeSiMe_2\text{-}Nu]^+X^-$ complexes is controlled by a combination of thermodynamic and kinetic factors.

For a particular silane, the equilibrium constant for the formation of silane-nucleophile salt is related to the electron donating properties of the incoming nucleophile. With donors of high nucleophilicity, such as HMPA and NMI, the resultant silane-nucleophile complexes are more stable accompanied by larger equilibrium constants. The enthalpy of reaction associated with adduct formation process provides information on the energy difference between the uncomplexed silane and its nucleophile salt. In contrast to the chloride analogues, the highly exothermic nature of the formation of solid 1:1 four coordinate ionic $[PhCHMeSiMe_2\text{-}Nu]^+Br^-$ adducts implies that dissociation of these complexes into their components requires a high activation energy and does not occur readily.

Furthermore, the silane-nucleophile adducts partake in three chemical exchange processes. The exchange with their parent silanes involves rate limiting dissociation of the complexes into individual components followed by rapid reassociation of these components. The rate of the initial dissociation step is governed by the nucleophilicity and the solvation of the counterion, as well as the degree of ion pairing of the adduct. Solvation and hence the stability of the ionic silane-nucleophile salts depend upon the nature of solvent. Thus in a more polar medium, solvent stabilization of ionic species is facilitated with a deceleration of the rate of adduct dissociation. The ability of the counterion to be solvated decreases in the following order OSO_2CF_3 > Br > Cl. In comparison with HMPA, NMI forms a relatively tighter ion pair

with the halide anion in the silane-nucleophile complex, resulting in an acceleration of the adduct dissociation process. The nucleophilicity of the counterion shares the same trend as the rate of complex dissociation, which decreases in the sequence Cl > Br > OSO_2CF_3.

$$PhCHMeSiMe_2X + Nu \rightleftharpoons [PhCHMeSiMe_2\text{-}Nu]^+X^-$$

Scheme 5.2.1

As a result of a direct, rate determining, nucleophilic attack by a second donor molecule at the silicon atom of a silylated complex, a dynamic equilibrium is established between the silane-nucleophile salt and its isomer with inverted configuration at silicon.

$$[PhCHMeSiMe_2\text{-}Nu]^+X^- + Nu^* \rightleftharpoons [PhCHMeSiMe_2\text{-}Nu^*]^+X^- + Nu$$

Scheme 5.2.2

The results from the variable temperature n.m.r. chemical shift studies provide evidence for the isomerizations of $PhCHMeSiMe_2X$ (X=Br, OSO_2CF_3) induced by the counterions of the silane-nucleophile complexes, which supports the observations by Prince.[71]

$$PhCHMeSiMe_2X + X^- \rightleftharpoons PhCHMeSiMe_2X + X^-$$

Scheme 5.2.3

5.3 The kinetic and thermodynamic behaviour of nucleophile assisted racemization of $PhCHMeSiMe_2X$ (X=Cl, Br)

The racemizations of $PhCHMeSiMe_2X$ (X=Cl, Br), involving four coordinate 1:1 silane-nucleophile ionic intermediates, proceed via two possible mechanistic pathways. The choice of reaction mechanism and the rate of racemization depend largely on the stability of the silane-nucleophile

adduct in the system, which are entirely consistent with the results from the kinetic and thermodynamic studies.

The discussion in the previous section pointed out that the stability of a silane-nucleophile complex is controlled by four major factors. These include the leaving group or counterion of silane, the nature of nucleophile, the concentration and the solvent of the system under investigation. With a particular nucleophile as the catalyst, the relative rate of racemization of $PhCHMeSiMe_2X$ (X=Cl, Br) decreases with leaving group or counterion in the following sequence Br > Cl.

The formation of a $[PhCHMeSiMe_2\text{-nucleophile}]^+X^-$ adduct in an initial, rapid, pre-equilibrium step, followed by the second rate determining nucleophilic attack at the silane-nucleophile complex is the preferred mechanistic route (Scheme 5.3.1) for the racemization of $PhCHMeSiMe_2Cl$ in the presence of strong nucleophiles and $PhCHMeSiMe_2Br$ with weak donor species.

$$PhCHMeSiMe_2X + Nu \rightleftharpoons [PhCHMeSiMe_2\text{-}Nu]^+X^-$$

$$[PhCHMeSiMe_2\text{-}Nu]^+X^- + Nu^* \rightleftharpoons [PhCHMeSiMe_2\text{-}Nu^*]^+X^- + Nu$$

rate determining step

Scheme 5.3.1

An approximate second order in nucleophile is found in each case which is in accord with the observations by Corriu, except that the mechanism proposed by him involves penta- and hexacoordinate molecular intermediates.[8] Aggregation of polar nucleophile molecules may be the rationale behind the unexpected high orders in nucleophile recorded for the racemization of $PhCHMeSiMe_2Cl$ with weak nucleophiles.

In the presence of strong donor species, $PhCHMeSiMe_2Br$ racemizes via a nucleophilic attack by the halide anion of the silane-nucleophile adduct at the silicon atom of the uncomplexed silane. In this mechanism (Scheme

5.3.2), the initial formation of the silane-nucleophile salt is followed by the attack of the counterion at the uncomplexed silane. The latter process may be the rate limiting step under equilibrium conditions. The orders in nucleophile tend towards unity and are similar to those reported by Prince[71] and Cartledge[73] on halide exchanges of halosilanes.

$$PhCHMeSiMe_2X + Nu \rightleftharpoons [PhCHMeSiMe_2\text{-}Nu]^+X^-$$

$$PhCHMeSiMe_2X + X^- \rightleftharpoons PhCHMeSiMe_2X + X^-$$

Scheme 5.3.2

Owing to the importance of the stability of the silane-nucleophile adduct in determining the mechanism for the racemization at silicon, factors affecting the stability will indirectly influence the mechanistic pathway. Thus with increasing stability of the complex, the reaction mechanism alters from one utilizing two molecules of nucleophile to one involving halide exchange.

The good correlation between the kinetic results from the racemization studies on $PhCHMeSiMe_2Cl$ and the nucleophilicity of the donor species (Beta values) assigned by Taft[41] provide evidence that the racemization process is dependent upon the nature of the incoming nucleophile. Furthermore, the plot of the kinetic results of the racemization of $PhCHMeSiMe_2Cl$ versus the rate of alcoholysis of Ph_2SiCl_2 published by Frye[57] produced an excellent linear correlation. The mechanism for the alcoholysis postulated by Frye is essentially the same as that proposed for the racemization of $PhCHMeSiMe_2Cl$. Thus the hypothesis that the four coordinate 1:1 ionic silane-nucleophile adducts are formed in an initial, rapid, pre-equilibrium step is verified.

The activation enthalpies evaluated from the thermodynamic studies on the racemizations of $PhCHMeSiMe_2X$ (X=Cl, Br) are about 10 and 40 $kJmol^{-1}$ for $PhCHMeSiMe_2Cl$ and $PhCHMeSiMe_2Br$ respectively. These results are in good

agreement with the two different mechanisms for the racemizations of $PhCHMeSiMe_2X$ (X=Cl, Br) in the presence of strong nucleophiles. In comparison with the bromide analogue, the activation entropy is more negative for the racemization of $PhCHMeSiMe_2Cl$. This indicates that the chlorosilane system is more ordered which may be induced by solvent stabilization and the steric effects in the silane-nucleophile complex.

5.4 The interactions of PhMeRSiCl (R=H, Me) with nucleophiles

In contrast to the diastereotopic $PhCHMeSiMe_2X$ (X=Cl, Br, OSO_2CF_3) system, pentacoordination at silicon of chloromethylphenylsilane (PhMeHSiCl) is observed with strong nucleophiles, for example NMI and HMPA, producing $[PhMeHSi-(Nu)_2]^+Cl^-$ complexes. However the formation of the $[PhMeHSi-(HMPA)_2]^+Cl^-$ adduct is accompanied by a low equilibrium constant at ambient temperatures. These five coordinate PhMeHSiCl-nucleophile salts undergo chemical exchanges with their four coordinate 1:1 ionic analogues, $[PhMeHSi-Nu]^+Cl^-$. Furthermore, no evidence for the presence of hexacoordinate silicon species is noted.

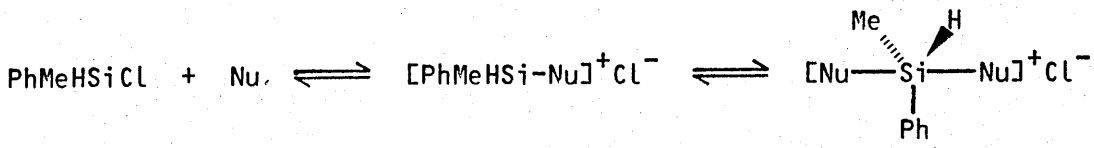

Scheme 5.4.1

With DMF as the nucleophile, significant complex formation cannot be detected for the interactions of PhMeRSiCl (R=H, Me). Nevertheless, interestingly, the collapse of the two N-methyl resonances of DMF is recorded on the proton n.m.r. spectra at low concentrations of DMF, which may be indicative of N-silylation of DMF.

The combined observations by Chojnowski, Bassindale and Stout, Frye as well as results from this project provide convincing evidence for the operation of the mechanism first postulated by Chojnowski,[9] which

applies in general to systems consisting of highly electrophilic silanes with good leaving groups and relatively strong nucleophiles. In a situation where poor leaving groups, such as Si—H, or very weak nucleophiles are involved, detailed investigations need to be performed to further elucidate the mechanism.

Chapter 6 Experimental

6.1 Instrumentation

The silanes used were extremely moisture sensitive; in order to eliminate contamination by moisture, all chemicals were treated as moisture sensitive compounds and handled under dry nitrogen (purchased from Air Products, high purity grade). A Faircrest dry nitrogen glove box enabled more convenient, easier transfers and handling of moisture sensitive reagents. Quantities of compounds were measured and transferred via stainless steel needles and Hamilton all glass-teflon, gas tight syringes. The syringes were calibrated by weighing measured volumes of distilled water, the accuracy was found to be ±0.7%.

Chemicals were stored in reagent bottles (previously heated in an oven) with either PTFE-silicon rubber septa valves (Pierce Mininert valves) or PTFE-silicon rubber septa caps. The septa were replaced regularly because they were attacked by the more reactive silanes e.g. chloromethylphenylsilane and also to prevent moisture entering through the punctures. PTFE-butyl rubber septa would be a better choice if their extremely poor resealability could be improved after being punctured by needles. Fine gauge stainless steel needles with non-coring tips were used to minimise the damage to septa. A Sartorius 2000 MP digital balance was used to provide accurate weighings of up to ±0.5mg.

The infrared spectra were obtained on a Perkin Elmer Model 1710 Fourier transform infrared spectrometer. For moisture sensitive or hygroscopic compounds, the samples (as Nujol mulls in the case of solids) were prepared under dry nitrogen. A Perkin Elmer 240C analyser was used to perform the elemental microanalyses.

All the n.m.r. spectra were recorded on a Jeol FX90Q n.m.r. spectrometer with a tunable, multinuclear probe. Tetramethylsilane (TMS) was normally taken as the reference. Nevertheless, in most experiments, an external reference was used when the diastereotopic SiMe groups of $PhCHMeSiMe_2X$ were under investigation since the SiMe signals were obscured by TMS. An outline of the various spectral parameters is given below.

	Proton	Carbon-13	Silicon-29
Spectral width	1000 or 1500Hz	5302Hz	2000 or 4000Hz
Frequency	89.56MHz	22.50MHz	17.76MHz
Pulse width	24 or 27μs	22 or 24μs	12 or 22μs
Pulse delay	0.1s	1.0s	10 to 50s
Irradiation mode	non-decoupling	complete decoupling	decoupling without nuclear overhauser enhancement
Exponential window	0.0Hz	0.0 or 1.24Hz	3.09Hz

Dynamic n.m.r. total line shape analyses were performed using the Dec-20 computing system with a modified version of the QCPE (Quantum Chemistry Program Exchange) DNMR4 program (No. 466). The calculated spectra were recorded on a Calcomp-81 flatbed plotter.

6.2 Purification of chemicals

Distillation under reduced pressure was predominantly used as the mode of purification. The choice of drying agents and the purification procedure are summarized in the following categories.

A. Deuterated solvents were stored over activated 4A molecular sieves and reagent grade chemicals were used without further purification.

From Aldrich Chemical Co. Ltd.:- tetramethylsilane 99.9+%, NMR grade
diphenylmethylsilane
chloroform-d_1 99.8 atom % D GOLD LABEL
acetonitrile-d_3 99 atom % D GOLD LABEL
dichloromethane-d_2 99.6 atom % D GOLD LABEL
benzene-d_6 99.5 atom % D GOLD LABEL
toluene-d_8 99+ atom % D GOLD LABEL
nitromethane-d_3 99 atom % D GOLD LABEL

From BDH Chemicals Ltd.:- magnesium turnings
potassium hydroxide 'AnalaR'
anhydrous magnesium sulphate

B. Prior to distilling and storing over activated 4A molecular sieves under nitrogen, these chemicals were allowed to stand over 4A sieves for a few days.

From Aldrich Chemical Co. Ltd.:- 1-methylimidazole 99%
1-methyl-2-pyrrolidinone 99%
1-methyl-2-pyridone 99+%
1,1,3,3-tetramethylurea 99%
N,N-dimethylformamide 99%
R-(+)-limonene 97%

From Fluka AG:- 1,3-dimethyl-3,4,5,6-tetrahydro-2(H)-pyrimidinone
1,3-dimethyl-2-imidazolidinone 98%

C. The following compounds were distilled from potassium hydroxide pellets and 4A molecular sieves.

From Aldrich Chemical Co. Ltd.:- pyridine 99%
2,6-dimethylpyridine 99%
3,5-dimethylpyridine 98+%
2,4-dimethylpyridine 96+%
2,6-di-tert-butylpyridine 97%
triethylamine 99+%

D. Due to the lack of suitable drying agents, halosilanes and corrosive chemicals were distilled in the absence of any drying agents.

From Aldrich Chemical Co. Ltd.:- trifluoromethanesulphonic acid
chlorodimethylphenylsilane

From Fluorochem Ltd.:- chloromethylphenylsilane

E. Reagents which serve as starting materials for syntheses were generally used without further purification.

From Aldrich Chemical Co. Ltd.:- (1-bromoethyl)benzene 97%
thionyl chloride
chlorodimethylsilane

From BDH Chemicals Ltd.:- carbon tetrachloride 'AnalaR'
DL-1-phenylethanol 99%
2-bromobutane

F. Individual routes of purification were carried out for these compounds.

Hexamethylphosphoramide:- Aldrich Chemical Co. Ltd., 99%; distilled from phosphorus pentoxide and stored over activated 4A molecular sieves under dry nitrogen before use.

n-Hexane, n-pentane:- Rathburn Chemicals Ltd., HPLC grade; previously dried and distilled from sodium wire, followed by storage over fresh sodium wire and activated 4A molecular sieves under nitrogen.

Benzene:- BDH Chemicals Ltd., 'AnalaR'; dried with calcium chloride prior to distillation.

Bromine liquid:- BDH Chemicals Ltd.; shaken with an equal volume of concentrated sulphuric acid and separated from the acid layer.

Tetrahydrofuran:- Rathburn Chemicals Ltd., HPLC grade; refluxed and distilled from calcium hydride under nitrogen.

Diethyl ether:- BDH Chemicals Ltd.; dried with sodium wire, followed by refluxing and distilling from calcium hydride under nitrogen.

Silver trifluoromethanesulphonate:- Aldrich Chemical Co. Ltd.; dried under reduced pressure at 50°C for four days.

Tetra-n-butylammonium bromide:- Aldrich Chemical Co. Ltd.; the recrystallization process involved dissolving in hot benzene (5 ml per gram) and adding n-hexane until the mixture became cloudy; the resulting solid was then filtered, washed with fresh n-hexane and dried under nitrogen.

6.3 Studies on halomethylphenylsilane (PhMeHSiX; X=Cl, OSO_2CF_3)

An aliquot of PhMeHSiX (X=Cl, OSO_2CF_3; 2.5 mmoles) was added to a solution of R-(+)-limonene (2.0 ml, 12.375 mmoles) in benzene-d_6 (0.2 ml) in a 10 mm screw cap n.m.r. tube, with a PTFE-silicon rubber septum. Proton, carbon-13 and silicon-29 n.m.r. spectra were recorded before and after the addition of silane. In the case of the silyl triflate, $PhMeHSiOSO_2CF_3$, the experiment was repeated in the presence of triethylamine (0.35 ml, 2.5 mmoles).

6.4 Syntheses

6.4.1 Synthesis of $RCHMeSiMe_2H$

$RCHMeSiMe_2H$ was prepared by the standard in situ Grignard reaction. The mixture of solvent, RCH(Br)Me and magnesium turnings, previously dried by heating in an oven, was activated with a small crystal of iodide. Chlorodimethylsilane was added dropwise and the stirred mixture was refluxed for four hours. Excess magnesium turnings were removed by the addition of hydrochloric acid (2M). The ethereal layer was washed with water and saturated sodium hydrogen carbonate solution, then dried with anhydrous magnesium sulphate. After removing the solvent, the remaining crude product was purified by distillation and stored under nitrogen prior to use.

$$RCH(Br)Me + Mg + Me_2HSiCl \xrightarrow{\text{solvent}} RCHMeSiMe_2H + MgClBr$$

When R=Et[84]	$CH_3CH_2CH(Br)CH_3$	56.48g, 0.412 mole
	Mg turnings	15.6g, 0.642 mole
	chlorodimethylsilane	59.64g, 0.630 mole
	diethyl ether	150 ml

Yield of sec-butyldimethylsilane	18.68g, 39.0%
b.p.	98-102°C 760mmHg

When R=Ph[85] Before (1-bromoethyl)benzene was commercially available, (1-chloroethyl)benzene was prepared by allowing a mixture of DL-1-phenylethanol (41.3g, 0.338 mole) and thionyl chloride (100.9g, 0.848 mole) to stir overnight at room temperature. Excess thionyl chloride was distilled off, the remaining liquid was dissolved in sodium dried diethyl ether. The resulting liquid was washed with water and saturated sodium hydrogen carbonate solution, dried and distilled to give 36.83g, 77.5% yield of (1-chloroethyl)benzene.

PhCH(Cl)Me	79.68g, 0.567 mole
Mg turnings	48.9g, 2.011 mole
chlorodimethylsilane	190.04g, 2.008 mole
tetrahydrofuran	300 ml

Yield of 1-methylbenzyldimethylsilane	78.05g, 83.8%
b.p.	28°C 0.3mmHg
Analysis	Found: C, 70.45%; H, 10.05%
	$C_{10}H_{16}Si$ requires C, 73.09%; H, 9.81%

When R=^{t}Bu[66] The precursor, 2-chloro-3,3-dimethylbutane (^{t}BuCHClMe) was synthesed by the same method as described above for the preparation of 1-chlorophenylethane. The n.m.r. spectral data of the crude product indicated the presence of a mixture of 2-chloro-3,3-dimethylbutane (^{t}BuCHClMe) and its rearranged product, 2,3-dimethyl-2-chlorobutane ($Me_2CClCHMe_2$). Further preparative work on this compound was abandoned.

^{13}C n.m.r. data ($CDCl_3$, external TMS)

Signals from $^tBuCH(Cl)Me$: 40.5 (CH), 30.3 ($\underline{C}Me_3$), 29.3 ($\underline{C}Me_3$), 18.3 (Me)

Resonances from $Me_2CHC(Cl)Me_2$: 74.4 (CCl), 31.3 ($CClMe_2$), 19.8 ($CHMe_2$), 15.7 (CH)

6.4.2 Synthesis of $RCHMeSiMe_2Cl$

The chlorosilanes were prepared by chlorination of the corresponding silanes $RCHMeSiMe_2H$.[84] Chlorine gas was bubbled through a stirred solution of silane in carbon tetrachloride (previously degassed) under nitrogen at 0°C. The mixture was irradiated with a 60W light bulb. The reaction was carefully monitored, by recording the proton spectra of the reaction mixture at regular intervals, to check for the disappearance of the SiH quintet. Further chlorination of the proton of the RCHMe group would result if excess chlorine gas was present. After the removal of solvent, the crude product was distilled under reduced pressure and stored under nitrogen before use.

$$RCHMeSiMe_2H + Cl_2\ (g) \xrightarrow[CCl_4]{h\nu,\ 0^oC} RCHMeSiMe_2Cl + HCl\ (g)$$

When R=Et

sec-butyldimethylsilane	4.47g, 0.038 mole
carbon tetrachloride	30 ml

Yield of sec-butyldimethylchlorosilane	4.34g, 74.9%
b.p.	132°C 760mmHg

When R=Ph

1-methylbenzyldimethylsilane	30.37g, 0.19 mole
carbon tetrachloride	50 ml

Yield of 1-methylbenzyldimethylchlorosilane	30.33g, 81.6%
b.p.	43-44°C 0.1mmHg

Analysis Found: C, 58.78%; H, 8.22%

$C_{10}H_{15}SiCl$ requires C, 60.43%; H, 7.61%

6.4.3 Synthesis of sec-butyldimethylsilyl triflate or trifluoromethanesulphonate ($^{S}BuSiMe_2OSO_2CF_3$)

Trifluoromethanesulphonic or triflic acid (0.68g, 4.535 mole) was syringed into a solution of sec-butyldimethylsilane (0.53g, 4.536 mole) in chloroform-d_1 (1.0 ml). Efferverscence of hydrogen gas was observed. The n.m.r. spectral results of the crude solution showed that it only contained a minute percentage of impurities.

$$^{S}BuSiMe_2H + CF_3SO_3H \longrightarrow {}^{S}BuSiMe_2OSO_3CF_3 + H_2\ (g)$$

6.4.4 Preparation of 1-methylbenzyldimethylsilyl triflate ($PhCHMeSiMe_2OSO_2CF_3$)

Cleavage of the phenyl group was observed, even at low temperatures, when triflic acid was employed for the conversion of the silane into its trifluoromethanesulphonate derivative. Hence an alternative and more expensive route had to be adopted.

1-Methylbenzylchlorodimethylsilane (4.86g, 0.024 mole) was added slowly to the viscous pale yellow solution of silver trifluoromethanesulphonate (5.87g, 0.029 mole) in acetonitrile-d_3 (2.5 ml) under nitrogen. Immediate precipitation of silver chloride was observed. On warming, the solid coagulated and became brownish pink, leaving a pale yellow, clear supernatant solution. After filtering off, the solid was washed with a further aliquot of solvent. When the removal of solvent from the combined solution was complete, the resulting liquid was distilled to give a yellow, extremely moisture sensitive liquid.

$$PhCHMeSiMe_2Cl + AgOSO_2CF_3 \longrightarrow PhCHMeSiMe_2OTf + AgCl\ (s)$$

Table 6.4.1
Summary of the n.m.r. data of $PhCHMeSiMe_2X$ (X=H, Cl, Br, OSO_2CF_3)

Assignments		$PhCHMeSiMe_2H$	$PhCHMeSiMe_2Cl$	$PhCHMeSiMe_2Br$	$PhCHMeSiMe_2OTf$
^1H	Ph	7.35-7.11m	7.44-7.17m	7.45-7.16m	7.44-7.10m
	SiH	3.93qn,3.3Hz	-	-	-
	$CH,^3J_{HH}$	2.40q,nr	2.52q,7.3Hz	2.59q,7.7Hz	2.61q,7.7Hz
	$Me,^3J_{HH}$	1.48d,7.3Hz	1.56d,7.3Hz	1.58d,7.7Hz	1.55d,7.7Hz
	$SiMe_{A,B}$	0.11dd	0.40,0.42	0.54,0.56	0.47
	A-B	3.7Hz	1.8Hz	1.8Hz	-
^{13}C	ipso C	145.6	143.2	142.9	140.6
	meta C	128.3	128.7	128.8	128.8
	ortho C	127.0	127.9	127.9	127.4
	para C	124.6	125.8	125.9	126.0
	$CF_3,^1J_{CF}$	-	-	-	118.4q,317.1Hz
	CH	27.8	32.1	32.3	29.5
	Me	15.5	14.8	15.3	13.6
	$SiMe_{A,B}$	-5.8,-5.9	-0.3,0.7	0.5,1.8	-2.8,-3.8
	A-B	2.6Hz	23.3Hz	29.8Hz	24.6Hz
^{29}Si	$SiMe_{A,B}$	nr	32.4	30.8	40.4
Quantities used:					
silane	mmol	3.01	3.01	3.18	3.36
solvent		2.0 ml chloroform-d_1			

Table 6.4.2
Summary of the n.m.r. data of $EtCHMeSiMe_2X$ (X=H, Cl, OSO_2CF_3)

Assignments	δ(ppm)	$EtCHMeSiMe_2H$	$EtCHMeSiMe_2Cl$	$EtCHMeSiMe_2OSO_2CF_3$
^1H	SiH	4.19qn,nr	-	-
	SiMe	0.10dd,3.7Hz	0.37	0.39
	^sBu	0.86-1.61m	0.88-1.55m	0.97 vbr
^{13}C	$CF_3,^3J_{CF}$	118.7q,315.9Hz	-	-
	$\underline{C}H(CH_3)$	25.9	24.1	23.3
	$CH_3\underline{C}H_2$	20.5	23.8	22.1
	$CH(\underline{C}H_3)$	14.5	13.1	12.6
	$\underline{C}H_3CH_2$	13.4	12.8	11.8
	$SiMe_{A,B}$	-5.9,-6.3	0.1	-3.3
	A-B	9.1Hz	-	

The spectra were recorded in chloroform-d_1.

Table 6.4.3

Infrared data of $PhCHMeSiMe_2X$ (X=H, Cl, Br, OSO_2CF_3)

Assignments (cm^{-1})	X = H	X = Cl	X = Br	X = OSO_2CF_3
Ph (=C-H stretch)	3083, 3062, 3024, 2999	3062, 3026	3083, 3061, 3025	3085, 3064, 3028
Me (C-H stretch)	2870 (sym) 2958 (asym)	2875 (sym) 2964 (asym)	2875 (sym) 2963 (asym)	2878 (sym) 2965 (asym)
CH (C-H stretch)	2929, 2903	2906, 2932	2904, 2931	2935
Ph (C=C stretch)	1601, 1580, 1495, 1451	1601, 1491, 1451	1601, 1495, 1451	1602, 1581, 1495, 1453
Si-benzyl	1194, 1034, 998	1194, 1034, 998	1195, 1034, 998	1207, 1034
Si-H	2113	-	-	-
Si-Me	1250, 775	1255, 792	1253, 790	1247, 761
Ph (=C-H in-plane bend)	1164, 1089 1047, 1011	1171, 1091, 1049, 1012	1169, 1091, 1049, 1013	1155, 1092, 1049, 1012
Ph (=C-H out-of-plane bend)	878, 837, 757, 699	845, 814, 760, 700	845, 812, 760, 700	852, 814, 761, 701
Me (C-H bend)	1423 (sym) 1377 (asym)	1407 (sym) 1378 (asym)	1407 (sym) 1378 (asym)	1392
CH (C-H bend)	1337	1337	nr	nr
Si-O	-	-	-	909
S-O	-	-	-	957
S=O	-	-	-	1155 (sym) 1392 (asym)
C-F	-	-	-	1262

Yield of 1-methylbenzyldimethylsilyl triflate 5.57g, 78.1%

b.p. 59-60°C 0.12mmHg

Analysis Found: C, 42.30%; H, 4.84%

$C_{11}H_{15}SiO_3SF_3$ requires C, 37.48%, H, 5.36%

6.4.5 Synthesis of 1-methylbenzyldimethylbromosilane ($PhCHMeSiMe_2Br$)

Analogous to the chlorination process, a stirred solution of 1-methylbenzyldimethylsilane (64.7g, 0.394 mole) in carbon tetrachloride (150 ml) was brominated by adding bromine liquid dropwise to the solution under nitrogen at 0°C with irradiation. Efferverscence of hydrogen bromide gas was observed. Proton n.m.r. spectroscopy was used to monitor the reaction. The mixture became orange when the reaction was complete. Removal of the solvent followed by distillation gave a slightly pale yellow, extremely moisture sensitive liquid.

$$PhCHMeSiMe_2H + Br_2\ (l) \longrightarrow PhCHMeSiMe_2Br + HBr\ (g)$$

Yield of 1-methylbenzylbromodimethylsilane 77.21g, 80.6%

b.p. 90-95°C 0.3mmHg

Analysis Found: C, 48.39%; H, 6.70%

$C_{10}H_{15}SiBr$ requires C, 49.38%, H, 6.22%

6.4.6 Syntheses of silane-nucleophile adducts

Generally, a nucleophile was mixed with a silane in n-pentane (0.2 ml) under dry nitrogen. The process of adduct formation was highly exothermic. After filtering and washing with a fresh aliquot of n-pentane, the extremely hygroscopic solids were analysed by elemental microanalysis as well as infrared and n.m.r. spectroscopies. The n.m.r. and infrared data are provided in the appropriate tables.

A. The $PhCHMeSiMe_2Cl$-NMI adduct ($C_{14}H_{21}N_2SiCl$)

The mixture of $PhCHMeSiMe_2Cl$ (1.0 ml, 5.957 mmoles) and NMI (0.47 ml, 5.925 mmoles) in n-pentane (0.2 ml) was cooled at -10^oC for an hour before the solid was observed.

Analysis Found: C 59.30%, H 7.87%, N 10.25%

Calculated: C 59.87%, H 7.54%, N 9.97%

B. The $PhCHMeSiMe_2Br$-NMI adduct ($C_{14}H_{21}N_2SiBr$)

A cloudy, viscous solution and an exothermic reaction resulted as NMI (0.44 ml, 5.488 mmoles) was added to $PhCHMeSiMe_2Br$ (1.0 ml, 5.480 mmoles) in n-pentane (0.2 ml) under nitrogen. The solid precipitated out after standing at -10^oC for six hours.

Analysis Found: C 52.54%, H 6.71%, N 8.48%

Calculated: C 52.01%, H 6.55%, N 8.66%

C. The $PhCHMeSiMe_2Br$-HMPA salt ($C_{16}H_{33}N_3POSiBr$)

A pale yellow, semi-solid mixture of $PhCHMeSiMe_2Br$ (1.0 ml, 5.515 mmoles) and HMPA (0.96 ml, 5.490 mmoles) in n-pentane (0.2 ml) was left to stand at -10^oC for six hours, prior to the formation of the solid. Heat was evolved during the addition.

Analysis Found: C 47.21%, H 8.19%, N 10.44%

Calculated: C 45.49%, H 7.87%, N 9.95%

D. The $PhCHMeSiMe_2Br$-NMPO adduct ($C_{16}H_{22}NOSiBr$)

The salt was formed instantaneously as NMPO (0.55 ml, 5.562 mmoles) was introduced to the solution of $PhCHMeSiMe_2Br$ (1.0 ml, 5.499 mmoles) in n-pentane (0.2 ml).

Analysis Found: C 52.94%, H 6.38%, N 7.22%

Calculated: C 54.54%, H 6.29%, N 3.94%

E. The $PhMeHSiCl$-$(NMI)_2$ salt ($C_{15}H_{21}N_4SiCl$)

NMI (1.22 ml, 15.273 mmoles) was mixed with PhMeHSiCl (1.0 ml, 7.647 mmoles) in n-pentane (0.2 ml) under nitrogen to give a gluey white solid, followed by recrystallization from hot chloroform-d_1 and n-pentane.

Table 6.4.4 N.M.R. data of silane-NMI adducts

	Assignments δ(ppm)	$PhCHMeSiMe_2Cl$	$PhCHMeSiMe_2Br$	PhMeHSiCl	NMI	$PhCHMeSiMe_2Cl$-NMI adduct	$PhCHMeSiMe_2Br$-NMI adduct	PhMeHSiCl-$(NMI)_2$ adduct
^1H	Ph	7.44-7.17m	7.45-7.16m	7.68-7.33m	-	7.19-7.14m	7.26-6.97m	7.60-7.32m
	CH, $^3J_{HH}$	2.52q,7.3Hz	2.59q,7.7Hz	-	-	2.42q,7.0Hz	2.91q	-
	Me, $^3J_{HH}$	1.56d,7.3Hz	1.58d,7.7Hz	-	-	1.45d,7.7Hz	1.39d,7.7Hz	-
	SiMe	0.40,0.42	0.54,0.56	-	-	0.32	0.66	-
	SiH, $^3J_{HH}$	-	-	5.29q,3.3Hz	-	-	-	5.48q,2.6Hz br
	SiMe, $^3J_{HH}$	-	-	0.73d,3.3Hz	-	-	-	0.77d,2.6Hz sbr
	$C_2(H)=N$	-	-	-	7.41	7.67 br	9.20 br	7.97 br
	$C_4(H)=C_5$	-	-	-	7.00	7.05 br	7.50 br	7.05 br
	$C_4=C_5(H)$	-	-	-	6.90	6.90 br	obscured	6.89 br
	$N-CH_3$	-	-	-	3.68	3.69 sbr	4.00	3.80
^{13}C	ipso C	143.2	142.9	133.9	-	142.6	140.7	136.1
	meta C	128.7	128.8	128.2	-	128.3	128.8	126.6
	ortho C	127.9	127.9	133.6	-	127.5	127.2	132.8
	para C	125.8	125.9	130.9	-	125.3	125.8	128.3
	CH	32.1	32.3	-	-	31.5	28.4	-
	Me	14.8	15.3	-	-	14.4	14.0	-
	SiMe	0.7,-0.3	0.5,1.8	0.1	-	-0.3	-4.1	1.3
	C_2	-	-	-	137.8	137.8 sbr	139.8 sbr	137.6 sbr
	C_4	-	-	-	129.5	124.4	126.0	129.9
	C_5	-	-	-	120.1	120.4 sbr	123.3 sbr	121.5
	$N-CH_3$	-	-	-	33.3	33.5	35.3	34.5
^{29}Si	SiMe	32.4	30.8	3.1	-	30.1 sbr	23.5	-50.9 vbr -64.7 vbr*
Quantities (mmol):		3.01	3.18	2.90	2.20	0.92	0.93	0.79

solvent all the adducts were dissolved in 1.5 ml chloroform-d_1 with 10% TMS, the spectra of silanes were recorded in 2.0 ml chloroform-d_1.

* recorded after three weeks

Table 6.4.5 Proton and silicon-29 n.m.r. data of $PhCHMeSiMe_2Br$-nucleophile (NMI, HMPA and NMPO) adducts

	Assignments δ(ppm)	$PhCHMeSiMe_2Br$	NMI	HMPA	NMPO	$PhCHMeSiMe_2Br$-NMI adduct	$PhCHMeSiMe_2Br$-HMPA adduct	$PhCHMeSiMe_2Br$-NMPO adduct
^1H	Ph	7.45-7.16m	-	-	-	7.26-6.97m	7.31-7.08m	7.29-6.96m
	$CH, {}^3J_{HH}$	2.59q,7.7Hz	-	-	-	2.91q,nr	2.51q,7.0Hz	2.66q,7.7Hz
	$Me, {}^3J_{HH}$	1.58d,7.7Hz	-	-	-	1.39d,7.7Hz	1.44d,7.7Hz	1.48d,7.3Hz
	SiMe	0.54,0.56	-	-	-	0.66	0.42	0.54
	$C_2(H)=N$	-	7.41	-	-	9.20 br	-	-
	$C_4(H)=C_5$	-	7.00	-	-	7.50 br	-	-
	$C_4=C_5(H)$	-	6.90	-	-	obscured	-	-
	$N-CH_3$	-	3.68	-	-	4.00	-	-
	$PNMe, {}^3J_{HH}$	-	-	2.66d 3.9Hz	-	-	2.71d,10.3Hz	-
	$C_{5,6}-H$	-	-	-	7.25-7.44m	-	-	7.29-6.96m
	C_3-H	-	-	-	6.55d,d	-	-	8.61d,d
	$^3J_{HH}$	-	-	-	9.8,1.4Hz	-	-	5.9,1.5Hz
	C_4-H	-	-	-	6.15t,d	-	-	7.96t,d
	$^3J_{HH}$	-	-	-	6.8,1.4Hz	-	-	7.3,1.8Hz
	$N-CH_3$	-	-	-	3.54	-	-	3.93
^{29}Si	SiMe	30.8	-	-	-	23.5	24.3	30.4
Quantities (mmol):		3.18	2.20	2.20	2.20	0.93	1.05	0.91

solvent 1.5 ml chloroform-d_1 with 10% TMS except for $PhCHMeSiMe_2Br$ which was in 2.0 ml chloroform-d_1

Table 6.4.6 Carbon-13 n.m.r. data of $PhCHMeSiMe_2Br$-nucleophile (NMI, HMPA and NMPO) adducts

Assignments δ(ppm)	$PhCHMeSiMe_2Br$	NMI	HMPA	NMPO	$PhCHMeSiMe_2Br$-NMI adduct	$PhCHMeSiMe_2Br$-HMPA adduct	$PhCHMeSiMe_2Br$-NMPO adduct
ipso C	142.9	-	-	-	140.7	141.5	141.7
meta C	128.8	-	-	-	128.8	128.7	128.6
ortho C	127.9	-	-	-	127.2	127.4	127.3
para C	125.9	-	-	-	125.8	125.9	125.8
CH	32.3	-	-	-	28.4	29.8	30.0 sbr
Me	15.3	-	-	-	14.0	14.1	14.2
SiMe	0.5,1.8	-	-	-	-4.1	-2.1	-1.6 sbr
C_2	-	137.8	-	-	139.8 sbr	-	-
C_4	-	129.4	-	-	126.0	-	-
C_5	-	120.1	-	-	123.2 sbr	-	-
$N-CH_3$	-	33.2	-	-	35.3	-	-
$P-N(CH_3)$	-	-	36.9d	-	-	37.0d	-
$^2J_{PC}$	-	-	3.9Hz	-	-	3.9Hz	-
C=O	-	-	-	163.1	-	-	159.8
C_3	-	-	-	139.6	-	-	144.9
C_6	-	-	-	138.5	-	-	142.2
C_5	-	-	-	120.5	-	-	117.3
C_4	-	-	-	105.9	-	-	114.4 sbr
$N-CH_3$	-	-	-	37.6	-	-	40.2
Quantities (mmol):	3.18	2.20	2.20	2.20	0.93	1.05	0.91

solvent 1.5 ml chloroform-d_1 with 10% TMS except for $PhCHMeSiMe_2Br$ which was recorded in 2.0 ml chloroform-d_1

Table 6.4.7

Infrared data of $PhCHMeSiMe_2X$-NMI adducts (X=Cl, Br)

Assignments (cm^{-1})	$PhCHMeSiMe_2Cl$-NMI salt	$PhCHMeSiMe_2Br$-NMI salt
Ph (=C-H stretch)	3089, 3041	nr
Me (C-H stretch)	2925	2903
CH (C-H stretch)	2854, 2703	2869
Ph (C=C stretch)	1601, 1494	1600, 1491, 1456
Ph (=C-H in-plane bend)	1178, 1064	1205, 1130, 1050
Ph (=C-H out-of-plane bend)	865, 780, 759, 700	856, 820, 754, 712
Me (C-H bend)	1455 (asym), 1377 (sym)	1427 (asym), 1378 (sym)
CH (C-H bend)	1342	1337
Si-benzyl	1178, 1064, 997	1176, 1030, 989
Si-Me	1254, 792	1256, 775
N-H stretch	3109	nr
N-H out-of-plane bend	835	805
C=N	1657	1695
C=C	1657	1568
C-N stretch	aromatic 1286 alkyl 1177, 1088	aromatic 1272, 1246 alkyl 1114, 1092, 1013
NMI (=C-H stretch)	3000	nr
NMI (=C-H out-of-plane bend)	944, 905	934, 897
NMe (C-H stretch)	2703, 2854	2869
NMe (C-H bend)	1455 (asym), 1377 (sym)	1427 (asym), 1351 (sym)
Si-N	865, 623	897, 820, 664, 651, 633

Table 6.4.8

Infrared data of $PhCHMeSiMe_2Br$-HMPA adduct

Assignments (cm^{-1})	$PhCHMeSiMe_2Br$-HMPA salt	HMPA
Ph (=C-H stretch)	3058, 3029	-
Me (C-H stretch)	2866, 2823	-
CH (C-H stretch)	2927	-
Ph (C=C stretch)	1600, 1490, 1455	-
Ph (=C-H in-plane bend)	1181, 1002	-
Ph (=C-H out-of-plane bend)	823, 762, 704	-
Me (C-H bend)	1455 (asym), 1376 (sym)	-
CH (C-H bend)	1314	-
Si-benzyl	1181, 1069	-
Si-Me	1256, 797	-
Si-O	1069, 1002, 823	-
P=O	1256	1211
C-N stretch	1069	1068
HMPA (C-H stretch)	2996	2996, 2880
HMPA (C-H bend)	1455 (asym), 1314 (sym)	1462 (asym),1296 (sym)

Table 6.4.9

Infrared data of $PhCHMeSiMe_2Br$-NMPO adduct

Assignments (cm^{-1})	$PhCHMeSiMe_2Br$-NMPO salt	NMPO
Ph (=C-H stretch)	3062	-
Me (C-H stretch)	2854	-
CH (C-H stretch)	2925	-
Ph (C=C stretch)	1604	-
Ph (=C-H in-plane bend)	1170, 1308	-
Ph (=C-H out-of-plane bend)	867, 835, 760, 725, 700	-
Me (C-H bend)	1462 (asym), 1378 (sym)	-
CH (C-H bend)	1351	-
Si-benzyl	1183, 1066, 926	-
Si-Me	1255, 781	-
Si-O	1066, 926, 867	-
C-N stretch	1308	1320
C=O	1646	1657
NMPO (=C-H stretch)	3062	3074
NMPO (C=C stretch)	1580, 1519, 1479	1587, 1471, 1541
NMPO (C-H stretch)	2925	3031
NMPO (C-H bend)	1462 (asym), 1378 (sym)	1437 (asym),1386 (sym)
NMPO (=C-H in-plane bend)	1170, 1308	1241, 1156, 1053, 1004
NMPO (=C-H out-of-plane bend)	867, 835, 760, 725	876, 844, 767, 730

Table 6.4.10

Infrared data of PhMeHSiCl, NMI and PhMeHSiCl-$(NMI)_2$ adduct

Assignments (cm^{-1})	PhMeHSiCl	NMI	PhMeHSiCl-$(NMI)_2$
Ph (=C-H stretch)	3073, 3054, 3025	-	3106,3040
Si-H	2169	-	2133
Ph (C=C stretch)	1592, 1487	-	1582, 1454
Si-Ph	1430, 1119	-	1178
Si-Me	1257	-	1273
Ph (=C-H in-plane bend)	1305	-	1332
Ph (=C-H out-of-plane bend)	882, 833, 729, 697, 672	-	836, 716
N-H stretch	-	3106	3106
N-H out-of-plane bend	-	819	836
C=N stretch	-	1518	1874
C=C stretch	-	1518	1529, 1582, 1546
C-N stretch	-	1286, 1232 1109, 1078, 1029	1285, 1236 1087, 1043, 1016
NMI (=C-H stretch)	-	2952	2926
NMe (C-H stretch)	-	2916	2854
NMe (C-H bend)	-	1421, 1359	1427, 1351
NMI (=C-H out-of-plane bend)	-	909, 743	956, 906, 746
Si-N stretch	-	-	956, 906, 836, 746, 666, 621

Analysis Found: C 56.31%, H 6.51%, N 17.09%

Calculated: C 56.14%, H 6.60%, N 17.46%

6.5 Kinetic studies on the exchange of $PhCHMeSiMe_2X$ (X=Cl, Br, OSO_2CF_3) with nucleophiles

6.5.1 The influence of nucleophile and leaving group

Successive aliquots of a nucleophile were syringed into a solution of $PhCHMeSiMe_2X$ (X=Cl, Br, OSO_2CF_3; 2.0 ml) in benzene-d_6 (0.2 ml) in a 10 mm screw top n.m.r. tube, with a PTFE-silicon rubber septum. The experiment was designed to minimise any medium effects, therefore only a small quantity of solvent, sufficient to lock on to the n.m.r. spectrometer, was used.

Instantaneous precipitation of silane-nucleophile adduct was observed when a minute quantity of a good nucleophile such as HMPA, NMI or NMPO was added to the $PhCHMeSiMe_2Br$ solution. Studies were therefore performed with a more dilute solution of silane (1.0 ml) in dichloromethane-d_2 (1.2 ml) for these systems. The exchange between the bromosilane and HMPA was extremely rapid and immeasurable even under the above conditions. The solution was made up of 0.4 ml of silane in 1.8 ml of dichloromethane-d_2.

6.5.2 The influence of solvent

The effect of altering the solvent, from an essentially non polar e.g. benzene-d_6 to a very polar one such as nitromethane-d_3, was investigated. The same procedure was followed, a nucleophile was added to $PhCHMeSiMe_2Cl$ (2.0 ml) in solvent (0.2 ml).

6.5.3 The influence of concentration

The dependence of the rate of reaction upon concentration was determined by varying the concentration of the silane solution. The experimental conditions are listed below.

Dilution	Quantity of $PhCHMeSiMe_2Cl$	Quantity and nature of solvent
Two fold	1.0 ml	1.2 ml benzene-d_6
Five fold	0.4 ml	1.8 ml benzene-d_6
Ten fold	0.2 ml	2.0 ml benzene-d_6
Two fold	1.0 ml	1.2 ml dichloromethane-d_2
Five fold	0.4 ml	1.8 ml dichloromethane-d_2
Ten fold	0.2 ml	2.0 ml dichloromethane-d_2

6.6 Variable temperature n.m.r. studies

Prior to the experiment, each sample was either cooled in a carbon dioxide-acetone bath ($-78^{o}C$) to test the solubility of the components for low temperature study or warmed in a water bath at $65^{o}C$ for high temperature work. The desired temperature was adjusted using a Jeol temperature controller. Calibration with a Comark microprocessor thermometer thermocouple indicated that the temperature accuracy was $\pm 2^{o}C$. After each readjustment of temperature, two minutes were allowed for the sample to reach thermal equilibrium. The reversibility of the reaction was examined by recording an n.m.r. spectrum after warming back to ambient temperature.

Two opposing factors were considered in preparing the samples for variable temperature studies. A moderately concentrated silane solution was required to reduce the accumulation time especially when recording silicon-29 n.m.r. spectrum. Sufficient solvent was needed, however, to avoid precipitation of silane-nucleophile adduct at low temperatures.

6.6.1 Variable temperature studies on $PhCHMeSiMe_2X$ (X=Cl, Br) and a mixture of the two silanes

Carbon-13 n.m.r. spectra of solutions of $PhCHMeSiMe_2X$ (X=Cl, Br or a mixture of silanes, 2.0 ml, 0.016 mole) in benzene-d_6 (0.2 ml) were recorded from 330K to 280K.

6.6.2 Thermodynamic studies on the exchange between $PhCHMeSiMe_2X$ (X=Cl, Br) and nucleophiles (HMPA, NMI)

Initially the experiment was performed with a solution of silane (2.0 ml) in dichloromethane-d_2 (0.2 ml), however on addition of an aliquot of nucleophile, less soluble silane-nucleophile salt, for example $PhCHMeSiMe_2Cl$-NMI, came out of solution as the temperature was lowered, hence a less concentrated solution of silane (1.0 ml) in dichloromethane-d_2 (1.2 ml) was employed.

Carbon-13 n.m.r. spectra were recorded as the temperature of the probe was progressively lowered until two well-separated diastereotopic SiMe signals were observed. The spectral data, observed rate constants at various temperatures and quantities of reagents used are listed in the accompanying tables.

6.6.3 Variable temperature chemical shift studies on the interactions of silanes with nucleophiles (HMPA, NMI, DMF)

A nucleophile was mixed with a silane (1.0 ml) in dichloromethane-d_2 (2.0 ml) except in the case where a mixture of silanes was studied. Carbon-13 or silicon-29 n.m.r. spectra were recorded at regular intervals on lowering of temperature. In certain experiments, n.m.r. spectra of other nuclei were obtained on returning to ambient probe temperature. The reaction between the mixture of $PhCHMeSiMe_2X$ (X=Cl, Br) and HMPA was

investigated by proton n.m.r. spectroscopy. The spectral data at particular temperatures and the quantities of compounds used are shown in the tables.

6.7 N.m.r. chemical shift titration studies of silanes against nucleophiles (HMPA, NMI, DMF)

Successive aliquots of nucleophiles were added to a silane solution in chloroform-d_1 (2.0 ml) under nitrogen in a 10 mm n.m.r. tube. Proton, carbon-13 and silicon-29 (oxygen-17 was studied in one of the experiments) n.m.r. spectra were recorded after each addition. All the spectral data are tabulated.

Table 6.5.1
Kinetic study on the exchange between $PhCHMeSiMe_2Cl$ and NMI

[$PhCHMeSiMe_2Cl$] (mol dm^{-3})	[NMI] (mol dm^{-3})	Ratio silane:NMI	Observed rate constant (s^{-1})
4.854	0.0	1.0 : 0.0	0.0
4.806	0.125	1.0 : 0.026	-
4.733	0.314	1.0 : 0.066	-
4.673	0.467	1.0 : 0.100	23.0
4.658	0.504	1.0 : 0.108	32.0
4.651	0.525	1.0 : 0.113	36.0
4.642	0.549	1.0 : 0.118	39.0
4.636	0.565	1.0 : 0.122	42.6
4.628	0.585	1.0 : 0.126	53.0*
4.620	0.605	1.0 : 0.131	58.0
4.610	0.632	1.0 : 0.137	68.0
4.594	0.673	1.0 : 0.147	78.0

ln observed rate constant = 3.367 ln [NMI] + 5.730

Table 6.5.2
Kinetic study on the exchange between $PhCHMeSiMe_2Cl$ and HMPA

[$PhCHMeSiMe_2Cl$] (mol dm^{-3})	[HMPA] (mol dm^{-3})	Ratio silane:HMPA	Observed rate constant (s^{-1})
4.914	0.0	1.0 : 0.0	0.0
4.862	0.061	1.0 : 0.012	-
4.836	0.151	1.0 : 0.031	-
4.737	0.207	1.0 : 0.044	16.5
4.710	0.238	1.0 : 0.051	22.0
4.694	0.257	1.0 : 0.055	26.0
4.683	0.270	1.0 : 0.058	29.2
4.672	0.283	1.0 : 0.061	32.5
4.672	0.283	1.0 : 0.061	33.2
4.656	0.302	1.0 : 0.065	36.8
4.644	0.315	1.0 : 0.068	42.0
4.629	0.333	1.0 : 0.072	46.5
4.617	0.347	1.0 : 0.075	55.0*
4.605	0.361	1.0 : 0.079	60.0
4.590	0.379	1.0 : 0.083	66.0

ln observed rate constant = 2.329 ln [HMPA] + 6.436

Quantities used in each experiment: silane 2.0 ml
solvent 0.2 ml benzene-d_6

* point of coalescence

Table 6.5.3

Kinetic study on the exchange between $PhCHMeSiMe_2Cl$ and NMPO

[$PhCHMeSiMe_2Cl$] (mol dm^{-3})	[NMPO] (mol dm^{-3})	Ratio silane:NMPO	Observed rate constant (s^{-1})
4.865	0.0	1.0 : 0.0	0.0
4.854	0.023	1.0 : 0.005	-
4.828	0.0795	1.0 : 0.016	-
4.774	0.191	1.0 : 0.040	-
4.651	0.448	1.0 : 0.096	-
4.594	0.568	1.0 : 0.124	-
4.488	0.789	1.0 : 0.176	6.0
4.292	1.199	1.0 : 0.279	25.8
4.252	1.282	1.0 : 0.301	32.0
4.231	1.327	1.0 : 0.314	35.8
4.219	1.354	1.0 : 0.321	38.0
4.207	1.379	1.0 : 0.328	40.5
4.194	1.406	1.0 : 0.335	48.0
4.181	1.432	1.0 : 0.343	55.0*
4.168	1.460	1.0 : 0.350	60.0
4.156	1.484	1.0 : 0.357	66.0
4.135	1.528	1.0 : 0.370	73.0

ln observed rate constant = 3.739 ln [NMPO] + 2.606

Quantities used: $PhCHMeSiMe_2Cl$ 2.0 ml
solvent 0.2 ml benzene-d_6

* point of coalescence

Table 6.5.4

Kinetic study on the exchange between $PhCHMeSiMe_2Cl$ and DMPU

[$PhCHMeSiMe_2Cl$] (mol dm^{-3})	[DMPU] (mol dm^{-3})	Ratio silane:DMPU	Observed rate constant (s^{-1})
4.865	0.0	1.0 : 0.0	0.0
4.833	0.039	1.0 : 0.008	-
4.766	0.154	1.0 : 0.032	-
4.637	0.374	1.0 : 0.081	-
4.525	0.565	1.0 : 0.125	-
4.311	0.931	1.0 : 0.216	-
4.128	1.245	1.0 : 0.302	8.0
4.090	1.310	1.0 : 0.320	28.5
4.063	1.356	1.0 : 0.334	34.0
4.049	1.380	1.0 : 0.341	39.0
4.038	1.398	1.0 : 0.346	42.0
4.012	1.443	1.0 : 0.360	43.0
4.001	1.462	1.0 : 0.366	51.0*
3.988	1.485	1.0 : 0.372	55.0
3.971	1.515	1.0 : 0.382	58.0
3.955	1.54	1.0 : 0.390	61.0
3.873	1.682	1.0 : 0.434	66.0

ln observed rate constant = 4.738 ln [DMPU] + 2.108

Quantities used: $PhCHMeSiMe_2Cl$ 2.0 ml
solvent 0.2 ml benzene-d_6

* point of coalescence

Table 6.5.5

Kinetic study on the exchange between $PhCHMeSiMe_2Cl$ and DMEU

[$PhCHMeSiMe_2Cl$] (mol dm^{-3})	[DMEU] (mol dm^{-3})	Ratio silane:DMEU	Observed rate constant (s^{-1})
4.849	0.0	1.0 : 0.0	0.0
4.623	0.431	1.0 : 0.093	-
4.415	0.828	1.0 : 0.187	-
4.220	1.198	1.0 : 0.284	-
4.046	1.530	1.0 : 0.378	-
3.888	1.831	1.0 : 0.471	-
3.740	2.114	1.0 : 0.565	13.0
3.602	2.378	1.0 : 0.660	23.5
3.535	2.506	1.0 : 0.709	28.6
3.469	2.632	1.0 : 0.759	33.2
3.434	2.696	1.0 : 0.785	35.8
3.417	2.729	1.0 : 0.799	38.8
3.396	2.770	1.0 : 0.815	40.0
3.381	2.800	1.0 : 0.828	40.2
3.358	2.841	1.0 : 0.846	46.0
3.343	2.871	1.0 : 0.859	53.0*
3.322	2.911	1.0 : 0.876	56.0
3.300	2.953	1.0 : 0.895	63.0

ln observed rate constant = 4.379 ln [DMEU] - 0.708

Quantities used: $PhCHMeSiMe_2Cl$ 2.0 ml
solvent 0.2 ml benzene-d_6

* point of coalescence

Table 6.5.6
Kinetic study on the exchange between $PhCHMeSiMe_2Cl$ and 3,5DMP

[$PhCHMeSiMe_2Cl$] (mol dm^{-3})	[3,5DMP] (mol dm^{-3})	Ratio silane:3,5DMP	Observed rate constant (s^{-1})
4.844	0.0	1.0 : 0.0	0.0
4.416	0.776	1.0 : 0.176	-
4.058	1.424	1.0 : 0.351	-
3.643	2.076	1.0 : 0.570	-
3.373	2.661	1.0 : 0.789	-
3.058	3.232	1.0 : 1.057	3.0
2.652	3.966	1.0 : 1.496	5.0
2.344	4.522	1.0 : 1.929	7.8
1.898	5.327	1.0 : 2.806	13.5
1.598	5.872	1.0 : 3.675	15.2
1.379	6.268	1.0 : 4.545	22.2
1.223	6.550	1.0 : 5.356	29.2
1.090	6.792	1.0 : 6.223	55.0*
0.983	6.985	1.0 : 7.108	72.0

ln observed rate constant = 3.758 ln [3,5DMP] - 3.544

Table 6.5.7
Kinetic study on the exchange between $PhCHMeSiMe_2Cl$ and py

[$PhCHMeSiMe_2Cl$] (mol dm^{-3})	[py] (mol dm^{-3})	Ratio silane:py	Observed rate constant (s^{-1})
4.618	0.0	1.0 : 0.0	0.0
3.755	2.311	1.0 : 0.615	-
2.733	5.049	1.0 : 1.848	-
1.773	7.617	1.0 : 4.296	-
1.629	8.003	1.0 : 4.912	-
1.507	8.331	1.0 : 5.529	7.2
1.401	8.615	1.0 : 6.151	12.8
1.354	8.741	1.0 : 6.458	18.5
1.292	8.906	1.0 : 6.894	27.0
1.243	9.036	1.0 : 7.269	31.5
1.184	9.194	1.0 : 7.766	33.1
1.093	9.439	1.0 : 8.639	33.7
0.986	9.729	1.0 : 9.867	38.4

ln observed rate constant = 8.982 ln [py] - 16.157

Quantities used in each experiment: silane 2.0 ml
solvent 0.2 ml benzene-d_6

* point of coalescence

Table 6.5.8

Kinetic study on the exchange between $PhCHMeSiMe_2Cl$ and TMU

[$PhCHMeSiMe_2Cl$] (mol dm^{-3})	[TMU] (mol dm^{-3})	Ratio silane:TMU	Observed rate constant (s^{-1})
4.647	0.0	1.0 : 0.0	0.0
4.443	0.366	1.0 : 0.082	-
4.167	0.863	1.0 : 0.207	-
3.922	1.305	1.0 : 0.333	-
3.638	1.816	1.0 : 0.499	-
3.393	2.256	1.0 : 0.665	13.2
3.229	2.550	1.0 : 0.790	19.5
3.125	2.737	1.0 : 0.876	27.0
3.111	2.763	1.0 : 0.888	33.0
3.097	2.789	1.0 : 0.901	31.8
3.083	2.813	1.0 : 0.912	32.0
3.069	2.838	1.0 : 0.925	36.2
3.056	2.862	1.0 : 0.936	34.5
3.043	2.886	1.0 : 0.948	38.0
3.025	2.918	1.0 : 0.965	39.2
3.011	2.942	1.0 : 0.977	38.5
2.994	2.973	1.0 : 0.993	43.2
2.981	2.997	1.0 : 1.005	43.0
2.963	3.029	1.0 : 1.022	53.0*
2.946	3.060	1.0 : 1.039	55.0
2.926	3.096	1.0 : 1.059	53.5
2.905	3.134	1.0 : 1.079	55.5

ln observed rate constant = 4.692 ln [TMU] - 1.337

Quantities used: $PhCHMeSiMe_2Cl$ 2.0 ml
solvent 0.2 ml benzene-d_6

* point of coalescence

Table 6.5.9

Kinetic study on the exchange between $PhCHMeSiMe_2Cl$ and NMP

[$PhCHMeSiMe_2Cl$] (mol dm^{-3})	[NMP] (mol dm^{-3})	Ratio silane:NMP	Observed rate constant (s^{-1})
4.625	0.0	1.0 : 0.0	0.0
4.514	0.247	1.0 : 0.055	-
4.316	0.696	1.0 : 0.161	-
4.051	1.292	1.0 : 0.319	-
3.747	1.976	1.0 : 0.527	-
3.546	2.428	1.0 : 0.685	10.5
3.367	2.833	1.0 : 0.841	19.5
3.285	3.016	1.0 : 0.918	24.0
3.208	3.189	1.0 : 0.944	31.8
3.193	3.224	1.0 : 1.010	31.0
3.168	3.279	1.0 : 1.035	34.5
3.145	3.331	1.0 : 1.059	37.5
3.117	3.395	1.0 : 1.089	41.5
3.089	3.456	1.0 : 1.119	43.2
3.057	3.529	1.0 : 1.154	46.0
3.033	3.581	1.0 : 1.181	57.0*
3.007	3.642	1.0 : 1.211	63.0
2.981	3.701	1.0 : 1.242	70.0

ln observed rate constant = 4.395 ln [NMP] - 1.629

Quantities used: $PhCHMeSiMe_2Cl$ 2.0 ml
solvent 0.2 ml benzene-d_6

* point of coalescence

Table 6.5.10

Kinetic study on the exchange between $PhCHMeSiMe_2Cl$ and DMF

[$PhCHMeSiMe_2Cl$] (mol dm^{-3})	[DMF] (mol dm^{-3})	Ratio silane:DMF	Observed rate constant (s^{-1})
4.855	0.0	1.0 : 0.0	0.0
4.625	0.610	1.0 : 0.132	-
4.415	1.171	1.0 : 0.265	-
4.225	1.675	1.0 : 0.396	-
3.896	2.552	1.0 : 0.655	-
3.612	3.305	1.0 : 0.915	32.0
3.603	3.330	1.0 : 0.924	35.0
3.589	3.368	1.0 : 0.938	36.5
3.587	3.373	1.0 : 0.940	36.5
3.585	3.377	1.0 : 0.942	37.0
3.582	3.386	1.0 : 0.945	37.0
3.569	3.420	1.0 : 0.958	39.0
3.558	3.449	1.0 : 0.969	43.0
3.550	3.471	1.0 : 0.978	45.0
3.538	3.504	1.0 : 0.991	47.0
3.526	3.535	1.0 : 1.003	53.0*
3.514	3.567	1.0 : 1.015	58.0
3.497	3.612	1.0 : 1.033	63.0

ln observed rate constant = 7.575 ln [DMF] - 5.607

Quantities used: $PhCHMeSiMe_2Cl$ 2.0 ml
solvent 0.2 ml benzene-d_6

* point of coalescence

Table 6.5.11
Kinetic study on the exchange between $PhCHMeSiMe_2Br$ and DMPU

[$PhCHMeSiMe_2Br$] (mol dm^{-3})	[DMPU] (mol dm^{-3})	Ratio silane:DMPU	Observed rate constant (s^{-1})
4.554	0.0	1.0 : 0.0	0.0
4.546	0.022	1.0 : 0.005	12.5
4.526	0.050	1.0 : 0.011	31.8
4.519	0.064	1.0 : 0.014	39.2
4.513	0.075	1.0 : 0.017	42.8
4.507	0.085	1.0 : 0.019	45.2
4.501	0.096	1.0 : 0.021	48.0
4.496	0.106	1.0 : 0.024	51.2
4.489	0.118	1.0 : 0.026	52.0
4.479	0.136	1.0 : 0.030	66.5
4.474	0.145	1.0 : 0.032	70.0

ln observed rate constant = 0.858 ln [DMPU] + 5.912

Table 6.5.12
Kinetic study on the exchange between $PhCHMeSiMe_2Br$ and DMEU

[$PhCHMeSiMe_2Br$] (mol dm^{-3})	[DMEU] (mol dm^{-3})	Ratio silane:DMEU	Observed rate constant (s^{-1})
4.549	0.0	1.0 : 0.0	0.0
4.506	0.086	1.0 : 0.019	-
4.461	0.180	1.0 : 0.040	16.0
4.426	0.251	1.0 : 0.057	26.5
4.393	0.319	1.0 : 0.073	39.5
4.379	0.348	1.0 : 0.080	46.5
4.371	0.365	1.0 : 0.084	50.5
4.363	0.379	1.0 : 0.087	51.8
4.356	0.395	1.0 : 0.091	55.2
4.347	0.414	1.0 : 0.095	66.8*
4.336	0.435	1.0 : 0.100	73.0
4.328	0.453	1.0 : 0.105	76.0

ln observed rate constant = 1.697 ln [DMEU] + 5.644

Quantities used in each experiment: silane 2.0 ml
solvent 0.2 ml benzene-d_6

* point of coalescence

Table 6.5.13
Kinetic study on the exchange between $PhCHMeSiMe_2Br$ and DMF

[$PhCHMeSiMe_2Br$] (mol dm^{-3})	[DMF] (mol dm^{-3})	Ratio silane:DMF	Observed rate constant (s^{-1})
4.515	0.0	1.0 : 0.0	0.0
4.470	0.129	1.0 : 0.029	7.6
4.424	0.260	1.0 : 0.059	38.4
4.417	0.280	1.0 : 0.063	43.2
4.413	0.292	1.0 : 0.066	48.8
4.408	0.308	1.0 : 0.070	54.5
4.402	0.323	1.0 : 0.073	65.0*
4.396	0.342	1.0 : 0.078	76.0
4.389	0.361	1.0 : 0.082	84.0

ln observed rate constant = 2.325 ln [DMF] + 6.776

Table 6.5.14
Kinetic study on the exchange between $PhCHMeSiMe_2Br$ and 2,4DMP

[$PhCHMeSiMe_2Br$] (mol dm^{-3})	[2,4DMP] (mol dm^{-3})	Ratio silane:2,4DMP	Observed rate constant (s^{-1})
4.542	0.0	1.0 : 0.0	0.0
4.219	0.617	1.0 : 0.146	-
3.812	1.394	1.0 : 0.366	-
3.475	2.037	1.0 : 0.586	-
3.353	2.270	1.0 : 0.677	18.0
3.187	2.587	1.0 : 0.812	26.7
3.132	2.692	1.0 : 0.859	31.7
3.079	2.792	1.0 : 0.907	34.4
3.029	2.889	1.0 : 0.954	37.7
2.980	2.983	1.0 : 1.001	40.4
2.915	3.106	1.0 : 1.066	40.6
2.849	3.233	1.0 : 1.135	43.7
2.766	3.391	1.0 : 1.226	43.7
2.672	3.569	1.0 : 1.335	51.2
2.596	3.714	1.0 : 1.430	51.8
2.509	3.881	1.0 : 1.547	52.0
2.415	4.060	1.0 : 1.681	59.6
2.301	4.278	1.0 : 1.859	66.5
2.197	4.476	1.0 : 2.037	78.0

ln observed rate constant = 1.812 ln [2,4DMP] + 1.603
Quantities used in each experiment: silane 2.0 ml
solvent 0.2 ml benzene-d_6

* point of coalescence

Table 6.5.15
Kinetic study on the exchange between $PhCHMeSiMe_2Br$ and TMU

[$PhCHMeSiMe_2Br$] (mol dm^{-3})	[TMU] (mol dm^{-3})	Ratio silane:TMU	Observed rate constant (s^{-1})
4.544	0.0	1.0 : 0.0	0.0
4.481	0.117	1.0 : 0.026	-
4.417	0.235	1.0 : 0.053	-
4.375	0.311	1.0 : 0.071	11.5
4.317	0.425	1.0 : 0.092	17.5
4.255	0.532	1.0 : 0.125	22.9
4.181	0.668	1.0 : 0.160	34.8
4.143	0.740	1.0 : 0.179	40.0
4.116	0.789	1.0 : 0.192	48.0
4.093	0.830	1.0 : 0.203	51.5
4.064	0.884	1.0 : 0.218	57.5
4.043	0.923	1.0 : 0.228	68.0
4.022	0.961	1.0 : 0.239	76.0

ln observed rate constant = 1.649 ln [TMU] + 4.273

Table 6.5.16
Kinetic study on the exchange between $PhCHMeSiMe_2Br$ and NMP

[$PhCHMeSiMe_2Br$] (mol dm^{-3})	[NMP] (mol dm^{-3})	Ratio silane:NMP	Observed rate constant (s^{-1})
4.547	0.0	1.0 : 0.0	0.0
4.441	0.244	1.0 : 0.055	25.7
4.432	0.265	1.0 : 0.060	28.6
4.421	0.289	1.0 : 0.065	37.0
4.409	0.316	1.0 : 0.072	40.0
4.399	0.339	1.0 : 0.077	47.0
4.389	0.363	1.0 : 0.083	52.0
4.382	0.379	1.0 : 0.087	62.0
4.371	0.416	1.0 : 0.092	72.0
4.364	0.419	1.0 : 0.096	78.0
4.354	0.442	1.0 : 0.102	84.0

ln observed rate constant = 2.022 ln [NMP] + 6.066

Quantities used in each experiment: silane 2.0 ml
solvent 0.2 ml benzene-d_6

Table 6.5.17
Kinetic study on the exchange between $PhCHMeSiMe_2Br$ and 3,5DMP

[$PhCHMeSiMe_2Br$] (mol dm^{-3})	[3,5DMP] (mol dm^{-3})	Ratio silane:3,5DMP	Observed rate constant (s^{-1})
4.533	0.0	1.0 : 0.0	0.0
4.066	0.904	1.0 : 0.223	-
3.825	1.369	1.0 : 0.358	18.0
3.678	1.652	1.0 : 0.449	25.6
3.607	1.790	1.0 : 0.496	32.5
3.540	1.919	1.0 : 0.542	37.2
3.443	2.109	1.0 : 0.613	42.3
3.406	2.178	1.0 : 0.639	46.2
3.355	2.276	1.0 : 0.678	48.8
3.305	2.374	1.0 : 0.718	55.5
3.256	2.468	1.0 : 0.758	62.0*
3.219	2.540	1.0 : 0.789	65.0
3.163	2.648	1.0 : 0.837	73.0

ln observed rate constant = 2.071 ln [3,5DMP] + 2.238

Table 6.5.18
Kinetic study on the exchange between $PhCHMeSiMe_2Br$ and py

[$PhCHMeSiMe_2Br$] (mol dm^{-3})	[py] (mol dm^{-3})	Ratio silane:py	Observed rate constant (s^{-1})
4.541	0.0	1.0 : 0.0	0.0
4.432	0.298	1.0 : 0.067	-
4.237	0.828	1.0 : 0.195	-
3.899	1.748	1.0 : 0.448	-
3.360	3.215	1.0 : 0.957	30.7
3.327	3.307	1.0 : 0.994	33.0
3.262	3.483	1.0 : 1.068	36.5
3.184	3.695	1.0 : 1.161	45.0
3.120	3.870	1.0 : 1.241	52.5
3.090	3.949	1.0 : 1.278	53.0
3.063	4.025	1.0 : 1.314	65.0*
3.040	4.088	1.0 : 1.345	71.0
3.017	4.149	1.0 : 1.375	74.0

ln observed rate constant = 3.422 ln [py] - 0.624

Quantities used in each experiment: silane 2.0 ml
solvent 0.2 ml benzene-d_6

* point of coalescence

Table 6.5.19
Kinetic study on the exchange between $PhCHMeSiMe_2Br$ and NMI

[$PhCHMeSiMe_2Br$] (mol dm^{-3})	[NMI] (mol dm^{-3})	Ratio silane:NMI	Observed rate constant (s^{-1})
2.295	0.0	1.0 : 0.0	0.0
2.285	0.056	1.0 : 0.024	28.5
2.284	0.062	1.0 : 0.027	36.4
2.283	0.068	1.0 : 0.030	40.0
2.282	0.073	1.0 : 0.032	45.3
2.281	0.079	1.0 : 0.035	51.2
2.279	0.085	1.0 : 0.038	60.0
2.278	0.091	1.0 : 0.040	65.0
2.277	0.096	1.0 : 0.042	-

ln observed rate constant = 1.635 ln [NMI] + 8.101

Table 6.5.20
Kinetic study on the exchange between $PhCHMeSiMe_2Br$ and DMPU with two fold dilution

[$PhCHMeSiMe_2Br$] (mol dm^{-3})	[DMPU] (mol dm^{-3})	Ratio silane:DMPU	Observed rate constant (s^{-1})
2.298	0.0	1.0 : 0.0	0.0
2.296	0.008	1.0 : 0.003	-
2.291	0.026	1.0 : 0.016	12.0
2.286	0.045	1.0 : 0.020	20.3
2.281	0.064	1.0 : 0.028	30.7
2.277	0.075	1.0 : 0.033	38.0
2.275	0.083	1.0 : 0.036	43.9
2.273	0.090	1.0 : 0.040	45.6
2.270	0.101	1.0 : 0.046	56.0*
2.267	0.112	1.0 : 0.050	64.0
2.262	0.131	1.0 : 0.058	76.0

ln observed rate constant = 1.174 ln [DMPU] + 6.694

Quantities used in each case: silane 1.0 ml
solvent 1.2 ml dichloromethane-d_2

* point of coalescence

Table 6.5.21
Kinetic study on the exchange between $PhCHMeSiMe_2Br$ and NMPO

[$PhCHMeSiMe_2Br$] (mol dm^{-3})	[NMPO] (mol dm^{-3})	Ratio silane:NMPO	Observed rate constant (s^{-1})
2.299	0.0	1.0 : 0.0	0.0
2.295	0.015	1.0 : 0.007	13.0
2.293	0.025	1.0 : 0.011	29.2
2.291	0.033	1.0 : 0.014	47.5
2.289	0.041	1.0 : 0.018	68.0
2.287	0.050	1.0 : 0.022	92.0
2.286	0.058	1.0 : 0.026	102.0

ln observed rate constant = 1.600 ln [NMPO] + 9.271
Quantities used: silane 1.0 ml
solvent 1.2 ml dichloromethane-d_2

Table 6.5.22
Kinetic study on the exchange between $PhCHMeSiMe_2Br$ and HMPA

[$PhCHMeSiMe_2Br$] (mol dm^{-3})	[HMPA] (mol dm^{-3})	Ratio silane:HMPA	Observed rate constant (s^{-1})
0.9197	0.0	1.0 : 0.0	0.0
0.9196	0.0053	1.0 : 0.006	11.2
0.9188	0.0105	1.0 : 0.011	34.1
0.9179	0.016	1.0 : 0.017	56.0

ln observed rate constant = 1.483 ln [HMPA] + 10.223
Quantities used: silane 0.4 ml
solvent 1.8 ml dichloromethane-d_2

Table 6.5.23
Kinetic study on the exchange between $PhCHMeSiMe_2Br$ and HMPA in the presence of 2,6DBP

[$PhCHMeSiMe_2Br$] (mol dm^{-3})	[HMPA] (mol dm^{-3})	Ratio silane:HMPA	Observed rate constant (s^{-1})
0.9268	0.0	1.0 : 0.0	0.0
0.9259	0.0053	1.0 : 0.0057	33.2
0.9255	0.0079	1.0 : 0.0085	57.0

ln observed rate constant = 1.335 ln [HMPA] + 10.503
Quantities used: silane 0.4 ml 2,6DBP 0.04 ml
solvent 1.8 ml dichloromethane-d_2

Table 6.5.24
Kinetic study on the exchange between $PhCHMeSiMe_2Cl$ (2.0 ml) and nucleophiles (2,6DMP; Et_3N; 2,4DMP) in benzene-d_6 (0.2 ml)

[$PhCHMeSiMe_2Cl$] (mol dm^{-3})	[2,6DMP] (mol dm^{-3})	Ratio silane:2,6DMP	Observed rate constant (s^{-1})
4.624	0.0	1.0 : 0.0	0.0
3.160	2.172	1.0 : 0.860	-
2.403	4.124	1.0 : 1.716	-
1.937	4.988	1.0 : 2.575	-
1.622	5.573	1.0 : 3.435	-
1.396	5.994	1.0 : 4.295	-
1.194	6.368	1.0 : 5.332	-
1.067	6.605	1.0 : 6.192	-
0.964	6.795	1.0 : 7.048	0.0

[$PhCHMeSiMe_2Cl$] (mol dm^{-3})	[Et_3N] (mol dm^{-3})	Ratio silane:Et_3N	Observed rate constant (s^{-1})
4.624	0.0	1.0 : 0.0	0.0
3.180	2.240	1.0 : 0.704	-
1.958	4.137	1.0 : 2.114	-
1.414	4.981	1.0 : 3.524	-
1.107	5.457	1.0 : 4.931	-
0.885	5.802	1.0 : 6.560	1.0

[$PhCHMeSiMe_2Cl$] (mol dm^{-3})	[2,4DMP] (mol dm^{-3})	Ratio silane:2,4DMP	Observed rate constant (s^{-1})
4.656	0.0	1.0 : 0.0	0.0
4.446	0.388	1.0 : 0.087	-
4.096	1.032	1.0 : 0.252	-
3.647	1.861	1.0 : 0.510	-
3.281	2.535	1.0 : 0.772	-
2.817	3.391	1.0 : 1.204	-
2.468	4.035	1.0 : 1.635	-
2.196	4.537	1.0 : 2.066	-
1.798	5.269	1.0 : 2.931	-
1.321	6.148	1.0 : 4.653	3.0
1.044	6.660	1.0 : 6.378	8.0

The change in the rate constant may be caused by medium effect.

Table 6.5.25

Kinetic study on the exchange between $PhCHMeSiMe_2Br$ and 2,6DMP

[$PhCHMeSiMe_2Br$] (mol dm^{-3})	[2,6DMP] (mol dm^{-3})	Ratio silane:2,6DMP	Observed rate constant (s^{-1})
4.541	0.0	1.0 : 0.0	0.0
4.159	0.722	1.0 : 0.174	-
3.830	1.344	1.0 : 0.351	-
3.553	1.868	1.0 : 0.526	-
3.313	2.321	1.0 : 0.700	-
3.102	2.719	1.0 : 0.876	-
2.682	3.514	1.0 : 1.310	-
2.362	4.119	1.0 : 1.745	-
1.906	4.982	1.0 : 2.632	-
1.212	6.294	1.0 : 5.196	-
0.952	6.785	1.0 : 7.125	3.0

Table 6.5.26

Kinetic study on the exchange between $PhCHMeSiMe_2Br$ and Et_3N

[$PhCHMeSiMe_2Br$] (mol dm^{-3})	[Et_3N] (mol dm^{-3})	Ratio silane:Et_3N	Observed rate constant (s^{-1})
4.531	0.0	1.0 : 0.0	0.0
3.680	1.347	1.0 : 0.366	-
2.682	2.928	1.0 : 1.091	-
1.901	4.164	1.0 : 2.190	-
1.473	4.842	1.0 : 3.288	-
1.201	5.273	1.0 : 4.390	-
1.014	5.569	1.0 : 5.490	0.0

Quantities used in each experiment: silane 2.0 ml
solvent 0.2 ml benzene-d_6

Table 6.5.27

Kinetic study on the exchange between $PhCHMeSiMe_2Cl$ and HMPA in the presence of 2,6DBP

[$PhCHMeSiMe_2Cl$] (mol dm^{-3})	[HMPA] (mol dm^{-3})	Ratio silane:HMPA	Observed rate constant (s^{-1})
4.589	0.0	1.0 : 0.0	0.0
4.204*	0.0	1.0 : 0.0	0.0
4.178	0.036	1.0 : 0.009	-
4.151	0.072	1.0 : 0.017	-
4.108	0.131	1.0 : 0.032	13.8
4.083	0.166	1.0 : 0.041	18.2
4.066	0.189	1.0 : 0.047	22.4
4.048	0.213	1.0 : 0.053	28.7
4.032	0.235	1.0 : 0.058	31.3
4.015	0.258	1.0 : 0.064	37.0
3.998	0.281	1.0 : 0.070	40.6
3.998**	0.281	1.0 : 0.070	42.0
3.983	0.303	1.0 : 0.076	47.0
3.967	0.324	1.0 : 0.082	57.0
3.951	0.346	1.0 : 0.088	64.0

ln observed rate constant = 1.569 ln [HMPA] + 5.748

Quantities used:

$PhCHMeSiMe_2Cl$	2.0 ml
2,6DBP	0.2 ml
solvent	0.2 ml dichloromethane-d_2

* after the addition of 2,6DBP

** sample left overnight

Table 6.5.28

Kinetic study on the exchange between $PhCHMeSiMe_2Cl$ and NMI in the presence of 2,6DBP

$[PhCHMeSiMe_2Cl]$ (mol dm^{-3})	[NMI] (mol dm^{-3})	Ratio silane:NMI	Observed rate constant (s^{-1})
4.592	0.0	1.0 : 0.0	0.0
4.207*	0.0	1.0 : 0.0	0.0
4.190	0.050	1.0 : 0.020	-
4.167	0.121	1.0 : 0.029	-
4.142	0.195	1.0 : 0.047	-
4.125	0.243	1.0 : 0.059	15.7
4.109	0.291	1.0 : 0.071	15.5
4.085	0.363	1.0 : 0.089	19.8
4.053	0.459	1.0 : 0.113	28.7
4.038	0.505	1.0 : 0.125	34.2
4.022	0.552	1.0 : 0.137	37.3
4.006	0.598	1.0 : 0.149	40.3
3.991	0.644	1.0 : 0.161	45.7
3.975	0.691	1.0 : 0.174	49.0
3.960	0.736	1.0 : 0.186	58.0
3.945	0.781	1.0 : 0.198	64.0

ln observed rate constant = 1.277 ln [NMI] + 4.392

Quantities used: $PhCHMeSiMe_2Cl$ 2.0 ml
2,6DBP 0.2 ml
solvent 0.2 ml dichloromethane-d_2

* after the addition of 2,6DBP

Table 6.5.29 Kinetic study on the exchange between $PhCHMeSiMe_2Br$ and NMI in the presence of 2,6DBP with two fold dilution

[$PhCHMeSiMe_2Cl$] (mol dm^{-3})	[NMI] (mol dm^{-3})	Ratio silane:NMI	Observed rate constant (s^{-1})
2.280	0.0	1.0 : 0.0	0.0
2.178 *	0.0	1.0 : 0.0	0.0
2.174	0.026	1.0 : 0.012	15.8
2.172	0.038	1.0 : 0.017	27.2
2.171	0.043	1.0 : 0.020	34.1
2.170	0.048	1.0 : 0.022	37.6
2.169	0.054	1.0 : 0.025	46.5
2.168	0.059	1.0 : 0.027	57.0

ln observed rate constant = 1.549 ln [NMI] + 8.384

Quantities used: $PhCHMeSiMe_2Br$ 1.0 ml 2,6DBP 0.1 ml
solvent 1.2 ml dichloromethane-d_2

* after the addition of 2,6DBP

Table 6.5.30
Kinetic study on the exchange between $PhCHMeSiMe_2H$ and HMPA

[$PhCHMeSiMe_2H$] (mol dm^{-3})	[HMPA] (mol dm^{-3})	Ratio silane:HMPA	Observed rate constant (s^{-1})
4.857	0.0	1.0 : 0.0	0.0
4.812	0.053	1.0 : 0.011	-
4.637	0.253	1.0 : 0.054	-
4.266	0.698	1.0 : 0.164	-
4.103	0.892	1.0 : 0.217	-
3.749	1.311	1.0 : 0.350	-
2.781	2.456	1.0 : 0.883	-
1.366	4.131	1.0 : 3.025	-
1.090	4.458	1.0 : 4.092	0.0

Table 6.5.31
Kinetic study on the exchange between $PhCHMeSiMe_2OSO_2CF_3$ and py

[$PhCHMeSiMe_2OTf$] (mol dm^{-3})	[py] (mol dm^{-3})	Ratio silane:py	Observed rate constant (s^{-1})
3.553	0.0	1.0 : 0.0	0.0
3.544	0.029	1.0 : 0.008	6367.2 **

Quantities used: $PhCHMeSiMe_2X$ (X=H, OTf) 2.0 ml
solvent 0.2 ml benzene-d_6

** calculated from the expression for coalescence based on the linewidth of the SiMe peak.

Table 6.5.32

Kinetic study on the exchange between $PhCHMeSiMe_2Cl$ and HMPA in toluene-d_8

[$PhCHMeSiMe_2Cl$] (mol dm^{-3})	[HMPA] (mol dm^{-3})	Ratio silane:HMPA	Observed rate constant (s^{-1})
4.626	0.0	1.0 : 0.0	0.0
4.542	0.104	1.0 : 0.023	-
4.503	0.153	1.0 : 0.034	-
4.457	0.210	1.0 : 0.047	11.0
4.439	0.231	1.0 : 0.052	15.7
4.398	0.281	1.0 : 0.064	25.4
4.378	0.307	1.0 : 0.070	32.3
4.368	0.320	1.0 : 0.073	37.6
4.356	0.335	1.0 : 0.077	42.0
4.346	0.346	1.0 : 0.080	51.0
4.337	0.357	1.0 : 0.082	57.0
4.326	0.371	1.0 : 0.086	64.0

ln observed rate constant = 2.995 ln [HMPA] + 7.076

Table 6.5.33

Kinetic study on the exchange between $PhCHMeSiMe_2Cl$ and NMI in toluene-d_8

[$PhCHMeSiMe_2Cl$] (mol dm^{-3})	[NMI] (mol dm^{-3})	Ratio silane:NMI	Observed rate constant (s^{-1})
4.636	0.0	1.0 : 0.0	0.0
4.592	0.12	1.0 : 0.026	-
4.516	0.324	1.0 : 0.072	12.0
4.484	0.410	1.0 : 0.092	20.4
4.461	0.472	1.0 : 0.106	28.6
4.452	0.498	1.0 : 0.112	32.7
4.440	0.530	1.0 : 0.119	40.6
4.430	0.557	1.0 : 0.126	46.6
4.425	0.570	1.0 : 0.129	52.0

ln observed rate constant = 2.557 ln [NMI] + 5.323

Quantities used in each experiment: silane 2.0 ml

solvent 0.2 ml toluene-d_8

Table 6.5.34
Kinetic study on the exchange between $PhCHMeSiMe_2Cl$ and HMPA in dichloromethane-d_2

[$PhCHMeSiMe_2Cl$] (mol dm^{-3})	[HMPA] (mol dm^{-3})	Ratio silane:HMPA	Observed rate constant (s^{-1})
4.599	0.0	1.0 : 0.0	0.0
4.536	0.079	1.0 : 0.017	8.0
4.493	0.132	1.0 : 0.029	19.0
4.468	0.163	1.0 : 0.036	28.0
4.446	0.190	1.0 : 0.043	35.8
4.439	0.198	1.0 : 0.045	39.8
4.431	0.209	1.0 : 0.047	41.6
4.423	0.219	1.0 : 0.049	45.7
4.416	0.228	1.0 : 0.052	52.0
4.404	0.242	1.0 : 0.055	57.0

ln observed rate constant = 1.745 ln [HMPA] + 6.440

Table 6.5.35
Kinetic study on the exchange between $PhCHMeSiMe_2Cl$ and NMI in dichloromethane-d_2

[$PhCHMeSiMe_2Cl$] (mol dm^{-3})	[NMI] (mol dm^{-3})	Ratio silane:NMI	Observed rate constant (s^{-1})
4.632	0.0	1.0 : 0.0	0.0
4.588	0.119	1.0 : 0.026	6.5
4.565	0.178	1.0 : 0.039	13.0
4.533	0.268	1.0 : 0.059	28.3
4.527	0.283	1.0 : 0.062	30.5
4.517	0.312	1.0 : 0.069	37.8
4.510	0.331	1.0 : 0.073	43.0
4.504	0.346	1.0 : 0.077	52.0*
4.497	0.364	1.0 : 0.081	57.0

ln observed rate constant = 1.921 ln [NMI] + 5.911

Quantities used in each case: silane 2.0 ml
solvent 0.2 ml dichloromethane-d_2

* point of coalescence

Table 6.5.36

Kinetic study on the exchange between $PhCHMeSiMe_2Cl$ and HMPA in nitromethane-d_3

[$PhCHMeSiMe_2Cl$] (mol dm^{-3})	[HMPA] (mol dm^{-3})	Ratio silane:HMPA	Observed rate constant (s^{-1})
4.629	0.0	1.0 : 0.0	0.0
4.610	0.024	1.0 : 0.005	-
4.601	0.035	1.0 : 0.008	28.0
4.597	0.040	1.0 : 0.009	33.5
4.592	0.047	1.0 : 0.010	39.2
4.587	0.053	1.0 : 0.012	47.0
4.583	0.058	1.0 : 0.013	53.0
4.579	0.063	1.0 : 0.014	60.0

ln observed rate constant = 1.256 ln [HMPA] + 7.547

Table 6.5.37

Kinetic study on the exchange between $PhCHMeSiMe_2Cl$ and NMI in nitromethane-d_3

[$PhCHMeSiMe_2Cl$] (mol dm^{-3})	[NMI] (mol dm^{-3})	Ratio silane:NMI	Observed rate constant (s^{-1})
4.630	0.0	1.0 : 0.0	0.0
4.610	0.055	1.0 : 0.012	15.4
4.604	0.070	1.0 : 0.015	21.5
4.602	0.074	1.0 : 0.016	21.9
4.597	0.089	1.0 : 0.019	25.3
4.593	0.099	1.0 : 0.022	29.2
4.588	0.114	1.0 : 0.025	34.4
4.582	0.129	1.0 : 0.028	40.3
4.574	0.153	1.0 : 0.033	51.0
4.570	0.161	1.0 : 0.035	53.0

ln observed rate = 1.141 ln [NMI] + 6.042

Quantities used in each case: silane 2.0 ml

solvent 0.2 ml nitromethane-d_3

Table 6.5.38
Two fold dilution study on the rate of exchange between $PhCHMeSiMe_2Cl$ and HMPA in benzene-d_6

[$PhCHMeSiMe_2Cl$] (mol dm^{-3})	[HMPA] (mol dm^{-3})	Ratio silane:HMPA	Observed rate constant (s^{-1})
2.287	0.0	1.0 : 0.0	0.0
2.255	0.080	1.0 : 0.036	-
2.225	0.157	1.0 : 0.071	-
2.197	0.234	1.0 : 0.107	-
2.164	0.308	1.0 : 0.142	6.6
2.144	0.359	1.0 : 0.167	10.8
2.124	0.409	1.0 : 0.192	18.5
2.118	0.424	1.0 : 0.200	22.0
2.113	0.437	1.0 : 0.207	26.0
2.105	0.458	1.0 : 0.217	32.5
2.093	0.488	1.0 : 0.233	39.3
2.081	0.517	1.0 : 0.248	56.0
2.072	0.541	1.0 : 0.261	68.0

ln observed rate = 4.210 ln [HMPA] + 6.751

Quantities used: $PhCHMeSiMe_2Cl$ 1.0 ml
solvent 1.2 ml benzene-d_6

Table 6.5.39
Five fold dilution study on the rate of exchange between $PhCHMeSiMe_2Cl$ and HMPA in benzene-d_6

[$PhCHMeSiMe_2Cl$] (mol dm^{-3})	[HMPA] (mol dm^{-3})	Ratio silane:HMPA	Observed rate constant (s^{-1})
0.927	0.0	1.0 : 0.0	0.0
0.907	0.131	1.0 : 0.144	-
0.868	0.368	1.0 : 0.424	-
0.826	0.626	1.0 : 0.758	10.3
0.816	0.688	1.0 : 0.843	15.9
0.806	0.748	1.0 : 0.928	28.0
0.801	0.777	1.0 : 0.970	41.7
0.798	0.797	1.0 : 0.998	63.0
0.797	0.807	1.0 : 1.012	73.0

ln observed rate constant = 7.664 ln [HMPA] + 5.767

Quantities used: $PhCHMeSiMe_2Cl$ 0.4 ml
solvent 1.8 ml benzene-d_6

Table 6.5.40

Ten fold dilution study on the rate of exchange between $PhCHMeSiMe_2Cl$ and HMPA in benzene-d_6

[$PhCHMeSiMe_2Cl$] (mol dm^{-3})	[HMPA] (mol dm^{-3})	Ratio silane:HMPA	Observed rate constant (s^{-1})
0.459	0.0	1.0 : 0.0	0.0
0.412	0.583	1.0 : 1.414	9.5
0.396	0.783	1.0 : 1.975	29.3
0.382	0.969	1.0 : 2.540	39.2
0.3810	0.975	1.0 : 2.559	48.0
0.3806	0.980	1.0 : 2.576	61.0
0.3802	0.986	1.0 : 2.593	100.0

ln observed rate constant = 3.504 ln [HMPA] + 4.159

Quantities used: $PhCHMeSiMe_2Cl$ 0.2 ml
solvent 2.0 ml benzene-d_6

Table 6.5.41

Ten fold dilution study on the rate of exchange between $PhCHMeSiMe_2Cl$ and HMPA in dichloromethane-d_2

[$PhCHMeSiMe_2Cl$] (mol dm^{-3})	[HMPA] (mol dm^{-3})	Ratio silane:HMPA	Observed rate constant (s^{-1})
0.464	0.0	1.0 : 0.0	0.0
0.464	0.008	1.0 : 0.017	-
0.463	0.021	1.0 : 0.045	8.5
0.462	0.029	1.0 : 0.062	12.2
0.461	0.037	1.0 : 0.079	15.5
0.461	0.044	1.0 : 0.096	17.0
0.460	0.057	1.0 : 0.125	26.3
0.459	0.070	1.0 : 0.153	40.0
0.458	0.080	1.0 : 0.176	48.0

ln observed rate constant = 1.282 ln [HMPA] + 7.012

Quantities used: silane 0.2 ml
solvent 2.0 ml dichloromethane-d_2

Table 6.5.42

Two fold dilution study on the rate of exchange between $PhCHMeSiMe_2Cl$ and HMPA in dichloromethane-d_2

[$PhCHMeSiMe_2Cl$] (mol dm^{-3})	[HMPA] (mol dm^{-3})	Ratio silane:HMPA	Observed rate constant (s^{-1})
2.320	0.0	1.0 : 0.0	0.0
2.307	0.031	1.0 : 0.014	12.4
2.301	0.047	1.0 : 0.020	21.8
2.297	0.056	1.0 : 0.024	28.3
2.293	0.066	1.0 : 0.029	31.7
2.288	0.078	1.0 : 0.034	39.5
2.284	0.088	1.0 : 0.038	46.0
2.279	0.100	1.0 : 0.044	54.0

ln observed rate constant = 1.244 ln [HMPA] + 6.864

Quantities used: silane 1.0 ml
solvent 1.2 ml dichloromethane-d_2

Table 6.5.43

Five fold dilution study on the rate of exchange between $PhCHMeSiMe_2Cl$ and HMPA in dichloromethane-d_2

[$PhCHMeSiMe_2Cl$] (mol dm^{-3})	[HMPA] (mol dm^{-3})	Ratio silane:HMPA	Observed rate constant (s^{-1})
0.925	0.0	1.0 : 0.0	0.0
0.916	0.052	1.0 : 0.056	27.5
0.9154	0.057	1.0 : 0.062	32.6
0.9146	0.062	1.0 : 0.068	39.0
0.9138	0.067	1.0 : 0.073	36.0
0.9130	0.072	1.0 : 0.079	40.0
0.912	0.077	1.0 : 0.085	42.0

ln observed rate constant = 0.961 ln [HMPA] + 6.223

Quantities used: silane 0.4 ml
solvent 1.8 ml dichloromethane-d_2

Table 6.6.1

Variable temperature study on the exchange between $PhCHMeSiMe_2Cl$ and HMPA

Temperature (K)	Observed rate constant (s^{-1})	^{13}C n.m.r. diastereotopic SiMe peak δ(ppm)	δν
300	52.0	0.23 br	-
300*	53.0	0.17 br	-
290	47.0	0.29 br	-
280	42.0	0.29 vbr	-
275	37.0	0.40,0.00	9.1Hz
270	34.1	0.40,0.00	9.1Hz
265	32.8	0.46,-0.06	11.6Hz
260	30.5	0.52,-0.17	15.5Hz
255	26.6	0.57,-0.11	15.5Hz
250	24.4	0.63,-0.17	18.1Hz
245	21.5	0.63,-0.23	19.4Hz
240	17.8	0.63,-0.23	19.4Hz
235	15.0	0.63,-0.29	20.7Hz
230	12.0	0.63,-0.29	20.7Hz
220	7.2	0.63,-0.29	20.7Hz
silane alone	0.0	0.69,-0.29	20.7Hz

Quantities used: $PhCHMeSiMe_2Cl$ 1.0 ml, 5.084 mmoles
HMPA 0.04 ml, 0.217 mmole
solvent 1.2 ml dichloromethane-d_2

The theoretical rate constant at coalescence is 46.0 s^{-1}.

* recorded on warming back to ambient temperature

Table 6.6.2

Variable temperature study on the exchange between $PhCHMeSiMe_2Cl$ and NMI

Temperature (K)	Observed rate constant (s^{-1})	^{13}C n.m.r. diastereotopic SiMe peak δ(ppm)	δν
295	-	0.17 vsh	-
290	-	0.17 vsh	-
280	-	0.17 vsh	-
270	-	0.11 vsh	-
260	-	0.06 vsh	-
250	-	-0.06	-
240	55.0	-0.29 br	-
230	23.6	0.52,-0.40	20.7Hz
225	13.7	0.57,-0.40	22.0Hz
220	6.4	0.63,-0.34	22.0Hz
228*	17.2	0.57,-0.40	22.0Hz
232	29.2	0.52,-0.40	20.7Hz
234	35.3	0.46,-0.40	19.4Hz
236	-	obscured	
238	-	obscured	
silane alone	0.0	0.69,-0.23	20.7Hz

Quantities used: $PhCHMeSiMe_2Cl$ 1.0 ml, 5.08 mmoles
NMI 0.04 ml, 0.469 mmole
solvent 1.2 ml dichloromethane-d_2

The theoretical rate constant at coalescence is 46.0 s^{-1}.

* recorded on warming back to ambient temperature

Table 6.6.3

Variable temperature study on the exchange between $PhCHMeSiMe_2Cl$ and HMPA in 9% dichloromethane-d_2

Temperature (K)	Observed rate constant (s^{-1})	^{13}C n.m.r. diastereotopic SiMe peak δ(ppm)	δν
290	65.0	0.52 br	-
290*	61.0	0.57 br	-
285	63.0	0.46 br	-
280	60.0	0.52 br	-
275	56.0	0.52 br	-
270	52.0	0.40 vbr	-
265	49.0	0.69,0.29	9.1Hz
260	43.1	0.69,0.11	13.0Hz
255	38.7	0.80,0.00	18.1Hz
250	32.8	0.86,-0.06	20.7Hz
245	27.6	0.92,-0.06	22.0Hz
240	22.5	0.92,-0.11	23.3Hz
235	19.8	0.98,-0.17	25.9Hz
230	16.8	0.98,-0.23	27.2Hz
silane alone	0.0	1.21,0.11	24.6Hz

Quantities used:

$PhCHMeSiMe_2Cl$	2.0 ml, 10.179 mmoles
HMPA	0.13 ml, 0.741 mmole
solvent	0.2 ml dichloromethane-d_2

The theoretical rate constant at coalescence is 57 s^{-1}.

* recorded on warming back to ambient temperature

Table 6.6.4

Variable temperature study on the exchange between $PhCHMeSiMe_2Br$ and NMI

Temperature (K)	Observed rate constant (s^{-1})	^{13}C n.m.r. diastereotopic SiMe peak δ(ppm)	δν
300	78.0	1.03 br	-
295	56.0	1.21 vbr	-
295*	60.0	0.98 br	-
290	41.4	1.49,0.69	18.1Hz
288	36.4	1.61,0.75	19.4Hz
286	32.0	1.67,0.69	22.0Hz
284	27.3	1.72,0.63	24.6Hz
282	23.8	1.72,0.63	24.6Hz
280	20.0	1.72,0.63	24.6Hz
278	17.3	1.78,0.63	25.9Hz
276	13.6	1.78,0.57	27.2Hz
273	12.9	1.78,0.57	27.2Hz
270	9.8	1.78,0.57	27.2Hz
dilution	30.3	1.49,0.52	22.0Hz
silane alone	0.0	1.84,0.63	27.2Hz

Quantities used: $PhCHMeSiMe_2Br$ 1.0 ml, 5.01 mmoles
NMI 0.02 ml, 0.20 mmole
solvent 1.2 ml dichloromethane-d_2

The theoretical rate constant at coalescence is 60.4 s^{-1}.

* recorded on warming back to ambient temperature

Table 6.6.5

Variable temperature study on the exchange between $PhCHMeSiMe_2Cl$ and HMPA in the presence of 2,6DBP

Temperature (K)	Observed rate constant (s^{-1})	^{13}C n.m.r. diastereotopic SiMe peak δ(ppm)	δν
301	52.0	0.23 br	-
290	47.0	0.29 br	-
290*	46.0	0.11 br	-
280	38.0	0.29 vbr	-
270	33.8	0.52,0.00	11.6Hz
265	31.7	0.52,-0.11	14.2Hz
260	29.6	0.57,-0.11	15.5Hz
255	27.2	0.63,-0.17	18.1Hz
250	24.8	0.63,-0.17	18.1Hz
245	22.9	0.63,-0.17	18.1Hz
240	18.5	0.63,-0.23	19.4Hz
235	16.8	0.69,-0.23	20.7Hz
230	14.8	0.69,-0.29	22.0Hz
220	9.0	0.69,-0.29	22.0Hz
silane alone	0.0	0.69,-0.23	20.7Hz

Quantities used:		
	$PhCHMeSiMe_2Cl$	1.0 ml, 5.086 mmoles
	2,6DBP	0.2 ml, 0.896 mmole
	HMPA	0.05 ml, 0.270 mmole
	solvent	1.2 ml dichloromethane-d_2

The theoretical rate constant at coalescence is 46.0 s^{-1}.

* recorded on warming back to ambient temperature

Table 6.6.6

Variable temperature study on the exchange between $PhCHMeSiMe_2Br$ and NMI in the presence of 2,6DBP

Temperature (K)	Observed rate constant (s^{-1})	^{13}C n.m.r. diastereotopic SiMe peak δ(ppm)	δν
304*	74.0	1.03 br	-
296	71.0	0.98 br	-
292	54.0	1.09 vbr	-
290	46.6	1.55,0.69	19.4Hz
288	39.0	1.67,0.75	20.7Hz
286	33.4	1.67,0.69	22.0Hz
284	29.7	1.72,0.69	23.3Hz
282	26.5	1.67,0.69	22.0Hz
280	21.6	1.78,0.63	25.9Hz
278	19.6	1.78,0.63	25.9Hz
276	17.0	1.78,0.63	25.9Hz
274	15.3	1.78,0.63	25.9Hz
silane alone	0.0	1.84,0.63	27.2Hz

Quantities used:

$PhCHMeSiMe_2Br$	1.0 ml, 5.008 mmoles
2,6DBP	0.2 ml, 0.907 mmole
NMI	0.02 ml, 0.222 mmole
solvent	1.2 ml dichloromethane-d_2

The theoretical rate constant at coalescence is 60.4 s^{-1}.

* recorded on warming back to ambient temperature

Table 6.6.7

Variable temperature study on the exchange between $PhCHMeSiMe_2Br$ and HMPA in the presence of 2,6DBP

Temperature (K)	Observed rate constant (s^{-1})	^{13}C n.m.r. diastereotopic SiMe peak δ(ppm)	δν
305	108.0	1.21	-
302	80.0	1.15 br	-
300	71.0	1.26 br	-
298	60.0	1.26 br	-
294	41.1	1.55,0.92	14.2Hz
292	37.7	1.67,0.80	19.4Hz
290	34.1	1.67,0.75	20.7Hz
288	30.3	1.72,0.69	23.3Hz
286	26.5	1.72,0.69	23.3Hz
284	24.5	1.78,0.69	24.6Hz
282	21.2	1.78,0.63	25.9Hz
280	18.0	1.78,0.63	25.9Hz
278	16.0	1.78,0.63	25.9Hz
275	12.7	1.84,0.63	27.2Hz
silane alone	0.0	1.84,0.63	27.2Hz

Quantities used:

$PhCHMeSiMe_2$ Br	1.0 ml, 5.01 mmoles
2,6DBP	0.2 ml, 0.904 mmole
HMPA	4.17 ul, 0.024 mmole
solvent	1.2 ml dichloromethane-d_2

The theoretical rate constant at coalescence is 60.4 s^{-1}.

Table 6.6.8 Variable temperature n.m.r. titration study of a 2:1 mixture of $PhCHMeSiMe_2Br$ and NMI

Assignments δ(ppm)		NMI	silane	Temperature (K) 300	295	280	260	240	220	200	185
^{13}C	ipso C	-	143.1	142.2 sbr	142.2 sbr	142.2 vbr	142.8 141.5	142.8 141.5	142.7 141.4	142.5	141.8
	meta C	-	128.9	128.9	128.9	128.9	129.1 128.7	129.1 128.7	129.1 128.7	128.6	128.0
	ortho C	-	128.0	127.8	127.8	127.8	127.9 127.7	127.9 127.7	128.0 127.8	127.9	127.2
	para C	-	125.9	126.0	126.0	126.0	126.2 125.8	126.3 125.8	126.2 125.9	125.8	125.1
	CH	-	32.3	30.3 vbr	31.5 vbr	31.8 vbr 28.6 vbr	31.9 28.5	31.8 28.4	31.7 28.4 sbr	31.4 28.1 br	30.6 br
	Me	-	15.3	14.7 sbr	14.7 sbr	14.7 vbr	15.1 14.2	15.1 14.1	14.9 14.1	14.8 13.8 sbr	14.0 sbr 12.4 vbr
	SiMe	-	1.7,0.6	-1.4 vbr	-1.4 vbr	0.9 vbr -3.8 vbr	1.0 vbr -3.4,-4.5	1.5,0.4 br -3.4,-4.7	1.5,0.3 -3.4,-4.9	1.3,0.1 -3.5,-5.2	0.6,-0.6 -4.2,-6.0
	C_2	137.8	-	141.7	141.7	141.7	141.7	141.5	141.4	141.3	140.6 br
	C_4	129.4	-	125.3	125.3	125.3	125.3	125.3 sbr	124.8 sbr	obscured	obscured
	C_5	120.1	-	124.1	124.1	124.1	124.2	124.3 sbr	124.3 sbr	124.3 vbr	obscured
	$N-CH_3$	33.2	-	36.6	36.6	36.6	36.6	36.5	36.5	36.4 sbr	35.7 br
^{29}Si	SiMe	-	29.2	26.2 vbr	28.4 vbr 23.9 vbr	29.6 vbr 23.3 vbr	29.8 23.2	30.0 23.1	30.2 23.0	30.3 22.8	30.2 22.5

Quantities used: $PhCHMeSiMe_2Br$ 1.0 ml, 5.056 mmoles
NMI 0.2 ml, 2.542 mmoles
solvent 1.2 ml dichloromethane-d_2

Si-29 n.m.r. spectra were recorded on warming back to ambient temperature. The spectrum recorded at 290K gave two peaks 29.2 (vbr) and 23.2 (vbr). Line broadening observed at 185K may be caused by the viscosity of the sample.

Table 6.6.9 Variable temperature n.m.r. titration study of a 2:1 mixture of $PhCHMeSiMe_2Br$ and HMPA

Assignments δ(ppm)		HMPA	silane	Temperature (K) 300	295	280	260	250	240	220	200
^{13}C	ipso C	-	143.1	142.5	142.5	142.5	142.5br	142.9 142.2	142.6 142.2	142.6 142.1	142.5 142.1
	meta C	-	128.9	128.8	128.8	128.8	128.8	129.0 128.6	129.0 128.6	129.0 128.6	129.0 128.6
	ortho C	-	128.0	127.8	127.8	127.8	127.8	127.8	127.8	127.9 127.7	127.8 127.7
	para C	-	125.9	125.9	125.9	125.9	125.9	125.9sbr	126.0 125.7	126.0 125.7	126.0 125.7
	CH	-	32.3	30.9sbr	30.9sbr	30.8br	31.5vbr 29.9vbr	31.6sbr 29.8sbr	31.6 29.8,29.7	31.5 29.7,29.6	31.4 29.6
	Me	-	15.3	14.7	14.7	14.7	14.6br	14.9br 14.2sbr	14.9 14.2	14.9 14.1	14.8 14.0
	SiMe	-	1.7,0.6	-0.6br	-0.5br	-0.5vbr	0.9vbr -1.9vbr	1.0sbr -1.8,-2.5	0.9 -1.8,-2.5	1.0vbr -1.9,-2.6	1.4,0.3sbr -1.9,-2.8
	$PN(CH_3)$	36.9d	-	37.2d	37.2d	37.1d	37.1d	37.0d	37.0d	36.9d	36.8d
	$^2J_{PC}$	3.9Hz	-	5.2Hz	5.2Hz	5.2Hz	5.2Hz	5.2Hz	5.2Hz	5.2Hz	5.2Hz
^{29}Si	SiMe	-	29.2	26.6br	26.4br	30.3vbr 23.9vbr	29.8,23.8d* 13.7Hz	nr	30.0,23.9d 12.7Hz	30.2,23.8d 11.7Hz	30.4,23.7d 11.7Hz

Quantities used: $PhCHMeSiMe_2Br$ 1.0 ml, 5.011 mmoles
HMPA 0.44 ml, 2.507 mmoles
solvent 1.2 ml dichloromethane-d_2

Si-29 n.m.r. spectra were recorded on warming back to ambient temperature. The spectrum at 210K gave two peaks 30.3 and 23.8d (11.7Hz).

* slightly broadened

Table 6.6.10

Variable temperature proton n.m.r. titration study of a 1:1:0.45 mixture of $PhCHMeSiMe_2X$ (X=Cl, Br) and HMPA

Temperature (K)	Assignments δ(ppm) Ph	$CH,^3J_{HH}$	$Me,^3J_{HH}$	SiMe	$PN(CH_3),^3J_{PH}$
mixture of silane *	7.35-6.90m	2.47q,7.3Hz 2.39q,7.3Hz	1.44d,7.3Hz 1.43d,7.7Hz	0.43,0.41 0.30,0.27	-
300	7.35-6.72m	2.44d br 6.6Hz	1.42d,7.3Hz	0.35 vbr	2.65d,10.6Hz
298	7.35-6.88m	obscured	1.42d,7.3Hz	0.35 vbr	2.64d,10.6Hz
294	7.35-6.88m	obscured	1.42d,7.3Hz	0.35 vbr	2.64d,10.6Hz
290	7.40-6.95m	obscured	1.42d,7.7Hz	0.33 vbr 0.37	2.64d,10.6Hz
288	7.35-6.95m	obscured	1.42d,7.7Hz	0.32 0.39	2.63d,10.3Hz
286	7.35-6.95m	obscured	1.42d,7.3Hz	0.31** 0.40	2.63d,10.3Hz
284	7.40-6.92m	obscured	1.42d,7.3Hz	0.31** 0.40	2.63d,10.3Hz
282	7.35-6.92m	obscured	1.42d,7.7Hz	0.31,0.28 0.40 sbr	2.62d,10.6Hz
280	7.35-6.91m	obscured	1.42d,7.3Hz	0.31,0.28 0.40 sbr	2.62d,10.3Hz
278	7.36-6.91m	obscured	1.42d,7.7Hz	0.31,0.28 0.40 sbr	2.62d,10.3Hz
274	7.35-6.92m	obscured	1.41d,7.3Hz	0.31,0.28 0.40 sbr	2.62d,10.6Hz
270	7.35-6.92m	obscured	1.42d,7.7Hz	0.31,0.28 0.40 sbr	2.62d,10.6Hz
260	7.35-6.90m	2.41q,7.3Hz	1.42d,7.3Hz	0.31,0.28 0.41 br	2.60d,10.6Hz
250	7.36-6.90m	2.41q,7.3Hz	1.42d,7.7Hz	0.31,0.27 0.38,0.33 0.43 sbr	2.59d,10.6Hz
240	7.41-6.90m	2.41q,7.3Hz	1.41d,7.3Hz 1.38d,7.3Hz	0.31,0.27 0.36,0.31 0.43 sbr	2.57d,10.3Hz
230	7.41-6.90m	obscured	1.42d,7.7Hz 1.39d,7.7Hz	0.31,0.27 0.36,0.31 0.43 sbr	2.56d,10.6Hz
HMPA	-	-	-	-	2.66d,9.3Hz

Quantities used:

$PhCHMeSiMe_2Cl$	0.59 ml, 2.99 mmoles
$PhCHMeSiMe_2Br$	0.60 ml, 3.01 mmoles
HMPA	0.24 ml, 1.36 mmoles
solvent	2.0 ml CD_2Cl_2 with 10% TMS

* in the absence of HMPA at ambient temperature

** a shoulder was observed on this peak

Table 6.6.11
Variable temperature silicon-29 n.m.r. titration studies of 1:3 mixtures of PhMeHSiCl and nucleophile (HMPA, DMF)

Temperature (K)	Si-29 n.m.r. chemical shifts δ(ppm) PhMeHSiCl-DMF mixture	PhMeHSiCl-HMPA mixture	PhMeHSiCl
300	-	-2.03	-
295	1.48 sbr	-1.37	3.35
280	0.77 br	-2.74	-
260	0.00 vbr	-6.31 sbr	-
240	0.44 vbr	-14.76 vbr	-
220	0.00 vbr	-35.28 vbr	-
200	0.00 vbr	-59.52 vbr	-

Quantities used in each case:

silane	1.0 ml, 6.93 mmoles
HMPA	3.0 ml, 17.28 mmoles
DMF	1.6 ml, 21.06 mmoles
solvent	2.0 ml CD_2Cl_2 with 10% TMS

Table 6.6.12
Variable temperature silicon-29 n.m.r. titration studies of $PhCHMeSiMe_2Cl$ and a 1:1.5 mixture of $PhCHMeSiMe_2Cl$ and HMPA

Temperature (K)	Silicon-29 n.m.r. chemical shifts δ(ppm) $PhCHMeSiMe_2Cl$	$PhCHMeSiMe_2Cl$-HMPA mixture
300	30.6	30.1
294	30.6	30.1
280	30.8	30.1
260	30.9	30.1
240	31.1	29.6
220	31.3	28.2
210 *	nr	27.5 vbr
200	31.5	22.7 vbr
180	31.7	nr

Quantities used:

$PhCHMeSiMe_2Cl$	1.0 ml, 5.08 mmoles
HMPA	1.3 ml, 7.70 mmoles
solvent	2.0 ml dichloromethane-d_2

* recorded on warming back to ambient temperature

Table 6.7.1 N.M.R. titration study of $PhCHMeSiMe_2Cl$ against NMI

Assignments		Ratio of $PhCHMeSiMe_2Cl$ to NMI							NMI
δ(ppm)		1.0 : 0.0	1.0 : 0.5	1.0 : 1.0	1.0 : 2.0	1.0 : 3.0	1.0 : 4.0	1.0 : 5.0	
^1H	Ph	7.48-7.11m	7.32-7.04m	7.15-6.90m	6.70-6.51m	6.81-6.29m	6.39-6.12m	6.28-6.01m	-
	CH, $^3J_{HH}$	2.52q,7.7Hz	2.41q,7.3Hz	2.29q,7.3Hz	2.10q sbr 7.3Hz	1.97q,7.3Hz	1.85q,7.7Hz	1.76q,7.7Hz	-
	Me, $^3J_{HH}$	1.56d,7.7Hz	1.43d,7.7Hz	1.26d,7.3Hz	0.89d sbr 7.3Hz	0.64d,7.7Hz	0.46d,7.7Hz	0.35d,7.7Hz	-
	SiMe	0.43,0.40	0.30	0.18	-0.07	-0.25	-0.38	-0.48	-
	$C_2(H)=N$	-	7.64 sbr	7.71 vbr	7.58 vbr	7.29 vbr	7.03 br	6.84	7.41
	$C_4(H)=C_5$	-	obscured	obscured	obscured	obscured	obscured	obscured	7.00t,1.0Hz
	$C_4=C_5(H)$	-	6.86 vbr	6.84 vbr	obscured	obscured	obscured	obscured	6.90t,1.0Hz
	N-CH_3	-	3.62	3.50	3.21	2.97	2.79	2.65	3.68
^{13}C	ipso C	142.8	142.4	141.8	140.6	140.1	139.7	139.4	-
	meta C	128.3	128.1	127.8	127.2	126.9	126.6	126.4	-
	ortho C	127.5	127.2	126.8	126.1	125.7	125.3	125.2	-
	para C	125.3	125.1	124.8	124.3	124.0	123.7	123.6	-
	CH	31.7	31.3	30.5	28.9	28.0	27.3	27.0	-
	Me	14.5	14.1	13.7	12.9	12.5	12.1	11.8	-
	SiMe	0.3,-0.7	-0.6	-1.4	-3.2	-4.3	-5.0	-5.4	-
	C_2	-	137.8	138.0 vbr	137.3 sbr	136.8 sbr	136.4	136.1	137.8
	C_4	-	125.9	127.0	126.7	126.4	126.1	126.0	129.3
	C_5	-	120.1 vbr	120.2 br	120.0 sbr	119.6 sbr	119.2	118.9	120.1
	N-CH_3	-	33.2	33.0	32.6	32.2	31.7	31.4	33.2
^{29}Si	SiMe	32.4	32.0	31.2	28.7	27.3	26.6	26.1	-
Quantities used:									
silane	mmol	3.00	3.00	3.00	3.00	3.00	3.00	3.00	-
NMI	mmol	0.00	1.50	3.01	6.02	9.04	12.05	15.06	2.20
solvent		2.0 ml chloroform-d_1							

Table 6.7.2 N.M.R. titration study of $PhCHMeSiMe_2Br$ against NMI

Assignments		Ratio of $PhCHMeSiMe_2Br$ to NMI							NMI
δ(ppm)		1.0 : 0.0	1.0 : 0.5	1.0 : 1.0	1.0 : 2.0	1.0 : 3.0	1.0 : 4.0	1.0 : 5.0	
^1H	Ph	7.45-7.16m	7.03-6.67m	6.80-6.26m	6.50-6.19m	6.26-6.05m	6.25-6.05m	6.24-5.99m	-
	CH, $^3J_{HH}$	2.59q,7.7Hz	2.52q vbr 2.29q vbr	2.35q br 7.7Hz	2.23q br 7.7Hz	2.07q br 7.7Hz	1.99q br 7.7Hz	1.91q br 7.3Hz	-
	Me, $^3J_{HH}$	1.58d,7.7Hz	1.12d br 7.7Hz	0.78d br 7.3Hz	0.64d br 7.7Hz	0.47d br 7.3Hz	0.38d br 7.7Hz	0.29d br 7.7Hz	-
	SiMe	0.56,0.54	0.25 vbr	0.06 sbr	-0.08	-0.25	-0.39	-0.43	-
	$C_2(H)=N$	-	9.90 br	9.40 br	8.02 br	7.42 sbr	7.12 br	6.91 br	7.41
	$C_4(H)=C_5$	-	7.57t br 1.1Hz	7.29 br	6.70 br	6.37 sbr	obscured	obscured	7.00t,1.0Hz
	$C_4=C_5(H)$	-	obscured	obscured	obscured	obscured	obscured	obscured	6.90t,1.0Hz
	$N-CH_3$	-	3.89	3.57	3.19	2.92	2.78	2.66	3.68
^{13}C	ipso C	142.9	142.4	140.6	140.6	140.6	140.6	140.6	-
	meta C	128.8	128.7	128.6	128.5	128.3	128.2	128.1	-
	ortho C	127.9	127.4	127.0	126.9	126.8	126.7	126.6	-
	para C	125.9	125.9	125.6	125.5	125.5	125.3	125.2	-
	CH	32.3	31.7 vbr 28.6 vbr	28.1	27.9	27.7	27.7	27.6	-
	Me	15.3	14.5 vbr	13.8	13.7	13.5	13.4	13.3	-
	SiMe	1.8,0.5	1.0 vbr -3.8 vbr	-4.2	-4.4	-4.7	-4.8	-4.9	-
	C_2	-	141.1	140.6	139.0	138.4	138.0	137.8	137.8
	C_4	-	125.2	124.8	126.2	126.8	127.1	127.7	129.3
	C_5	-	123.8	123.9	122.4	121.5	121.0	120.8	120.1
	$N-CH_3$	-	36.5	36.1	34.6	33.9	33.5	33.2	33.2
^{29}Si	SiMe	30.8	30.8 br 25.2 br	24.9	24.7	24.5	24.4	24.2	-
Quantities used:									
silane	mmol	3.18	3.18	3.18	3.18	3.18	3.18	3.18	-
NMI	mmol	0.00	1.63	3.27	6.43	9.62	12.88	16.10	2.20
solvent		2.0 ml chloroform-d_1							

Table 6.7.3 N.M.R. titration study of $PhCHMeSiMe_2OSO_2CF_3$ against NMI

Assignments		Ratio of $PhCHMeSiMe_2OSO_2CF_3$ to NMI								NMI
	δ(ppm)	1.0 : 0.0	1.0 : 0.5	1.0 : 1.0	1.0 : 1.5	1.0 : 2.0	1.0 : 3.0	1.0 : 4.0	1.0 : 5.0	
^1H	Ph	7.44-7.10m	7.24-6.96m	7.26-6.80m	7.01-6.69m	6.89-6.60m	6.78-6.48m	6.72-6.36m	6.70-6.06m	-
	$CH, {}^3J_{HH}$	2.61q,7.7Hz	2.68q,7.7Hz 2.50q,7.3Hz	2.58q sbr 7.3Hz	2.51q sbr 7.3Hz	2.43q,7.7Hz	2.29q,7.7Hz	2.17q,7.7Hz	2.05q,7.7Hz	-
	$Me, {}^3J_{HH}$	1.55d,7.7Hz	1.42d,7.7Hz 1.32d,7.3Hz	1.21d sbr 7.3Hz	1.13d sbr 7.3Hz	1.04d,7.7Hz	0.90d,7.7Hz	0.76d,7.3Hz	0.65d,7.3Hz	-
	SiMe	0.47	0.35 0.57,0.48	0.41 sbr	0.33	0.25	0.10	-0.02	-0.14	-
	$C_2(H)=N$	-	8.76	8.59 sbr	8.13 br	7.84 br	7.48 sbr	7.24 sbr	7.06 sbr	7.41
	$C_4(H)=C$	-	7.41t,1.6Hz	7.33 sbr	7.07 br	obscured	obscured	obscured	obscured	7.00t,1.0Hz
	$C=C_5(H)$	-	obscured	obscured	obscured	obscured	obscured	obscured	obscured	6.90t,1.0Hz
	$N-CH_3$	-	3.92	3.81	3.62	3.48	3.26	3.10	2.96	3.68
^{13}C	ipso C	140.6	140.5,140.3	140.3	140.2	140.0	139.8	139.7	139.5	-
	meta C	128.8	128.5	128.3	128.0	127.9	127.6	127.4	127.1	-
	ortho C	127.4	127.1,126.8	126.6	126.4	126.2	126.1	126.3	126.3	-
	para C	126.0	125.7	125.5	125.3	125.6	126.0	125.8	125.5	-
	CF_3	118.4q	119.4q	120.3q	120.1q	120.0q	119.8q	119.7q	119.5q	-
	$^1J_{CF}$	317.1Hz	318.4Hz	319.7Hz	319.7Hz	321.0Hz	321.0Hz	321.0Hz	321.0Hz	-
	CH	29.5	29.1,28.0	27.8	27.6	27.4	27.1	26.9	26.7	-
	Me	13.6	13.4,13.3	13.2	13.0	12.8	12.5	12.2	12.0	-
	SiMe	-2.8,-3.8	-3.5 -4.9,-5.5	-5.3 sbr	-5.5	-5.7	-6.0	-6.3	-6.5	-
	C_2	-	139.8	139.3	138.4	138.0	137.4	137.0	136.7	137.8
	C_4	-	124.5	124.1	124.9	125.1	124.8	124.5	124.3	129.4
	C_5	-	123.7	123.6	122.6	121.7	120.7	120.1	119.7	120.1
	$N-CH_3$	-	35.7	35.3	34.2	33.5	32.8	32.3	31.9	33.2
^{29}Si	SiMe	40.4	40.8,25.7	25.7 sbr	25.7	25.5	25.2	25.0	24.9	-
Quantities used:										
silane	mmol	3.36	3.36	3.36	3.36	3.36	3.36	3.36	3.36	-
NMI	mmol	0.00	1.69	3.39	5.08	6.77	10.16	13.55	16.93	2.20
solvent		2.0 ml chloroform-d_1								

Table 6.7.4 N.M.R. titration study of $PhCHMeSiMe_2Cl$ against HMPA

Assignments		Ratio of $PhCHMeSiMe_2Cl$ to HMPA									
	δ(ppm)	1.0 : 0.0	1.0 : 0.2	1.0 : 0.4	1.0 : 0.6	1.0 : 0.8	1.0 : 1.0	1.0 : 1.2	1.0 : 1.6	1.0 : 2.0	1.0 : 3.0
^1H	Ph	7.44-7.17m	7.37-7.09m	7.19-7.01m	7.16-6.93m	7.13-6.85m	7.05-6.84m	6.88-6.69m	6.85-6.40m	6.75-6.30m	
	CH	2.52q	2.44q	obscured	obscured	obscured	obscured	obscured	obscured	obscured	
	$^3J_{HH}$	7.3Hz	7.3Hz	-	-	-	-	-	-	-	
	Me	1.56d	1.48d	1.40d	1.32d	1.25d	1.17d	1.09d	0.91d	0.72d	
	$^3J_{HH}$	7.3Hz	7.3Hz	7.3Hz	7.7Hz	7.7Hz	7.3Hz	7.3Hz	7.3Hz	7.3Hz	
	SiMe	0.42,0.40	0.33	0.25	0.18	0.10	0.02	-0.05	-0.23	-0.42	
	NMe	-	2.66d	2.58d	2.51d	2.43d	2.35d	2.28d	2.10d	1.91d	
	$^3J_{PH}$	-	9.2Hz	9.5Hz	9.5Hz	9.2Hz	9.2Hz	9.2Hz	9.5Hz	9.2Hz	
^{13}C	ipsoC	143.2	143.0	142.9	142.8	142.8	142.6	142.5	142.4	142.2	141.8
	metaC	128.7	128.7	128.6	128.5	128.5	128.4	128.3	128.2	128.0	127.6
	orthoC	127.9	127.8	127.7	127.6	127.6	127.5	127.4	127.2	127.1	126.7
	paraC	125.8	125.7	125.6	125.6	125.5	125.4	125.3	125.2	125.1	124.7
	CH	32.1	31.9	31.9	31.8	31.7	31.6	31.5	31.3	31.1	30.7
	Me	14.8	14.8	14.7	14.6	14.5	14.5	14.4	14.2	14.1	13.8
	SiMe	0.7,-0.3	0.6,-0.3	0.06 br	0.0 sbr	-0.06	-0.2	-0.2	-0.4	-0.5	-0.9
	NMe	-	37.2d	37.1d	37.1d	37.0d	36.9d	36.8d	36.6d	36.5d	36.2d
	$^2J_{PC}$	-	3.9Hz	3.9Hz	3.9Hz	3.9Hz	3.9Hz	5.2Hz	3.9Hz	3.9Hz	3.9Hz
^{29}Si	SiMe	32.4	32.3	32.1	32.0	31.9	31.8	31.7	31.4	31.2	30.8

Quantities used (mmol):										
silane	3.01	3.01	3.01	3.01	3.01	3.01	3.01	3.01	3.01	-
HMPA	0.00	0.61	1.21	1.81	2.42	3.03	3.63	4.84	6.05	2.20
solvent	2.0 ml chloroform-d_1									

Table 6.7.5 N.M.R. titration study of $PhCHMeSiMe_2Br$ against HMPA

Assignments		Ratio of $PhCHMeSiMe_2Br$ to HMPA							HMPA
	δ(ppm)	1.0 : 0.0	1.0 : 0.5	1.0 : 1.0	1.0 : 2.0	1.0 : 3.0	1.0 : 4.0	1.0 : 5.0	
^1H	Ph	7.45-7.16m	6.86-6.62m	6.45-6.10m	6.11-5.91m	5.87-5.70m	5.82-5.48m	5.65-5.37m	-
	CH, $^3J_{HH}$	2.59q,7.7Hz	2.06q,7.7Hz	obscured	obscured	obscured	obscured	obscured	-
	Me, $^3J_{HH}$	1.58d,7.7Hz	1.00d,7.7Hz	0.49d,7.7Hz	0.25d,7.7Hz	0.19d sbr 7.7Hz	-0.12d,7.7Hz	-0.22d,7.3Hz	-
	SiMe	0.56,0.54	-0.01	-0.51	-0.74	-0.97	-1.12	-1.20	-
	$PN(CH_3)$	-	2.25d	1.77d	1.50d	1.25d	1.10d	1.00d	2.66d
	$^3J_{PH}$	-	10.3Hz	10.6Hz	9.9Hz	9.9Hz	9.5Hz	9.5Hz	9.3Hz
^{13}C	ipso C	142.9	140.6 br	141.3	141.0	141.0	140.9	140.9	-
	meta C	128.8	127.2	128.2	127.9	127.8	127.5	127.4	-
	ortho C	127.9	126.1	127.0	126.7	126.6	126.4	126.4	-
	para C	125.9	124.3	125.3	125.0	124.7	124.4	124.3	-
	CH	32.3	29.9,28.6	29.2	28.8	28.6	28.3	28.1	-
	Me	15.3	13.2 br	13.8	13.5	13.3	13.1	13.0	-
	SiMe	1.8,0.5	-0.7,-3.3	-2.5	-2.8	-3.0	-3.2	-3.3	-
	$PN(CH_3)$	-	35.7d	36.5d	36.2d	36.0d	35.7d	35.6d	36.9d
	$^2J_{PC}$	-	5.2Hz	5.2Hz	3.9Hz	3.9Hz	3.9Hz	3.9Hz	3.9Hz
^{29}Si	SiMe	30.8	30.8 br 25.9 vbr	25.3	24.9	24.7	24.5	24.4	-

Quantities used:

silane	mmol	3.18	3.18	3.18	3.18	3.18	3.18	3.18	-
HMPA	mmol	0.00	1.61	3.21	6.37	9.53	12.71	15.88	2.20
solvent		2.0 ml chloroform-d_1							

Table 6.7.6

N.M.R. titration study of $PhCHMeSiMe_2Br$ with tetrabutylammonium bromide ($^nBu_4NBr$)

Assignments		$^nBu_4NBr$	Ratio of $^nBu_4NBr$: $PhCHMeSiMe_2Br$			$PhCHMeSiMe_2Br$
δ(ppm)			1.0 : 0.1	1.0 : 0.6	1.0 : 1.0	
^1H	Ph	-	6.94-6.75m	7.04-6.78m	7.06-6.65m	7.49-7.13m
	CH, $^3J_{HH}$	-	no	2.22q,7.3Hz	2.24q,7.3Hz	2.61q,7.7Hz
	Me, $^3J_{HH}$	-	no	1.14d,7.3Hz	1.17d,7.7Hz	1.59d,7.3Hz
	SiMe	-	0.11	0.15	0.18	0.57,0.59
	CH_3	0.74-0.54m	0.72-0.56m	0.76-0.62m	0.79-0.63m	-
	$(CH_2)_2$	1.60-0.88m	1.50-0.88m	1.55-0.94m	1.57-0.97m	-
	CH_2N	3.24-2.90m	3.17-2.98m	3.23-2.94m	3.28-2.87m	-
^{13}C	ipso C	-	142.6	142.6	142.6	143.1
	meta C	-	128.5	128.5	128.6	128.9
	ortho C	-	127.6	127.7	127.8	128.1
	para C	-	125.6	125.6	125.7	126.0
	CH	-	31.7	31.8	32.8	32.3
	Me	-	14.9	15.0	15.0	15.4
	SiMe	-	0.8	0.9	0.9	1.8,0.6
	CH_3	13.7	13.7	13.8	13.9	-
	$CH_3\underline{C}H_2$	19.9	19.9	20.0	20.0	-
	$\underline{C}H_2CH_2N$	24.4	24.4	24.5	24.5	-
	CH_2N	59.1 sbr	59.2 sbr	59.2 sbr	59.2 sbr	-
^{29}Si	SiMe	-	29.6	29.4	29.3	29.2

Quantities used:

silane	mmol	-	0.50	2.96	4.94	5.05
$^nBu_4NBr$	mmol	4.97	4.97	4.97	4.97	-
solvent		2.0 ml dichloromethane-d_2 with 10% TMS				

Table 6.7.7 N.M.R. titration study of tetrabutylammonium bromide ($^{n}Bu_4NBr$) against $PhCHMeSiMe_2Br$ and HMPA

N.M.R. assignments		$^{n}Bu_4NBr$	Ratio $^{n}Bu_4NBr$: $PhCHMeSiMe_2Br$: HMPA			$PhCHMeSiMe_2Br$	HMPA
δ(ppm)			1.0 : 0.1 : 0.1	1.0 : 0.5 : 0.5	1.0 : 1.0 : 1.0		
^{1}H	CH_3	0.73-0.54m sbr	0.73-0.52m sbr	0.63-0.44m br	0.54-0.45m br	-	-
	CH_2CH_2	1.50-0.88m br	1.48-0.88m br	1.48-0.85m br	1.48-0.77m br	-	-
	CH_2N	3.20-2.97m br	3.18-2.97m br	3.16-2.95m br	3.13-2.88m br	-	-
	Ph	-	6.99-6.70m	6.95-6.58m	6.76-6.55m br	7.49-7.13m	-
	$CH,^{3}J_{HH}$	-	obscured	obscured	obscured	2.61q,7.7Hz	-
	$Me,^{3}J_{HH}$	-	1.06d,7.7Hz	0.98d,7.7Hz	0.88d br,7.3Hz	1.59d,7.3Hz	-
	SiMe	-	0.04	-0.05	-0.12 sbr	0.57,0.59	-
	$PNMe,^{3}J_{PH}$	-	2.31d,10.3Hz	2.23d,10.3Hz	2.17d,10.3Hz	-	2.66d,9.3Hz
^{13}C	CH_3	13.7	13.7	13.8	13.8	-	-
	$CH_3\underline{C}H_2$	19.9	19.9	19.9	19.8	-	-
	$\underline{C}H_2CH_2N$	24.4	24.4	24.4	24.3 sbr	-	-
	CH_2N	59.1 sbr	59.1 sbr	59.0 sbr	58.9 sbr	-	-
	ipso C	-	142.2	142.3	142.4	143.1	-
	meta C	-	128.7	128.7	128.6	128.9	-
	ortho C	-	127.6	127.6	127.6	128.1	-
	para C	-	125.8	125.6	125.5	126.0	-
	CH	-	nr	29.9	29.6	32.3	-
	Me	-	nr	14.2	14.1	15.4	-
	SiMe	-	-2.0 sbr	-1.8	-1.9	1.8,0.6	-
	$PNMe,^{2}J_{PC}$	-	36.9d,5.2Hz	36.9d,5.2Hz	36.9d,5.2Hz	-	36.9d,3.9Hz
^{29}Si	SiMe	-	28.4 vbr	25.0 sbr	24.2 sbr	29.2	-
Quantities used:							
$^{n}Bu_4NBr$	mmol	5.01	5.01	5.01	5.01	-	-
$PhCHMeSiMe_2Br$	mmol	0.00	0.50	2.49	4.99	5.05	-
HMPA	mmol	0.00	0.49	2.46	4.99	-	2.20
solvent		2.0 ml dichloromethane-d_2					

Table 6.7.8

N.M.R. titration study of $PhCHMeSiMe_2Br$ against DMPU with the addition of tetrabutylammonium bromide ($^nBu_4NBr$)

Assignments		DMPU	$^nBu_4NBr$	Ratio PhCHMeSiMe$_2$Br : DMPU : $^nBu_4NBr$		
δ(ppm)				1.0:0.0:0.0	1.0:0.04:0.0	1:0.04:0.04
^1H	Ph	-	-	7.49-7.13m	7.45-7.19m	7.44-7.09m
	CH	-	-	2.61q	2.60q	2.57q
	$^3J_{HH}$	-	-	7.7Hz	7.7Hz	7.3Hz
	Me	-	-	1.59d	1.58d	1.54d
	$^3J_{HH}$	-	-	7.3Hz	7.7Hz	7.3Hz
	SiMe	-	-	0.59,0.57	0.56	0.53
	$C_{4,6}H$	3.25t	-	-	3.31t sbr	obscured
	$^2J_{HH}$	6.0Hz	-	-	5.86Hz	-
	N-CH_3	2.92	-	-	3.03	3.02
	C_5-H	1.98qn	-	-	obscured	obscured
	CH_3	-	0.73-0.54m	-	-	0.82-0.76m
	CH_2	-	1.50-0.88m	-	-	1.22-0.98m
	CH_2N	-	3.20-2.97m	-	-	3.55-3.20m br
^{13}C	ipsoC	-	-	143.1	143.1	143.0
	metaC	-	-	128.9	128.9	128.9
	orthoC	-	-	128.1	128.1	128.1
	paraC	-	-	126.0	126.0	126.0
	CH	-	-	32.3	32.3	32.3
	Me	-	-	15.4	15.4	15.4
	SiMe	-	-	1.8,0.6	1.6 br,0.7 br	1.2
	C=O	156.8	-	-	no	no
	N-CH_3	47.9	-	-	48.6	48.6
	$C_{4,6}$	35.6	-	-	37.1	37.3
	C_5	22.2	-	-	22.2	22.0
	CH_3	-	13.7	-	-	14.2
	CH_2	-	19.9	-	-	20.4
	CH_2	-	24.4	-	-	24.8
	CH_2N	-	59.1 sbr	-	-	59.6 br
^{29}Si	SiMe	-	-	29.2	29.2	29.2
Quantities used:						
silane	mmol	-	-	5.33	5.33	5.33
DMPU	mmol	2.20	-	0.00	0.19	0.19
$^nBu_4NBr$	mmol	-	5.01	0.00	0.00	0.18
solvent		1.2 ml dichloromethane-d_2				

Table 6.7.9

N.M.R. titration study of $PhCHMeSiMe_2Br$ against tetrabutylammonium bromide ($^nBu_4NBr$) with the addition of DMPU

Assignments		Ratio $PhCHMeSiMe_2Br$: $^nBu_4NBr$: DMPU			$^nBu_4NBr$	DMPU
δ(ppm)		1.0:0.0:0.0	1.0:0.03:0.0	1.0:0.03:0.03		
^1H	Ph	7.49-7.13m	7.44-7.12m	7.42-7.10m	-	-
	CH, $^3J_{HH}$	2.61q,7.7Hz	2.58q,7.3Hz	2.57q,7.7Hz	-	-
	Me, $^3J_{HH}$	1.59d,7.3Hz	1.56d,7.3Hz	1.55d,7.3Hz	-	-
	SiMe	0.59,0.57	0.55	0.54	-	-
	CH_3	-	0.84-0.77m	0.85-0.77m	0.74-0.54m	-
	CH_2CH_2	-	1.60-0.88m	1.23-1.02m	1.30-1.10m	-
	CH_2N	-	3.55-3.35m	3.40-3.28m	3.24-2.90m	-
	$C_{4,6}H$	-	-	obscured	-	3.25t
	$C_{3,5}H$	-	-	obscured	-	1.98qn
	$N-CH_3$	-	-	3.04	-	2.92
^{13}C	ipso C	143.1	143.1	143.0	-	-
	meta C	128.9	128.9	128.9	-	-
	ortho C	128.1	128.1	128.1	-	-
	para C	126.0	126.0	126.0	-	-
	CH	32.3	32.3	32.3	-	-
	Me	15.4	15.4	15.4	-	-
	SiMe	1.8,0.6	1.2	1.2	-	-
	CH_3	-	14.2	14.2	13.8	-
	$CH_3\underline{CH_2}$	-	20.5	20.5	20.2	-
	$CH_2\underline{CH_2}$	-	24.8	24.8	24.5	-
	CH_2N	-	59.6 br	59.6 sbr	59.5 sbr	-
	C=O	-	-	nr	-	156.8
	$N-CH_3$	-	-	48.6	-	47.9
	$C_{4,6}$	-	-	37.4	-	35.6
	C_5	-	-	21.9	-	22.2
^{29}Si	SiMe	29.2	29.2	29.2	-	-
Quantities used:						
silane	mmol	5.05	5.05	5.05	-	-
$^nBu_4NBr$	mmol	0.00	0.18	0.18	5.01	-
DMPU	mmol	0.00	0.00	0.18	-	2.20
solvent		1.2 ml dichloromethane-d_2				

Table 6.7.10

Proton n.m.r. titration study of $PhCHMeSiMe_2X$ (X=Cl, Br) against HMPA

Ratio	Assignments δ(ppm)				
Cl:Br:HMPA	Ph	$CH, {}^3J_{HH}$	$Me, {}^3J_{HH}$	SiMe	$PN(CH_3), {}^3J_{PH}$
1.0:0.0:0.0	7.33-7.10m	2.45q,7.3Hz	1.47d,7.3Hz	0.35,0.33	-
1.0:1.0:0.0	7.39-7.02m	2.58q,6.6Hz 2.51q,7.0Hz	1.56d,7.7Hz 1.55d,7.3Hz	0.56,0.54 0.42,0.40	-
1.0:1.0:0.1	7.35-7.06m	2.55q,6.6Hz 2.47q,7.3Hz	1.51d,7.7Hz	0.50 0.38,0.36	2.71d,10.6Hz
1.0:1.0:0.2	7.35-7.09m	obscured	1.46d,7.3Hz	0.45 sbr 0.34sbr	2.67d,10.6Hz
1.0:1.0:0.3	7.36-6.92m	obscured	1.42d,7.7Hz	0.40 sbr 0.31 sbr	2.63d,10.6Hz
1.0:1.0:0.4	7.19-6.85m	obscured	1.38d,7.7Hz	0.31 vbr	2.59d,10.3Hz
1.0:1.0:0.5	7.16-6.82m	obscured	1.34d,7.7Hz	0.27 vbr	2.56d,10.6Hz
1.0:1.0:0.6	7.18-6.90m	obscured	1.30d,7.3Hz	0.23 sbr	2.53d,10.3Hz
1.0:1.0:0.8	7.18-6.70m	obscured	1.23d,7.3Hz	0.16 sbr	2.46d,10.3Hz
1.0:1.0:1.0	7.18-6.70m	obscured	1.20d,7.7Hz	0.12	2.42d,10.3Hz
1.0:1.0:2.0	7.05-6.72m	obscured	1.12d,7.3Hz	0.04	2.32d,9.9Hz
1.0:1.0:3.0	6.90-6.73m	obscured	1.06d,7.7Hz	-0.06	2.25d,9.5Hz
1.0:1.0:4.0	6.97-6.55m	obscured	1.01d,7.7Hz	-0.06	2.19d,9.5Hz
1.0:1.0:5.0	6.95-6.48m	obscured	1.00d,7.3Hz	-1.06	2.14d,9.5Hz
HMPA	-	-	-	-	2.66d,9.3Hz

Quantities used:

$PhCHMeSiMe_2Cl$	0.59 ml, 2.984 mmoles
$PhCHMeSiMe_2Br$	0.60 ml, 2.986 mmoles
solvent	2.0 ml dichloromethane-d_2

Table 6.7.11 Carbon-13 and silicon-29 n.m.r. titration studies of $PhCHMeSiMe_2X$ (X=Cl, Br) against HMPA

Ratio SiCl : SiBr : HMPA	^{13}C n.m.r. assignments δ(ppm) ipso C	meta C	ortho C	para C	CH	Me	SiMe	$PNCH_3$, $^2J_{CP}$	^{29}Si n.m.r. SiMe
1.0 : 0.0 : 0.0	143.3	128.7	127.9	125.8	32.0	14.7	0.5,-0.4	-	30.7
1.0 : 1.0 : 0.0	143.3 143.1	128.5	128.0	125.9 126.0	32.1,32.3	14.9,15.3	0.6,-0.2 1.7,0.5	-	30.7,29.2
1.0 : 1.0 : 0.1	143.3 143.0	128.8	128.0	125.8 126.0	32.1	14.9,15.2	0.6,-0.3 0.8	37.3d,5.2Hz	30.6sbr 29.0br
1.0 : 1.0 : 0.2	143.2 142.9	128.8	128.0	125.8	32.0	14.9,15.1	0.6,-0.3 0.6sbr	37.3d,5.2Hz	30.6sbr 28.1vbr
1.0 : 1.0 : 0.3	143.2vbr	128.8	127.9	125.9sbr	31.9vbr	14.9sbr	0.5,-0.3 0.5br	37.3d,5.2Hz	30.6sbr 28.1vbr
1.0 : 1.0 : 0.4	143.0vbr	128.8	127.9	125.8	31.8vbr	14.8	0.5,-0.3 0.3vbr	37.2d,5.2Hz	30.6br 26.9vbr
1.0 : 1.0 : 0.5	142.9vbr	128.8	127.9	125.8	31.7vbr	14.8	0.5,-0.3 -0.3vbr	37.2d,5.2Hz	30.6br 27.0vbr
1.0 : 1.0 : 0.6	142.9vbr	128.8	127.9	125.8	31.5vbr	14.7	0.2vbr -0.4br	37.2d,5.2Hz	30.4br 25.9vbr
1.0 : 1.0 : 0.8	142.7br	128.7	127.8	125.8	31.1vbr	14.6	-0.7vbr	37.2d,5.2Hz	30.0vbr 26.5vbr
1.0 : 1.0 : 1.0	142.7	128.7	127.8	125.8	31.0	14.5	-0.8	37.1d,5.2Hz	27.7br
1.0 : 1.0 : 2.0	142.6	128.6	127.7	125.6	30.8	14.4	-0.9	36.9d,5.2Hz	27.6
1.0 : 1.0 : 3.0	142.6	128.6	127.6	125.6	30.7	14.4	-0.9	36.8d,3.9Hz	27.5
1.0 : 1.0 : 4.0	142.6	128.5	127.6	125.5	30.6	14.3	-1.0	36.8d,3.9Hz	27.5
1.0 : 1.0 : 5.0	142.6	128.5	127.6	125.4	30.6	14.3	-1.0	36.7d,3.9Hz	27.5
HMPA	-	-	-	-	-	-	-	36.9d,3.9Hz	-

Quantities used: $PhCHMeSiMe_2Cl$ 0.59 ml, 0.59g, 2.984 mmoles
$PhCHMeSiMe_2Br$ 0.60 ml, 0.73g, 2.986 mmoles
solvent 2.0 ml dichloromethane-d_2

Table 6.7.12 Proton n.m.r. titration study of $PhCHMeSiMe_2X$ (X=Cl, Br) against NMI

Ratio SiCl : SiBr : NMI	Ph	CH, $^3J_{HH}$	Me, $^3J_{HH}$	SiMe	δ(ppm) $C_2(H)=N$	C_4H, $^3J_{HH}$	C_5H, $^3J_{HH}$	$N-CH_3$
1.0 : 0.0 : 0.0	7.24-7.06m	2.41q,7.7Hz	1.44d,7.3Hz	0.31,0.29	-	-	-	-
1.0 : 1.3 : 0.0	7.22-7.05m	2.46q,7.3Hz 2.38q,6.6Hz	1.44d,7.7Hz	0.43,0.42 0.30,0.28	-	-	-	-
1.0 : 1.3 : 0.1	7.31-7.05m	2.48q,7.3Hz 2.40q,7.3Hz	1.43d,7.3Hz	0.44 0.30,0.28	10.20 vbr	5.16 vbr	obscured	4.06sbr
1.0 : 1.3 : 0.2	7.32-6.98m	2.50 vbr 2.40 br	1.43d,7.3Hz	0.46 0.30,0.28	10.24 vbr	7.57 vbr	obscured	4.10sbr
1.0 : 1.3 : 0.3	7.32-7.05m	2.50 vbr 2.40 br	1.42d,7.7Hz	0.48 sbr 0.30,0.28	10.30 vbr	7.68t vbr	obscured	4.11
1.0 : 1.3 : 0.4	7.32-7.05m	2.55 vbr 2.40q br	1.42d,7.7Hz	0.50,0.30	10.30 br	7.75t br	obscured	4.12
1.0 : 1.3 : 0.5	7.31-7.05m	2.60 vbr 2.40q vbr	1.41d sbr 7.7Hz	0.52,0.30	10.30 br	7.80t br	obscured	4.13
1.0 : 1.3 : 0.6	7.28-7.00m	2.80 vbr 2.40 vbr	1.40d sbr 7.3Hz	0.56 br 0.30 br	10.30 br	7.86t br 1.5Hz	7.32t br 1.5Hz	4.14
1.0 : 1.3 : 0.7	7.28-6.90m	2.83 vbr 2.40 vbr	1.40d sbr 7.7Hz	0.56 vbr 0.31 vbr	10.30 br	7.89 br	7.35t br 1.5Hz	4.15
1.0 : 1.3 : 0.8	7.28-7.00m	2.80 vbr 2.40 vbr	1.39d sbr 7.3Hz	0.49 vbr	10.30 br	7.92 br	7.38t br 1.5Hz	4.16
1.0 : 1.3 : 0.9	7.28-7.06m	2.75q vbr	1.38d,7.7Hz	0.47 sbr	10.09 br	7.87 br	7.39 br	4.12
1.0 : 1.3 : 1.2	7.23-7.06m	2.76q,7.3Hz	1.38d,7.7Hz	0.48	9.45 br	7.66 br	7.31 br	4.20
1.0 : 1.3 : 1.6	7.17-7.05m	2.78q,7.3Hz	1.37d,7.7Hz	0.49	9.08 br	7.52 br	7.25 br	3.91
NMI	-	-	-	-	7.41	7.00t,1.0Hz	6.90t,1.0Hz	3.68

Quantities used: $PhCHMeSiMe_2Cl$ 0.43 ml, 0.45g, 2.242 mmoles
$PhCHMeSiMe_2Br$ 0.50 ml, 0.70g, 2.859 mmoles
solvent 2.0 ml dichloromethane-d_2 with 10% TMS

Table 6.7.13 Carbon-13 and silicon-29 n.m.r. titration studies of $PhCHMeSiMe_2X$ (X=Cl, Br) against NMI

Ratio SiCl : SiBr : NMI	^{13}C n.m.r. assignments δ(ppm) C_i	C_m	C_o	C_p	CH	Me	SiMe	C_2	C_4	C_5	NCH_3	^{29}Si SiMe
1.0 : 0.0 : 0.0	143.2	128.6	127.8	125.6	31.9	14.5	0.3,-0.6	-	-	-	-	30.5
1.0 : 1.3 : 0.0	143.0 142.8	128.5	127.7	124.7 125.5	32.0 31.8	14.5 14.9	0.3,-0.6 1.3,0.3	-	-	-	-	30.5 29.0
1.0 : 1.3 : 0.1	142.9 142.6	128.5	127.7	125.5 125.6	31.8	14.5 14.9	0.3,-0.6 0.3vbr	140.5	124.0	122.5	36.4	30.5 28.9
1.0 : 1.3 : 0.2	142.9br 142.2br	128.5	127.6	125.5 125.6	31.7	14.5 14.8	0.2,-0.6 0.2 vbr	141.2br	124.5	123.1	36.4	30.6sbr 28.0vbr
1.0 : 1.3 : 0.3	142.9 142.1vbr	128.5	127.6	125.5 125.8	31.7	14.5	0.3,-0.6 obscured	141.3sbr	124.7	123.3	36.4	30.5 28.0vbr
1.0 : 1.3 : 0.4	142.9 142.1br	128.6	127.6	125.5 125.8	31.7 30.5vbr	14.5	0.3,-0.6 obscured	141.3	124.8	123.5	36.4	30.6 28.0vbr
1.0 : 1.3 : 0.5	142.9 142.0br	128.6	127.6	125.5 125.8	31.7 30.6vbr	14.5	0.3,-0.6 obscured	141.3	124.9	123.5	36.4	30.6 27.0vbr
1.0 : 1.3 : 0.6	143.0br 142.0br	128.6	127.6	125.7br	31.7sbr 29.5vbr	14.4	0.2,-0.6 -2.7vbr	141.4	125.0	123.7	36.4	30.6sbr 25.5vbr
1.0 : 1.3 : 0.7	142.5br 141.4br	128.6	127.6	125.8	31.6br 29.2vbr	14.4	0.0,-0.6 -3.3vbr	141.4	125.1	123.7	36.4	30.7br 25.2vbr
1.0 : 1.3 : 0.8	142.0vbr	128.6	127.5	125.7	31.4vbr 29.1vbr	14.3sbr	-0.6vbr -3.4vbr	141.3	125.1	123.8	36.4	30.8vbr 24.3vbr
1.0 : 1.3 : 0.9	142.1	128.6	127.5	125.7	29.9sbr	14.2	-2.2sbr	141.1sbr	124.8br	124.1	36.1	26.8br
1.0 : 1.3 : 1.2	142.1	128.7	127.6	125.8	29.8	14.2	-2.4	140.3sbr	125.4	123.7sbr	35.5	26.6sbr
1.0 : 1.3 : 1.6	142.1	128.7	127.6	125.8	29.7	14.2	-2.5	139.9sbr	126.1	123.1sbr	35.0	26.4sbr
NMI	-	-	-	-	-	-	-	137.8	129.5	120.1	33.2	-

Quantities used:
$PhCHMeSiMe_2Cl$ 0.43 ml, 0.45g, 2.242 mmoles
$PhCHMeSiMe_2Br$ 0.50 ml, 0.70g, 2.859 mmoles
solvent 2.0 ml dichloromethane-d_2 with 10% TMS

Table 6.7.14 Proton n.m.r. titration study of chloromethylphenylsilane (PhMeHSiCl) against NMI

Ratio PhMeHSiCl : NMI	Proton n.m.r. assignments δ(ppm) Ph	SiH, $^3J_{HH}$	SiMe, $^3J_{HH}$	$C_2(H)=N$	C_4H, $^3J_{HH}$	$C_4=C_5(H)$	$^3J_{HH}$	$N-CH_3$
1.0 : 0.0	7.78-7.42m	5.38q,3.4Hz	0.82d,3.3Hz	-	-	-	-	-
1.0 : 0.2	7.79-7.32m	5.33q,3.2Hz	0.77d,3.2Hz	9.06 br	7.27 br	6.95t br	1.5Hz	3.94
1.0 : 0.5	7.60-7.26m	5.30q,2.9Hz	0.69d,2.9Hz	8.21 br	7.02t br	6.79t br	1.5Hz	3.76
1.0 : 0.7	7.55-7.20m	5.27q,2.9Hz	0.63d,2.7Hz	8.27 br	6.95 br	6.78 br	-	3.70
1.0 : 0.9	7.43-7.12m	5.24q,2.7Hz	0.57d,2.4Hz	8.11 br	6.90t br, 1.5Hz	6.68t br	1.5Hz	3.62
1.0 : 1.1	7.43-7.12m	5.24q,2.4Hz	0.56d,2.7Hz	8.10 vbr	6.89 br	6.68 br	-	3.62
1.0 : 1.4	7.28-6.97m	5.18q,2.5Hz	0.45d,2.2Hz	7.94 br	6.81t br, 1.5Hz	6.56t br	1.5Hz	3.50
1.0 : 1.6	7.21-6.97m	5.13q,2.4Hz	0.38d,2.2Hz	7.73 br	6.75 br	6.45 br	-	3.43
1.0 : 1.8	7.47-6.85m	5.09 vbr	0.30 vbr	7.63 vbr	6.66 br	6.40 br	-	3.35 sbr
1.0 : 2.1	7.00-6.78m	5.04 vbr	0.27 vbr	7.57 vbr	6.59 vbr	6.37 vbr	-	3.27 sbr
1.0 : 2.2	7.10-6.76m	5.01 vbr	0.24 vbr	7.49 vbr	6.54 br	6.35 br	-	3.23 sbr
1.0 : 3.3	6.92-6.59m	4.88q br, 2.2Hz	0.12d,1.8Hz	7.19 vbr	6.37 br	6.25 br	-	3.06
1.0 : 3.7	6.99-6.58m	4.82 br	0.08 vbr	7.09 vbr	6.31 br	6.21 br	-	2.99
1.0 : 4.6	6.78-6.48m	4.72 vbr	-0.02d br, 1.8Hz	6.93 vbr	6.19 br	6.12 br	-	2.87
NMI	-	-	-	7.41	7.01t,1.0Hz	6.90t	1.0Hz	3.68

Quantities used: PhMeHSiCl 0.35 ml, 0.37g, 2.35 mmoles
solvent 2.0 ml chloroform-d_1

Table 6.7.15 Carbon-13 and silicon-29 n.m.r. titration studies of chloromethylphenylsilane (PhMeHSiCl) against NMI

Ratio PhMeHSiCl : NMI	^{13}C n.m.r. assignments δ(ppm) ipso C	ortho C	para C	meta C	SiMe	C_2	C_4	C_5	N-CH_3	^{29}Si n.m.r. SiMe
1.0 : 0.0	134.2	133.6	130.9	128.7	0.1	-	-	-	-	5.2
1.0 : 0.2	nr	nr	nr	nr	nr	nr	nr	nr	nr	-1.9 sbr
1.0 : 0.5	134.6	133.6	130.9	128.6	0.7	138.0	125.5	122.5	35.3	-14.0 sbr
1.0 : 0.7	135.1	133.4	130.9	128.6	1.0	137.9	125.6	122.3	35.2	-24.3 sbr
1.0 : 0.9	135.0	133.1	130.3	128.5	1.3	137.9	125.6	122.2	35.1	-39.2 sbr
1.0 : 1.1	134.9	132.9	130.1	128.5	1.4	137.9	125.6	122.1	35.0	-51.7 br
1.0 : 1.4	134.9	132.6	129.7	128.5	1.6	137.8	125.5	122.1	35.0	-60.2 sbr
1.0 : 1.6	obscured	132.5	129.5	128.3	1.8	137.5	125.6	122.0	34.8	-69.5 sbr
1.0 : 1.8	134.8	132.3	129.5	128.3	1.9	137.5	125.8	121.9	34.6	-75.4 sbr
1.0 : 2.1	134.7	132.2	129.1	128.2	2.0	137.6	126.0	121.7	34.5	-80.3
1.0 : 2.2	134.7	132.1	129.0	128.8	2.0	137.5	126.2	121.6	34.4	-81.6
1.0 : 2.7	134.8	128.9	125.1	125.8	-1.1	134.4	123.5	118.2	31.0	-85.5
1.0 : 3.3	134.5	132.0	128.8	128.0	2.0	137.5	126.8	121.1	33.9	-83.2
1.0 : 3.7	134.5	131.9	128.7	128.0	1.9	137.5	127.0	120.9	33.7	-83.4
1.0 : 4.6	134.4	131.8	128.6	127.9	1.8	137.4	127.2	120.6	33.4	-83.7
NMI	-	-	-	-	-	137.8	129.4	120.1	33.2	-

Quantities used: PhMeHSiCl 0.35 ml, 0.37g, 2.35 mmoles
solvent 2.0 ml chloroform-d_1

Table 6.7.16 N.M.R. titration study of chloromethylphenylsilane (PhMeHSiCl) against HMPA

Assignments		Ratio of PhMeHSiCl to HMPA								HMPA
	δ(ppm)	1.0 : 0.0	1.0 : 0.2	1.0 : 0.5	1.0 : 0.7	1.0 : 1.0	1.0 : 1.4	1.0 : 2.0	1.0 : 5.0	
^1H	Ph	7.66-7.33m	7.60-7.20m	7.55-7.20m	7.44-7.03m br	7.43-7.10m sbr	7.24-6.92m	7.25-6.77m	6.60-6.18m vbr	-
	SiH	5.29q	5.24q	5.25q	5.08q br	5.06q sbr	4.88q	4.74q	4.18 vbr	-
	$^3J_{HH}$	3.3Hz	3.2Hz	3.2Hz	3.2Hz	3.2Hz	3.2Hz	3.2Hz	-	-
	SiMe	0.72d	0.68d	0.61d	0.53d br	0.51d	0.34d	0.20d	-0.31 vbr	-
	$^3J_{HH}$	3.3Hz	3.2Hz	3.2Hz	2.9Hz	3.2Hz	2.9Hz	2.9Hz	-	-
	$PN(CH_3)$	-	2.64d	2.53d	2.44d	2.42d	2.24d	2.10d	1.56d	2.66d
	$^3J_{PH}$	-	10.3Hz	9.8Hz	9.8Hz	9.8Hz	9.5Hz	9.5Hz	9.3Hz	9.3Hz
^{13}C	ortho C	133.6	133.3	133.2	133.0	133.0	132.6	132.4	131.1	-
	para C	130.9	130.9	130.7	130.6	130.5	130.2	129.9	128.6	-
	meta C	128.2	128.1	127.9	127.8	127.8	127.5	127.2	126.0	-
	SiMe	0.1	-0.5	-0.6	-0.7	-0.7	-1.1	-1.3	-2.1	-
	$PN(CH_3)$	-	36.7d	36.4d	36.3d	36.3d	35.9d	35.6d	34.5d	36.9d
	$^2J_{PC}$	-	3.9Hz	3.9Hz	3.9Hz	3.9Hz	3.9Hz	3.9Hz	3.9Hz	3.9Hz
^{29}Si	SiMe	5.3	5.0	4.8	4.5	4.5	3.4	2.4	-2.9	-
Quantities used:										
silane	mmol	2.33	2.33	2.33	2.33	2.33	2.33	2.33	2.33	-
HMPA	mmol	0.00	0.55	1.10	1.67	2.22	3.32	4.42	11.57	2.20
solvent		2.0 ml chloroform-d_1								

External reference was used for proton and Si-29 spectra, the carbon spectra were referenced to the chloroform-d_1 peaks. The ipso C signal was obscured.

Table 6.7.17 N.M.R. titration study of chloromethylphenylsilane (PhMeHSiCl) against N,N-dimethylformamide (DMF)

Assignments		Ratio of PhMeHSiCl to DMF									DMF
	δ(ppm)	1.0 : 0.0	1.0 : 0.4	1.0 : 0.8	1.0 : 1.3	1.0 : 1.7	1.0 : 2.0	1.0 : 2.5	1.0 : 3.3	1.0 : 4.0	
^{1}H	Ph	7.70-7.28m	7.68-7.30m	7.68-7.30m	7.68-7.30m	7.68-7.30m	7.68-7.30m	7.66-7.30m	7.68-7.30m	7.68-7.30m	-
	SiH	5.30q	5.29q	5.28q	5.29q	5.28q	5.28q	5.28q	5.28q	5.28q	-
	$^{3}J_{HH}$	2.9Hz	3.3Hz	2.9Hz	3.3Hz	2.9Hz	3.3Hz	2.9Hz	2.9Hz	2.9Hz	-
	SiMe	0.72d	0.75vbr	0.75d	0.75d	0.75d	0.75d	0.75d	0.75d	0.75d	-
	$^{3}J_{HH}$	3.3Hz	3.3Hz	3.3Hz	3.3Hz	3.3Hz	3.3Hz	2.9Hz	2.9Hz	3.3Hz	-
	H-C=O	-	7.98br	7.98br	8.00br	7.99br	7.99br	7.99br	7.99br	7.98br	8.01
	NMe_A	-	2.83	2.83	2.83	2.83	2.83	2.83	2.83	2.82	2.87
	NMe_B	-	2.86	2.88	2.89	2.90	2.90	2.91	2.92	2.92	2.94
	A-B	-	7.8Hz	2.9Hz	4.4Hz	5.1Hz	5.9Hz	7.0Hz	7.7Hz	8.4Hz	7.8Hz
^{13}C	ortho C	133.6	133.6	133.6	133.7	133.6	133.6	133.6	133.6	133.6	-
	para C	130.9	130.9	130.9	130.9	130.9	130.9	130.9	130.9	130.9	-
	meta C	128.3	128.2	128.2	128.3	128.3	128.3	128.3	128.3	128.3	-
	SiMe	0.2	0.0	0.1	0.0	0.1	0.0	0.0	0.0	0.0	-
	C=O	-	162.4	162.5	162.5	162.4	162.4	162.4	162.4	162.3	162.4
	NMe_A	-	31.3sbr	31.3	31.3	31.3	31.3	31.3	31.2	31.2	31.3
	NMe_B	-	36.3sbr	36.4	36.4	36.4	36.4	36.4	36.4	36.4	36.4
	A-B	-	113.9Hz	113.9Hz	113.9Hz	113.9Hz	113.9Hz	115.2Hz	116.5Hz	115.2Hz	115.0Hz
^{29}Si	SiMe	3.0	3.1	1.4vbr	2.2vbr	2.1vbr	1.2vbr	1.5vbr	1.1vbr	1.4vbr	-
Quantities used:											
silane	mmol	2.63	2.63	2.63	2.63	2.63	2.63	2.63	2.63	2.63	-
DMF	mmol	0.00	1.06	2.19	3.37	4.39	5.39	6.47	8.71	10.51	2.20
solvent		2.0 ml chloroform-d_1									

The ipso C signal was obscured.

Table 6.7.18 Proton n.m.r. titration study of PhMeHSiCl against DMF in the presence of 2,6DBP

Ratio PhMeHSiCl : 2,6DBP : DMF	Proton n.m.r. assignments δ(ppm) Ph	$SiH, {}^3J_{HH}$	$SiMe, {}^3J_{HH}$	H-C=O	$NMe_{A,B}$	A-B	$C_{3,5}$-H	C_4-H	^tBu
1.0 : 0.0 : 0.0	7.88-7.21m	5.29q,3.3Hz	0.73d,3.3Hz	-	-	-	-	-	-
1.0 : 1.1 : 0.0	7.67-7.32m	5.30q,3.9Hz	0.70d,3.3Hz	-	-	-	obscured	7.04d,7.7Hz 7.03d,8.1Hz	1.35
1.0 : 1.1 : 0.1	7.67-7.30m	5.29q,2.9Hz	0.71d br 3.3Hz	nr	2.80	-	obscured	7.05d,7.7Hz nr	1.35
1.0 : 1.1 : 0.2	7.67-7.30m	5.29q,2.9Hz	0.71d vbr 3.3Hz	7.93 sbr	2.80	-	obscured	7.05d,7.3Hz	1.35
1.0 : 1.1 : 0.4	7.67-7.28m	5.29q,3.3Hz	0.71d vbr 2.6Hz	7.94 sbr	2.80 sbr	-	obscured	7.05d,7.3Hz	1.35
1.0 : 1.1 : 0.6	7.67-7.33m	5.29q,3.3Hz	0.72d sbr 2.9Hz	7.95 sbr	2.81,2.82	1.1Hz	obscured	7.05d,7.7Hz	1.35
1.0 : 1.1 : 0.8	7.67-7.32m	5.29q,3.3Hz	0.72d sbr 2.9Hz	7.95 sbr	2.81,2.83	2.2Hz	obscured	7.05d,7.7Hz	1.35
1.0 : 1.1 : 1.0	7.67-7.31m	5.28q,3.3Hz	0.72d sbr 3.3Hz	7.96 sbr	2.81,2.84	2.6Hz	obscured	7.05d,7.3Hz	1.35
1.0 : 1.1 : 1.2	7.67-7.34m	5.29q,3.3Hz	0.72d,3.3Hz	7.96 sbr	2.81,2.84	2.9Hz	obscured	7.05d,7.3Hz	1.35
1.0 : 1.1 : 1.6	7.67-7.30m	5.29q,2.9Hz	0.72d,2.9Hz	7.95 sbr	2.81,2.85	3.7Hz	obscured	7.05d,7.7Hz	1.34
1.0 : 1.1 : 2.0	7.65-7.33m	5.29q,2.9Hz	0.73d,3.3Hz	7.96 sbr	2.81,2.86	4.4Hz	obscured	7.06d,7.7Hz	1.35
1.0 : 1.1 : 3.0	7.65-7.34m	5.29q,2.9Hz	0.73d,2.9Hz	7.97 sbr	2.81,2.88	5.9Hz	obscured	7.06d,7.7Hz	1.34
1.0 : 1.1 : 4.0	7.66-7.33m	5.29q,3.3Hz	0.73d,2.9Hz	7.97 sbr	2.81,2.88	6.6Hz	obscured	7.07d,7.3Hz	1.34
1.0 : 1.1 : 5.0	7.65-7.33m	5.28q,2.9Hz	0.73d,3.3Hz	7.97 sbr	2.81,2.89	7.7Hz	obscured	7.08d,7.7Hz	1.34
DMF	-	-	-	8.01	2.87,2.94	7.8Hz	-	-	-

Quantities used: PhMeHSiCl 0.38 ml, 2.558 mmoles
2,6DBP 0.60 ml, 2.697 mmoles
solvent 2.0 ml chloroform-d_1 with 5% TMS

Table 6.7.19 Carbon-13 and silicon-29 n.m.r. titration studies of PhMeHSiCl against DMF in the presence of 2,6DBP

Ratio PhMeHSiCl : 2,6DBP : DMF	Carbon-13 n.m.r. assignments δ(ppm) C_o	C_p	C_m	SiMe	$C_{2,6}$	C_4	$C_{3,5}$	$\underline{C}Me_3$	^tBu	C=O	$NMe_{A,B}$	A-B	Si-29 SiMe
1.0 : 0.0 : 0.0	133.6	130.9	128.2	0.1	-	-	-	-	-	-	-	-	3.1
1.0 : 1.1 : 0.0	133.6	130.8	128.2	0.1	167.5	135.9	115.2	37.6	30.2	-	-	-	3.0
1.0 : 1.1 : 0.1	133.6	130.8	128.2	0.1	167.4	135.9	115.1	37.5	30.1	nr	nr,36.1	nr	3.0 sbr
1.0 : 1.1 : 0.2	133.6	130.9	128.2	0.2	167.4	136.0	115.2	37.6	30.2	162.3	31.3,36.2	111.3Hz	3.0 sbr
1.0 : 1.1 : 0.3	133.6	130.9	128.2	0.1	167.4	136.0	115.2	37.6	30.2	162.3	31.0,36.2	112.6Hz	3.0 sbr
1.0 : 1.1 : 0.4	133.6	130.8	128.2	0.1	167.3	135.9	115.2	37.5	30.1	162.3	31.2,36.2	112.6Hz	3.0 sbr
1.0 : 1.1 : 0.6	133.6	130.9	128.2	0.1	167.4	136.0	115.2	37.6	30.2	162.3	31.2,36.2	112.6Hz	3.0 vbr
1.0 : 1.1 : 0.8	133.6	130.9	128.2	0.1	167.4	136.0	115.2	37.6	30.2	162.3	31.3,36.2	112.6Hz	3.0 vbr
1.0 : 1.1 : 1.0	133.6	130.9	128.3	0.1	167.3	136.0	115.2	37.6	30.2	162.3	31.3,36.2	112.6Hz	2.7 vbr
1.0 : 1.1 : 1.2	133.6	130.9	128.2	0.1	167.3	136.0	115.2	37.5	30.1	162.3	31.2,36.2	113.9Hz	2.7 sbr
1.0 : 1.1 : 1.6	133.6	130.9	128.2	0.1	167.3	136.0	115.2	37.5	30.1	162.3	31.2,36.2	112.6Hz	2.7 sbr
1.0 : 1.1 : 2.0	133.6	130.9	128.3	0.1	167.3	136.1	115.3	37.6	30.2	162.3	31.2,36.2	113.9Hz	2.7 sbr
1.0 : 1.1 : 3.0	133.6	130.9	128.3	0.1	167.3	136.1	115.3	37.5	30.2	162.3	31.1,36.2	113.9Hz	2.6 sbr
1.0 : 1.1 : 4.0	133.6	130.9	128.3	0.1	167.2	136.1	115.3	37.5	30.1	162.3	31.1,36.2	115.2Hz	2.5 sbr
1.0 : 1.1 : 5.0	133.6	131.0	128.3	0.0	167.2	136.3	115.4	37.5	30.2	162.3	31.1,36.2	115.2Hz	2.6 sbr
DMF	-	-	-	-	-	-	-	-	-	162.4	31.3,36.4	115.0Hz	-

Quantities used: PhMeHSiCl 0.38 ml, 2.558 mmoles
2,6DBP 0.60 ml, 2.697 mmoles
solvent 2.0 ml chloroform-d_1 with 5% TMS

The ipso C peak was not observed throughout the titration.

Table 6.7.20 N.M.R. titration study of chlorodimethylphenylsilane ($PhMe_2SiCl$) against N,N-dimethylformamide (DMF)

N.M.R. assignments		Ratio of $PhMe_2SiCl$ to DMF						DMF
	δ(ppm)	1.0 : 0.0	1.0 : 0.3	1.0 : 0.5	1.0 : 0.8	1.0 : 2.1	1.0 : 2.6	
^1H	Ph	7.59-7.30m	7.65-7.31m	7.65-7.35m	7.59-7.31m	7.58-7.30m	7.59-7.32m	-
	SiMe	0.59	0.63	0.63	0.63	0.64	0.64	-
	H-C=O	-	7.91 br	7.91 br	7.92 br	7.92 br	7.93 br	8.01
	$NMe_{A,B}$	-	2.75	2.76,2.77	2.76d,0.5Hz 2.78	2.77d,0.7Hz 2.81	2.77,2.81	2.87,2.94
	A-B	-	-	0.7Hz	2.7Hz	3.3Hz	3.7Hz	7.8Hz
^{13}C	ipso C	nr	136.1	136.1	136.0	nr	nr	-
	ortho C	133.0	133.0	133.0	133.0	nr	nr	-
	para C	130.3	130.3	130.3	130.3	nr	nr	-
	meta C	128.0	128.0	128.1	128.0	nr	nr	-
	SiMe	2.1	2.0	2.0	2.0	nr	nr	-
	C=O	-	162.3	162.3	162.2	nr	nr	162.4
	$NMe_{A,B}$	-	31.2,36.2	31.1,36.2	31.1,36.1	nr	nr	31.3,36.4
	A-B	-	112.6Hz	113.9Hz	113.9Hz	nr	nr	115.0Hz
Quantities used:								
$PhMe_2SiCl$	mmoles	7.13	7.13	7.13	7.13	7.13	7.13	-
DMF	mmoles	0.00	1.93	3.68	5.53	15.06	18.76	2.20
solvent		2.0 ml chloroform-d_1 with 5% TMS						

Table 6.7.21 Carbon-13 n.m.r. titration study of $PhMe_2SiCl$ against DMF in the presence of 2,6DBP

Ratio $PhMe_2SiCl$: 2,6DBP : DMF	Carbon-13 n.m.r. assignments δ(ppm)												
	C_o	C_p	C_m	SiMe	$C_{2,6}$	C_4	$C_{3,5}$	^tBu	$\underline{C}Me_3$	C=O	$NMe_{A,B}$	A-B
1.0 : 0.0 : 0.0	133.0	130.3	128.0	2.1	-	-	-	-	-	-	-	-
1.0 : 1.1 : 0.0	133.0	130.3	128.0	2.1	167.5	136.0	115.2	37.6	30.2	-	-	-
1.0 : 1.1 : 0.1	133.0	130.3	128.0	2.1	167.4	135.9	115.2	37.6	30.2	162.2	nr,36.1	nr
1.0 : 1.1 : 0.2	133.0	130.3	128.1	2.1	167.5	136.0	115.2	37.6	30.2	162.3	31.3,36.2	111.3Hz
1.0 : 1.1 : 0.3	133.0	130.3	128.0	2.1	167.4	136.0	115.2	37.6	30.2	162.3	31.2,36.2	112.6Hz
1.0 : 1.1 : 0.4	133.0	130.3	128.0	2.1	167.4	136.0	115.2	37.6	30.2	162.3	31.2,36.2	112.6Hz
1.0 : 1.1 : 0.5	133.0	130.3	128.1	2.1	167.4	136.0	115.2	37.6	30.2	162.3	31.2,36.2	112.6Hz
1.0 : 1.1 : 0.6	133.0	130.3	128.0	2.1	167.4	136.0	115.2	37.6	30.2	162.3	31.2,36.2	112.6Hz
1.0 : 1.1 : 0.7	133.0	130.3	128.0	2.0	167.3	136.0	115.2	37.5	30.2	162.3	31.2,36.2	112.6Hz
1.0 : 1.1 : 0.8	133.0	130.3	128.1	2.1	167.4	136.0	115.2	37.6	30.2	162.3	31.2,36.2	112.6Hz
1.0 : 1.1 : 0.9	133.0	130.3	128.0	2.1	167.3	136.0	115.2	37.6	30.2	162.3	31.2,36.2	112.6Hz
1.0 : 1.1 : 1.0	133.0	130.3	128.0	2.0	167.3	136.1	115.2	37.5	30.2	162.2	31.1,36.2	113.9Hz
1.0 : 1.1 : 1.1	133.0	130.3	128.1	2.1	167.3	136.1	115.3	37.6	30.2	162.3	31.2,36.2	112.6Hz
1.0 : 1.1 : 1.2	133.0	130.3	128.0	2.1	167.3	136.1	115.3	37.6	30.2	162.3	31.2,36.2	112.6Hz
1.0 : 1.1 : 1.3	133.0	130.3	128.0	2.0	167.3	136.1	115.3	37.5	30.2	162.2	31.1,36.2	113.9Hz
1.0 : 1.1 : 1.4	133.0	130.3	128.0	2.0	167.3	136.1	115.3	37.5	30.1	162.2	31.1,36.1	112.6Hz
1.0 : 1.1 : 1.6	133.0	130.3	128.0	2.0	167.3	136.2	115.3	37.5	30.2	162.2	31.1,36.2	113.9Hz
1.0 : 1.1 : 4.8	133.0	130.4	128.1	2.0	167.2	136.9	115.8	37.5	30.1	162.2	31.0,36.1	115.2Hz
DMF	-	-	-	-	-	-	-	-	-	162.4	31.3,36.4	115.0Hz

Quantities used: $PhMe_2SiCl$ 0.42 ml, 2.519 mmoles
2,6DBP 0.61 ml, 2.717 mmoles
solvent 2.0 ml chloroform-d_1 with 5% TMS

The ipso C signal was obscured which made assignment difficult.

Table 6.7.22 Proton and silicon-29 n.m.r. titration studies of $PhMe_2SiCl$ against DMF in the presence of 2,6DBP

Ratio $PhMe_2SiCl$: 2,6DBP : DMF	Proton n.m.r. assignments δ(ppm) Ph	SiMe	$C_{3,5}$-H	C_4-H	^tBu	H-C=O	$NMe_{A,B}$	A-B	Si-29 n.m.r. SiMe
1.0 : 0.0 : 0.0	7.63-7.26m	0.59	-	-	-	-	-	-	20.2
1.0 : 1.1 : 0.0	7.66-7.31m	0.64	obscured	7.04d,7.7Hz	1.35	-	-	-	20.1
1.0 : 1.1 : 0.1	7.66-7.31m	0.64	obscured	7.04d,7.7Hz	1.35	7.96	2.79	-	20.1
1.0 : 1.1 : 0.2	7.66-7.31m	0.64	obscured	7.05d,7.7Hz	1.35	7.93	2.80	-	nr
1.0 : 1.1 : 0.3	7.66-7.31m	0.65	obscured	7.05d,7.7Hz	1.35	7.94 sbr	2.80	-	nr
1.0 : 1.1 : 0.4	7.66-7.31m	0.65	obscured	7.05d,7.7Hz	1.35	7.93 sbr	2.80	-	nr
1.0 : 1.1 : 0.5	7.66-7.31m	0.64	obscured	7.05d,7.7Hz	1.35	7.94 sbr	2.80	-	20.2
1.0 : 1.1 : 0.6	7.66-7.34m	0.65	obscured	7.05d,7.7Hz	1.35	7.94 sbr	2.81	-	20.2
1.0 : 1.1 : 0.7	7.66-7.32m	0.65	obscured	7.05d,7.7Hz	1.35	7.94 sbr	2.80,2.81	0.7Hz	nr
1.0 : 1.1 : 0.8	7.66-7.31m	0.64	obscured	7.05d,7.7Hz	1.34	7.94 sbr	2.80,2.81	1.1Hz	nr
1.0 : 1.1 : 0.9	7.66-7.32m	0.65	obscured	7.05d,7.7Hz	1.35	7.94 sbr	2.80d,0.7Hz / 2.82	1.8Hz	nr
1.0 : 1.1 : 1.0	7.66-7.32m	0.65	obscured	7.05d,7.7Hz	1.35	7.94 sbr	2.80,2.82	1.8Hz	20.2
1.0 : 1.1 : 1.1	7.63-7.31m	0.64	obscured	7.05d,7.7Hz	1.35	7.94 br	2.80d,0.7Hz / 2.82	2.2Hz	nr
1.0 : 1.1 : 1.2	7.66-7.31m	0.65	obscured	7.06d,7.7Hz	1.35	7.94 br	2.80,2.83	2.2Hz	nr
1.0 : 1.1 : 1.3	7.66-7.31m	0.65	obscured	7.06d,7.7Hz	1.35	7.94 br	2.80,2.83	2.6Hz	20.2
1.0 : 1.1 : 1.4	7.66-7.32m	0.65	obscured	7.06d,7.7Hz	1.35	7.94 br	2.80,2.83	2.6Hz	nr
1.0 : 1.1 : 1.6	7.66-7.31m	0.65	obscured	7.07d,7.7Hz	1.35	7.95 sbr	2.80,2.83	3.3Hz	nr
1.0 : 1.1 : 1.8	7.66-7.32m	0.65	obscured	7.07d,7.7Hz	1.35	7.95 sbr	2.80,2.84	3.3Hz	nr
1.0 : 1.1 : 2.0	7.63-7.33m	0.65	obscured	7.07d,7.7Hz	1.35	7.95 sbr	2.80d,0.7Hz / 2.85	4.0Hz	nr
1.0 : 1.1 : 2.2	7.61-7.32m	0.65	obscured	7.07d,7.7Hz	1.35	7.95 sbr	2.80,2.85	4.0Hz	nr
1.0 : 1.1 : 2.7	7.65-7.35m	0.65	obscured	7.08d,7.7Hz	1.35	7.95 sbr	2.81,2.86	4.8Hz	nr
1.0 : 1.1 : 3.2	7.67-7.33m	0.65	obscured	7.10d,7.7Hz	1.36	7.96 sbr	2.81,2.87	5.5Hz	20.4
1.0 : 1.1 : 4.8	7.67-7.31m	0.66	obscured	7.12d,7.7Hz	1.36	7.96 sbr	2.80,2.88	7.7Hz	20.5
DMF	-	-	-	-	-	8.01 sbr	2.87,2.94	7.8Hz	-

Quantities used: $PhMe_2SiCl$ 0.42 ml, 2.519 mmoles
2,6DBP 0.61 ml, 2.717 mmoles
solvent 2.0 ml chloroform-d_1 with 5% TMS

Table 6.7.23

Proton and oxygen-17 n.m.r. titration studies of $PhMe_2SiCl$ against DMF in the presence of 2,6DBP

Ratio $PhMe_2SiCl$: 2,6DBP : DMF	^1H n.m.r. δ(ppm) $NMe_{A,B}$	A-B	Oxygen-17 n.m.r. δ(ppm) C=O
0.0 : 1.1 : 0.4	nr	nr	312.7
1.0 : 1.1 : 0.4	2.80	-	315.1
1.0 : 1.1 : 0.6	2.81	-	313.5
1.0 : 1.1 : 0.9	2.80,2.81	1.1Hz	313.5
1.0 : 1.1 : 1.1	$\overset{2.80d,0.7Hz}{2.82}$	2.2Hz	313.5
1.0 : 1.1 : 1.5	$\overset{2.80d,0.7Hz}{2.83}$	2.6Hz	313.5
1.0 : 1.1 : 2.1	2.80,2.84	3.7Hz	314.3
1.0 : 1.1 : 3.2	2.80,2.86	5.5Hz	314.3
1.0 : 1.1 : 4.2	$\overset{2.80d,0.7Hz}{2.87}$	6.2Hz	315.1
1.0 : 1.1 : 6.4	2.80,2.89	8.1Hz	316.7
1.0 : 1.1 : 8.5	2.80,2.90	9.2Hz	317.5
DMF	2.87,2.94	7.8Hz	310.2

Quantities used: $PhMe_2SiCl$ 0.41 ml, 2.450 mmoles

2,6DBP 0.60 ml, 2.678 mmoles

solvent 2.0 ml chloroform-d_1 with 5% TMS

Chapter 7 References

[1] W.P. Weber
"Silicon Reagents for Organic Synthesis", Springer-Verlag, Berlin, 1983.

[2] C.A. Pierce
"Silylation of Organic Compounds", Pierce, Rockford, Illinois, 1968.

[3] I. Fleming
"Comprehensive Organic Chemistry", Pergamon, Oxford, 1979, vol. 3, part 13.

[4] D.J. Ager and I. Fleming
J. Chem. Res. (S), 1977, 6-7.

[5] D.Y. Sogah and W.B. Farnham
"Group Transfer Polymerization Mechanistic Studies" in "Organosilicon and Bioorganosilicon Chemistry: Structure, Bonding, Reactivity and Synthetic Application", edited by H. Sakurai, Ellis Horwood Ltd., Chichester, UK, 1985, 219-230.

[6] E.W. Colvin
"Silicon in Organic Synthesis", Butterworths, London, 1981.

[7] S.K. Chaudhary and O. Hernandez
Tet. Lett., 1979, vol. 2, 99-102.

[8] R.J.P. Corriu, G. Dabosi and M. Martineau
J. Organomet. Chem., 1980, vol. 186, 25-37.

[9] J. Chojnowski, M. Cypryk and J. Michalski
J. Organomet. Chem., 1978, vol. 161, C31-C35.

[10] T.R. Forbus Jr. and J.C. Martin
J. Am. Chem. Soc., 1979, vol. 101, number 17, 5057-5059.

[11] J.C. Martin
Science, 1983, vol. 221, number 4610, 509-514.

[12] R.R. Holmes, R.O. Day, J.J. Harland, A.C. Sau and J.M. Holmes
Organometallics, 1984, vol. 3, number 3, 341-353.

[13] E.A.V. Ebsworth
"Physical Basis of the Chemistry of the Group IV Elements" in "Organometallic Compounds of the Group IV Elements", vol. 1, part 1, edited by A.G. MacDiarmid, Marcel Dekker, New York, 1968.

[14] D.A. Armitage
"Comprehensive Organometallic Chemistry", edited by G. Wilkinson, F.G.A. Stone and E.W. Abel, Pergamon, Oxford, 1982.

[15] L.H. Sommer
Intra-Science Chemistry Reports, 1973, vol. 7, number 4.

[16] C.G. Pitt
J. Organomet. Chem., 1973, vol. 61, 49-70 and references cited therein.

[17] T. Veszpremi and J. Nagy
J. Organomet. Chem., 1983, vol. 255, 41-47.

[18] R. Ponec
"Theoretical Aspects of Bonding in Organosilicon Chemistry" in "Carbon-Functional Organosilicon Compounds", edited by V. Chvalovsky and J.M. Bellama, Plenum Press, New York, 1984, 233-298.

[19] P.J. Kanyha and W.S. Brey
Proc: Magnetic Resonance Related Phenomena, 22nd Congress, Zurich, September 1984, 341-342.

[20] C.G. Pitt
J. Organomet. Chem., 1970, vol. 23, C35-C37.

[21] A.G. MacDiarmid
Intra-Science Chemical Reports, 1973, vol. 7, number 4, 83-95.

[22] K. Hensen, T. Zengerly, P. Pickel and G. Klebe
Angew. Chem., Int. Ed. Eng., 1983, vol. 22, 725.

[23] E.A. Williams and J.D. Cargioli
"Annual Reports on NMR Spectroscopy", Academic Press, 1979, vol. 9, 221-318.

[24] E.A. Williams
"Annual Reports on NMR Spectroscopy", edited by G.A. Webb, Academic Press, London, 1983, vol. 15, 235-289.

[25] G.C. Levy and J.D. Cargioli
"Nuclear Magnetic Resonance Spectroscopy of Nuclei other than Protons", edited by T. Axenrod and G.A. Webb, John Wiley & Sons, Inc., 1974, 251-274.

[26] J. Schraml and J.M. Bellama
"Determination of Organic Structure by Physical Methods", Academic Press, New York, 1976, vol. 6, 203-269.

[27] T.A. Blinka, B.J. Helmer and R. West
"Advances in Organometallic Chemistry", edited by F.G.A. Stone and R. West, Academic Press, Inc., 1984, vol. 23, 193-218.

[28] E.A. Williams, J.D. Cargioli and R.W. Larochelle
J. Organomet. Chem., 1976, vol. 108, 153-158.

[29] V. Gutmann
Angew. Chem., Int. Ed. Eng., 1970, vol. 9, number 11, 843-860.

[30] V. Gutmann
Coord. Chem. Rev., 1976, vol. 18, 225-255.

[31] R.K. Harris, J. Jones and S. Ng
J. Magn. Res., 1978, vol. 30, 521-535.

[32] G. Binsch and H. Kessler
Angew. Chem., Int. Ed. Eng., 1980, vol. 19, number 6, 411-494.

[33] J. Sandstrom
"Dynamic NMR Spectroscopy", Academic Press Inc. Ltd., London, 1982, and references cited therein.

[34] N.T. Anh and C.J. Minot
J. Am. Chem. Soc., 1980, vol. 102, 103.

[35] R.J.P. Corriu, C. Guerin and J.J.E. Moreau
"Topics in Stereochemistry", edited by E.L. Eliel, S.H. Wilen and N.L. Allinger, John Wiley & Sons, Inc., 1984, vol. 15, 43-198.

[36] A.D. Allen, J.C. Charlton, C. Eaborn and G. Modena
J. Chem. Soc., 1957, 3668-3670.

[37] A.D. Allen and G. Modena
J. Chem. Soc., 1957, 3671-3678.

[38] F.K. Cartledge
Organometallics, 1983, vol. 2, number 3, 425-430.

[39] R.S. Drago
J. Chem. Educ., 1974, vol. 51, number 5, 300-307.

[40] R.W. Taft, T. Gramstad and M.J. Kamlet
Journal of Organic Chemistry, 1982, vol. 47, number 23, 4557-4563.

[41] M.J. Kamlet, J.-L.M. Abboud, M.H. Abraham and R.W. Taft
Journal of Organic Chemistry, 1983, vol. 48, number 17, 2877-2887.

[42] M.J. Kamlet and R.W. Taft
J. Chem. Soc., Perkin Trans. 2, 1985, 1583-1589.

[43] R.H. Prince
"Reaction Mechanisms in Inorganic Chemistry" in "International Review of Science, Inorganic Chemistry Series One", edited by M.L. Tobe, Butterworths, London, 1972, vol. 9, chapter 9.

[44] L.H. Sommer
"Stereochemistry, Mechanism and Silicon", McGraw-Hill, New York, 1965.

[45] J.B. Lambert, J.A. McConnell and W.J. Schulz Jr.
J. Am. Chem. Soc., 1986, vol. 108, number 9, 2482.

[46] S.A.I. Al-Shali, C. Eaborn and F.M.S. Mahmoud
J. Organomet. Chem., 1982, vol. 232, 215-218.

[47] W.H. Stevenson III, S. Wilson, J.C. Martin and W.B. Farnham
J. Am. Chem. Soc., 1985, vol. 107, 6340-6352.

[48] W.H. Stevenson III and J.C. Martin
J. Am. Chem. Soc., 1985, vol. 107, 6352-6358.

[49] F. Klanberg and E.L. Muetterties
Inorg. Chem., 1968, vol. 7, 155.

[50] A.F. Janzen, J.A. Gibson and D.G. Ibott
Inorg. Chem., 1972, vol. 11, 2853.

[51] W.B. Farnham and R.L. Harlow
J. Am. Chem. Soc., 1981, vol. 103, 4608-4610.

[52] W.H. Stevenson III and J.C. Martin
J. Am. Chem. Soc., 1982, vol. 104, 309-310.

[53] E.F. Perozzi and J.C. Martin
J. Am. Chem. Soc., 1979, vol. 101, number 6,
1591-1593.

[54] J. Boyer, R.J.P. Corriu, A. Kpoton, M. Mazhar, M. Poirier, G. Royo
J. Organomet. Chem., 1986, vol. 301, 131-135.

[55] R.J.P. Corriu, M. Mazhar, M. Poirier and G. Royo
J. Organomet. Chem., 1986, vol. 306, C5-C9.

[56] A.R. Bassindale and T. Stout
J. Organomet. Chem., 1982, vol. 238, C41-C45.

[57] H.K. Chu, M.D. Johnson and C.L. Frye
J. Organomet. Chem., 1984, vol. 271, 327-336.

[58] K. Mislow and M. Raban
"Stereoisomeric Relationships of Groups in Molecules" in "Topics
in Stereochemistry vol. 1", edited by N.L. Allinger and
E.L. Eliel, Interscience, New York, 1967, 1-38.

[59] K. Mislow and M. Raban
"Modern Methods of the Determination of Optical Purity" in
"Topics in Stereochemistry vol. 2", edited by N.L. Allinger and
E.L. Eliel, Interscience, New York, 1969.

[60] J. Jacobus and M. Raban
J. Chem. Educ., 1969, vol. 46, 351.

[61] W.B. Jennings
Chem. Rev., 1975, vol. 75, number 3, 307-322.

[62] H.H. Hergott and G. Simchen
Liebigs Ann. Chem., 1980, 1718.

[63] A.R. Bassindale and T. Stout
Tet. Lett., 1985, vol. 26, number 28, 3403-3406.

[64] H. Emde
Synthesis, 1982, 1.

[65] G.A. Olah and S.C. Narang
Tetrahedron, 1982, vol. 38, 2225.

[66] F.R. Jensen and T.I. Moder
J. Am. Chem. Soc., 1975, vol. 97, 2281.

[67] M. Nogradi
"Stereochemistry Basic Concepts and Applications", Pergamon Press, 1981, 123.

[68] R.J. Pugmire, D.M. Grant, L.B. Townsend and R.K. Robins
J. Am. Chem. Soc., 1973, vol. 95, number 9, 2791-2793.

[69] G.B. Barlin and T.J. Batterham
J. Chem. Soc. (B), 1967, 516-518.

[70] A.R. Bassindale and T. Stout
J. Chem. Soc., Perkin Trans. 2, 1986, 221-225.

[71] M.W. Grant and R.H. Prince
Nature, 1969, vol. 222, 1163-1164.

[72] B.G. McKinnie and F.K. Cartledge
J. Organomet. Chem., 1976, vol. 104, 407-411.

[73] F.K. Cartledge, B.G. McKinnie and J.M. Wolcott
J. Organomet. Chem., 1976, vol. 118, 7-18.

[74] A.R. Bassindale and T. Stout
J. Organomet. Chem., 1984, vol. 271, C1.

[75] R.B. Homer and C.D. Johnson
"Acid-base and complexing properties of amides" in "The Chemistry of amides", edited by J. Zabicky, Interscience, 1970, 187-243.

[76] G. Fraenkel and C. Franconi
J. Am. Chem. Soc., 1960, vol. 82, 4478-4483.

[77] C.L. Hausman and C.H. Yoder
J. Organomet. Chem., 1978, vol. 161, 313-317.

[78] H. Marsmann
"Oxygen-17 and Silicon-29" in "NMR: Basic Principles and Progress Grundlagen und Fortschritte, vol. 17", edited by P. Diehl, E. Fluck and R. Kosfeld, Springer-Verlag, Berlin, 1965, 65.

[79] A.T. Balaban, C. Uncuta, M. Elian, F. Chiraleu and A. Dinculescu
Tetrahedron, 1984, vol. 40, number 13, 2547-2553.

[80] Quantum Chemistry Program Exchange (QCPE) DNMR4 program No. 466, Indiana University.

[81] M.B. Robin, F.A. Bovey and H. Basch
"Molecular and electronic structure of the amide group" in "The Chemistry of amides", edited by J. Zabicky, Interscience, 1970, 18-19.

[82] T.J. Barton and C.R. Tully
J. Org. Chem., 1978, vol. 43, number 19, 3649-3653.

[83] K.J. Laidler
"Reaction Kinetics: vol. One Homogeneous Gas Reactions", Pergamon Press, 1966.

[84] H.J. Reich and D.A. Murcia
J. Am. Chem. Soc., 1973, vol. 95, number 10, 3418-3420.

[85] Y. Kiso and M. Kamada
J. Organomet. Chem., 1973, vol. 1, part 50, 297-310.